Kulturhistoriska Dokumentationer nr 28

# REBURIAL AND ANALYSES OF ARCHAEOLOGICAL REMAINS

## Phase II – Results from the 4th retrieval in 2009 from Marstrand, Sweden

## THE RAAR PROJECT

Eds. Inger Nyström Godfrey, Thomas Bergstrand and Håkan Petersson

REBURIAL AND ANALYSES OF ARCHAEOLOGICAL REMAINS THE RAAR PROJECT Eds. Inger Nyström Godfrey, Thomas Bergstrand and Håkan Petersson

Kulturhistoriska Dokumentationer nr 28

# Reburial and analyses of archaeological remains The RAAR project

## Phase II - Results from the 4th retrieval in 2009 from Marstrand, Sweden

Kulturhistoriska Dokumentationer nr 28

# Reburial and analyses of archaeological remains The RAAR project

## Phase II - Results from the 4th retrieval in 2009 from Marstrand, Sweden

Stefan Almström
Thomas Bergstrand
Carola Bohm (co-ordinator)
Eva Christensson
Charlotte Gjelstrup Björdal (co-ordinator)
David Gregory (co-ordinator)
Inger Nyström Godfrey (co-ordinator)
Ian MacLeod (co-ordinator)
Anders Nord
Elizabeth E. Peacock (co-ordinator)
Håkan Petersson
Vicki Richards (co-ordinator)
Kate Tronner
Gordon H. Turner-Walker

Eds. Inger Nyström Godfrey, Thomas Bergstrand and Håkan Petersson

BOHUSLÄNS MUSEUM

VÄSTRA GÖTALANDSREGIONEN
VÄSTARVET

ISSN 1102-528X
ISBN 978-91-7686-239-1

**Språkgranskning** Ian Godfrey
**Grafisk form** Gabriella Kalmar
**Layout och teknisk redigering** Lisa K Larsson
**Omslagsbild** Marine Photo

Kartor godkända från sekretessynpunkt för spridning
Lantmäteriverket 2006-12-04. Dnr 601-2006/2076

**Tryck** Bording AB, Borås 2011

Bohusläns museum och Studio Västsvensk konservering
Kulturhistoriska dokumentationer nr 28
Bohusläns museums förlag
Museigatan 1
Box 403
451 19 Uddevalla
tel 0522-65 65 00, fax 0522-126 73
www.vastarvet.se, www.bohuslansmuseum.se

# Innehåll

# Summary

The general purpose of Reburial and Analyses of Archaeological Remains (RAAR) project is to evaluate reburial as a method for long-term storage and preservation of waterlogged archaeological remains. Five sub-projects aim to investigate the effects of the burial environment in Marstrand harbour on a wide range of material types. These include organic materials such as wood, textile, leather, bone, horn and antler and inorganic materials such as silicates and metals. The stability of these, the most commonly encountered materials in archaeological excavations, as well as packing and labelling materials has been studied in this investigation. The sixth sub-project has monitored the reburial environment. The project is designed to last for 50 years and the following report discusses the findings of Phase II, the 4th retrieval of samples after a seven-year burial phase (2002-2009).

Phase II has so far confirmed most of the results from the previous phase. It has underlined the importance of understanding the processes occurring within a given sediment prior to carrying out any reburial. If any form of reburial is to be successful, the primary aim should be to understand the agents of deterioration on a site and their effects on artefacts with a view to the development and implementation of mitigation strategies. Buried sites have better preservation because of the limited oxygen levels, which minimise chemical, physical and especially biological deterioration.

The optimal depth of reburial has been a point of discussion throughout the project and the results of Phase II have assisted in answering some of the questions that have arisen over the years. These results show that it is not simply a matter of depth of burial per se, but the type of sediment used, its properties and the processes occurring within it – all of which vary from sediment to sediment. Porosity and organic content in particular will have an effect on the rates of microbial activity. The lower the porosity and organic content the better the sediment is for preservation of archaeological materials.

Based upon the results from RAAR Phases I and II, materials such as porcelain, stoneware, clay pipes and wood are likely to survive a long-term reburial, whereas glass and fibrous material should not be reburied. The exception could be tarred cordage recovered in large amounts, which, due to their physical bulk and the biocidal effect of the tar coating, will survive for a longer period. Soft and hard animal products like leather, bone and antler can be considered for medium-term reburial.

Low-fired earthenware is unlikely to survive long-term exposure and should not be reburied. However, the resistance of earthenware to a marine environment varies, largely dependent on the firing conditions during manufacture. Hence, the poor results for the very low-fired 'modern' earthenware samples in this project cannot be extrapolated to issue a general recommendation against reburial of all earthenware artefacts.

It is believed that copper alloys could be recommended for short-term reburial in these types of sediments. Although it is probable that pure copper and brass alloy types may be buried for longer periods of time and at shallower depths, more information from the next phase of the experiment is required to support this inference. On the other hand, due to the significant increase in corrosion rate of the bronze coupons over the past four years, it is not possible to recommend longer term reburial times for these alloy types at this point. Ferrous alloys could not be recommended for reburial even in the medium term, based on their extensive degradation after six years and the significant increases in their corrosion rates since 2005, which may indicate that corrosion will increase significantly over time.

The impact of packing archaeological material prior to reburial is considered very important. Of the three packing systems investigated the Zip-lock® bags generally seemed to offer the best protection against degradation and/or infiltration of salts. However, potentially unfavourable micro-climates can develop inside the zip-lock bags. For example, micro-organisms were detected on the model potash glass deposited in zip-lock bags. While geotextile readily allows for free flow of the soluble salts, it also protects against direct influence of the burial sediment. Results indicate that the geotextile offers protection from micro-organisms within the sediment and isolates the material inside from some microstructural alteration. It does not appear to protect against chemical alteration. Polyethylene netting offered the least protection and should be avoided.

Most of the synthetic packing materials tested seem very stable and could be used in situations when archaeological artefacts are to be reburied. Only the polyethylene netting should be avoided since it lost more than half of its strength during the in situ and laboratory exposure periods. To label finds the preferred option would be to use either prefabricated tags, like the so-called 'ear-tags' for livestock, or embossed PVC tags (Table 7).

As more results have been obtained the RAAR project perception on reburial has modified slightly; not from yes to no or vice versa, but in the realisation that there is more complexity to it than we originally and, maybe naively, thought. The degradation processes are complex and there are more nuances within the categories of materials than was first acknowledged. Maybe even more complex are the implications for heritage management.

A heritage institution could provide curation for its archaeological archive by using reburial depots provided they follow recommended restrictions. Reburied artefacts are not meant to be forgotten in the sediments, nor should reburial be chosen instead of conscious disposal of artefacts that have been evaluated as of no use based on, for example, scientific, technological, educational, or aesthetic grounds. In the same way as traditional conservation and storage preserves an object for study

or exhibition purposes, artefact reburial is also designed for preservation so that it can be accessed and researched in the future.

To accomplish this, collection strategies including time frames are necessary. The project report presents a first draft of a suggested model for a reburial collection strategy that includes short, medium and long-term reburial. Collection strategies and programs should be added to these time frames; documents that describe the intentions with the reburied finds, time schedules and funding proposals. To make reburial a useful and complete tool for heritage management we also need to consider possible failures in our reburial programs and suggest remedies.

## Acknowledgements

The Reburial and Analyses of Archaeological Remains (RAAR) project was initiated thanks to funding from the Nordic Cultural Fund, the National Heritage Board of Sweden, Carl Jacob Lindebergs Fornminnesfond and Wilhelm and Martina Lundgrens fund.

Each co-ordinating institute contributes to the funding of the project to varying degrees by providing work time for the co-ordinators, covering analytical costs, etc. This self-funding is quite substantial in some cases and the project is in great debt to these institutions. In particular the Western Australian Museum should be mentioned, since their contribution to the project has been fully funded by that museum.

## Introduction

To protect the fragile and non-renewable archaeological heritage, non-destructive and non-intrusive conservation strategies, such as in situ preservation, are emphasised in the UNESCO Convention of 2001. Reburial can be seen as the other side of the coin in that it seeks to emulate a pre-excavation (in situ) environment that has been relatively benign for the preservation of archaeological remains for centuries. Therefore reburial and in-situ preservation of shipwrecks and other archaeological underwater sites represents a new field of interest that is being given increased attention. The approach offers the potential to understand and identify the processes of deterioration of archaeological materials in underwater environments. However, more importantly, it also offers the possibility to find methods of counteracting these processes and to create alternative storage for the preservation of underwater archaeological heritage.

The extensive archaeological investigations and reburial of recovered archaeological artefacts that took place in Marstrand harbour during 1998 to 1999, was the catalyst for the international reburial research project 'Reburial and Analyses of Archaeological Remains' (RAAR), which was initiated in 2001. The project is co-ordinated by Bohusläns

Museum and Studio Västsvensk Konservering in Sweden and consists of six sub-projects co-ordinated in turn by museums and universities in Sweden, Denmark, Norway and Australia (Table 1).

The general purpose of RAAR is to evaluate reburial as a method for long-term storage and preservation of waterlogged archaeological remains.

The study aims to determine the effects of the burial environment in Marstrand harbour on a wide range of material types. These are organic materials (e. g. wood, textile and leather) as well as inorganic materials such as silicates and metals. The stability of these, the most commonly encountered materials on archaeological excavations, has been studied, as well as that of packing and labelling materials. Understanding the degradation patterns of packing and labelling materials is important, since it affects the ability to identify artefacts at a later stage. The different material groups were divided into sub-projects, each with its own specific objectives. These objectives together with the materials and methods of analyses are described in the sub-project reports.[1]

| Sub-project | Co-ordinator | Institute/University |
|---|---|---|
| Silicates | Carola Bohm & Eva Christensson | The National Heritage Board, Sweden, (RAÄ) |
| Metals | Vicki Richards & Ian MacLeod | Western Australian Museum, Fremantle, Australia, (WAM) |
| Wood | Charlotte Björdal & Thomas Nilsson | Swedish University of Agricultural Science, Uppsala, Sweden, (SLU) |
| Organic non-wood material | Elizabeth Peacock | The Norwegian University of Science and Technology, Trondheim, Norway, (NTNU) |
| Packing and labelling materials | Inger Nyström Godfrey | Studio Västsvensk Konservering, Göteborg, Sweden, (SVK) |
| Environmental monitoring | David Gregory | The National Museum of Denmark, Brede, Denmark, (NM) |

*Table 1. The six subprojects and their co-ordinators.*

The project concurrently monitors and assesses the burial environment in Marstrand with the aim to complement the studies on materials and to discuss important physical and chemical criteria necessary for an acceptable reburial environment. The environmental sub-project also aims to develop methods to assess and monitor the reburial environment.

It is the scope of the study to provide, where possible, guidelines for material types that can be safely reburied in environments similar to those in Marstrand harbour and to identify those that should not be reburied. Hopefully, this wide-ranging study will provide valuable information linking environmental parameters with the degradation of included materials. Studying the environmental parameters and the degradation of test materials will also provide insight into the preservation status of the reburied archaeological artefacts from the Marstrand project.

1 See Appendices

## Main objectives

- Evaluate reburial as a method for preserving wet archaeological remains
- Determine the effects of the burial environment on a range of material types
- Gain information about the preservation status of the reburied archaeological artefacts

In order to determine the long-term effects of reburial on the different material types, sufficient samples were buried to allow sampling to continue for up to 50 years. The wood, other organics, ceramics/silicates and polymeric samples were buried in Marstrand Harbour, Sweden in September 2002 (trench 1), whereas the metal sample units were buried in a separate trench (trench 2) the following year in September 2003 (Table 2 & Figure 1). The project, methodology and results from the first 3-year burial phase (2002-2005) have been reported extensively (e.g. Bergstrand and Nyström 2007; Nyström Godfrey et al. 2009). The final report for the first phase is also available on the project website: http://www9.vgregion.se/vastarvet/svk/reburial/index.htm.

The following report presents the work, analyses and results of the second phase of the RAAR project (2009). For details regarding the history and background of the project, readers are referred to the aforementioned publications.

*Figure 1. The reburial site at Marstrand (photo Inger Nyström Godfrey, SVK).*

| Phase | Proposed Retrieval Year | Proposed Reburial Interval (yr) | Retrieval Year | Reburial Interval (yr) | Comments |
|---|---|---|---|---|---|
| 1 | 2003 | 1 | 2003 | 1 | Final report published in 2007 |
| | 2004 | 2 | 2004 | 2 (1)[1] | |
| | 2005 | 3 | 2005 | 3 (2) | |
| 2 | 2008 | 6 | 2009 | 7 (6) | Final report completed in 2011 |
| 2 | 2014 | 12 | | | Subject to funding |
| 3 | 2026 | 24 | | | Subject to funding |
| 3 | 2050 | 48 | | | Subject to funding |

*Table 2. Retrieval programme for the project.*
*[1] Numbers in brackets denote the reburial interval for the metal samples, which were reburied in 2003, one year after the other sample units.*

# Phase II – The 4th retrieval (2009)

## Conditions

Lack of funding meant that the 4th retrieval of samples was postponed from 2008 to 2009. The second phase began with the retrieval of samples in September 2009. The funds received for the 4th retrieval were less than those required to follow through with the initial research plan but through prioritisation within the project, some analyses could be carried out.

This was an unfortunate and difficult task and it has to be stressed that the outcome was in no way a reflection of the quality of our respective work. It was decided that it was most important to continue the analyses of materials that were generally less well studied or where results from Phase I were not conclusive. Therefore the focus was on areas where the 4th retrieval would hopefully provide answers to questions arising in Phase 1. In the decision making process we also had to take into consideration the restrictions of some funding bodies.

As a result of these discussions with co-ordinators and the co-ordinating institutions, the RAAR project decided to fund the organic sub-project, the environmental sub-project and the silicate project. The Western Australian Museum was able to fully support the metal sub-project, for which we are truly thankful. The packing and marking sub-project was scaled down by half. All travel expenses, apart from those related to the retrieval, were not funded and part of the administration cost was covered by Västarvet[2]. We decided not to fund the wood sub-project, since it is our belief that wood is the most studied material under these circumstances and would therefore contribute least to new knowledge

2 Västarvet is the regional heritage organisation within Västra Götalandsregionen, Sweden and consists of museums and other heritage institutions, amongst these are Bohusläns Museum and Studio Västsvensk Konservering, the co-ordinators of RAAR.

and understanding. However, the wood samples were retrieved together with the other samples and sent to the co-ordinator, in case analyses were possible at a later stage.

### Fieldwork

The 4th retrieval took place on the 22nd September 2009 with participants from Bohusläns Museum, Studio Västsvensk Konservering and the National Museum of Denmark. The site was scanned, photographed and marked before sediment cores were taken in the two trenches and the material samples retrieved. Redox potentials and pH values of the metal samples were measured and recorded on the seabed as soon as possible after they were removed from the sediment. Note that the iron samples for the 4th retrieval numbered 8, 9 & 10, could not be found since visibility was zero. Instead iron samples numbered 14, 15 & 16 were retrieved. Samples and/or sample units were photographed before they were packed for transport.

Special care was taken to pack the metal samples in an oxygen-free environment in order to prevent corrosion processes occurring before their analysis. The metal samples were demounted and each plate with samples was rinsed with deionised water and lightly padded with tissue paper to remove some of the water before being wrapped in polyester wadding. Each parcel was packed and sealed in gas tight bags together with an oxygen scavenger and an oxygen indicator. [3] The whole procedure, from when the metal samples were extracted from the sediment to when they were packed, took approximately one hour.

## Experimental and results -Summaries of the sub-project reports

### Environmental monitoring

The environmental monitoring sub-project for Phase II of the RAAR project focused on three specific questions:

- What are the conditions within sediments deeper than 50 cm below the sediment surface and is the 50cm reburial depth sufficient for protection?
- As the sediments in the metals reburial trench were not studied in Phase I, what are the conditions within these sediments?
- Is the environment in Marstrand harbour still conducive to the preservation of reburied archaeological material?

3 ESCAL barrier film and clip. Oxygen scavenger RP-A 2000 ml and RP oxygen eye.

Following on from the completion of Phase I in 2006, sediments were examined in April 2007 and September 2009. A new system of coring was developed whereby it was possible to sample sediments to ca. 70cm below the sediment surface. Two systems were successfully used: the first, for analysing pore water parameters and the second for analysing sediment properties themselves. Cores were taken in an undisturbed area and from the organic and metals reburial trenches.

Pore water parameters were primarily measured using microelectrodes: dissolved oxygen, sulphide, redox potential, carbon dioxide and pH. Aliquots of pore water were also taken for determination of sulphate content. Measurements were taken at 5cm intervals along the total core length. Sediment analyses were carried out on sections taken every 5cm through the cores. For each section the porosity, particle size, loss on ignition (organic content) and iron content were determined.

All results reflect that the environments within the organic and metal reburial trenches are conducive to the preservation of the materials within them. Results of the pore water analyses indicated that the conditions within the organic and metals reburial trenches were sub-oxic to anoxic and dominated by anaerobic processes. Dissolved oxygen levels were low: sub-oxic (0.1-0.3 mg dm-3) to anoxic (< 0.01 mg dm-3). Redox potentials were strongly reducing with potentials between -150mV and -200mV (vs SHE). pH of sediments were near neutral (pH 7.0-7.5). The processes ongoing in the sediments were dominated by sulphate reduction, where generally a loss of sulphate was seen with increasing depth with the concomitant evolution of sulphide.

However, the analyses of the sediments themselves (Figures 2 and 3) showed there was a distinct difference between those used in the organic and metals reburial trenches. In both trenches the upper 30 cm consisted of porous (porosity of 0.8), coarse silts with a high organic content (20-30% weight/dry weight). In the metals trench, sediments were graded to medium silts below this depth and were still porous with a relatively high organic content. In the organic trench after 40 cm the sediment consisted of very fine, low porous (porosity of 0.4) sands with a low organic content (ca. 5% weight/dry weight). The profiles of sulphate and sulphide showed that the rates of sulphate reduction were highest in the finer grained sediments with high organic contents. Seasonal changes in the rate of reduction were seen in the metals trench, surprisingly with rates higher in April than in September. Modelling mineralisation of organic material due to sulphate reduction showed that ca. 80g and 44g of organic material per $m^2$ per year could be oxidised in the metals trench in April and September, respectively. Sulphate had been completely reduced at a depth of 50 cm in both April 2007 and September 2009. In the organic trench sulphate reduction was also the dominant process. The rate of mineralisation of organic material was lower at ca. 20g per $m^2$ per year and there did not appear to be a significant seasonal variation. All sulphate had not been utilised in the organic trench

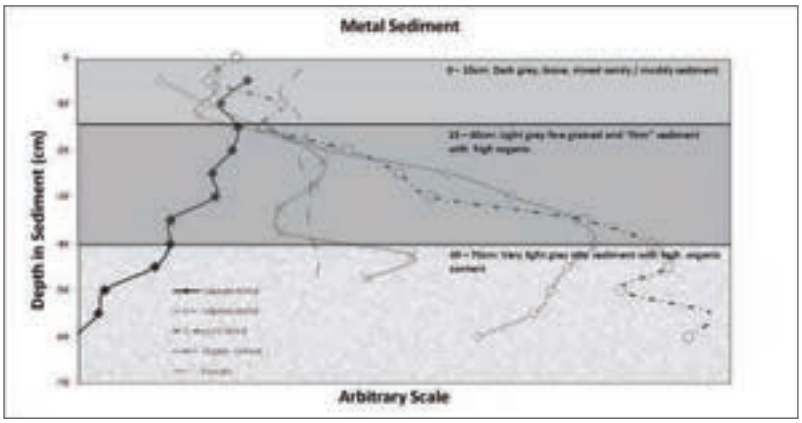


*Figure 2. Results (September 2009) of sediment analyses in the Metal trench (trench 2).*

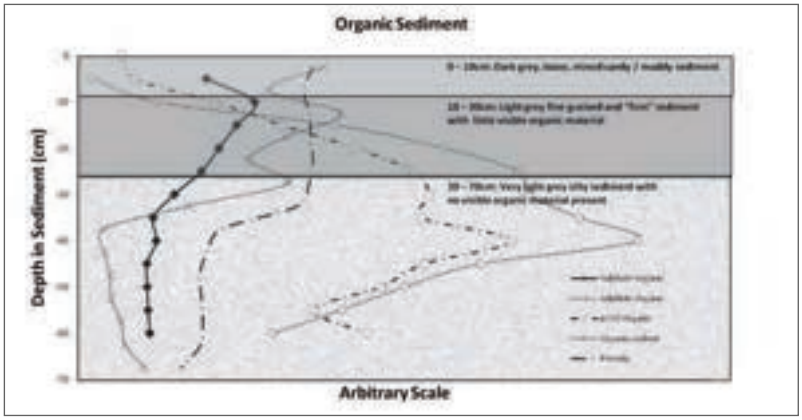


*Figure 3. Results (September 2009) of sediment analyses in the Organic trench (trench 1).*

but sulphate reduction ceased at ca. 40 cm below the sediment surface where the concentration remained at about 7mM from 35 cm down to 6 5cm (Figure 3).

## *General implications for reburial?*

The implications of these results to the question of depth of burial show that it is not just depth of burial per se that is important. An explicit understanding of the physical, chemical and biological properties of the sediment used, or to be used in reburial, is required in order to understand what processes take place, at what rates they occur and only knowing this information can an optimal depth of burial be selected. Differences in the rates of sulphate reduction are probably due to the different particle sizes, porosity and importantly, organic contents of the sediments. Based on the results of Phase II it is believed that conditions

in the reburial trenches are still conducive to preservation. However, the sulphate reducing bacteria responsible for sulphate reduction can affect the sulphur content of wood, cause microbial induced corrosion of metals and potentially affect the other materials reburied in Marstrand. To this end the environmental results should be co-ordinated with the results of the other sub-projects to confirm or refute this. Such an action has already been agreed with the coordinators of the metals sub-project.

In order to classify sediments for their potential use in future reburial projects it is recommended that the following parameters be measured and that the time (season) of sampling be considered:

Pore water parameters: Dissolved oxygen, redox potential, pH, dissolved and total iron, sulphate and sulphide content, temperature.

Sediment parameters: Particle size, porosity, organic content.

For further information on the environmental sub-project see Appendix 1.

## Metals

The aim of the metals sub-project is to investigate the corrosion behaviour of metals buried in the marine environment. The corrosion of modern metal coupons reburied in the sediment and exposed to the open marine environment will be examined and compared over time. This study will ascertain the effect of reburial on the deterioration of archaeological metals commonly found on underwater cultural heritage sites and assist in evaluating the effectiveness of reburial as a long-term in-situ preservation strategy for metallic archaeological remains.

The sample units consisted of prefabricated proprietary metal coupons of known composition mounted utilising high density polyethylene (HDPE) materials. The metal coupons deployed in the experiment were ferrous alloys: duplicate coupons of cast iron and mild steel and one standard Defence Science and Technology Organisation (DSTO) copper steel coupon and copper alloys: duplicate coupons of brass, copper and bronze. The ferrous and copper alloys were mounted separately to minimise galvanic and proximity corrosion since the latter form of decay has been known to exert its effects over separation distances of many metres on historic shipwreck sites (North 1989). Each sample unit consisted of three sets of duplicate metal coupons mounted at three different depth intervals (totally exposed above the sediment, just below the sediment and buried 50 cm in the sediment) on the HDPE rod (Figure 4).

In September 2009, six years after the initial reburial in 2003, the third set of metal sample units (copper and iron alloys) were retrieved. Each sample unit was removed by physically extracting the rods from the sediment and the corrosion parameters (Ecorr and pH) of each coupon

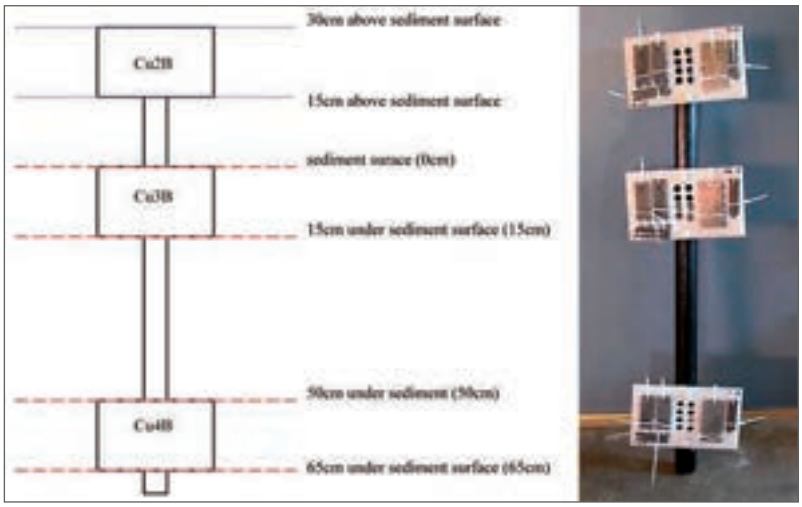


*Figure 4. Schematic diagram and image of the completed copper alloy coupon sample unit (photo Vicki Richards, WAM).*

measured in-situ on the seabed prior to recovery. The metal coupons were documented and each coupon with the associated corrosion products was analysed by scanning electron microscopy/electron dispersive x-ray analysis (SEM/EDX). One of the duplicate coupons was then chemically stripped of all corrosion products, weighed and analysed again by the same technique. Digital electron micrographs (SEM) and energy dispersive x-ray analyses (EDX) were collected as the primary data.

At the end of six years it is clear that the precise burial microenvironment plays a major role in determining the fate of the metal coupons. From extended and detailed analyses of the surfaces and their corrosion products, annualised normalised percentage weight loss data and normalised corrosion rates it is possible to gain a good understanding of the parameters that dominate the deterioration of the metals. The effect of the reburial environment on the extent of corrosion of the metals after six years is summarised below.

- It is very important to fully understand the physico-chemical and biological nature of the local sedimentary environment prior to deployment of any reburial strategy.
- It was found that the behaviour and characteristics of the metal surfaces that were fully exposed to the local microenvironment provided a better insight into long term corrosion of metals in a marine environment than the side that lay directly against the HDPE support plate despite the pre-drilled flow holes. However the complimentary data collected from this reverse side provided corroboration of the overall corrosion mechanism and provided an insight into how variations in the microenvironment affect the corrosion processes.

- The manner in which metals are packed for reburial is extremely important. Metals of significantly different composition must be physically separated by sufficient distance to avoid the complications of galvanic and proximity corrosion and even artefacts of similar composition should be separated in some way (e.g. geotextile barrier) to minimise abrasion and damage to the inherently protective corrosion product layer.
- Copper alloy artefacts recovered from a saline environment should always be stored wet. It was noted that desiccation can cause changes in the nature of the surface corrosion products that may not accurately reflect the microenvironment from which the object was recovered.
- If further analysis of the corrosion product layer and underlying residual metal will be undertaken in the context of the deposition and site formation processes then all metal artefacts should be stored in a similar environment to that from which they had been recovered (e.g. deoxygenated environments if the artefact is recovered from under the sediment). For example, both the copper and the ferrous alloy plates from above the sediment where stored in a low oxygen environment after recovery, which caused a significant change in the nature of the outer surface of the corrosion product layer. This could have lead to misinterpretation of the local microenvironment and the corrosion mechanisms and hence, the associated archaeological record.
- It is vitally important that metals are reburied to depths where there is no chance of partial exposure to the aerobic marine environment through sediment movement, since the non-ferrous metal coupons were found to be particularly sensitive to being in a mixed aerobic/anaerobic microenvironment.
- The resistance of a metal to corrosion is very dependent on the elemental composition and the associated microstructure, which records the impact of fabrication processes and depositional stress.
- The reburial environment surrounding the metal coupons has finally stabilised and as a result the long-term corrosion processes and associated mechanisms are becoming better indicators of the final corrosion outcomes.
- The concretions and corrosion product layers on the metal coupons are more extensively developed than after the first two years of exposure/reburial and therefore, the coupons are beginning to more accurately reflect the corrosion behaviour of marine archaeological metal artefacts.

- The extent of corrosion of all metal coupons decreased once the coupons were buried, even at shallow depths and this protective effect increased with increasing burial depth. This decrease was most marked for the brass and bronze coupons, but much less dramatic for the ferrous alloy coupons. Burial seemed to have the least effect on the pure copper coupons, however the extent of corrosion of the exposed copper coupons was also very low due to their pure composition and single phase microstructure.
- Despite a general decrease in the extent of corrosion with burial, all metal coupons exposed to the three different environments (exposed, buried just below the sediment and buried 50 cm below the sediment), showed some increase in corrosion rate over the past four years. The greatest increases were found for the bronze and ferrous metal coupons buried at both depth intervals but the rate increases for the buried brass and copper coupons were considerably less. These results indicate that the greatest microenvironmental changes are occurring in the sediment and these changes are mainly affecting the corrosion behaviour of the buried bronze and ferrous alloy coupons.
- It appears that reburial has the most positive effect on brasses and to a lesser extent, bronzes. This significant decrease in corrosion would be primarily due to the biological toxicity of copper, zinc and tin corrosion products, which inhibit concretion formation and corrosion by effectively limiting bacterial counts in the surrounding sediment. The bronze coupons show more corrosion than the brass coupons as the three different phases in the bronze microstructure have significantly different electrochemical voltages as compared to the brass microstructure, which causes increased intergranular (micro-galvanic) corrosion.
- Reburial has less affect on the preservation of pure copper as it is a single phase alloy, with uniform composition and therefore, exhibits less intergranular galvanic corrosion.
- The positive effect of burial is significantly reduced on ferrous alloys due to the fact that iron corrosion products can be utilised by microbes and therefore, microbially induced corrosion (MIC) can become more significant in controlling the corrosion rates than direct access to dissolved oxygen.
- Since the major process in the Marstrand sediments is sulphate reduction and the metals trench contains sulphate, albeit at low concentrations at deeper depths and

> significant quantities of organic matter, it is probable that sulphate reducing bacteria are causing microbially influenced corrosion of the buried ferrous alloy coupons.

Based on the 2009 results, copper alloys could be recommended for reburial in these types of sediments for a period of six years. It is probable that pure copper and brass alloy types may be buried for longer periods of time and at shallower depths, however more information from the next phase of the experiment is required to support this inference. On the other hand, due to the significant increase in corrosion rate of the bronze coupons over the past four years, it is not possible to recommend longer term reburial times for these alloy types at this point in time.

Conversely, ferrous alloys could not be recommended for reburial even in the medium term, based on their extensive degradation after six years and the significant increases in their corrosion rates since 2005, which may indicate that corrosion will increase parabolically over time. However, despite the concretion layers on the ferrous metal coupons being considerably better developed after six years they are not yet totally encapsulating, making extrapolation to the corrosion behaviour of totally concreted archaeological ferrous artefacts difficult at this stage. Even after six years, it is still difficult to make any definitive statements regarding the longer term stability of these alloy types. It is of paramount importance therefore that this project continues to the next phase, so as much information as possible regarding the corrosion processes of these metal coupons can be obtained. This will allow us to establish whether or not the present conclusions are real indicators of the effects of the different microenvironments on long-term metal corrosion and whether reburial is indeed, an appropriate preservation strategy for maritime archaeological metals.

For further information on the metal sub-project see Appendix 2.

## Silicates

In order to study the effects of reburial in a marine environment, twelve categories of silicate samples, typically found at shipwreck sites, were chosen for this sub-project. Each material category has been reburied in three different packing envelopes: zip-lock bags, plastic netting, and geotextile to ascertain if preservation of the samples is affected by packing methods. Samples were deposited in perforated HDPE crates. In Tables 3 and 4 the material categories are listed along with the preliminary results from Phase I.

The analyses of the glass and ceramic samples retrieved in 2009, after seven years of burial, have, in many instances, have confirmed the results from the first phase of the project. These analyses have also provided some new and intriguing features that have raised questions concerning local microenvironments in the burial trench, although this does not appear to be confirmed by the environmental data. It might simply be attributed to the longer burial period.

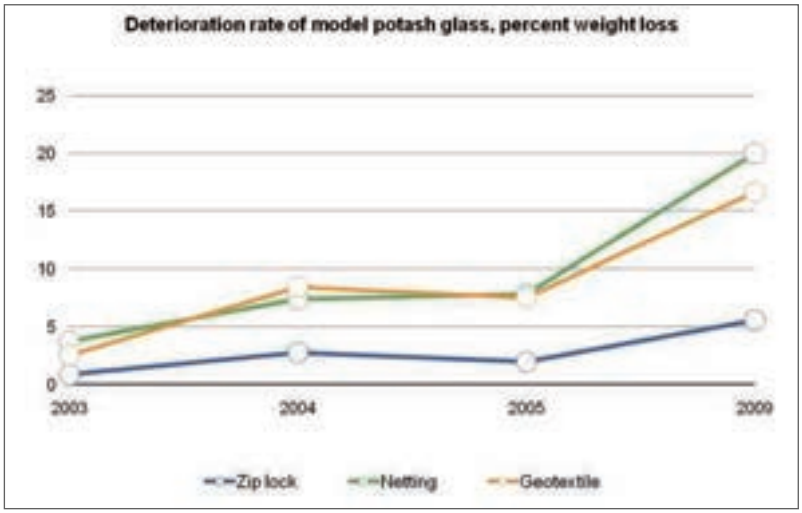


*Figure 5. Model potash glass packed in zip-lock bags, netting and geotextile envelopes. Measured weight loss after reburial for 1, 2, 3 and 7 years burial*

| Archaeological samples | | Model samples | |
|---|---|---|---|
| Clear table glass | Bottle glass, green | Soda glass | Potash glass |
| Thin iridescent surface layers with reduced alkali levels. | Thick silica-rich surface layers with areas of elevated NaCl, S, Fe | Accelerating depletion of Na | Depletion of alkali components in surface layers |
| Surface exfoliation | Heavy surface exfoliation | | Severe disintegration and loss of surface |
| One sample in zip-lock bag broken | No clear difference between reburied sample and reference | | Zip-lock bag represses leaching, but promotes biological growth |
| | | | Discolouration of weathered layers |

*Table 3. Summary of the results for the glass samples.*

| Archaeological samples | | | | Modern samples | | | |
|---|---|---|---|---|---|---|---|
| Porous | | | Non-porous | Porous | | Non-porous | |
| Earthenware, lead glazed | Flintware, lead glazed | Clay pipes | Stoneware, salt glazed | Earthenware, low-fired | Flintware, lead glazed | Stoneware, feldspatic glaze | Porcelain, feldspatic glaze |
| No visible alteration | No visible alteration | Black stained in wet condition | No visible alteration | Severe disintegration | No visible alteration | No alteration | No alteration |
| Absorption of NaCl, S | Absorption of NaCl, S | Absorption of NaCl, S, Fe | Traces of NaCl, S | Absorbed NaCl, S | Some absorption of NaCl | | |

*Table 4. Summary of the results for the ceramic samples.*

An apparent difference in the deterioration process is manifested in the model potash glass samples. It is the texture, rather than the chemical composition of the weathering layers of these samples that differs strongly from that of the earlier samples, in that it is hard and sugary and adheres more strongly to the substrate. All the earlier samples have been conspicuously and increasingly flaky. The rate of deterioration – one of the questions raised by the results from Phase I – has not abated as is illustrated in Figure 5. The zip-lock bags still prove to be inhibiting, whereas the netting seems to allow for quicker leaching of the alkali components and thereby, loss of coherence in the surface layers.

Another question that arose from the earlier retrievals was the nature of the biological growth detected on all the samples of model potash glass deposited in zip-lock bags. The organisms are again present on the 2009 samples, but do not appear to have grown or expanded (Figure 6). At high magnification, groups of pits can be seen on the glass surface, which correspond in size and shape to the detected micro-organisms and could be a sign of etching caused by these microbes (Figure 7). Investigations into these phenomena are on-going, but are not conclusive and the micro-organisms have not yet been identified.

Although the model soda glass samples still appear undeteriorated to the naked eye, the SEM analyses reveal a continuing depletion of sodium from the superficial layers and the sample packed in the zip-lock bag is now starting to show a tendency towards flaking. The leaching is most consistently observed in the samples deposited in netting where the sodium remaining at the surface after seven years of burial has decreased by a third. Leaching is however, observed in all three packing systems,

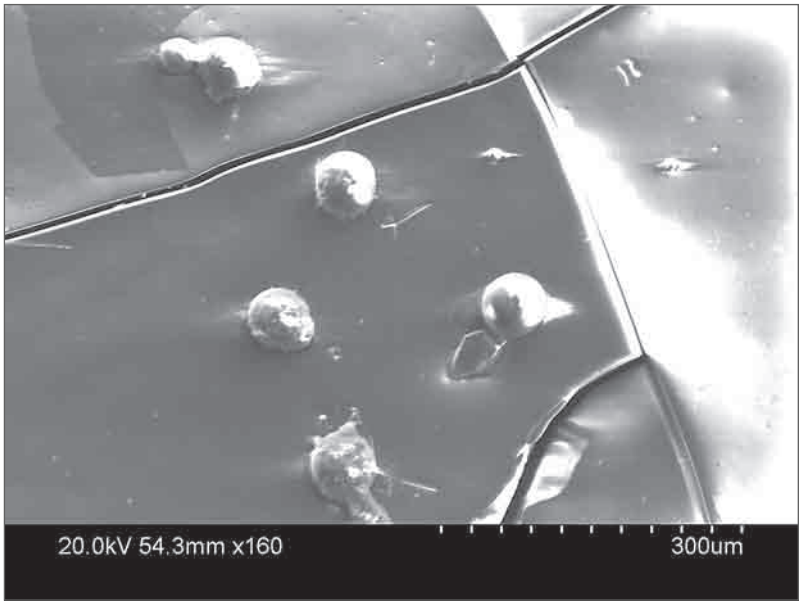


*Figure 6. SEM image of model potash glass with micro-organisms on the surface (photo Margareta Ekroth-Edebo,Conservation Institute, Göteborg University).*

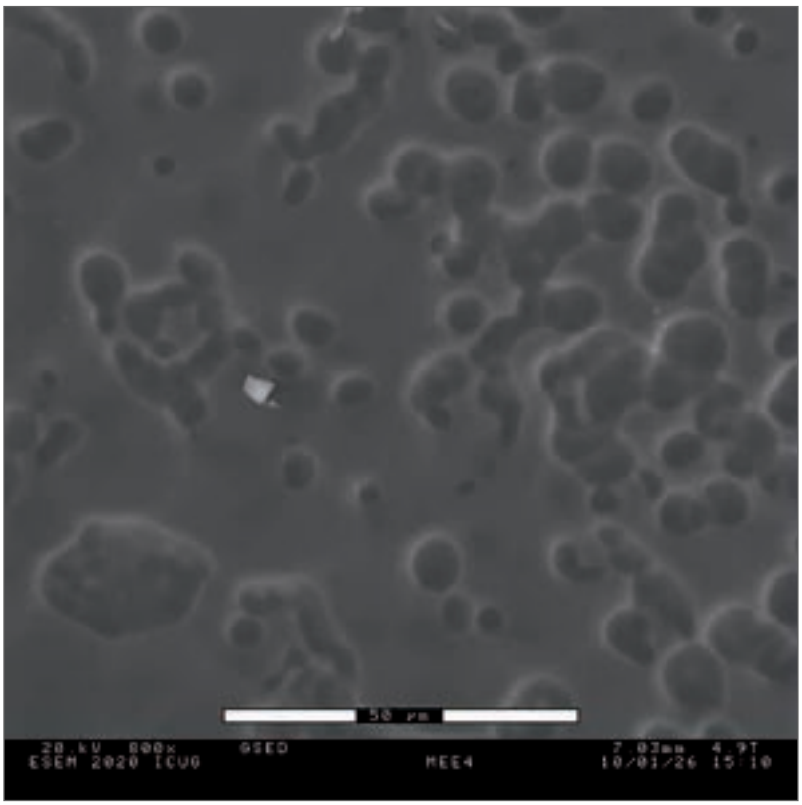


*Figure 7. SEM image of the "etched" surface on model potash glass surface (photo Margareta Ekroth-Edebo, Conservation Institute, Göteborg University).*

but occurs least in the zip-lock bags. Of the archaeological glass, little change has been observed compared to earlier retrievals.

Most samples of a porous nature, the earthenware, flintware and clay pipes, as well as the depleted, layered surfaces of the glass samples can be seen to include ever higher concentrations of both sulphides/sulphates and chlorides. Non-porous modern samples, porcelain and stoneware, are generally still quite unaltered, as seen both visually and in the elemental analyses.

Tentative recommendations for reburial provided in the conclusion of Phase I are still appropriate. Material categories that might be considered "safe" for reburial are porcelain, stoneware and clay pipes, with the exception of items with over-glaze decoration.

For further information on the silicate sub-project see Appendix 3.

## Organic non-wood materials

The non-wood organic materials sub-project of RAAR is evaluating the effect of burial in a marine environment on the more sensitive non-wood organic materials that make up the marine archaeological record. Samples have been drawn from modern materials of vegetable-tanned

leather, undyed and dyed (madder, indigo and weld) woven wool fabric (vadmel), raw (grey) woven linen fabric, undyed woven silk fabric, hemp rope, tarred/treated cotton fishing net, antler, horn, and fresh bovine bone (metapodials). Dyestuffs, tanning agents and pre-treatments of the experimental materials were kept as close to those used in antiquity or historical times as practically possible. One sample of each material was sewn into a nylon open mesh envelope, and half of these envelopes were further enclosed in envelopes made of a non-woven geotextile fabric. One set each of the geotextile-covered and uncovered samples was laced side-by-side with nylon cord in the bottom of a perforated plastic tray (Figure 8).

The materials included in this study are modern in origin, and thus at the outset do not simulate burial-degraded archaeological artefacts of similar materials or artefacts recovered from a marine burial environment. For these materials the study is of burial rather than reburial. Moreover, the sample materials were not packed in polyethylene or similar slow-biodegradable packaging film to protect them from interaction with the surrounding sediment solution and sediment. Artefacts of these materials selected for deposition in a marine archive would undoubtedly be packaged prior to deposition. Therefore, these results reflect degradation of non-protected materials and of materials once the protective packaging fails either through leakage or failure of the packaging material itself.

All the non-wood materials included in this study exhibited degradation as the result of one to seven years burial in 50 cm of sediment in Marstrand harbour. In this seven year time frame there was no indication that the degradation was levelling off to establish an equilibrium state. Results indicate that the geotextile envelope offers protection from micro-organisms within the sediment and isolates the material inside from some microstructural alteration. The envelope does not appear to protect against chemical alteration.

One aim of RAAR has been to assist in evaluating the technique of reburial in the marine environment as an alternative to traditional museum storage for marine archaeological finds. The Phase I three year burial period was sufficient to be able to draw conclusions for the fibre-based materials included in the study, but was not long enough to be able to draw conclusions with regard to recommendations for or against long-term reburial for leather, bone and antler (Peacock 2007, Nyström Godfrey et al. 2009, Peacock and Turner-Walker 2009).

Results of the Phase II seven year burial period support results of the Phase I burial period in that deterioration has progressed in the same manner as revealed at the end of Phase I. Based upon Phase II results, fibre artefacts and horn are not recommended for reburial; whereas, leather, bone and antler could be reburied for at least a period of seven years (Table 6). The twelve and twenty four year retrievals will be important determinants for making long-term recommendations for these latter materials.

*Figure 8. The non-wood organic materials sample unit containing one uncovered and one covered set of samples before burial in Marstrand harbour, September 2002 (photo Elizabeth Peacock, VM-NTNU).*

Finds of the more perishable organic materials, especially fibre-based ones such as textile fabrics, basketry and rope make up a small percent of total recovered artefacts from the sea both in number of items and in physical bulk. Being a rarer category of find they are usually given a higher priority, and it is less likely that such finds would be selected for reburial. The exception could be in instances where large volumes of similar rope/cables, nets and sails are recovered, in which case representative samples might be conserved with the remaining finds reburied. Regardless, fibre materials are demanding in that their conservation is labour-intensive and therefore costly. In a water-degraded condition their polymer substance is highly degraded and their physical structure disintegrated. Frequently, in an attempt to preserve physical integrity, such artefacts must be recovered together with their surrounding sediment matrix as blocklifts. Once documented, analysed and accessioned into an archive, these artefacts are not likely to be robust enough to survive the reburial process. Finds of basketry, nets and rope/cables also fall into this category.

Based upon the Phase I results for the modern fibre-based materials investigated, buried at a depth of 50 cm in harbour sediment, it was already concluded after three years that reburial cannot be recommended for recovered fibre artefacts. The exception is tarred cables recovered in massive amounts, which due to their physical bulk and the biocidal effect of the tar coating, will survive for a longer period.

Finds of leather can make up a sizeable portion of non-wood organic artefacts recovered from a marine site. It is possible that following full documentation leather artefacts may be selected for reburial in a marine environment. Based upon the Phase II results for the modern vegetable-tanned leather buried at a depth of 50 cm in porous and sandy sediment with a low organic content as in trench 1, short-term reburial can be recommended for recovered tanned leather artefacts.

The marine reburial of skeletal material poses several potential problems. Human skeletal remains require specialised handling and disposal protocols because of the obvious culturally sensitive nature of the material. It is highly unlikely that reburial at sea is suggested for human remains unless this involves returning bones to a recognised war grave. Horn and antler are such rare finds in marine archaeological sites that it is very unlikely that any finds made of these materials as well as worked bone would be selected for reburial. Only animal bones are likely to be selected for reburial/disposal at sea.

Based upon the Phase II results for the modern hard animal products investigated, buried at a depth of 50cm in porous and sandy sediment with a low organic content as in trench 1, short-term reburial can be recommended for recovered bone ecofacts and antler; although, as mentioned above, antler may not be selected due to its less-frequent nature as a material. It is advised that all material be packaged in materials recommended by the polymer sub-project, and buried in sediments with

low microbiological activity. The burial depth should be determined based on the results of the environmental monitoring.

Due to health issues within the non-wood organic sub-project no final report is available as an appendix.

## Packing and labelling materials

As reburial of archaeological material is anticipated to last for an extended period, the packing and labelling materials need to be able to survive for the same period of time. Consequently the durability of these products is of great importance.

This sub-project focuses on how a burial environment will affect the mechanical properties of some relevant packing products, mainly made from different polymers, and if different types of labels and written identifications can be read after being exposed to a marine sediment environment. Apart from in-situ exposure, Phase I also included accelerated ageing of some materials in the laboratory. Those results were published in Nyström Godfrey (2009).

Table 5 shows all materials investigated in the sub-project. Due to lack of funding, the tensile strength of some of these materials could not be tested in 2009. The materials excluded were chosen on the basis of bad preservation results in Phase I or their importance in the archaeological process.

The labelling materials were investigated using ocular inspection and colorimetric analyses and the mechanical strength of the packing materials was evaluated by tensile testing. Results were compared with references and previously retrieved samples.

When commercial products are studied a few problems arise. One is that the actual composition of a specific product can be difficult to obtain because of trade secrets. Therefore only the main ingredient(s), the base material, of each product can be given in a study like this. Hence conclusions from the analyses in this study are valid primarily for the tested products and to a lesser extent for the base materials.

We know from previous results (Nyström Godfrey 2009) that the wooden crate (B) and the polyethylene net (D) lost considerable strength after 3 years. After seven years in the marine sediments the mechanical strength of the HDPE crate (A), the polyethylene bag (C), the polyethylene/polypropylene geotextile (F), the polyethylene rope and the PETR/PUR prefabricated tag (N) were unchanged. The polyester rope (J) is still strong, but the maximum load has decreased from 800 to 625 N and it could be considered a trend (Figure 9) that may make a polyester rope less suitable for long-term reburials. This will have to be confirmed through future analyses.

The interpretation of the tensile tests on the polyamide products cord (L) and yarn (M) was inconclusive after Phase I. Polyamide is a material sensitive to humidity. Moisture does not affect the ageing, but it

| Sample ID | Product | Material | Abbreviation | Tested in Phase I | Tested in Phase II - 2009 |
|---|---|---|---|---|---|
| A | Crate | Polyethylene | HDPE | x | x |
| B | Crate | Pine | | x | |
| C | Bag | Polyethylene | LDPE | x | x |
| D | Net | Polyethylene | PE | x | |
| E | Sack, woven | Polypropylene | PP | x | |
| F | Geotextile | Polyethylene/ Polypropylene | PP/PE | x | x |
| G | Geotextile | Polyester | | x | |
| H | Tarpaulin | Synthetic rubber | EPDM | x | |
| J | Cord | Polyester | | x | x |
| K | Cord | Polyethylene | PE | x | x |
| L | Cord, spun | Polyamide | PA | x | x |
| M | Yarn | Polyamide | PA | x | x |
| N | Tag, prefabricated | Polyether/ Polyurethane | PETR/PUR | x | x |
| O | Tag, Dymo ® | Polyvinyl chloride | PVC | x | x |
| P | Tag, Dymo ® | Steel | | x | x |
| Q | Marker | Permanent ink on PE bag | | x | x |
| R | Marker for OH | Permanent ink on PE bag | | x | x |
| S | Pen, ball point | Archival proof ink on PE bag | | x | x |
| T | Pencil | Graphite on PE -bag | | x | x |

*Table 5. Packing and labelling materials tested.*

strongly affects the strength of the material (Almström pers. comm.). The inconclusive and odd results for the mechanical strength in Phase I was thought to be a result of differences in moisture content and recrystallisation, despite all samples being conditioned in the same manner.

The tests performed on the 2009 in situ samples showed no degradation of the mechanical properties (Figure 10), with smaller variations within the standard deviation. This suggests that polyamide rope is suitable for reburial. However, it would be wise to wait for future analyses before making statements on the long-term preservation of polyamide in anaerobic reburial environments.

After seven years of burial all labels were easily readable with the naked eye. Ocular inspection and chromaticity readings show, however, that text written with the black marker, Stabilo OHpen Universal (R) and the blue archival proof pen, Svenskt arkiv (S) had continued to deteriorate and change quite considerably. Neither the lead “graphite” pencil writing (T) nor the permanent marker Edding 404 (Q) changed at all.

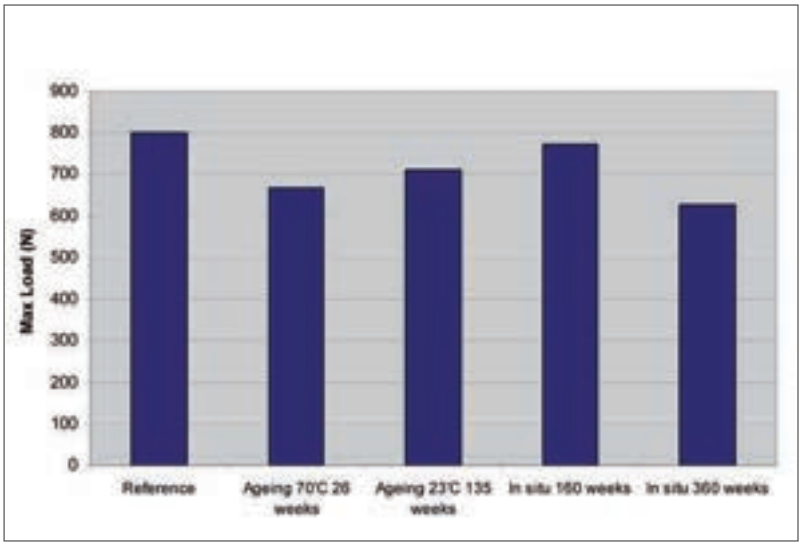


*Figure 9. Diagram showing the tensile strength of the polyester rope (J) after accelerated ageing in the laboratory and exposed in situ in the Marstrand sediments.*

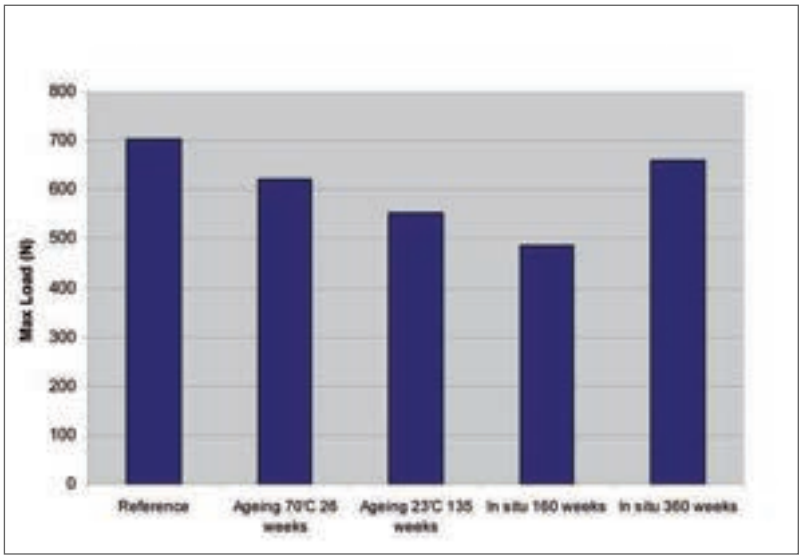


*Figure 10. Diagram showing the tensile strength of the polyamide rope (L) after accelerated ageing in the laboratory and exposed in situ in the Marstrand sediments.*

It is therefore recommended to use pencils or markers of good permanent quality and not for example, over-head markers, such as the one tested. As the archival ink pen (S) showed signs of degradation in this particular environment it is not suitable for anaerobic clay sediments. Another reason to avoid this pen is the fineness of the tip of the pen, which makes the lines very thin and difficult to read when the ink fades and changes in colour.

Although the prefabricated and Dymo labels all looked good after seven years of burial, the steel label is difficult to read. It is also known that stainless steel corrodes in anaerobic environments due to the action of sulphate reducing bacteria, making it a less attractive choice. A better choice for labelling artefacts reburied in sediments would be to use PVC Dymo labels or prefabricated embossed tags, so called "ear-tags". Table 7 summarises the results and evaluations of the stability of the tested materials.

For further information on the packing and labelling sub-project see Appendix 4.

# Discussion and conclusion

## Findings of the RAAR project after seven years of burial

Phase II has so far confirmed most of the results from the previous phase, both with regard to the environmental and material studies. It has underlined the importance of understanding the processes occurring within a given sediment prior to carrying out any reburial. If any form of reburial is to be successful, the primary aim should be to understand the agents of deterioration on a site and the effects on artefacts with a view to developing and implementing mitigation strategies. Sites that are buried have better preservation characteristics because of the limited oxygen levels, which minimise chemical, physical and especially biological deterioration.

The optimal depth of reburial is not simply a matter of depth of burial per se, but also depends on the type of sediment used, its properties and the processes occurring within it. These vary from sediment to sediment. Porosity and organic content in particular will have an effect on the rates of microbial activity. The lower the porosity and organic content the better the sediment is for preservation of archaeological materials.

The degradation processes have not yet stabilised for many of the tested materials and future analyses will be required in order to provide more conclusive evidence regarding reburial as a preservation strategy. Therefore, it is of paramount importance that this project continues so that as much information as possible can be obtained regarding the degradation processes of the test materials. This information, in conjunction with analyses of actual shipwreck artefacts, will allow evaluation of the long-term effectiveness of reburial as a preferred means of preservation for archaeological remains.

Many of the material degradation results were expected based on known material properties, and on the known survival trends for materials excavated from shipwreck sites. However, studies like these are important, since they acquire basic scientific foundations for each individual material and situation. The broad perspective is valuable and

although the RAAR Marstrand investigation aims to provide informed guidelines for the reburial of recovered marine artefacts in the seabed, the various sub-projects are yielding information of a much broader nature. At the outset, it might be questioned as to why more perishable organic materials were included in such a reburial study when it is not likely that artefacts of such materials would be selected for reburial. It should be noted that at the same time that the study provides information on the preservation of materials in and above the seabed, it also sheds light on deterioration processes and contributes knowledge to artefact conservation. For example, the non-wood organic sub-project is providing insight into the properties of dyestuffs, which can slow the deterioration rate of dyed wool fabric. This confirms anecdotal evidence for the better preservation of madder-dyed wool in actual artefacts. Furthermore, it is noted that many of these same experimental materials have been or will be included in other burial studies; thus providing a comparative degradation/preservation dataset with broader implications than just the RAAR study (Richards et al 2009, Turner-Walker and Peacock 2008, Peacock 2004).

Based on the results from the first and second phases (7 years of exposure) of the Marstrand reburial project, some conclusions can be drawn and recommendations made. These are outlined below and summarised in Tables 6 and 7.

### *Environment*

1. Both trenches in Marstrand appear to have generally good preservation conditions for the reburied artefacts and the experimental samples. At the depths where the artefacts and most of the material samples are buried (~ 50 cm) the sediments are anoxic and strongly reducing with the predominant ongoing process being sulphate reduction. In both trenches the upper 30cm consisted of porous (porosity of 0.8), coarse silts with a high organic content (20 – 30% weight/dry weight). In the metals trench, sediments were graded to medium silts below this depth and were still porous with a relatively high organic content. In the organic trench after 40 cm the sediment consisted of very fine, low porous (porosity of 0.4) sands with a low organic content (ca. 5 % weight/dry weight).

2. It is recommended that the following pore water parameters are measured and that the season of sampling is considered: Dissolved oxygen, redox potential, pH, dissolved and total iron, sulphate and sulphide content, temperature.

3. It is recommended that the following sediment parameters are measured and that the season of sampling is considered: Particle size, porosity, organic content.

*Metals*

4. The reburial environments surrounding the metal coupons have finally stabilised and as a result the long term corrosion processes and associated mechanisms are becoming better indicators of the final corrosion outcomes.

5. The concretions and corrosion product layers on the metal coupons are more extensively developed than after the first two years of exposure/reburial and therefore, the coupons are beginning to more accurately reflect the corrosion behaviour of marine archaeological metal artefacts.

6. The extent of corrosion of all metal coupons decreased significantly once the coupons were buried, even at shallow depths and this protective effect increased with increasing burial depth.

7. Despite a general decrease in the extent of corrosion with burial, all metal coupons showed some increase in corrosion rate over the past four years.

8. Copper alloys could be recommended for reburial in these types of sediments for a period of six years. Although it is probable that pure copper and brass alloy types may be buried for longer periods of time and at shallower depths, more information from the next phase of the experiment is required to support this inference. On the other hand, due to the significant increase in corrosion rate of the bronze coupons over the past four years, it is not possible to recommend longer term reburial times for these alloy types at this point.

9. Ferrous alloys could not be recommended for reburial even in the medium term, based on their extensive degradation after six years and the significant increases in their corrosion rates since 2005, which may indicate that corrosion will increase significantly over time. However, despite the concretion layers on the ferrous metal coupons being considerably better developed after six years they are not yet totally encapsulating, making extrapolation to the corrosion behavior of totally concreted archaeological ferrous artefacts difficult at this stage.

*Silicates*

10. Reburial cannot be recommended for any type of glass.

11. Although reburial cannot be recommended for low-fired earthenware, the resistance of earthenware in a marine environment varies, largely dependent on the firing conditions during manufacture. The poor results for the very low-fired 'modern'

earthenware samples, after seven years of reburial, cannot be extrapolated to issue a general recommendation against the reburial of earthenware.

12. High-fired ceramic wares, such as porcelain, stoneware and also clay pipes are highly stable and should survive reburial but consideration should still be given to the problems of over-glaze decoration and gilding on porcelain and salt infiltration in clay pipes and less high-fired stoneware.

### *Wood*

13. Reburial is a simple, useful and effective method for decreasing wood degradation.

14. As wooden structures, above the sediment, degrade very fast in saline seawater, a burial depth of at least 50 cm is recommended for wooden artefacts. Further studies on degradation at even greater depths, in combination with knowledge of individual site parameters, will be most important to guide decisions on the thickness of the applied protective layer.

### *Non-wood organic material*

15. Burial is not recommended for fibre artefacts, with the possible exception of large tarred cables/ropes, if similar representative samples are conserved.

16. Soft and hard animal products like leather, bone and antler can be considered for short-term reburial (at least 7 years), in porous and sandy sediments with low levels of organic matter. The actual depth will have to be chosen according to the individual site. In Marstrand (trench 1) a depth greater than 40 cm was sufficient to enhance preservation.

### *Packing and labelling material*

17. With respect to packing materials, zip-lock bags generally seemed to offer the best protection against degradation and/or infiltration of salts. Geotextile readily allows for free flow of soluble salts, but protects against the direct influence of the burial sediment. It possibly offers some protection from microorganisms within the sediment and isolates the material inside from some microstructural alteration, but it does not appear to protect against chemical alteration. Finally, polyethylene netting offers the least protection and should be avoided.

18. Potentially unfavourable micro-climates can develop in zip-lock bags. Micro-organisms were detected on the model potash glass deposited in zip-lock bags and corresponding pits were seen on the glass surface, a possible sign of etching caused by the microbes.

19. Appropriate containers for groups of finds include high-density polyethylene crates, polyethylene bags and geotextile envelopes, with the former the most highly recommended.

20. Polyethylene, polyamide and polyester cords are suitable to tie and secure artefacts and labels for short term reburials (at least 7 years). For longer term reburials polyethylene ropes are recommended at this stage.

21. Preferred options for identifying finds include the use of prefabricated tags (live stock 'ear tags'), embossed PVC labels (eg. Dymo® labels), pencils or black permanent markers. Ball-point pens, even those labelled, as 'archival' should not be used.

### *General considerations*

22. Recovered marine archaeological organic materials routinely undergo desalination at an early stage of post-excavation processing. It is important that the use of this method be re-evaluated in circumstances in which finds may be selected for later reburial in a saline marine environment. Problems may arise with rewetting dried-out organic materials for reburial.

23. A general viewpoint is that reburial should be avoided if artefacts have decorative surfaces or show traces of production or wear.

## Consequences for heritage management

The consequences for heritage management discussed previously after the completion of Phase I (Nyström Godfrey et al. 2009) are still valid. The findings from the last four years of exposure in the sediments have not changed the overall picture but have improved the overall understanding of reburial by providing a more nuanced picture of the different materials and the reburial environment, information that was not conclusive after the completion of the first phase.

Many recommendations and inferences were made based on the results from the seven year RAAR project, but one important aspect that should be mentioned is that our perception on reburial has changed. It is now understood that reburial is significantly more complicated than we first, and maybe naively imagined. The degradation processes are complex and there are more nuances within the categories of materials than was first acknowledged.

| Material | No or minimal degradation > Long term reburial possible* | Some degradation > Medium term reburial possible - at least 7 years | Unacceptable degradation > Reburial not recommended |
|---|---|---|---|
| Copper | x | | |
| Brass | x | | |
| Bronze | | x | |
| Ferrous alloys | | | x |
| Porcelain | x | x | |
| Stone ware | x | x | |
| Clay pipes | x | x | |
| Earthen ware, low-fired | | | x |
| Glass | | | x |
| Wood | x | x | |
| Fibre artefacts | | | x |
| Tanned leather | | x | |
| Animal bones | | x | |
| Antler | | x | |
| Horn | | | x |

*Table 6. Recommendations on archaeological materials suited for reburial in anaerobic sediments with low microbiological activity (low porosity, sandy sediments with low organic content). X marks the type of material suitable or not for reburial.*

** The suitability of these material types for long-term reburial has been suggested but these predictions are to be confirmed through future retrievals.*

Even more complex is the heritage management aspect of reburial: the whats, the whys, the wheres, the hows, the time frames and not least of all, the legal aspects. Within this discourse we have the reburial versus disposal debate; is any reburial a better option than disposal, since at least the artefacts are then not immediately lost, or should we have a more stricter view on reburial depots as proper museum storages with strategies for handling, administration and annual assessment; reburial with plans for future use of artefacts and with time frames. The latter will inevitably also include a much stricter stand on which artefacts that should be part of such a reburial and consequently there would be artefacts that would, after documentation, be disposed of.

## *Collection strategies for reburial?*

There remains three ways of dealing with physical finds from an excavation: conservation, reburial and disposal. In the same way that traditional conservation and storage preserves an object for study or exhibition purposes, artefact reburial is also designed for preservation so that

| Sample ID & Product | Material | No or minimal degradation > Long term reburial possible* | Some degradation > Medium term reburial possible - at least 7 years | Unacceptable degradation > Reburial not recommended |
|---|---|---|---|---|
| A. Crate | Polyethylene, HDPE | x | x | |
| B. Crate | Pine | | | x |
| C. Bag | Polyethylene, LDPE | x | x | |
| D. Net | Polyethylene | | | x |
| E. Sack, woven | Polypropylene | | x** | |
| F. Geotextile | Polyethylene/ Polypropylene | x | x | |
| G. Geotextile | Polyester | | x** | |
| H. Tarpaulin | Synthetic rubber | x | x** | |
| J. Cord | Polyester | | x | |
| K. Cord | Polyethylene | x | x | |
| L. Cord, spun | Polyamide | | x | |
| M. Yarn | Polyamide | | x | |
| N. Tag, prefabricated | Polyether/ Polyurethane | x | x | |
| O. Tag, dymo | Polyvinyl chloride | x | x | |
| P. Tag, dymo | Stainless steel | | x | x |
| Q. Marker | Permanent ink | x | x | |
| R. Marker for OH | Permanent ink | | x | x |
| S. Pen, ball point | Archival proof ink | | x | x |
| T. Pencil | Graphite | x | x | |

*Table 7. Recommendations on packing and labelling materials suitable for reburial in anaerobic sediments with low microbiological activity.*

** The suitability of these material types for long-term reburial has been suggested but these predictions are to be confirmed through future retrievals.*

*** These materials were only tested after 3 years of exposure, hence short term reburial of less than 3 years can only be safely recommended, however it is highly likely that they are suitable for medium term reburial and the EPDM tarpaulin also for long term reburial.*

artefacts can be accessed and researched in the future. If there are no thoughts or ideas about future needs or use of an artefact or a collection, there seems little point preserving it at all. This might lead to some problems, since it would perhaps be easy to use reburial as an "artefact dump" when the decision to discard is difficult or controversial. However, it is important to make a clear distinction between reburial and disposal. It is vital to stress that reburied artefacts are not meant to be forgotten in the sediments, nor should reburial be chosen instead of conscious disposal if the artefacts have been evaluated as of no or little use based on, for example, scientific, technological, educational or aesthetic grounds.

Today many museums are updating their collection strategies regarding what to collect and keep but also what to deaccession from their collections. With a constant increase in the number of finds comes a need for bigger storage areas. Already many museum storage areas are almost full. With often limited economic funds, it is valid to question what should be preserved and at what cost. A similar attitude and strategy for reburial depots seems appropriate.

Collection and preservation strategies and evaluations of archaeological finds obviously varies from one country to another and changes over time. A common dilemma though, seems to be a delayed thought process. The questions of what and why are often raised too late during an archaeological investigation. Decision making is often not easy but it will become less difficult if the process begins early and is coherent and consistent with regional and/or national collection policies.

### *Collection dilemmas*

Preservation strategies should be based on scientific reasoning – first of all site specific questions, but sometimes also taking into account regional and national aspects. While most practitioners would agree with this, in reality it is not always that easy and an examination of existing archaeological storage areas would confirm the presence of an endless number of small flint artefacts (cheap to preserve and store) but much less in the way of large conservation costly artefacts. A preservation strategy based on what can be afforded, while realistic, is not really sufficient as it gives an unrepresentative picture of a certain archaeological site or region.

This should be borne in mind also for reburial strategies. Results from the RAAR project have pointed out material categories that should not be reburied. These materials types are conserved and stored or they are disposed of. However, there are also some types of materials, like porcelain and stoneware, which are perfectly fine to rebury from a degradation point of view, but would not necessarily be chosen for reburial since conservation and storage costs are normally relatively low. This cost might be below the cost of handling and administering a reburial depot. It is at this point where the choice becomes more difficult. If we do not want to create another "flint collection", with an unrepresentative amount of "cheap" artefacts we need to discuss this more thoroughly before deciding on strategies for each reburial project.

### *Reburial time frames*

If we accept that reburied artefacts should be available in the future we need to discuss time frames for reburial depots and also strategies for closure. In previous reports the RAAR project has recommended that stipulated time frames should be part of a reburial strategy: i.e. depending on the materials to be reburied, a reburial program should be designed to last a certain number of years or maybe even decades.

The project has previously used the terms short- and long-term reburial as a way of categorising the reburial potential of different materials, but it was not until recently we really contemplated what we actually meant by these terms. How long is long-term and does the length of the short-term increase with future retrievals, if the material survives?

Long term certainly does not mean eternity, since reburial depots are not meant to last forever. Retrievability has been discussed as a way of defining long-term reburial, relating it to the working life of a person, e.g. approximately 25-30 years. This definition suggests that information may get lost and foci and agendas may change when a person retires. Against this one could argue that a reburial depot is the responsibility of a museum or similar institution and is thereby secure in the longer term. Unfortunately this is often not the case. Possibly 25 years is too short – should it be 50 or 100 years? Eventually it was decided that, for the RAAR project, long-term reburial means 25 to 50 years, since 50 years is the planned life of the project. We decided to define short-term reburial as lasting between 0 to 5 years. This leaves a rather big time period between 5 and 25 years. Therefore a third term was introduced; medium-term reburial. Below is a first draft of a suggested model for reburial collection strategies.

> Short term: 0-5 years. Storage solution while preparing for documentation, conservation, traditional storage and/or analyses.
>
> Medium term: 5-25 years. Artefacts or collections in a 'capsule' awaiting analysis to answer future research questions, improved analytical techniques and/or the development of more suitable conservation treatments.
>
> Long term: 25-50 years. Exceptional conditions. Finds with a very high archaeological potential, but where documentation and conservation is not possible due to a lack of resources and/or competence.

Collection strategies and programs must be developed in addition to these time frames. That is, documents that describe the intentions with the reburied finds, time schedules and funding proposals.

We also have to consider failure in this system. Even if we design a reburial program with strategies for retrievals and funding, there is always the potential risk that something may go wrong. What if the structural problems still exist after 50 years? How do we prepare for that? Do we physically dispose of the artefacts in such circumstances or can we "only" rid ourselves of the problem legally and administratively? To make reburial a useful and complete tool for heritage management we need to be aware of this issue, discuss it and propose solution strategies.

With the above discussion in mind, a heritage institution could provide short-, medium- and long-term curation for some part of its archaeological archive by using reburial depots provided they are used within certain guidelines formulated on the results of rigorous scientific research.

# Future

The findings after seven years have revealed and confirmed many interesting results and have so far generally fulfilled the objectives of the project. However, seven years of exposure in the sediments of Marstrand is an insufficient time for some materials for degradation processes to take place and for other materials to stabilise. Some conclusions are therefore pending or awaiting confirmation from the results of the next experimental phase. Further analyses and more comprehensive studies over a longer period of time is of great importance to allow more complete conclusions to be drawn on reburial as a tool for heritage management.

The metal coupons are now beginning to more accurately reflect the corrosion behaviour of marine archaeological metal artefacts; therefore the next retrievals will give us valuable knowledge about corrosion processes and corrosion rates for archaeological metal objects of different alloys. Questions like whether or not the iron coupons have continued to corrode at a high rate or not, or if the corrosion rate of the brass samples has stabilised, should be possible to answer. The situation is similar for leather and antler, where a longer burial period would shed light on whether or not the slow but existing degradation is continuing at the same pace or has decreased. With a fifth retrieval in 2014 after a12 year burial period it might be possible to predict the life span of a particular material in this given environment.

A fifth retrieval would conclude Phase II and hopefully also give us the opportunity to look at all the materials without exclusion, something that will yield highly valuable information.

The participating institutions have all announced their willingness to continue with Phase II of the project, which also includes retrieval in 2014 and we hope that the project managers will find the funds to enable the second phase to continue.

# References

Almström S., (pers. comm. 2009), SP Technical Research Institute of Sweden.

Bergstrand T. and Nyström Godfrey I. (editors), (2007), Reburial and Analyses of Archaeological Remains. Studies on the Effect of Reburial on Archaeological Materials Performed in Marstrand, Sweden 2002-2005, Kulturhistoriska dokumentationer nr 20, Uddevalla, Bohusläns Museum and Studio Västsvensk Konservering.

North, N.A., (1989), 'Proximity corrosion in seawater', Corrosion Australasia 14, 8-11.

Nyström Godfrey I., Bergstrand T., Bohm C., Christensson E., Gjelstrup Björdal C., Gregory D., MacLeod I., Nilsson T., Peacock E.E., Richards V., (2009), Reburial and Analyses of Archaeological Remains. The RAAR Project. Project Status and Cultural Heritage Management Implications Based on the First Preliminary Results, in K. Strætkvern and D.J. Huisman (editors), Proceedings of the 10th ICOM Group on Wet Organic Archaeological Materials Conference, Amsterdam, 10-15 September 2007, Rijksdienst voor Archeologie, Cultuurlandschap en Monumenten (RACM), Amersfoort, 2009, pp. 169-196.

Nyström Godfrey I., (2009), Reburial and Analyses of Archaeological Remains (RAAR). Investigation of the Effects of Burial on Materials Used at Archaeological Excavations to Separate and Mark Objects, in K. Strætkvern and D.J. Huisman (editors), Proceedings of the 10th ICOM Group on Wet Organic Archaeological Materials Conference, Amsterdam, 10-15 September 2007, Rijksdienst voor Archeologie, Cultuurlandschap en Monumenten (RACM), Amersfoort, 2009, pp. 215-251.

Peacock E. E., (2007), Reburial and Analyses of Archaeolgical Remains (RAAR): Investigation of the Effects of Burial on Organic Materials Other Than Wood (Textile, Leather, Antler, Horn and Bone), T. Bergstrand and I. Nyström Godfrey (editors), Reburial and Analyses of Archaeological Remains – Studies on the Effect of Reburial on Archaeological Materials Performed in Marstrand, Sweden 2003-2005. The RAAR Project, Uddevalla, Bohusläns Museum and Studio VästSvensk Konservering, pp. 35-38.

Peacock, E. E. and Turner-Walker, G., (2009), Reburial and Analysis of Archaeological Remains (RAAR):Iinvestigation of the Effects of Burial

on Non-Wood Organic Materials. Preliminary Results, in K. Strætkvern and D.J. Huisman (editors), Proceedings of the 10th ICOM Group on Wet Organic Archaeological Materials Conference, Amsterdam, 10-15 September 2007, Rijksdienst voor Archeologie, Cultuurlandschap en Monumenten (RACM), Amersfoort, 2009, pp. 197-213.

The RAAR web site: http://www9.vgregion.se/vastarvet/svk/reburial/index.htm

UNESCO, (2001), Convention on the Protection of the Underwater Cultural Heritage 2001. The General Conference of the United Nations Educational, Scientific and Cultural Organisation, 31st Session, Paris, 15 October to 3 November 2001http://portal.unesco.org/en/ev.php-URL_ID=13520&URL_DO=DO_TOPIC&URL_SECTION=201.html

NATIONALMUSEET

*Department of Conservation*

# RAAR Phase II: Environmental monitoring of the re-burial trenches 2007 - 2009

David Gregory

REPORT no

11051216-001

Report from the

Department of Conservation
National Museum of Denmark
IC Modewegsvej, Brede
DK-2800 Lyngby
Denmark
Telephone +45 33 47 35 02
Telefax +45 33 47 33 27

Case: 11031041
Date: 10th May 2010

**Title:**
RAAR Phase II: Environmental monitoring of the re-burial trenches 2007 - 2009
.

**Author:**
David Gregory

**Executive Summary**
The environmental monitoring sub-project for Phase II of the RAAR project focused on three specific questions:

- What are the conditions within sediments deeper than 50cm below the sediment surface and is the 50cm reburial depth sufficient for protection?
- As the sediments of the metals re-burial trench were not studied in phase I, what are the conditions within these sediments?
- Is the environment in the harbour of Marstrand still conducive to the preservation of re-buried archaeological material?

Following on from completion of Phase I in 2006, sediments were examined in April 2007 and September 2009. A new system of coring was developed whereby it was possible to sample sediments to ca. 70cm below the sediment surface. Two systems were successfully used: the first, for analysing pore water parameters and the second for analysing sediment properties themselves.

All results reflect that the environments within the organic and metal re-burial trenches are conducive to the preservation of the materials within them. Results of the pore water analyses indicated that the conditions within the organic and metals re-burial trenches were sub-oxic to anoxic and dominated by anaerobic processes. Dissolved oxygen levels were low: sub-oxic (0.1 – 0.3 mg $dm^{-3}$) to anoxic (<0.01 mg $dm^{-3}$). Redox potentials were strongly reducing with potentials

between -150 and -200 (vs SHE). pH of sediments were near neutral (pH 7 – 7.5). The processes ongoing in the sediments were dominated by sulphate reduction, where generally a loss of sulphate was seen with increasing depth with the concomitant evolution of sulphide.

However, the analyses of the sediments themselves showed there was a distinct difference between those used in the organic and metals re-burial trenches. In both trenches the upper 30cm consisted of porous (porosity of 0.8), coarse silts with high organic content (20 – 30% weight/dry weight). In the metals trench, sediments graded to medium silts below this and were still porous with relatively high organic content. In the organic trench after 40 cm the sediment consisted of very fine low porous (porosity of 0.4) sands with low organic content (ca. 5% weight/dry weight). The profiles of sulphate and sulphide showed that the rates of sulphate reduction were highest in the finer grained sediments with high organic contents. Seasonal changes in the rate of reduction were seen in the metals trench, surprisingly with rates higher in April than in September. Modelling mineralisation of organic material due to sulphate reduction showed that ca. 80g and 44g of organic material per $m^2$ per year could be oxidised in the metals trench in April and September respectively. Sulphate had been completely reduced at a depth of 50cm in both April 2007 and September 2009. In the organic trench sulphate reduction was also the dominant process. The rate of mineralisation of organic material was lower at ca. 20g per $m^2$ per year and there did not appear to be a significant seasonal variation. All sulphate had not been utilised in the organic trench but sulphate reduction ceased at ca. 40 cm below the sediment surface where the concentration remained at about 7mM from 35 cm down to 65cm.

The implications of these results to the question of depth of burial show that it is not just depth of burial per se. that is important. An explicit understanding of the physical, chemical and biological properties of the sediment used, or to be used in reburial, is required in order to understand what processes take place, at what rates they occur and only knowing this information can an optimal depth of burial be selected. Differences in the rates of sulphate reduction are probably due to the different particle sizes, porosity and importantly organic contents of the sediments. Based on the results of Phase II it is believed that conditions in the re-burial trenches are still conducive to preservation. However, the Sulphate Reducing Bacteria responsible for Sulphate reduction can affect the sulphur content of wood, cause microbial corrosion of metals and potentially affect the other materials re-buried in Marstrand. To this end the results should be coordinated with the results of the other sub-projects to confirm or refute this. Such an action has already been agreed with the coordinators of the metals sub-project.

# Table of Contents

David Gregory
Author
Senior Scientist

Henning Matthiesen
Quality Assurer
Senior Scientist

# 1. Introduction

## 1.1 Phase I of RAAR: 2002 - 2005

Phase I of the environmental monitoring sub project of *Reburial and Analyses of Archaeological Remains (RAAR)* project ran between 2002 and 2005, with an extra set of sediment cores taken in April of 2006. During this time the Environmental Monitoring programme focused upon the following:

- Developing methods to assess and monitor the reburial environment
- Assess the processes (aerobic / anaerobic) ongoing in the reburial environment
- Based on the results of the monitoring give an estimate of ongoing deterioration in the re-burial trench.

The monitoring of the environment was carried out in two ways: *In situ* using a data logger, with sensors placed within dip wells to record long term variations in open seawater and within the sediment. *Ex situ,* and in the laboratory, by taking spot measurements in sediment cores taken from the organic re-burial mound and an "undisturbed" area close to this. It should be noted that during Phase I, the sediments from the metals reburial trench were not assessed.

A full description of the methods and results is given in Gregory (2007). Summarily, in the organic re-burial trench:

- The dissolved oxygen content was seen to be suboxic (0.1 – 0.3 mg $dm^{-3}$) after the first few centimetres within the cores and thereafter bordering on anoxic (<0.01 mg $dm^{-3}$).
- Sediments were strongly reducing with potentials between –160 to –250mV (vs SHE).
- The predominant processes ongoing in the sediments were sulphate reduction – especially at the depths where archaeological material was reburied.
- Seasonal variations were seen
- The reburial sediments used in the organic trench were primarily of a sandy nature (by observation), with an organic matter content of <5% at the levels where archaeological materials was re-buried.
- From the set of core data collected in April of 2006, it was apparent that there was still sulphate available for deterioration of organic matter. However, an initial

model shows that this equates to a turnover of organic matter of 20g of organic matter per $m^2$ of sediment per year (or 2 kg per 100 years). This equates to the organic content of sediment 6 cm below where sulphate has been presently measured.

## 1.2 Phase II of RAAR: 2006 – 2009

Following the presentation of the monitoring sub-project results of Phase I (RAAR seminar, Studio Västsvensk Konservering, Göteborg May 2006), the following recommendations were made for Phase II of the project.

- Assess the sediments in the metals re-burial trench as well as those from the organic re-burial trench and the undisturbed area. Analysis of the metal trench sediments, as part of the metals sub-project, showed significantly different results from those of the organic re-burial trench.
- Develop a sediment core sampling technique, whereby sediments deeper than 50cm could be sampled. This was in order to better understand the sulphate – sulphide system, which dominated the anoxic processes in the re-burial sediments. Concerns had also been expressed by the metals and wood sub projects that the depth of burial of 50cm was not sufficient to afford optimal protection of these materials.

Further to these recommendations the aim of Phase II was to check that the environment was still conducive to the preservation of the re-buried artefacts and also to shed more light on the potential mechanisms of deterioration.

As funding for Phase II was not obtained until 2009, development of sediment coring devices and subsequent sampling of sediment cores in April 2007 was funded by the National Museum of Denmark. Analyses of these cores, as for Phase I of the project, included: dissolved oxygen, sulphate, sulphide, pH and redox potential of sediment pore water and loss on ignition (organic content) and porosity of the sediment. Furthermore the total iron content of the sediment was determined as iron can also contribute to the mineralisation of organic matter in marine sediments (Berner, 1984). Following the securing of funding, a further set of cores were taken in September 2009 and, in addition to the aforementioned parameters, carbon dioxide content of the pore water and particle size of the sediments was determined. One of the end products of microbial deterioration is carbon dioxide and profiles in the sediments may confirm or refute the other measurements in the pore water. Particle

size analysis would enable quantification and comparison of the sediments from the three separate areas in question, namely the undisturbed area and the sediments from the organic and metals trench.

Data logging was discontinued at this stage.

## 2. Sediment core sampling

During Phase I, sediment core samples were taken using an Uwitec corer (http://www.uwitec.at/html/frame.html) fitted with transparent, 6cm Ø x 60cm long PVC sample tubes. Although effective and simple to use, it was difficult to retrieve sediment core samples over 40 cm in length.

In order to take deeper sediment cores, and facilitate subsequent analysis, two types of corer system were used. For pore water analyses (pH, redox potential, dissolved oxygen, sulphate, sulphide and carbon dioxide), 7cm Ø x 125cm clear PVC tubes were used. These were pressed into the sediment as far as possible and then, if and where necessary, hammered as far into the sediment as possible using a protective metal cap placed over the end of the PVC tube. This was designed to prevent breakage of the tube and had holes drilled into it to allow the free passage of water, which resulted from pressing the tubes into the sediment. Following this, the top of the PVC tube was capped with a rubber bung and the tube and sediment retrieved by placing a metal ring, attached to a thin rope, over the tube and pulling the rope in order to get the tube out of the sediment. A second diver followed the removal of the tube and when the open end came out, quickly capped it with a further rubber bung. The area where the core was taken from was marked with a metal rod, which had red and white marking tape tied to it, in order to aid relocation for the second core sample to be taken. The PVC tubing / sediment core, held in a vertical position, was taken immediately to the surface where the quality of the core was assessed and, if satisfactory, the bungs were sealed with Gaffer Tape and the core labelled.

A second core, adjacent to the first (15-30 cm away), was taken for sediment analysis (porosity, loss on ignition, particle size analysis and total iron). In this case, the corer consisted of an outer PVC tube – as above – into which 20 clear acrylic tubes,

6.9cm Ø x 5cm long, were stacked. The point of having the separate acrylic tubes was to make sampling of sediments at discrete depths easier and give sample sizes of a known volume, which was required for porosity determination. The bottom and top acrylic tubes were fixed in place with four grub screws, which had O-rings fitted on to them to prevent loss of water. The 1mm gap between the outer PVC tube and the bottom most acrylic tube was sealed with silicone mastic to prevent loss of water from the sediment. The method of sediment collection was as previously described. Following retrieval, the sediment samples were kept submerged in the harbour (max. 24 hours) prior to transport back to the laboratories of the National Museum in an insulated transportation box, which ensured the cores were held vertically and cool. Once at the National Museum, the cores were stored in a holding tank flushed with 4°C water and analysis was commenced within 24 - 48 hours.

# 3. Laboratory Methods

## 3.1 Visual Description of Sediment

The cores were initially assessed by looking through the walls of the PVC tubes. Following the pore water analyses, the sediment from these cores was pressed out into lengths of plastic guttering, sectioned longitudinally and visually assessed.

## 3.2 Analysis of pore water

The methods and sensors for analysing the pore water parameters and pore water itself were the same as for Phase I of the project and the reader is referred to Gregory (2007) for details on sensors types, their calibration and use. In addition, a carbon dioxide micro sensor and an optical oxygen sensor were trialled, as will be discussed. Measurements were taken in the following order: dissolved oxygen (with Unisense microelectrode), sulphide, carbon dioxide, redox potential and pH. Measurements were taken first from the top of the core and then working down through the core. In between measurements the sensors were rinsed with deionised water, superfluous matter removed with a fine haired brush under a magnifying glass and finally rinsed with a wetted cotton bud. To check for carry over and reproducibility, repeat measurements were taken in several holes working from bottom to top. Following, this the oxygen was measured using the optical sensor (see section 3.3.1) and finally, the

holes were expanded to 12 mm and sediment taken out, using an adapted 10cm$^3$ syringe, for porewater extraction in order to determine the sulphate content.

## 3.3 Pore water analysis

### 3.3.1 Dissolved Oxygen with Presens optical sensor

In September 2009 a new method, whereby the oxygen concentration was measured optically, i.e. using light rather than traditional chemical or electrochemical methods was trialled alongside the Unisense microsensor. The method has only relatively recently become commercially available (http://www.presens.de/) and has been trialled at the National Museum (Matthiesen, 2007). The principle is based on luminescence, in which molecules are excited with light at one wavelength and emit the energy at another. Various oxygen-sensitive molecules have been developed, where the presence of oxygen quenches the emission of light and the oxygen concentration can be determined from the luminescence decay time or the intensity of the emitted light. One of the great advantages of optical sensors (optodes) is that unlike large Clarke type sensors they do not themselves consume any oxygen in the measurement.

The oxygen-sensitive compound in this system is a ruthenium complex that is excited using light at 505 nm. The complex is fixed to a polyester base and is delivered as foil or as sensor spots of 5–10 mm diameter. The sensor spots work equally well in air and in water and were thus suitable to trial here. Sensor spots of 5 mm diameter were fixed to the bottom of small (5mm Ø x 30mm L), flat bottomed, glass vials with a bead of silicone mastic and allowed to dry for 24 hours. The glass vials were pressed into the previously drilled holes in the PVC tubes and allowed to equilibrate for 24 hours prior to measuring with the fibre optic. One end of the optical fibre is placed inside the vial and measures through the glass to the sensor spot, while the other end was connected to a Presens Fibox3 meter. The measurements are temperature sensitive and the Fibox3 has a temperature sensor connected to allow for compensation for variation. The system was calibrated as for the Unisense sensors by dipping the vial, with the fibre optic inside, into 100% and 0% saturated aliquots of seawater taken from Marstrand. Results were converted to concentrations in mg/ Litre knowing the temperature and salinity (determined by conductivity) of the surrounding seawater at the time of sampling.

### 3.3.2 Carbon Dioxide

Microelectrodes INC (*http://www.microelectrodes.com/*) Dip Type MI-720 $CO_2$ sensor was used and was connected to a high impedance pH meter (Model: IQ 150) set to read mV. The sensor operates by measuring the pH in a thin layer of sodium hydrogen Carbonate ($NaHCO_3$) trapped between the tip of a pH sensor and a $CO_2$ permeable hydrophobic membrane. The hydrogen ion concentration in the $NaHCO_3$ inner solution is linearly related to the inner solutions carbon dioxide concentration. At equilibrium this equals the partial pressure of the carbon dioxide in the solution outside the $CO_2$ permeable hydrophobic membrane and is linearly related to the EMF or pH (Cai and Reimers, 2000). The electrode was calibrated in a solution with a known concentration of $CO_2$, produced from a standard solution of $NaHCO_3$, on titration with standard HCl, where the exact $CO_2$ concentration is calculated using stability constants from Stumm and Morgan (1981).

### 3.3.3 Sulphate

The pre-drilled holes in the cores were expanded to a diameter of 12mm with a drill. Samples of sediment were taken out using an adapted $10cm^3$ syringe. This was transferred to a sintered glass filter and filtered under vacuum. The filtrate from the sediment was collected in a centrifuge tube and re-filtered using a disposable membrane (0.45um) filter. Separate aliquots of the pore water were analysed spectrophotometrically using a Lange (http://www.hach-lange.com/) water quality testing kit for sulphate content following the manufacturer's instructions.

## 3.2 Sediment analysis

The individual inner acrylic tubes were "pressed" out of the outer PVC tubes using the same machined nylon cylinder as used for the pore water sediment cores. The sediment core was held vertically with the machined nylon tube placed in the bottom of the core. Using a long metal rod the PVC tube was forced downward so that the inner acrylic tubes were "pressed" upwards. As each individual acrylic tube came out of the top of the outer PVC tube, the sediment was cleanly cut and the tube containing sediment was removed. The porosity, Loss On Ignition (Organic content), total iron content and particle size analysis were determined on each sediment section as follows.

### 3.2.1 Porosity of sediments

By general definition, sediment is a collection of particles – the sediment grains. The voids between the sediment grains – the pores- form the pore space. In water saturated sediments it is filled with water. The porosity ($\phi$) characterizes the relative amount of pore space within a sample volume and is defined by the ratio:

$$\phi = \frac{\text{Volume of pore space}}{\text{Total sample volume}} = \frac{V_f}{V} \qquad \text{Equation 1}$$

Equation 1 describes the fractional porosity, which ranges from 0 in the case of non-porous sediment to 1 as would be in the case of a pure water sample. Taking the wet weight of a known volume of sediment and subsequently drying this at 100ºC to constant weight and using these data in Equation 1 determined porosity. The sediment within each acrylic tube (volume : 141.3 $cm^3$) was transferred to an empty pre-weighed aluminium container. The container and sample was re-weighed and then dried at 100ºC to constant weight (24-36 hours). The container and dry sediment was cooled to room temperature and re-weighed and the water content of the sample calculated.

### 3.2.2 Loss on Ignition: Organic content of sediments

Following determination of porosity the dried samples were ground using a mill to break the sediment up and passed through a 2mm sieve to remove any large pieces of organic matter / stones. Approximately 1 gram of this material was ashed in a muffle oven at 600 ºC to constant weight and the Loss on Ignition, which approximates to the organic content of the sediment, determined.

### 3.2.3 Particle Size Analysis

Particle size analysis of sieved oven dried sediment was determined at the laboratories of the Department of Geography and Geology, University of Copenhagen, by Malvern Laser Diffraction (http://www.malvern.com/LabEng/products/Mastersizer/MS2000/). Samples were pretreated by dispersing in water with Sodium Pyrophosphate ($Na_4P_2O_7$), added as a dispersing agent, in an ultrasonic bath. The intensity of scattered light was

measured on the detector placed in the focal plane and the resulting raw data converted to spherical grain sizes using the Mie theory (Hodkinson and Greenleaves, 1963; Agrawal et al., 1991).

### 3.2.4 Iron Content

"Reactive Iron" is often defined as the iron oxides present in sediment that can be utilised by iron reducing bacteria to oxidise organic material. This is of interest in this instance as it thus possible to calculate how much organic material can be oxidised as a result of iron reduction (Canfield, 1989).

The iron content of the sediment was determined by Atomic Absorption Spectrophotometry (AAS), on sieved oven dry samples at the laboratories of the Department of Geography and Geology, University of Copenhagen. Their method 8a (Sodium citrate – sodium hydrogen carbonate – sodium dithionite (CBD) was used. Summarily, the iron was extracted using a sodium bicarbonate buffer and after heating reduced using sodium dithionite. The iron content of the resulting extracts was determined by Atomic Absorption Spectropohotometry (AAS).

# 4. Results

## 4.1 Description of Sediment cores

### 4.1.1 April 2007

#### 4.1.1.1 Undisturbed / Control Core

0 – 15cm: Dark grey, loose, mixed sandy / muddy sediment.

15 – 40cm: Dark grey, fine grained sediment with visible organic material.

40 – 65cm: Light grey, very fine grained and very "firm" sediment with little visible organic material.

#### 4.1.1.2 Metal Re-burial Trench Core

0 – 15cm: Dark grey very loose and flocculated mixed muddy sediment.

15 – 60cm: Dark grey, fine grained sediment with visible organic material present

60 – 75cm: Dark grey, sandy sediment with no visible organic material present.

#### 4.1.1.3 Organic Re-burial Trench Core

0 – 10cm: Dark grey, loose, mixed sandy / muddy sediment.

10 – 35cm: Light grey, fine grained and "firm" sediment with little visible organic material.

35 – 70cm: Very light grey and sandy sediment with no visible organic material present.

### 4.1.2 September 2009

#### 4.1.2.1 Undisturbed / Control Core

0 – 5cm: Dark grey, loose, mixed sandy / muddy sediment.

5 – 20cm: Dark grey, fairly fine grained and "firm" sediment with little visible organic material.

20 – 40cm: Light grey, fairly fine grained sediment with little visible organic material.

40 – 75cm: Light grey, very fine grained and very "firm" sediment with little visible organic material.

#### 4.1.2.2 Metal Re-burial Trench Core

0 – 15cm: Dark grey very loose and flocculated mixed muddy sediment.

15 – 40cm: Dark grey, fine grained sediment with visible organic material present

40 – 65cm: Dark grey, fine grained sediment as above but with higher organic content.

#### 4.1.2.3 Organic Re-burial Trench Core

0 – 10cm: Dark grey, loose, mixed sandy / muddy sediment.

10 – 30cm: Light grey fine grained and "firm" sediment with little visible organic material.

30 – 70cm: Very light grey and sandy sediment with no visible organic material present.

### 4.2 Pore water Analyses: General conditions in the re-burial trenches.

The analyses of the sediments in April of 2007 and September of 2009 show that the conditions within all the sediments studied were still anoxic and dominated by anaerobic processes. Dissolved oxygen levels (Figure 1a,b,c), were still low: sub-oxic (0.1 – 0.3 mg $dm^{-3}$) to anoxic (<0.01 mg $dm^{-3}$). Redox potentials (Figure 2a,b,c) were still strongly reducing with potentials between -150 and -200 (vs SHE). pH of sediments (Figure 3a,b,c) were near neutral (pH 7 – 7.5). The processes ongoing in the sediments were dominated by sulphate reduction (Figure 4a,b,c), where generally an increase in sulphate reduction (i.e. loss of sulphate) was seen with increasing depth with the concomitant evolution of sulphide (Figure 5a,b,c). Carbon dioxide measurements, measured on cores from September 2009, are at this stage inconclusive but are shown in Figure 6

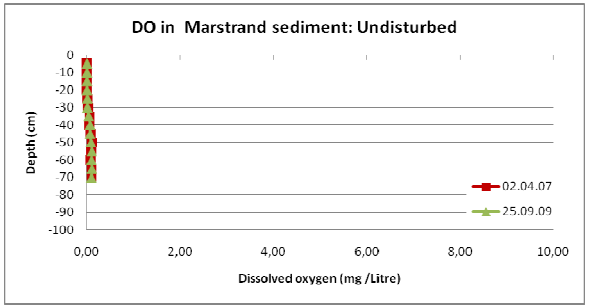


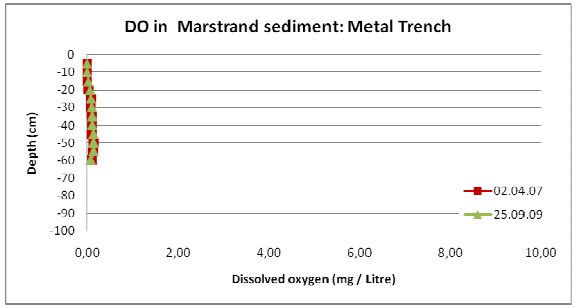


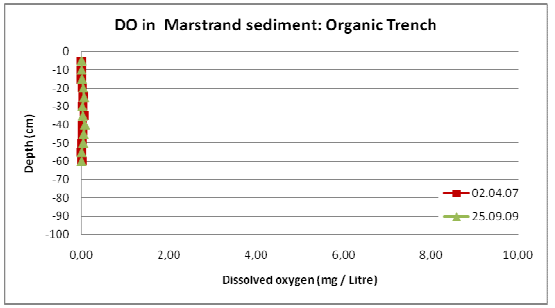


Figure 1: Dissolved oxygen content of a) undisturbed, b) metal trench and c) organic trench sediments in Marstrand.

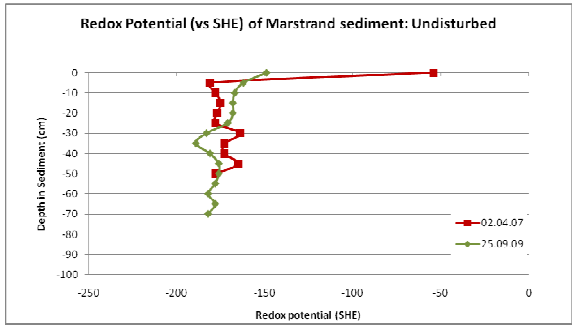


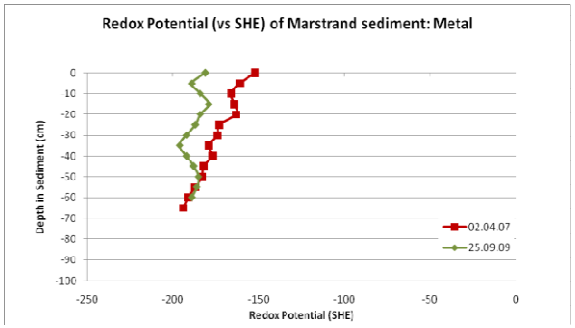


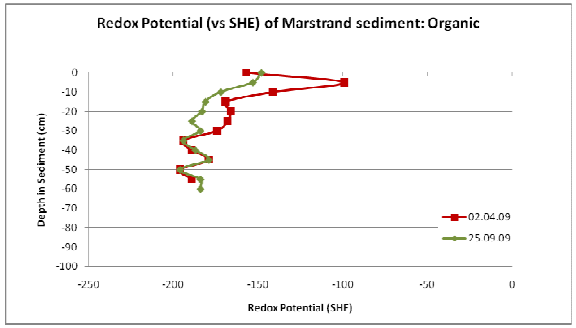


Figure 2: Redox potential of a) undisturbed, b) metal trench and c) organic trench sediments in Marstrand.

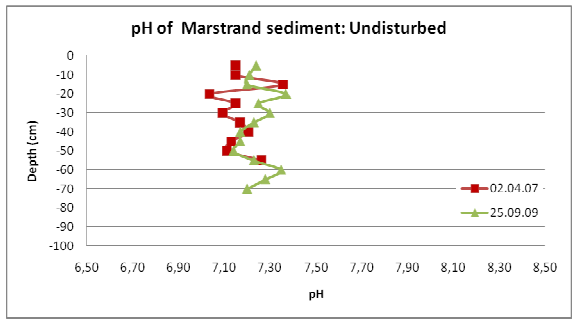


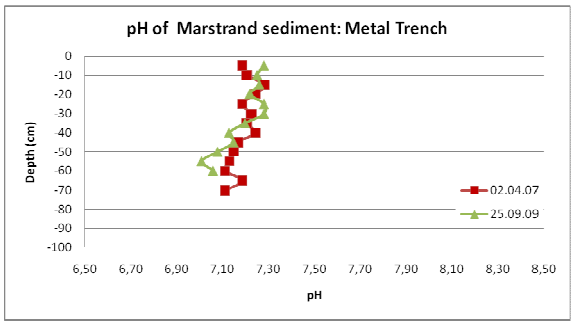


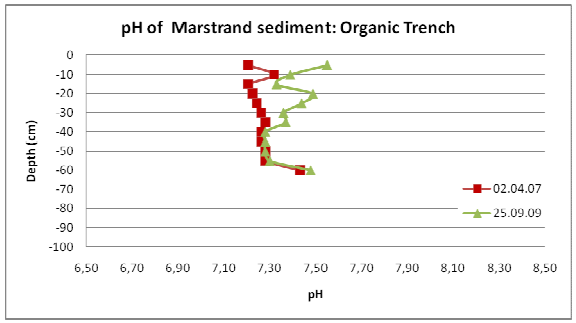


Figure 3: pH of a) undisturbed, b) metal trench and c) organic trench sediments in Marstrand.

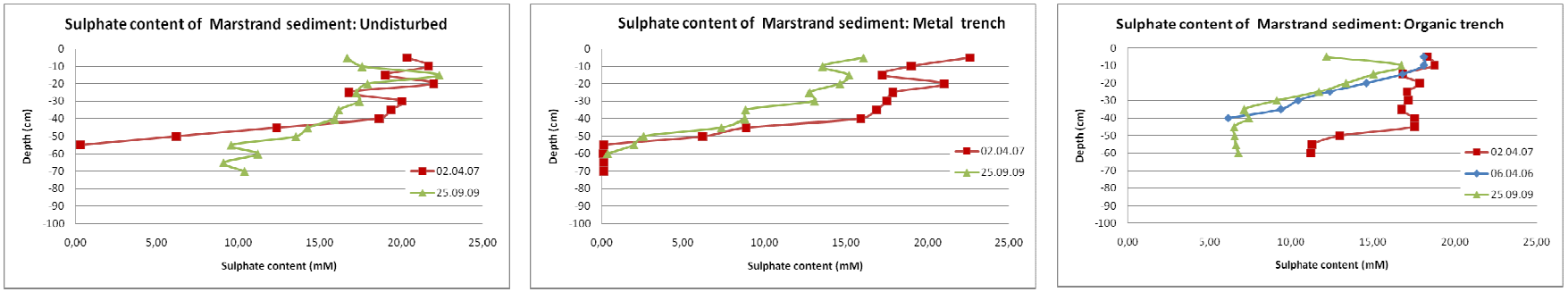


Figure 4: Sulphate content of a) undisturbed, b) metal trench and c) organic trench sediments in Marstrand.

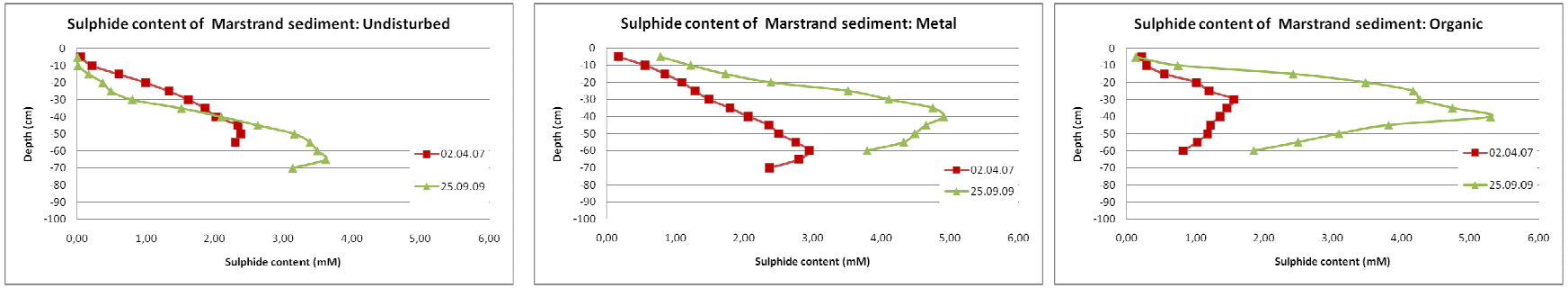


Figure 5: Sulphide content of a) undisturbed, b) metal trench and c) organic trench sediments in Marstrand.

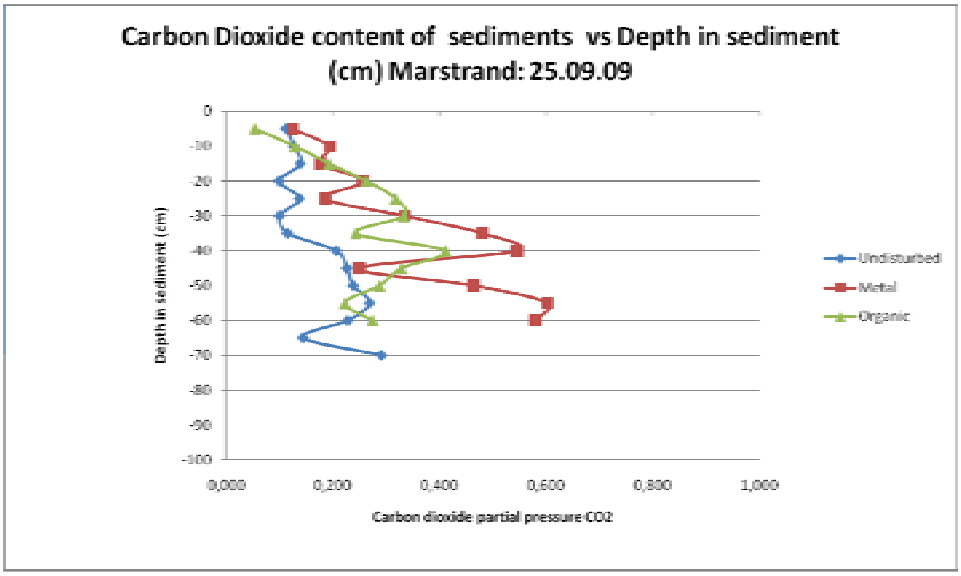


Figure 6: Carbon dioxide levels in sediments from Marstrand, September 2009.

## 4.3 Sediment Analysis

### 4.3.1 Particle Size Analysis

A plot of the mean particle size of the sediment cores taken in September 2009 is shown in Figure 7. The results show that in the undisturbed / control area, particle sizes are mainly of medium to fine silts below 15cm depth and down to 60cm. The organic trench shows that from 5cm below the surface to 30cm they are coarse silts, which then changes to a layer of fine to very fine sands from 40 – 60cm below the surface and then a change back to coarse silts at 60 – 70cm. The sediments in the metals trench are homogeneous throughout, consisting of coarse to medium silts.

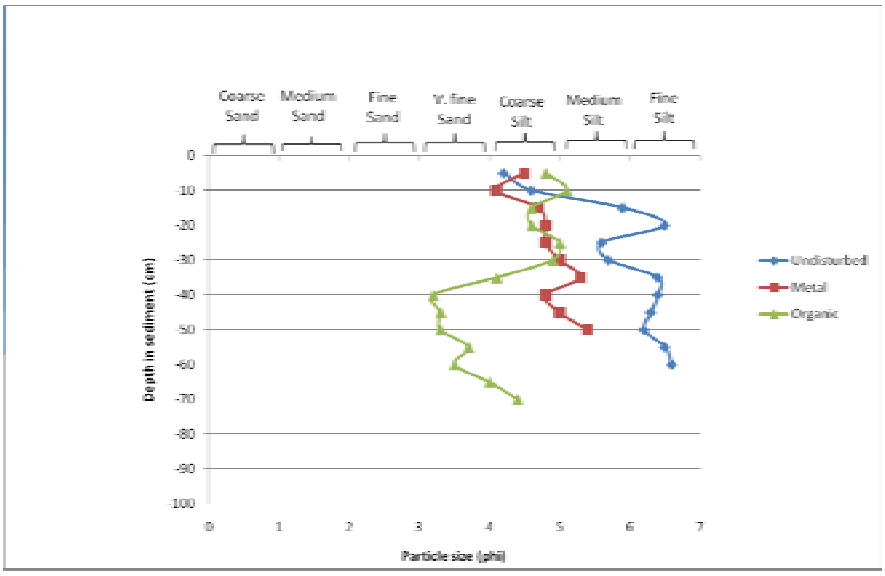


Figure 6: Mean particle size (phi) of sediments in Marstrand 25.09.09.

4.3.2 Porosity

The porosity of the sediments in the undisturbed, metals and organic re-burial trenches, for 02.04.07 and 25.09.09, are shown in Figures 7a, b and c, respectively. In the cores from the undisturbed area the sediments are very porous between 0.8 and 0.9. The porosity of sediment in the metals trench taken in April of 2007 are very porous from the sediment surface and down to 60cm, thereafter they become decreasingly porous, approximately 0.5, from 70 – 75cm. The sediments of the core taken in September 2009 show similar results, with high porosities between 0.75 and 0.90, from the surface of the sediment down to 55cm. Unfortunately, porosity deeper than this could not be calculated on this occasion due to the presence of large pieces of wood / organic material in the sediment.

The sediments from the organic re-burial trench show a distinct change in porosity with increasing depth. From the surface of the sediment down to approximately 30cm the sediments are very porous, 0.8 to 0.9, thereafter and down to approximately 70cm, the porosity decreases to between 0.4 and 0.5.

4.2.3 Loss on Ignition: Organic Content

The Loss on Ignition (organic content; %w/w = % weight/dry weight) of the sediments in the undisturbed, metals and organic re-burial trenches, for 02.04.07 and 25.09.09, are shown in Figures 8a, b and c respectively. Sediment from the undisturbed area taken on the two dates showed quite varying organic contents. The core from April 2007 showed a low organic content within the first 15cm, 5-15%w/w, which then increased to a maximum content of ca. 33% at 50 cm depth. Thereafter the organic content decreased to ca. 17% at 60cm below the sediment surface. The core from September 2009 showed an initial content of 15%w/w organic content which increased to over 25% w/w at 15cm and then decreased to 15%w/w at 30 cm. Thereafter the organic content varied between 15 – 20% w/w down to 60 cm below the sediment surface.

The organic content of the sediment from the metals re-burial trench taken on the two dates also showed similar trends. However, data for the core from September 2009 does not go as deep as that from April due to sampling problems (see porosity results). The core from April 2007 showed a low organic content in the

first 5cm, ca. 10%, which increased to ca 20% at 10cm. Thereafter the organic content ranges between 20 and 25%w/w down to 60cm whereupon it decreases down to ca. 8% at 70 – 75cm. The core from September 2009 shows a similar overall trend to the April core, with lower organic content in the upper 15cm, ca. 12%w/w, which increases to ca. 20%w/w by 20cm below the surface and thereafter fluctuates between ca. 20 and 25%w/w down to 40cm. There is an increase in organic content between 40 and 45cm below the surface (same trend seen in April core) to ca 32%w/w and then the organic content decreases down to 50cm below the surface, which was unfortunately the last sample analysed in the core.

The organic content from the organic re-burial trench taken on the two dates showed similar trends, although the amounts of organic matter did vary within them. The core from April 2007 showed organic contents of between 10 and 15% w/w down to 20cm thereafter there was a decrease in organic content down to ca. 5% at 35cm below the sediment surface. Thereafter this was fairly constant down to 55cm whereupon the organic content increased to ca. 8%w/w at 65 cm below the sediment surface. The core from September 2009 showed the same trend but the amounts of organic matter differed. In the upper 30cm of sediment, organic contents ranged from 15 to 25% w/w. Thereafter there was a decrease down to ca. 3% at 40cm below the sediment surface, whereupon there was a slight increase from 40 to 70 cm where the content at this depth was ca. 7%w/w.

### 4.2.4 Iron Content

The iron content of sediments from the undisturbed / control, organic and metals re-burial trenches are shown in Figures 9a, b and c respectively. The iron results are not necessarily the total iron content as the method used in this instance only extracts iron oxide and hydroxide minerals ($Fe^{3+}$) and not necessarily minerals bound to sulphide ($Fe^{2+}$) (Haese, 2000); which would likely form a large proportion of iron minerals in Marstrand. However, the iron oxides and hydroxides measured here are of prime interest as it these minerals that may be used by iron reducing bacteria to oxidise organic matter. It can be seen that generally more iron is recorded in the sediments of a silty nature (undisturbed, metals and upper 30 cm of the organic trench) in the September cores when compared with the April cores. Highest levels of

iron were recorded in the upper 10-15cm of April core of the metals trench and September core of the organic trench. The implications of the iron results recorded, in relation to the other parameters will be discussed in the following section.

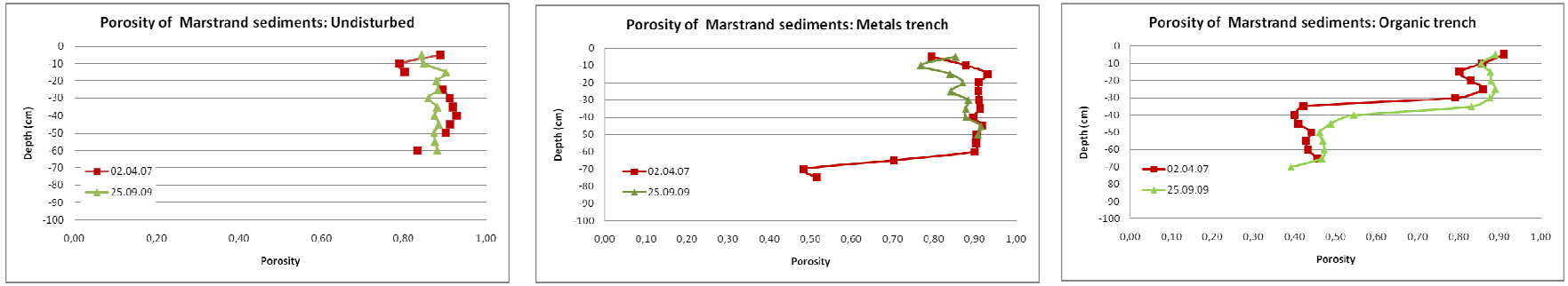


Figure 7: Porosity in a) undisturbed, b) metal trench and c) organic trench from sediments in Marstrand.

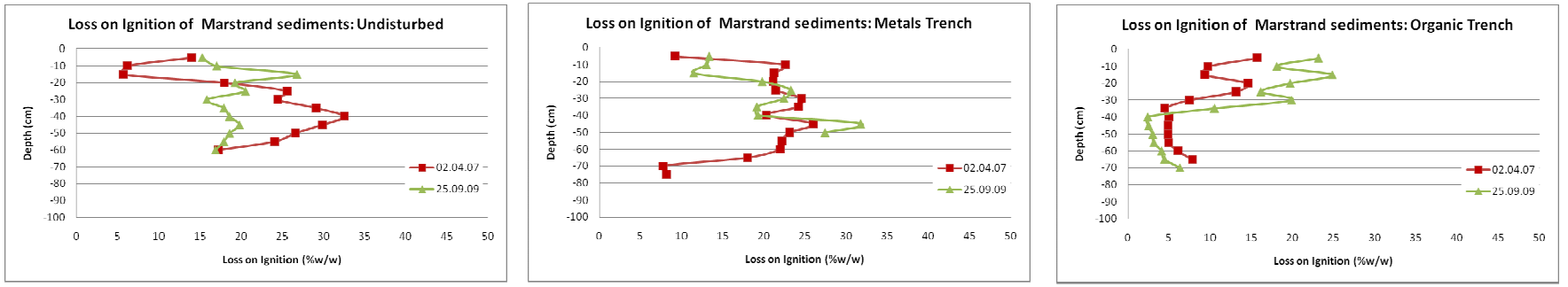


Figure 8: Loss on ignition (organic content) in a) undisturbed, b) metal trench and c) organic trench sediments in Marstrand.

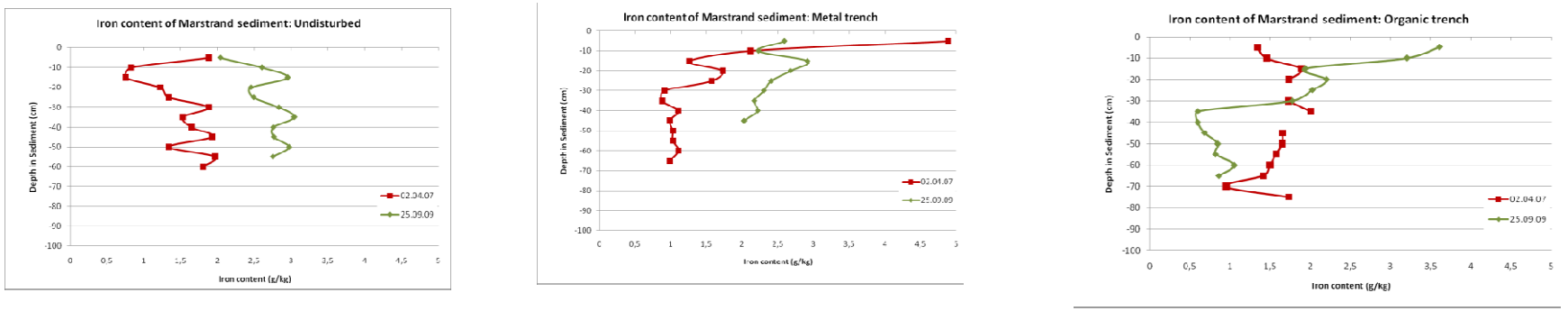


Figure 9: Iron content in a) undisturbed, b) metal trench and c) organic trench sediments in Marstrand

# 5. Interpretation and Discussion of Results

## 5.1 Pore Water Chemistry

As the results of Phase I of the project indicated, sulphate reduction was prevalent at Marstrand. Sulphate reduction may contribute by more than 50% to the mineralisation of organic matter in continental shelf sediments (Jørgensen, 1982) and in certain environments has accounted for over 90% of mineralisation (Jensen et al., 2003). Sulphate reduction still appears to be the predominant terminal metabolism pathway in Marstrand, certainly at the depths where archaeological material has been buried. As was discussed in the Final Report of Phase I (Gregory, 2007) the utilisation of organic matter by microorganisms within sediments involves oxidation – reduction (Redox) reactions. These reactions follow a well documented succession with various chemical species being utilised by microorganisms based on the amount of energy they yield. In marine sediments the sequence of utilisation can be observed spatially in horizontal layers of increasing depth. Typically the sequence in order of depth is: dissolved oxygen > nitrate > manganese > iron > sulphate > carbon dioxide (Froelich et al., 1979). As mentioned in section 4.2, dissolved oxygen contents were very low and redox potentials highly reducing in all sediments indicating that the sediments were sub anoxic / anoxic and thus anaerobic microbial processes would dominate. Sulphate and sulphide measurements show that sulphate reduction was the predominant process ongoing at the depths where archaeological material was buried. The undisturbed sediments showed similarities with the metals trench but there were differences between these and the sediments of the organic re-burial trench. The undisturbed and metal sediments showed similar trends, with slower rates of sulphate reduction in the upper 40cm, thereafter sulphate was rapidly reduced. In the cases of the undisturbed sediment and metal re-burial trench, sulphate was seen to have been completely reduced by 55cm in both cases in the cores from April 2007. In the September cores there was still sulphate present at 55 cm in the undisturbed sediments but sulphate had been completely reduced by 60cm in the metal re-burial sediments. This is most likely explained by the levels of organic material in the sediments (Berner, 1984). In the metal re-burial sediment from April and September and undisturbed core from April, where all sulphate was seen to have been reduced, it can be seen that the organic contents were highest with maximums

of 26-32%w/w at approximately 40cm below the surface of the sediment. In the undisturbed core from September, where sulphate was still present at 70cm depth, the organic content was lower at 19%w/w. It is also interesting to note that the evolution of carbon dioxide, which was only measured in the cores from September 2009, shows that lower levels of carbon dioxide (half as much) were present in the undisturbed sediments when compared with the metals sediments, indicating that microbial activity was less in this instance.

The organic content of the sediment may also help explain the sulphate reduction seen in the organic re-burial sediments. As noted, the cores from April 2007 are difficult to explain why there was little discernible sulphate reduction in the upper 45cm of sediment and then a period of rapid sulphate reduction down to 55cm and thereafter little sign of reduction in the remainder of the core with ca. 10mM of sulphate still present in the sediment. However, a core taken in April 2006, where sulphate and sulphide were measured has been included in Figure 10 for comparison with the core from September 2009.

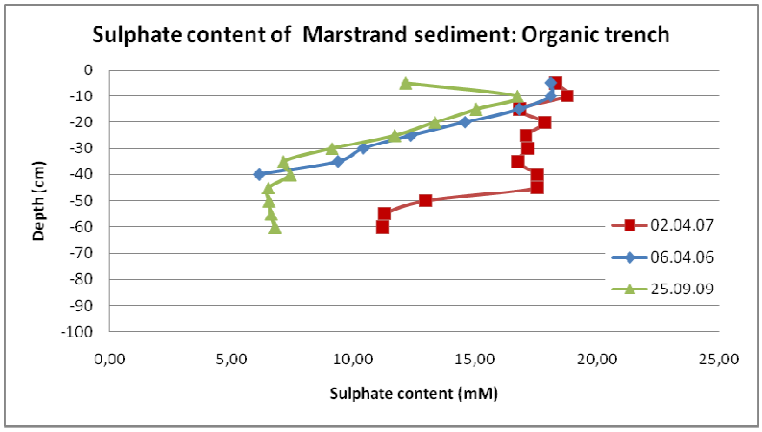


Figure 10: Sulphate content of the organic trench from Marstrand 2006 – 2009.

In the September 2009 core, sulphate reduction began at 10cm below the surface of the sediment and continued relatively rapidly down to 35cm where it reached ca. 8mM sulphate. Thereafter sulphate levels remained constant indicating no further reduction. When looking at the other measured parameters for the organic re-burial cores it is apparent that in the upper layers the sediments are porous and silty with maximum organic contents of between 15 and 25%. Between 30 and 40cm below the

surface of the sediment there is a change to a coarser, less porous fine grained sand with organic contents of between 2 and 8%w/w. It is therefore possible that the combination of less porous, coarser grained sediment and a lower organic content mean that conditions are unfavourable for decomposition of organic material by sulphate reduction and therefore sulphate is still present in the sediment. Looking at the carbon dioxide levels, below 40 cm they are decreasing again indicative of reduced microbial respiration.

To get an impression of a "worst case scenario" of decomposition of organic matter, due to the reduction of sulphate in the reburied sediments at Marstrand, a simplified diffusion model was developed based on porosity of the sediments and the sulphate content of the pore water as a function of depth. The model was used to estimate the potential amount of organic material that could be oxidised through sulphate reduction at the depths where archaeological material was buried and sulphate reduction was the predominant process. The model assumes that the environment is in a steady state and that flux of sulphate in the sediment is due to diffusion (Li and Gregory, 1974). Fick's first law describes flux in water:

$$F_{sed} = -D_{i,sed} \cdot \frac{dC}{dx} \qquad \left[mol \cdot cm^{-2} \cdot s^{-1}\right] \qquad Eqn.3$$

Where:

$F_{sed}$: The flux of ion "i" per area unit per time unit

$D_{i, sed}$: a diffusion constant

dC/dx: concentration gradient of ion "i"

However, in sediment we have to take into account that only a part of the sediment is water where diffusion can take place, so we have to correct for the porosity ($\phi$):

$$F_{sed} = -\phi \cdot D_{i,sed} \cdot \frac{dC}{dx} \qquad \left[mol \cdot cm^{-2} \cdot s^{-1}\right] \qquad Eqn.4$$

In the present model, influence from the pore structure of the sediment (tortuosity), which would slow the diffusion rate, is ignored as we are considering a worst-case scenario.

Using Equation 4 with a diffusion coefficient for sulphate in seawater of $6 \cdot 10^{-6}$ $cm^2 \cdot second^{-1}$ (at 5° C after Li and Gregory; 1974), and the average porosities of sediments and concentration gradients (dC/dx), the sulphate fluxes as a function of depth were calculated for all sediment cores. Using the calculated flux of sulphate and assuming that 1 mole of sulphate can oxidise 2 moles of organic carbon from $CH_2O$, (brutto formula) to carbon dioxide, the amount of organic material, which will be decomposed as a result of sulphate reduction, could be calculated.
These data are shown in Table 1.

| **Core** | **dC / dx (mmol/L/cm)** | | **Porosity ($cm^3$ / $cm^3$)** | | **Flux (mol/cm2/s)** | | **Organic Mineralisation (g /m2/yr)** | |
|---|---|---|---|---|---|---|---|---|
| | *Apr 07* | *Sep 09* | *Apr 07* | *Sep 09* | *Apr 07* | *Sep 09* | ***Apr 07*** | ***Sep 09*** |
| **Undisturbed** | 0.816 | 0.213 | 0.88 | 0.88 | $6.47 \times 10^{-12}$ | $1.12 \times 10^{-12}$ | **123** | **21** |
| **Metal** | 0.784 | 0.438 | 0.9 | 0.88 | $4.24 \times 10^{-12}$ | $2.31 \times 10^{-12}$ | **80** | **44** |
| **Organic** | 0.396* | 0.387 | 0.38 | 0.47 | $9.03 \times 10^{-13}$ | $1.09 \times 10^{-12}$ | **17** | **21** |

Table 1: Data and results used to calculate mineralisation of organic matter due to sulphate reduction. *: Calculated from data taken in April 2006

The results in Table show that there are seasonal variations in the rate of sulphate reduction and surprisingly that there is more mineralisation in the April cores in the undisturbed and metal sediments than in the September cores. There does not appear to be a significant seasonal variation in the sediment from the organic reburial trench sediment. One may anticipate that sulphate reduction would be higher in September due to higher temperatures (Al Raei et al., 2009). Unfortunately temperature was only measured in the seawater and not through the cores so it is not certain if there is a significant change in temperature at these depths in the

sediment. Temperature within the sediment should be measured if future cores are taken. Concomitant with sulphate reduction was the evolution of sulphide with increasing depth. Levels of sulphide were highest in the Autumn – in the September 2009 cores - for all sediment types, where levels of between 4 and 5mM Sulphide were measured. This compares to between 1-5 and 3mM sulphide for the April cores. In all cases levels of sulphide increased as the levels of sulphate decreased and peaked at the levels where measured sulphate was at a minimum, thereafter levels of sulphide decreased. Further interpretation of the data should be made with caution as there is not a direct "one to one" relationship between sulphate reduction and measurements of resulting sulphide in the sediment pore water. This is due to the complexities of the potential reaction of the produced sulphide with metal ions in the sediment, e.g. iron, leading to the production of iron sulphides. Re-oxidation of the sulphide may also take place.

## 5.2 Sediment Properties of the Reburial Trenches

The analysis of the sediments themselves has shed light on the question raised at the end of Phase I of the project – notably, that the sediments used for the re-burial of the organic materials and the metals were different and if so what effect does this have on the re-buried materials? The particle size, porosity and loss on ignition (organic content) analyses confirmed that there were gross differences in the sediments.

The sediments used in the metals trench were very similar to the naturally occurring harbour sediments. In these sediments the particle sizes were predominantly medium to fine silts (5-7 phi) and in the metals trench coarse to medium silts (4-6 phi). Both sediment types were highly porous (0.8 – 0.95), although the core in the metals trench from April 2007, which went down to 70cm, showed that the sediment was less porous after 60cm and was more sandy. The organic content of both sediments was generally between 15 and 25% w/w. However, there were occasions when this was higher, up to ca. 30%w/w at 40 – 50 cm below the sediment surface. In the cases where this was measured, it corresponded with a layer of dead eel grass and other large particles of organic material.

The sediments from the organic trench were quite different. The particle size of sediment in the upper 30 cm was very similar to the metals trench being coarse to medium silts (4-6 phi). However, there was then a clear transition from 30 – 40 cm below the sediment surface, whereby the sediments became coarser. From 40 – 60cm the sediments were graded as very fine sands (3-4 phi) and then between 60 – 70 cm they became finer, grading back to coarse silts. These results were reflected and corresponded with the porosity measurements which were very porous, 0.8 – 0.95, in the upper 30cm. As with the particle size there was a clear transition from 30 – 40 cm with the sediment becoming less porous and then from 40 cm to 70 cm the sediment was less porous at ca. 0.4. Again, the organic content of the sediment reflected and corresponded with these results. In the upper porous and finer grained sediments the organic contents were higher, between 10 and 25%w/w. However, the transition to the coarser sediment at 30 – 40 cm also corresponded to the organic content, with it decreasing to between ca 3 and 8% between 40 and 70cm.

Generally the finer grained sediments corresponded with higher porosities, as could be expected there was also a higher concentration of organic matter in the finer grained sediments. This trend is corroborated in the literature relating to organic decomposition in coastal marine sediments, whereby organic matter (OM) load is often associated with the sedimentary mud fractions (grain size fractions below 63 μm) (Al Raei et al., 2009). Furthermore, bacterial cell numbers, as a measure for overall potential microbial activity, show a positive correlation with the sedimentary mud fraction with finer grained sediments containing more bacteria (DeFlaun and Mayer, 1983). When attempting to understand the processes ongoing in the sediments at Marstrand these results can also be related to what was measured within the interstitial pore waters of the sediments.

As discussed the iron results are not necessarily the total iron but an attempt to measure the “reactive” iron available for oxidation of organic material. Nevertheless, iron has been shown to contribute quite considerably to the oxidation of organic material in marine sediments (Canfield, 1983) but, as noted previously, mineralisation through iron reduction tends to occur higher up in the sediments where it predominates over sulphate reduction. Furthermore, the presence of dissolved sulphide in the sediments indicates that reactive iron has been consumed

(Canfield, 1983). Although the reduction rate due to iron cannot be concluded from these results, an estimate of the potential future mineralisation due to iron reduction may be given. An Iron (III) content of for instance 2 g/ kg (average measurement seen in Marstrand) may oxidise the following amount of organic material:

$$\frac{2\ \frac{g\ Fe}{kg}}{55\frac{g\ Fe}{kg}} \frac{\cdot 30\ \frac{g\ CH_2O}{mol}}{\cdot 4\ \frac{mol\ Fe}{mol\ CH_2O}} = \sim 0.28\ \frac{g\ CH_2O}{kg}$$

Assuming that 4 moles of iron can oxidise 1 mole of organic carbon from $CH_2O$ (brutto formula) to carbon dioxide (Froelich et al., 1979), the amount of mineralisation due to the oxidation of iron will, certainly at the depths where archaeological material are present, be limited. For comparison the total amount of organic material varies between 5 and 25% or 50 – 250 $\frac{g\ CH_2O}{kg}$ i.e. reduction due to iron will be very low.

The results themselves somewhat reflect this hypothesis with higher amounts of iron being measured in the upper sediments of the organic and metals trench. Here, iron would likely be present as ferric iron and thus, by the method used, more of these fractions would be extracted. Deeper in the sediments, where iron would be bound in the ferrous form and the method was not suitable for extraction of these minerals, the levels of iron are lower.

In hindsight the ferrous ($Fe^{2+}$) and ferric ($Fe^{3+}$) fractions of all the mineral groups present in the sediments should have been determined in order to gain more information about the role of iron in oxidation of organic matter. However, as the sulphate and sulphide results show sulphate reduction is the dominant process in Marstrand.

# 6. Conclusions, implications and recommendations.

The aims for the environmental monitoring of Phase II of the RAAR project were threefold:

- Check that the environment was still conducive to preservation of the archaeological materials present in the re-burial trenches.
- Develop a coring system whereby sediment samples deeper than 50 cm could be taken and assess the processes ongoing below this depth.
- Assess the sediments of the metals re-burial trench as well as the organic materials re-burial trench.

## 6.1 Is the re-burial environment in Marstrand conducive to preservation?

Assuming that the organic materials and silicates are best preserved in waterlogged and anoxic conditions then the organic re-burial trench is still conducive to their preservation. The environment, over the two year period of Phase II, was seen to be sub-oxic to anoxic and highly reducing with a neutral pH. Sulphate reduction, with concomitant sulphide production, was still the predominant process ongoing in the trench.

The aforementioned conditions hold true for the metals trench too and as Richards and MacLeod (2007) concluded in Phase I of the sub metals project, corrosion of metal coupons decreased with increasing depth in the sediment when compared with corrosion in the open seawater. However, as they also note (ibid.) microbial induced corrosion may play a part in the deterioration of the metal coupons. It has already been agreed with the coordinators of the metals sub-project to coordinate the results of their research with the environmental sub-project results.

## 6.2 Sediments deeper than 50cm

The PVC tubing (pore water analysis) and coring system (sediment analysis) worked well and it was possible to obtain cores deeper than 50cm. However, it is still difficult to obtain these deeper cores. This is in part due to the very mobile and “fluffy” nature of the upper 30 – 40 cm of the undisturbed sediment and metals trench

sediments, which were easily compacted when the cores were pressed into them. On several occasions it was possible to press the core below the sediment surface by several centimetres yet on retrieval only 30 – 40 cm of sediment were collected. The organic re-burial sediments were a little easier to retrieve due to the more sandy nature of the sediments lower down. Nevertheless, the cores were deemed to be reliable as looking at parameters, which were comparable and not susceptible to seasonal change, such as porosity (Figure 7), the profiles were remarkably similar for the April and September cores. The vertical precision of the cores would appear to be ± 5 – 10cm, which is deemed acceptable bearing in mind that visibility was often less than 50cm during sampling. Development of taking cores will continue, trying to improve the way the cores are pressed into the sediment.

### 6.3 Sediments and processes in the Metals and Organic re-burial trenches

The particle size analysis of the September cores showed that the sediments in the two re-burial trenches were of different composition. In all sediments sampled, the upper 30cm were coarse to fine silts. In the organic trench this then graded to very fine sand at the depth where the archaeological material was buried. This can possibly be explained by the way the materials were re-buried in the two areas. In the organic trench the materials were backfilled with sediment from different areas whereas in the metals trench the materials were covered with material from the surrounding area. The porosity results reflect the particle size analysis with the upper sediments being highly porous and the lower sandier sediments of the organic trench being less porous. The particle size also relates to the amount of organic material within the sediments. Generally, the finer grained sediments had higher amounts of organic material and the coarser grained sediment lower amounts of organic material. This is significant as the amount of organic material has affected the rates of the processes ongoing in the sediments. Sulphate reduction is the dominant process in the Marstrand sediments and will be responsible for the majority of organic mineralisation. From this research the rate of mineralisation due to iron reduction cannot be concluded although it is deemed to be minimal at the depths where archaeological materials are present. Sulphate reduction was greatest in the metals trench and showed seasonal variation with ca. 80 and 40 g of organic matter

being mineralised per $m^2$ of sediment per year in April and September respectively. In the organic trench sulphate reduction was lower and did not appear to show seasonal a seasonal trend with ca. 20 g of organic material being mineralised per $m^2$ per year in both April and September.

## 6.4 Implications of Marstrand for Re-burial of archaeological materials as a means of long term storage

### 6.4.1 Correlation of deterioration of materials and the re-burial environment

The results have shown that the conditions in the re-burial trenches are still certainly conducive to the preservation of the organic materials. However, what effect does the iron and sulphate have on the materials? Certainly, in terms of wood, there is an ongoing debate on the effects of iron and sulphur in the deterioration of conserved archaeological wood (Fors, 2005). Are there similar implications for the textile materials and silicates?

Microbially induced corrosion in environments with high sulphate contents is documented and, as discussed, the results of this sub-project will be coordinated with the results of the metals sub project in order to better understand the preservation of the metals.

### 6.4.2 General implications for re-burial

Phase II has shown the importance of understanding the processes ongoing within a given sediment prior to carrying out any re-burial. Fortuitously, this was seen when comparing the results from the metals and organic materials trenches. The optimal depth of re-burial has been a point of discussion throughout the project and the results of Phase II help shed light on this question. These results show that it is not simply a matter of depth of burial per se. but the type of sediment used, its properties and the processes ongoing within it – all of which vary from sediment to sediment. Based on the results from Marstrand the implications for re-burial are that sandy sediments, which are less porous and naturally contain less organic material due to their larger particle size, appear to have lower rates of mineralisation when

the dominant process is sulphate reduction. This contrasts with the higher rates of mineralisation in more porous finer grained sediment with higher organic contents.

These factors could be used to our advantage when re-burying; for instance the use of coarse grained sediment with inclusion of a layer of “sacrificial organic matter” in order to “induce” mineralisation in the upper sediment; in this way it may not be necessary to re-bury archaeological materials so deeply. This effect can be seen in the metals trench where all available sulphate had been utilised higher up in the sediment above where artefacts had been buried.

In order to classify sediments for their potential use in future re-burial projects it is recommended that the following parameters at least be measured and that the time (season) of sampling be considered:

Pore water parameters:

Dissolved oxygen, redox potential, pH, dissolved and total iron, sulphate and sulphide content, temperature.

Sediment parameters:

Particle size, porosity, organic content.

# 7. References


Agrawal, Y. C., McCave, I. N., Riley, J. B. (1991): Laser diffraction size analysis. In: Principles, methods, and application of particle size analuses. (ed. J. P. M. Siyvitski). Cambridge University Press. ISBN 0-521-36472-8.

Al-Raei, M.A., Bosselmann, K., .Böttcher, M.E., Hespenheide, B and Tauber, F. (2009), Seasonal dynamics of microbial sulfate reduction in temperate intertidal surface sediments: controls by temperature and organic matter. In *Ocean Dynamics*, **59:** 351-370.

Berner, R.A. (1984) Sedimentary pyrite formation: An update. In Geochimica et Cosmochimica Acta, **48**:4, 605-615.

Cai, W.J. and Reimers, C.E. (2000) Sensors for in situ pH and $pCO_2$ measurements in seawater and at thesediment-water interface. In J. Buffle and G. Horvai (eds) *In situ monitoring of Aquatic Systemes*. IUPAC, Chichester, 75-121.

Canfield, D. E. (1989) Reactive iron in marine sediments. In Geochimica et Cosmochimica Acta, **63**:3, 619-632.

DeFlaun,M. F. and Mayer,L M. (1983) Relationships Between Bacteria and Grain Surfaces in Intertidal Sediments. *Limnology and Oceanography*, **28:**5, 873-881.

Fors, Y. (2005) Sulfur speciation and Distribution in the *Vasa's* wood. Protection by water pollution leaves a sour aftertaste. Unpublished Licentiate Thesis, Dept. Of Structural Chemistry, Stockholm University.

Froelich, P.N., Klinkhammer, G.P:, Bender, M.L., Luedtke, N.A:, Heath, G.R., Cullen, D., Dauphin, P., Hammond, D., Hartman, B. and Maynard, V. 1979. Early oxidation of organic matter in pelagic sediments of the eastern equatorial Atlantic: Suboxic diagenesis. *Geochim. Cosmochim. Acta,* 43: 1075-1090

Gregory, D. (2007) Environmental monitoring. In Reburial and Analyses of Archaeological Remains. Studies on the effects of reburial on archaeological materials performed in Marstrand, Sweden 2002-2005, The RAAR project. Eds. T. Bergstrand and I. Nyström Godfrey.

Haese, R.R. (2000). The Reactivity of Iron. In H.D. Schulz and M Zabel (eds.), *Marine Geochemistry*: 233-261. Springer-Verlag, Berlin.

Hodkinson, J. R., Greenleaves, I. (1963). Computations of Light-Scattering and Extinction by spheres according to diffraction and geometrical optics, and some comparisons with the Mie Theory. Jour. Of the Optical Soc. Of Am. Vol 53. no. 5, 577-588.

Jensen, M.M., Thamdrup, B., Rysgaard, S., Holmer, M. and Fossing, H. (2003) Rates and Regulation of Microbial Iron Reduction in Sediments of the Baltic-North Sea Transition. In *Biogeochemistry, **65:**3, 295 – 317.*

Jørgensen, B.B. (1977) The Sulfur Cycle of a Coastal Marine Sediment (Limfjorden, Denmark). In *Limnology and Oceanography*, **22**:5, 814-832.

Li, Y.H. and Gregory, S. 1974: Diffusion of ions in seawater and in deep sea sediments. *Geochimica et Cosmochimica Acta*, 38, 703-714.

Matthiesen, H. (2007) A Novel Method to Determine Oxidation Rates of Heritage Materials in Vitro and in situ. In *Studies in Conservation, **52**, 1-11*

Richards, V. and MacLeod, I. (2007) Metlas. In Reburial and Analyses of Archaeological Remains. Studies on the effects of reburial on archaeological materials performed in Marstrand, Sweden 2002-2005, The RAAR project. Eds. T. Bergstrand and I. Nyström Godfrey.

GOVERNMENT OF WESTERN AUSTRALIA

WESTERN AUSTRALIAN museum

# REBURIAL AND ANALYSES OF ARCHAEOLOGICAL REMAINS

## Investigation into the Effects of Reburial on Metals

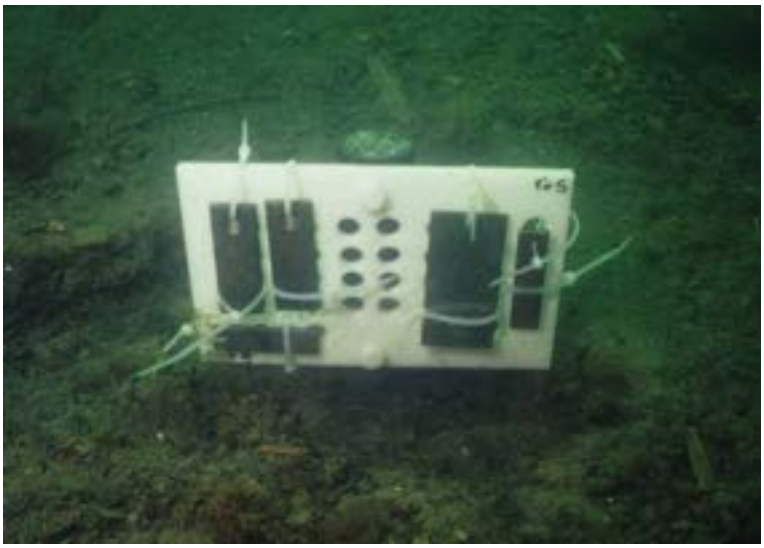

**Marstrand, Sweden**
**December 2010**


**Vicki Richards (MPhil)**
Research Officer
Western Australian Museum
Shipwreck Galleries
47-49 Cliff St
FREMANTLE WA 6160
Tel: +61 8 9431 8472
Fax: +61 8 9431 8489

Email: vicki.richards@museum.wa.gov.au

**Dr Ian MacLeod**
Executive Director
Collection Management & Conservation
Western Australian Museum
Locked bag 49
WELSHPOOL DC WA 6986
Tel: +61 8 9427 2839
Fax: +61 8 9427 2892
Email: ian.macleod@museum.wa.gov.au

# ACKNOWLEDGEMENTS

The authors wish to thank the co-ordinators Inger Nyström Godfrey, Studio of Western Sweden Conservators and Thomas Bergstrand, County Museum of Bohusläns for the opportunity to be involved in this important reburial project. We would like to acknowledge The National Heritage Board, Sweden, The Nordic Cultural Fund, Carl Jacob Lindebergs Fornminnesfond, Wilhelm & Martina Lundgrens Vetenskapsfond and the Western Australian Museum for co-funding the project and Dr Diana Jones, former Acting Chief Executive Officer of the Western Australian Museum for facilitating our participation in this project. We would especially like to acknowledge Dr Ian Godfrey, Head of the Department of Materials Conservation, Western Australian Museum for funding the purchase of the materials for the metals sub-project. Special thanks must also go to Michael Verrall, CSIRO for providing access to the SEM/EDAX instrument at no cost. Last but not least, we would like to thank the collaborators of the other sub-projects.

# CONTENTS

# EXECUTIVE SUMMARY

The major purpose of the 'Reburial and Analyses of Archaeological Remains' project is to investigate and evaluate the effect of reburial on the most common material types found on underwater cultural heritage sites as a means of preserving archaeological remains *in-situ*. The project consists of six sub-projects. Four of the six sub-projects analyse the extent of deterioration of more commonly found materials on archaeological sites: wood; other organics such as leather, textiles, etc; ceramics/silicates; metals. Another sub-project concentrates on assessing the stability of packing and marking materials used in archaeological documentation and the final sub-project involves monitoring chemical and physical changes occurring in the reburial environment over time.

In order to determine the long-term effects of reburial on the different material types, sufficient samples were buried to allow sampling to continue for up to 50 years. The wood, other organics, ceramics/silicates and polymeric samples were buried in Marstrand Harbour, Sweden in September 2002, whereas the metal sample units were buried the following year in September 2003. The environmental monitoring began in March 2003. The sample units were to be retrieved in the pre-determined order of 1, 2, 3, 6, 12, 24 and 48 years (Table 1). The first phase of the project covered the initial three year time interval (2003-2005) and the final report was published in 2007 (Nyström Godfrey and Berstrand 2007; Richards and MacLeod 2007). The final report for the first phase is available on the project website http://www.svk.com/reburial. However, since retrieval of the reburied samples are almost totally dependent on external funding, the six year retrieval period was postponed to 2009 and as such the reburial period was extended to seven years for the samples reburied in 2002.

Table 1. Retrieval programme for the project.

| Phase | Proposed Retrieval Year | Proposed Reburial Interval (yr) | Retrieval Year | Reburial Interval (yr) | Comments |
|---|---|---|---|---|---|
| 1 | 2003<br>2004<br>2005 | 1<br>2<br>3 | 2003<br>2004<br>2005 | 1<br>2 (1)[1]<br>3 (2) | Final report published in 2007 |
| 2 | 2008 | 6 | 2009 | 7 (6) | Final report due in 2010 |
| 3 | 2014 | 12 | | | Subject to funding |
| 4 | 2026 | 24 | | | Subject to funding |
| 5 | 2050 | 48 | | | Subject to funding |

[1] Number in brackets denote the reburial interval for the metal samples, which were reburied in 2003 one year after the other sample units.

The aim of the metals sub-project is to investigate the corrosion behaviour of metals buried in the marine environment. The corrosion of reburied and exposed modern metal coupons will be examined and compared over time. This study will ascertain the effect of reburial on the deterioration of archaeological metals commonly found on underwater cultural heritage sites and assist in evaluating the effectiveness of reburial as a long-term *in-situ* preservation strategy for metallic archaeological remains.

The samples units consisted of prefabricated proprietary metal coupons of known metal composition mounted utilising high density polyethylene (HDPE) materials.

The metal coupons deployed in the experiment were ferrous alloys: duplicate coupons of cast iron and mild steel and one standard Defence Science and Technology Organisation (DSTO) copper steel coupon and copper alloys: duplicate coupons of brass, copper and bronze. The ferrous and copper alloys were mounted separately to minimise galvanic and proximity corrosion since the latter form of decay has been known to exert its effects over separation distances of some metres on historic shipwreck sites (North 1989). Each sample unit consisted of three sets of duplicate metal coupons mounted at three different depth intervals (totally exposed above the sediment, just below the sediment and buried 50cm in the sediment) on the HDPE rod (Figure 1). Fourteen copper (7) and ferrous (7) alloy sample units were buried in Marstrand Harbour, Sweden on 30 September 2003 in two rows separated by a distance of approximately 3m with about 1-2m between each sample unit.

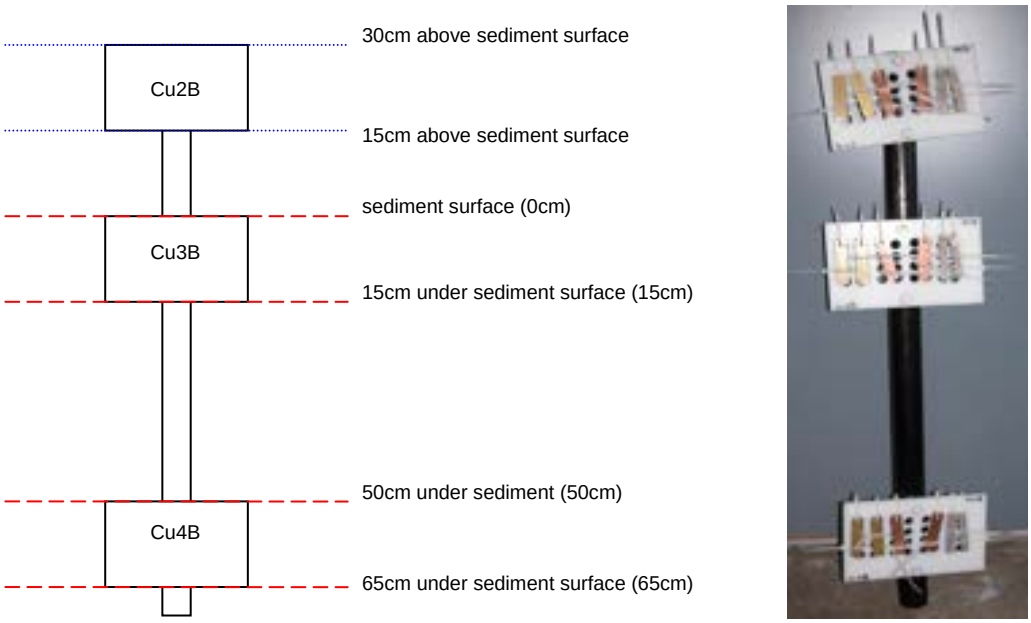


*Figure 1. Schematic diagram and image of a completed copper alloy coupon sample unit.*

The first set of metal sample units (copper and ferrous alloys) was retrieved in 2004 after 1 year on-site and the second set was retrieved in 2005 after 2 years on-site. The interim report for the metals sub-project was finalised in 2006 and the final report for the first phase of the reburial project was published in 2007. In September 2009, six years after the initial reburial in 2003, the third set of metal sample units (copper and iron alloys) were retrieved.

The sample units were photographed *in-situ* prior to any physical disturbance. Each sample unit was then removed by physically extracting the rods from the sediment and the corrosion parameters ($E_{corr}$ and pH) of each coupon measured *in-situ* on the seabed prior to recovery. Immediately after recovery each sample plate was photographed, packed separately for transport and couriered to the conservation laboratories of the Western Australian Museum in Fremantle, Western Australia. The metal coupons were documented and each coupon with the associated corrosion products was analysed by scanning electron

microscopy/electron dispersive x-ray analysis (SEM/EDAX). One of the duplicate coupons was then chemically stripped of corrosion products, weighed and analysed again by the same technique. Digital electron micrographs (SEM) and energy dispersive x-ray analyses (EDX) were collected as the primary data.

At the end of six years it is clear that the precise burial microenvironment plays a major role in determining the fate of the metal coupons. From extended and detailed analyses of the surfaces and their corrosion products, annualised normalised percentage weight loss data and normalised corrosion rates it is possible to gain a good understanding of the parameters that dominate the deterioration of the metals. The effect of the reburial environment on the extent of corrosion of the metals after six years is summarised below.

- It is very important to fully understand the physico-chemical and biological nature of the local sedimentary environment prior to deployment of any reburial strategy.
- It was found that the behaviour and characteristics of the metal surfaces that were fully exposed to the local microenvironment provided a better insight into long term corrosion of metals in a marine environment than the side that lay directly against the HDPE support plate despite the pre-drilled flow holes. However the complimentary data collected from this reverse side provided corroboration of the overall corrosion mechanism and an insight into how variations in the microenvironment affect the corrosion processes.
- The manner in which metals are packed for reburial is extremely important. Metals of significantly different composition must be physically separated by sufficient distance to avoid the complications of galvanic and proximity corrosion and even artefacts of similar composition should be separated in some way (e.g. geotextile barrier) to minimise abrasion and damage to the inherently protective corrosion product layer.
- Copper alloy artefacts recovered from a saline environment should always be stored wet. It was noted that desiccation can cause changes in the nature of the surface corrosion products that may not accurately reflect the microenvironment from which the object was recovered.
- If further analysis of the corrosion product layer and underlying residual metal will be undertaken in the context of the deposition and site formation processes then all metal artefacts should be stored in a similar environment to that from which they had been recovered (e.g. deoxygenated environments if the artefact is recovered from under the sediment). For example, both the copper and the ferrous alloy plates from above the sediment where stored in a low oxygen environment after recovery, which caused a significant change in the nature of the outer surface of the corrosion product layer. This could have lead to misinterpretation of the local microenvironment and the corrosion mechanisms and hence, the associated archaeological record.
- It is vitally important that metals are reburied to depths where there is no chance of partial exposure to the aerobic marine environment through sediment movement, since the non-ferrous metal coupons were found to be particularly sensitive to being in a mixed aerobic/anaerobic microenvironment.
- The resistance of a metal to corrosion is very dependent on the elemental composition and the associated microstructure, which records the impact of fabrication processes and depositional stress.

- The reburial environment surrounding the metal coupons has finally stabilised and as a result the long-term corrosion processes and associated mechanisms are becoming better indicators of the final corrosion outcomes.
- The concretions and corrosion product layers on the metal coupons are more extensively developed than after the first two years of exposure/reburial and therefore, the coupons are beginning to more accurately reflect the corrosion behaviour of marine archaeological metal artefacts.
- The extent of corrosion of all metal coupons decreased once the coupons were buried, even at shallow depths and this protective effect increased with increasing burial depth. This decrease was most marked for the brass and bronze coupons, but much less dramatic for the ferrous alloy coupons. Burial seemed to have the least effect on the pure copper coupons, however the extent of corrosion of the exposed copper coupons was also very low due to their pure composition and single phase microstructure.
- Despite a general decrease in the extent of corrosion with burial, all metal coupons exposed to the three different environments (exposed, buried just below the sediment and buried 50cm below the sediment), showed some increase in corrosion rate over the past four years. The greatest increases were found for the bronze and ferrous metal coupons buried at both depth intervals but the rate increases for the buried brass and copper coupons were considerably less. These results indicate that the greatest microenvironmental changes are occurring in the sediment and these changes are mainly affecting the corrosion behaviour of the buried bronze and ferrous alloy coupons.
- It appears that reburial has the most positive effect on brasses and to a lesser extent, bronzes. This significant decrease in corrosion would be primarily due to the biological toxicity of copper, zinc and tin corrosion products, which inhibit concretion formation and corrosion by effectively limiting bacterial counts in the surrounding sediment. The bronze coupons show more corrosion than the brass coupons as the three different phases in the bronze microstructure have significantly different electrochemical voltages as compared to the brass microstructure, which causes increased intergranular (micro-galvanic) corrosion.
- Reburial has less affect on the preservation of pure copper as it is a single phase alloy, with uniform composition and therefore, exhibits less intergranular galvanic corrosion.
- The positive effect of burial is significantly reduced on ferrous alloys due to the fact that iron corrosion products can be utilised by microbes and therefore, microbially induced corrosion (MIC) can become more significant in controlling the corrosion rates than direct access to dissolved oxygen.
- Since the major process ongoing in the Marstrand sediments is sulphate reduction and the metals trench contains sulphate, albeit at low concentrations at deeper depths and significant quantities of organic matter, it is probable that sulphate reducing bacteria are causing microbially influenced corrosion of the buried ferrous alloy coupons.

Based on the 2009 results, copper alloys could be recommended for reburial in these types of sediments for a period of six years. It is probable that pure copper and brass alloy types may be buried for longer periods of time and at shallower depths, however more information from the next phase of the experiment is required to support this inference. On the other hand, due to the significant

increase in corrosion rate of the leaded zinc bronze coupons over the past four years, it is not possible to recommend longer term reburial times for these alloy types at this point in time.

Conversely, ferrous alloys could not be recommended for reburial even in the medium term, based on their extensive degradation after six years and the significant increases in their corrosion rates since 2005, which may indicate that corrosion will increase parabolically over time. However, despite the concretion layers on the ferrous metal coupons being considerably better developed after six years they are not yet totally encapsulating, making extrapolation to the corrosion behaviour of totally concreted archaeological ferrous artefacts difficult at this stage. Even after six years, it is still difficult to make any definitive statements regarding the longer term stability of these alloy types. It is of paramount importance therefore that this project continues to the next phase, so as much information as possible regarding the corrosion processes of these metal coupons can be obtained. This will allow us to establish whether or not the present conclusions are real indicators of the effects of the different microenvironments on long-term metal corrosion and whether reburial is indeed, an appropriate preservation strategy for maritime archaeological metals.

# 1 INTRODUCTION

## 1.1 BACKGROUND

Reburial of underwater archaeological sites and excavated archaeological material is becoming increasingly common practice. Reburial may be an appropriate means of stabilizing and decreasing the deterioration rate of a site and the associated artefacts, however, there needs to be a holistic approach to the study of the material types and the environment, before and after reburial to gain a full understanding of the changes that are occurring on the site and determine the effectiveness of the technique.

The major purpose of the 'Reburial and Analyses of Archaeological Remains' project is to investigate and evaluate the effect of reburial on the most common material types found on underwater cultural heritage sites as a means of preserving archaeological remains *in-situ*. The project consists of six sub-projects. Four of the six sub-projects analyse the extent of deterioration of more commonly found materials on archaeological sites: wood; other organics such as leather, textiles, rope, etc; ceramics/silicates; metals. Another sub-project concentrates on assessing the stability of packing and marking materials used in archaeological documentation and the final sub-project involves monitoring chemical and physical changes occurring in the reburial environment over time.

In order to determine the long-term effects of reburial on the different material types, sufficient samples were buried to allow sampling to continue for up to 50 years. The wood, other organics, ceramics/silicates and polymers were buried in Marstrand Harbour, Sweden in September 2002, whereas the metal samples were buried the following year in September 2003. The environmental monitoring began in March 2003. The sample units were to be retrieved in the pre-determined order of 1, 2, 3, 6, 12, 24 and 48 years (Table 1). The first phase of the project covered the initial three year time interval (2003-2005) and the final report was published in 2007 (Nyström Godfrey and Berstrand 2007; Richards and MacLeod 2007). The final report for the first phase is available on the project website http://www.svk.com/reburial. However, since retrieval of the reburied samples are almost totally dependent on external funding, the six year retrieval period was postponed to 2009 and as such the reburial period was extended to seven years for the samples reburied in 2002. The final report for this retrieval interval is due in 2010.

*Table 1. Retrieval programme for the project.*

| Phase | Proposed Retrieval Year | Proposed Reburial Interval (yr) | Retrieval Year | Reburial Interval (yr) | Comments |
|---|---|---|---|---|---|
| 1 | 2003<br>2004<br>2005 | 1<br>2<br>3 | 2003<br>2004<br>2005 | 1<br>2 (1)[1]<br>3 (2) | Final report published in 2007 |
| 2 | 2008 | 6 | 2009 | 7 (6) | Final report due in 2010 |
| 3 | 2014 | 12 | | | Subject to funding |
| 4 | 2026 | 24 | | | Subject to funding |
| 5 | 2050 | 48 | | | Subject to funding |

[1] Number in brackets denote the reburial interval for the metal samples, which were reburied in 2003 one year after the other sample units.

## 1.2 AIMS

The aim of the metals sub-project is to investigate the corrosion of metals buried in the marine environment. The corrosion of reburied and exposed modern metal coupons will be examined and compared over time. This study will ascertain the effect of reburial on the deterioration of archaeological metals commonly found on underwater cultural heritage sites and assist in evaluating the effectiveness of reburial as a long-term *in-situ* preservation strategy for these types of archaeological remains.

## 1.3 SCOPE OF WORK

In September 2003, Vicki Richards travelled to Gothenburg, Sweden to prepare and rebury the metal sample units in Marstrand Harbour, Sweden. Two sets of metal sample units were retrieved and received in the Materials Conservation laboratory, Fremantle in 2004 and 2005. The interim report for the metals sub-project was finalised in 2006 and the final report for the first phase of the reburial project was published in 2007.

In 2009, six years after the initial reburial in 2003, another set of metal sample units (copper and iron alloys) were retrieved in September 2009. The following report will discuss the results of the metal sample analyses and the effect of the reburial environment on the extent of deterioration after this six year reburial period.

# 2 EXPERIMENTAL

## 2.1 METALS

### 2.1.2 Preparation of Sample Units

The samples units consisted of metal coupons of known metal composition mounted utilising high density polyethylene (HDPE) materials (Table 2). The metal coupons were prefabricated and purchased from Amac Alloys, Australia. The metal coupons deployed in the experiment were ferrous alloys: duplicate coupons of cast iron and mild steel and one standard Defence Science and Technology Organisation (DSTO) copper steel coupon (Figure 1) and copper alloys: duplicate coupons of brass, copper and bronze (Figure 2). All metal coupons were accurately weighed prior to mounting. The ferrous and copper alloys were mounted separately to minimise galvanic and proximity corrosion (Figure 3). Therefore, seven sample units for each alloy group were prepared to allow recovery and analysis after 1, 2, 3, 6, 12, 24 and 48 years (Table 1).

*Table 2. Metal coupon and support dimensions.*

| Material | Length (mm) | Width (mm) | Thickness (mm) | Surface Area ($cm^2$) |
|---|---|---|---|---|
| ***Copper Alloys*** | | | | |
| Brass[1] | 75 | 19 | 5 | 37.9 |
| Copper | 75 | 19 | 5 | 37.9 |
| Bronze | 75 | 12 | 5 | 26.7 |
| ***Ferrous Alloys*** | | | | |
| Cast Iron | 80 | 30 | 5 | 59.0 |
| Mild Steel | 75 | 20 | 5 | 39.5 |
| DSTO Copper Steel[2] | 100 | 50 | 3 | 109.0 |
| ***Supports*** | | | | |
| HDPE Plate[3] | 250 | 150 | 10 | na |
| HDPE Rod | 1000 | na | 50 (OD) | na |

1 All coupons had 5mm ID pre-drilled holes for attachment to the HDPE plates.

2 Some copper steel standard coupons were too heavy for the four figure balance at SVK (max = 120g), therefore a 10mm hole was drilled through the bottom of the coupon so that they could be weighed accurately prior to reburial.

3 The plates were perforated with 16mm pre-drilled holes to allow the flow of seawater through the plates and minimise differential aeration corrosion.

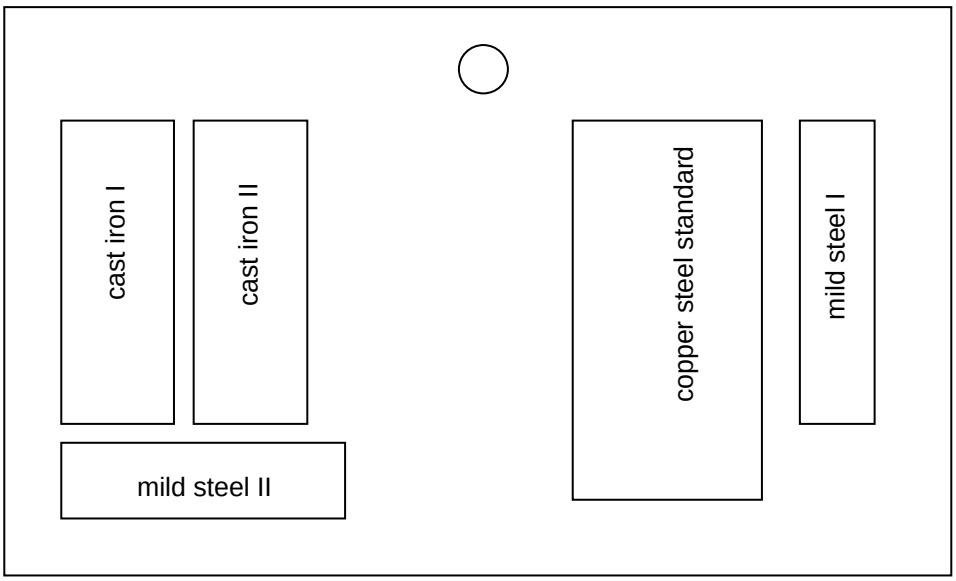


*Figure 1. Schematic diagram (scale 1:2) of the coupon orientation on the ferrous alloy support plate.*

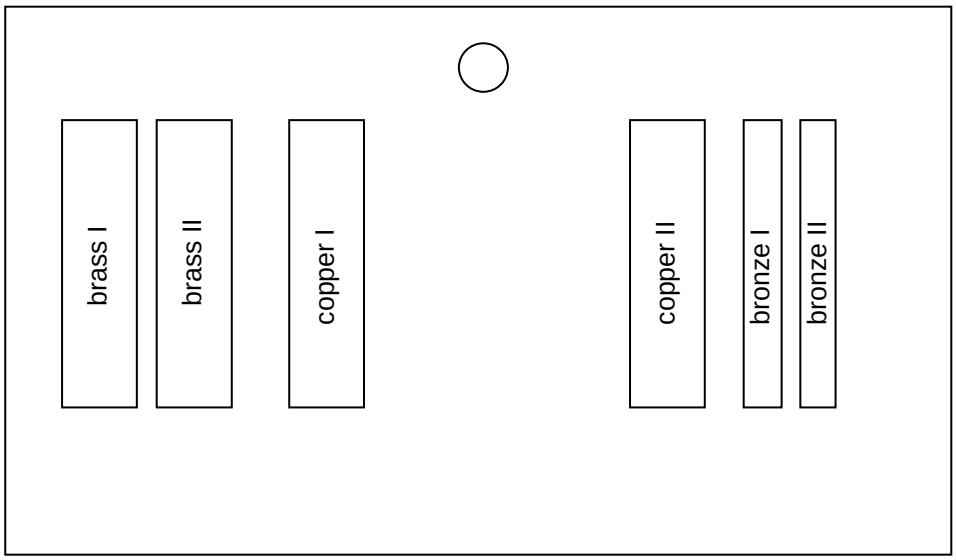


*Figure 2. Schematic diagram (scale 1:2) of the coupon orientation on the copper alloy support plate.*

*Figure 3. Completed metal alloy support plates: (left) copper alloy coupons; (right) ferrous alloy coupons.*

Each sample unit consisted of three sets of duplicate metal coupons, with the exception of the copper steel coupon where only one coupon was included, mounted at three different depth intervals on the HDPE rod so that one plate was totally exposed above the sediment, the second plate was buried just below the sediment and the third plate was buried approximately 50cm in the sediment (Figure 4). Each set of duplicate metal samples were separated and secured with plastic cable ties to three perforated HDPE plates then attached to a HDPE rod at the specified depth intervals with HDPE nuts and bolts (Figure 5).

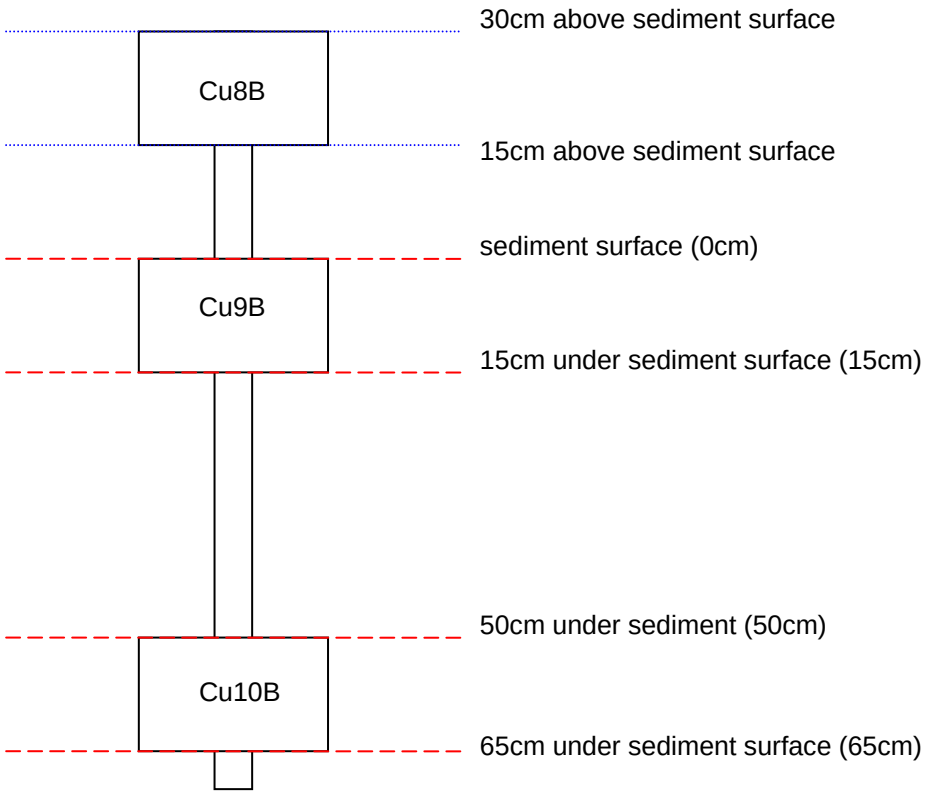


*Figure 4. Schematic diagram (scale 1:10) of the copper alloy coupon support plate arrangement on rod 3 retrieved in 2009.*

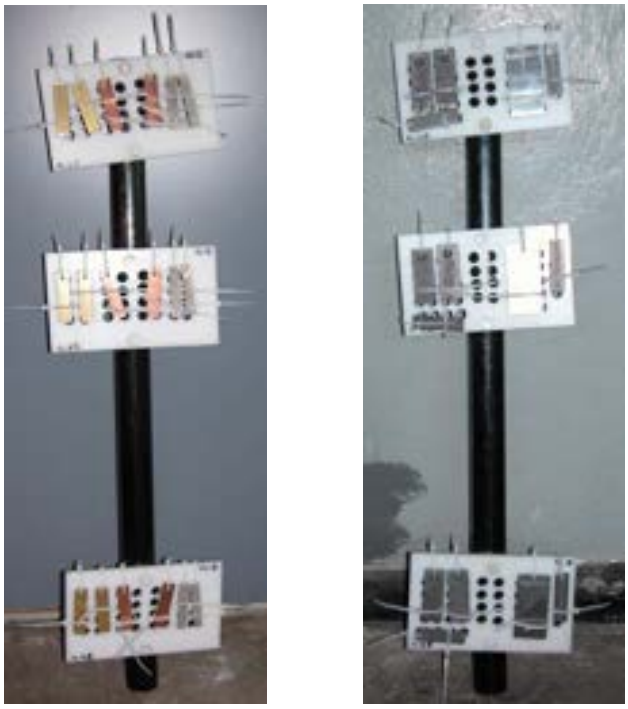

*Figure 5. Completed sample units: copper alloys (left); ferrous alloys (right).*

In addition, three sets of metal control samples were accurately weighed and stored in the laboratory in oxygen barrier bags with Ageless© oxygen scavenger packets and Ageless© oxygen eyes. Finally the storage bags were flushed with argon and heat sealed. The oxygen scavenger packets consist of finely divided iron powder which reacts with any oxygen that may infiltrate the bags and the eyes indicate any oxygen ingress by turning from pink to blue in the presence of oxygen.

### 2.1.2 Reburial of Sample Units

The fourteen sample units were placed on-site on 30 September 2003 (Figure 6). Fortunately the sediment in the metal reburial trench was loosely packed and the units were simply pushed into the sediment to the required depth without the need for dredging and subsequent backfilling. The copper and ferrous alloy sample units were reburied in two rows separated by a distance of approximately 3m with about 1-2m between each sample unit. The position of the sample units are shown diagrammatically in Figure 7.

*Figure 6. Examples of the metal sample units in-situ immediately after reburial in 2003 (copper alloys:left; ferrous alloys:right).*

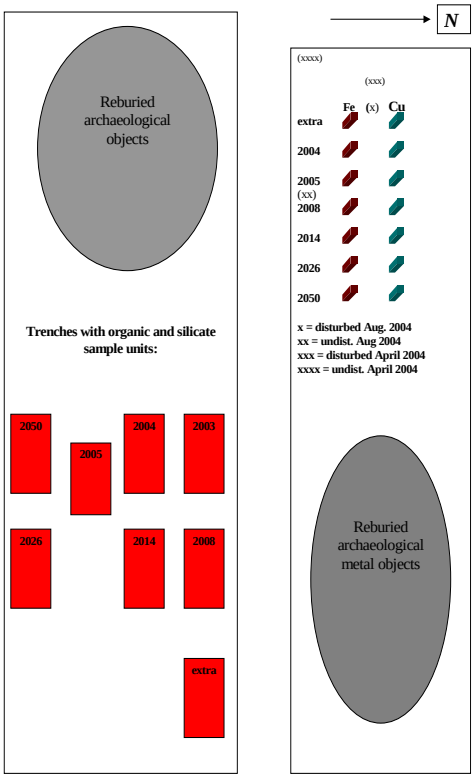


*Figure 7. Schematic plan of the reburial trenches and sediment sampling positions.*

### 2.1.3 Retrieval of Sample Units

The third set of metal sample units [copper alloys sample unit (rod 3) and ferrous alloys sample unit (rod 5)] were retrieved on 22 September 2009, after 6 years on-site. The ferrous alloy sample unit (rod 3) could not be located due to zero in-water visibility, therefore another sample unit (rod 5) was recovered (Table 3). The sample units were photographed *in-situ* prior to any physical disturbance (Figure 8). Each sample unit was then removed by physically extracting the rods from the sediment and the surface pH and corrosion potentials ($E_{corr}$) of each coupon measured *in-situ* on the seabed prior to recovery.

*Figure 8. Sample units in-situ prior to removal in 2009: copper alloy (rod 3) (left); ferrous alloy (rod 5) (right).*

Biological growth and the corrosion product layer were mechanically removed from a small section of each coupon prior to the electrochemical measurements. The surface pH was determined by using a BDH GelPlas flat surface pH electrode connected to a Cyberscan 200 pH meter sealed inside a custom-built plexiglass waterproof housing. Immediately after removal of the biological and corrosion layers the corrosion potential ($E_{corr}$) was measured on a high impedance digital multimeter, sealed in a custom-built plexiglass waterproof housing, set to read at 2V direct current. The measured voltage refers to the difference in electrical potential between a platinum working electrode and a silver/silver chloride/seawater electrode ($Ag/AgCl_{seawater}$). The $E_{corr}$ of the point was measured by firmly pressing the platinum electrode onto the exposed metal surface of the coupon. Good electrical contact was made when the voltage reading was very stable, changing only ±1mV. The surface pH of the each metal coupon was then measured with a flat surface pH electrode held directly against the same exposed metal surface area and the minimum pH reading was recorded.

The sample units were recovered, placed on the adjacent jetty and photographed (Figure 9). The plates were unbolted from the rods and as much biological growth as practicable was removed from the plates to satisfy Australian quarantine regulations without damaging the corrosion product layers. The plates were then photographed separately.

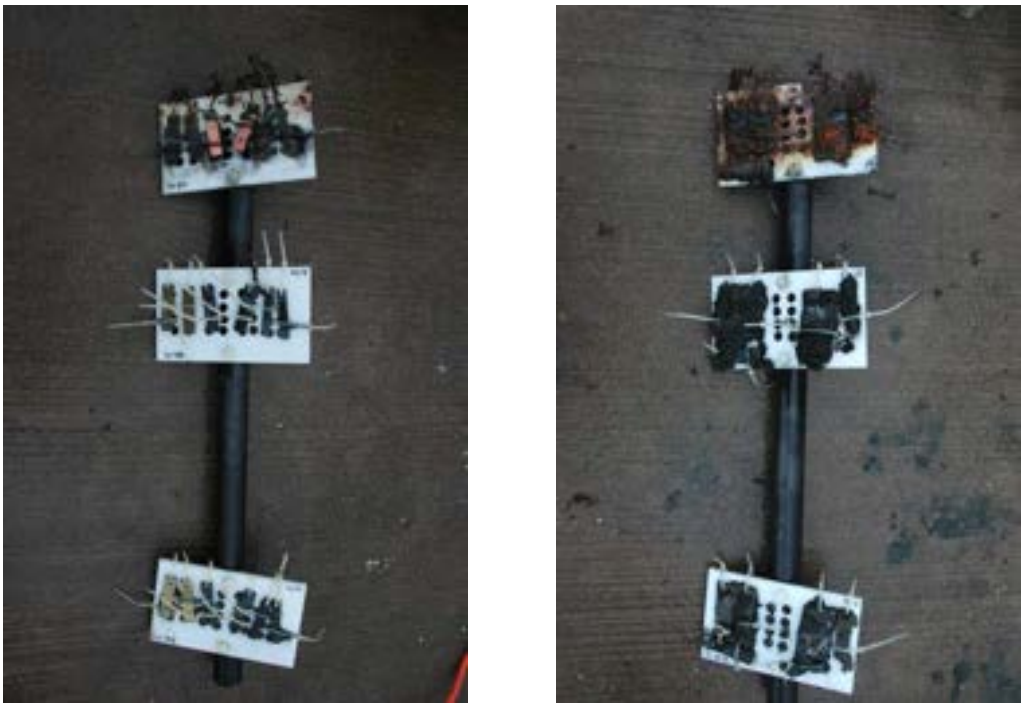

*Figure 9. Sample units immediately after recovery in 2009: copper alloys (left); ferrous alloys (right).*

The plates were rinsed with deionised water and lightly patted with tissue paper to remove the excess water and wrapped in polyester wadding. Each plate was placed in an oxygen barrier bag (ESCAL barrier film) together with an oxygen scavenger RP-A (2000 ml) and an oxygen indicator eye, which was then sealed with an ESCAL clip. The entire procedure from recovery to sealing the oxygen barrier bags took approximately one hour. Initially the oxygen indicators turned

blue or bluish pink in the bag indicating the presence of some oxygen. The bags were placed in an insulated cold box with ice packs for transportation back to the SVK laboratories in Gothenburg. After 36 hours all indicators had turned pink indicating that no oxygen was present in the bags. The bags were then placed in a freezer prior to being packed in one box and couriered to the conservation laboratories in Fremantle. The coupons arrived in October 2009. On arrival in the Materials Conservation laboratories, each barrier bag was opened and approximately 15 fresh Ageless© oxygen scavenger sachets were added and the bags resealed awaiting further analysis.

### 2.1.4 Preparation of Metal Coupons

The metal coupons were documented, prepared and analysed over an eight week period from March to April 2010. A general analytical regime is outlined below and metal coupon descriptions after sample preparation are shown in Table 3.

1. All control coupons, stored in an oxygen barrier bag with Ageless© oxygen scavengers since 2009, were removed, photographed and resealed in the bag with fresh oxygen scavengers.
2. The recovered experimental coupons were photographed on their plates (front view of all coupons and close ups of each alloy type).
3. The cable ties attaching the coupons to the plate were removed and the coupons rotated.
4. The rotated coupons were then re-photographed (rear view of all coupons and close ups of each alloy type).
5. All copper and ferrous alloy coupons recovered from just below the sediment and 50cm below the sediment were replaced in their oxygen barrier bags with fresh Ageless© oxygen scavengers, flushed with argon and resealed awaiting SEM/EDX analysis.
6. The rear surfaces (surfaces laying against the HDPE plates) of all copper alloy I coupons and the front surfaces (exposed to the environment) of all copper alloy II coupons were analysed by SEM/EDX spectroscopy.
7. The rear surfaces (surfaces laying against the HDPE plates) of the cast iron I and mild steel II coupons and the front surfaces of the cast iron II, the standard DSTO copper steel and the mild steel I coupons were analysed by SEM/EDX spectroscopy.
8. Immediately after SEM/EDX analysis all copper and ferrous alloy coupons recovered from just below the sediment and 50cm below the sediment were replaced in their oxygen barrier bags with fresh Ageless© oxygen scavengers, flushed with argon and resealed awaiting mechanical and chemical stripping.
9. The corrosion products from all copper alloy I coupons and the cast iron I, the standard DSTO copper steel and the mild steel II coupons above the sediment were mechanically removed by carefully scraping the surface with a scalpel blade and placed in vials awaiting XRD analysis.
10. The corrosion products were removed from the cast iron I, the standard DSTO copper steel and the mild steel II coupons recovered from just below the sediment and 50cm below the sediment and placed in vials, flushed with argon and stored in a vacuum dessicator filled with argon to minimise aerial oxidation prior to XRD analysis.

11. The mechanically cleaned coupons were then placed in solutions to chemically remove any adherent corrosion products. Note the chemical stripping of the coupons was not taken to completion and some adherent corrosion products remained on the surfaces, especially on the coupons recovered from the sediment. This was so the effect of the corrosion on the underlying metallographic structure could be ascertained and the changes could not be attributed to chemical etching of the parent metal.
12. Copper alloys were placed in 0.5% (w/v) benzotriazole (previously dissolved in 20ml ethanol)/25% (w/v) copper sulphate in 50% concentrated hydrochloric acid (specific gravity 1.19) for approximately 2 hours, removed, gently scrubbed under running water then ethanol and dewatered in acetone. This procedure was repeated at longer time intervals to a maximum of 5 hours until the visible corrosion products were removed.
13. Ferrous alloys were placed in Clarke's solution [2% antimony oxide/5% tin chloride in concentrated hydrochloric acid (specific gravity 1.19)] for approximately 4 hours, removed, gently scrubbed under running water, dewatered with acetone and allowed to air dry. Again this procedure was repeated until the visible corrosion products were removed.
14. The stripped coupons were weighed and normalised for surface area.
15. All chemically stripped ferrous coupons were repacked in oxygen barrier bags with Ageless© oxygen scavengers and indicator eyes, flushed with argon and heat sealed prior to SEM/EDX analysis.
16. All stripped coupons were reanalysed by SEM/EDX and resealed in the oxygen barrier storage bags where appropriate.

*Table 3. Description of metal coupons from sample units retrieved 22/9/09.*

| Rod No. | Plate No. | Plate Description | Metal Coupon No. | Coupon Description |
|---|---|---|---|---|
| ***Copper Alloy Coupons*** | | | | |
| Rod 3 | Plate Cu8 | above sediment | Cu8 Bs I (s) | brass I (stripped) |
| | | | Cu8 Bs II | brass II (unstripped) |
| | | | Cu8 Cu I (s) | copper I (stripped) |
| | | | Cu8 Cu II | copper II (unstripped) |
| | | | Cu8 Bz I (s) | bronze I (stripped) |
| | | | Cu8 Bz II | bronze II (unstripped) |
| | Plate Cu9 | just below sediment (0-15cm) | Cu9 Bs I (s) | brass I (stripped) |
| | | | Cu9 Bs II | brass II (unstripped) |
| | | | Cu9 Cu I (s) | copper I (stripped) |
| | | | Cu9 Cu II | copper II (unstripped) |
| | | | Cu9 Bz I (s) | bronze I (stripped) |
| | | | Cu9 Bz II | bronze II (unstripped) |
| | Plate Cu10 | 50cm below sediment (50-65cm) | Cu10 Bs I (s) | brass I (stripped) |
| | | | Cu10 Bs II | brass II (unstripped) |
| | | | Cu10 Cu I (s) | copper I (stripped) |
| | | | Cu10 Cu II | copper II (unstripped) |
| | | | Cu10 Bz I (s) | bronze I (stripped) |
| | | | Cu10 Bz II | bronze II (unstripped) |
| ***Ferrous Alloy Coupons*** | | | | |
| Rod 5 | Plate Fe14 | above sediment | Fe14 Fc I (s) | cast iron I (stripped) |
| | | | Fe14 Fc II | cast iron II (unstripped) |
| | | | Fe14 FCu (s) | copper steel (stripped) |
| | | | Fe14 Fw I | mild steel[1] (unstripped) |
| | | | Fe14 Fw II (s) | mild steel (stripped) |
| | Plate Fe15 | just below sediment (0-15cm) | Fe15 Fc I (s) | cast iron I (stripped) |
| | | | Fe15 Fc II | cast iron II (unstripped) |
| | | | Fe15 FCu (s) | copper steel (stripped) |
| | | | Fe15 Fw I | mild steel (unstripped) |
| | | | Fe15 Fw II (s) | mild steel (stripped) |
| | Plate Fe16 | 50cm below sediment (50-65cm) | Fe16 Fc I (s) | cast iron I (stripped) |
| | | | Fe16 Fc II | cast iron II (unstripped) |
| | | | Fe16 FCu (s) | copper steel (stripped) |
| | | | Fe16 Fw I | mild steel (unstripped) |
| | | | Fe16 Fw II (s) | mild steel (stripped) |

1 The contemporary mild steel coupons were used to approximate wrought iron.

### 2.1.5 Scanning Electron Microscopy/Electron Dispersive X-ray Analysis (SEM/EDX)

Each stripped and unstripped metal coupon was examined using a Philips XL40 CP variable pressure scanning electron microscope equipped with a Robinson scintillator back-scatter electron detector and an EDX energy dispersive (EDS) system. The microscope was operated at 0.5m Bar and 30kV at a working distance of approximately 10-15mm. Digital electron micrographs (SEM) and energy dispersive x-ray analyses (EDX) were collected as the primary data.

# 3 RESULTS AND DISCUSSION

## 3.1 REFERENCE COUPONS

In order to facilitate discussions about the changes to the metals that occur over this extended reburial experiment it is essential to understand the composition, morphology and surface detail of the original metals since it is the interaction of these surfaces with the marine environment that dictates the ultimate survival of the metals. The composition of the reference coupons are listed in Tables 4 and 5.

*Table 4. Composition of copper alloy coupons.*

| Alloy Name[1] | Cu | As | Sn | Zn | Pb | Fe |
|---|---|---|---|---|---|---|
| **Copper** | 99.90[2] | - | - | - | - | - |
| **Brass** | 55.0 - 60.0 | - | - | 36.2 – 43.4 | 1.5 – 3.0 | 0.00 – 0.25 |
| **Bronze** | 85.93 | 0.01 | 10.0 | 2.7 | 1.1 | 0.02 |

1 All metal compositions were provided by the supplier of the metal coupons.

2 Oxygen by difference.

*Table 5. Composition of the iron alloy coupons.*

| Alloy Name | Fe | C | Si | Mn | P | S | Ti | Ni | Cr | Cu |
|---|---|---|---|---|---|---|---|---|---|---|
| **Copper Steel** | 98.53 | 0.16 | 0.05 | 0.61 | 0.01 | 0.03 | - | 0.27 | 0.12 | 0.22 |
| **Cast Iron** | 92.6-94.0 | 3.0-3.6 | 2.4-2.9 | 0.35-0.65 | <0.1 | residual | 0.12-0.20 | residual | residual | residual |
| **Mild steel** | 98.94 | 0.14 | 0.16 | 0.71 | 0.12 | 0.04 | - | - | - | - |

### 3.1.1 Copper Coupons

The reference copper coupons were a standard high quality electrolytic tough pitch metal with a lustrous finish (Figure 10). The EDX analysis of the pure copper coupon detected no other elements except copper. The surface showed longitudinal striations due to the rolling processes in the manufacturing of the coupon (Figure 10). This feature dominated the distribution of localised corrosion processes during all phases of the experiment to date.

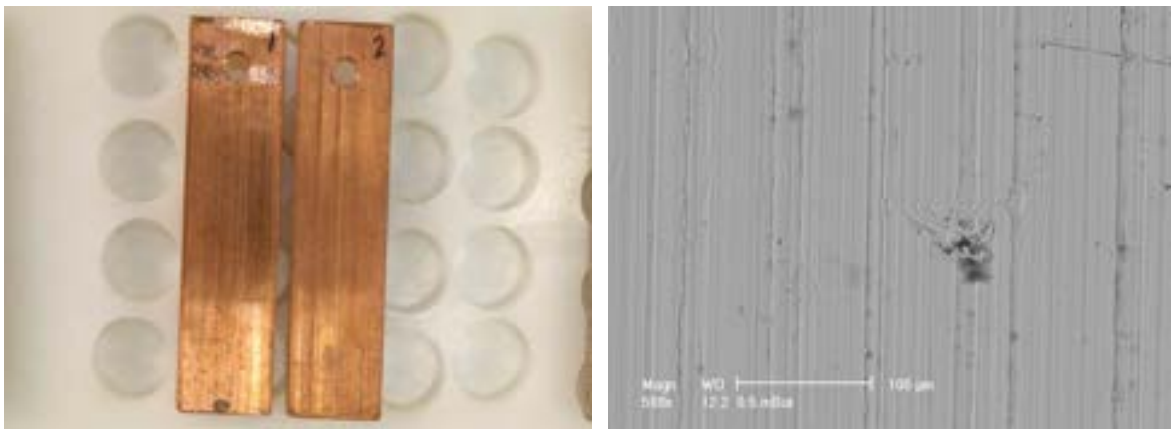

*Figure 10. Copper reference coupons (left); SEM image of the copper reference coupon (right) indicating the longitudinal rolling lines associated with cold working.*

### 3.1.2 Brass Coupons

The coupon had the typical appearance of a duplex brass with a rich yellow finish as expected of a 36 – 43% leaded zinc brass alloy (Figure 11). The striations from the rolling of the parent alloy are clearly visible to the naked eye. The SEM images showed up the presence of the lead along the striations and the EDX analysis reflected the wet chemical analytical data on the parent alloy (Figure 11).

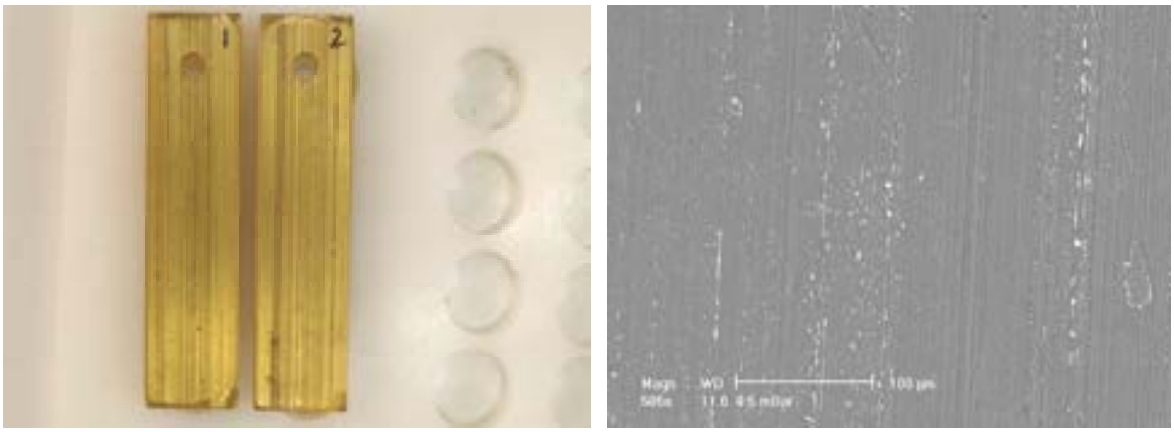

*Figure 11. Brass reference coupons (left); SEM image of the brass reference coupon (right) indicating the lead (bright areas) concentrated along the longitudinal lines of working.*

### 3.1.3 Bronze Coupons

The coupon as received was characterised by a rough surface which had the appearance of the fine sand casting associated with its manufacture (Figure 12). Where mechanical working had taken place the underlying metal was a soft yellow-brown colour. The bronze reference coupons are approximately 86% Cu, 10% Sn, 1% Pb and 3% Zn and as such, are classified as a medium leaded zinc bronze typical of 19$^{th}$ century marine bronzes. The SEM image of the reference coupon (Figure 12) clearly showed the strong coring and segregation of the alloy into tin-rich (α+δ) eutectic phases, where the lead was concentrated as droplets and the copper rich α phases, where the zinc tends to be present in solid solution.

Even in the uncorroded state the SEM image showed up the localised concentrations of lead at the edge of the tin-rich (α+δ) eutectoid.

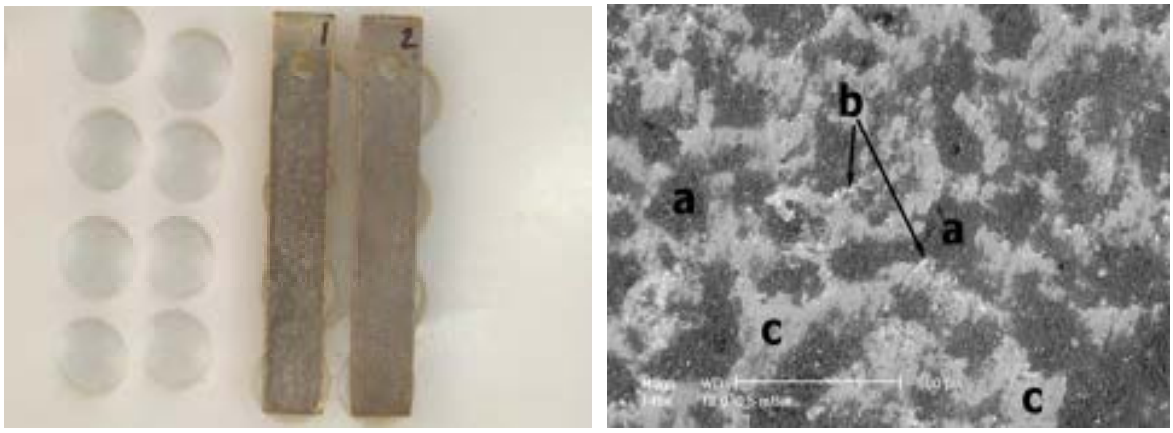


*Figure 12. Bronze reference coupons (left); SEM image of the bronze reference coupon (right) indicating the tin-rich phases (a) with the lead concentrated along the grain boundaries (b – bright spots) and the copper-rich phases (c).*

### 3.1.4 Copper Steel Coupons

Copper steel may be classed as a low alloy steel. The addition of relatively low concentrations of copper markedly improves the atmospheric corrosion resistance of steels however, the beneficial effects are doubtful under sheltered conditions of atmospheric exposure, burial in soil or immersion in natural waters, such as seawater. It is speculated that the copper in copper steels consolidates the rust by forming a corrosion product layer that is lower in porosity and more dense than that present on non-alloyed mild steel. The addition of copper may also influence the rate of rusting by raising the potential of the surface to more noble values and so encourage passivation of the surface. However, in this experiment even though the corrosion resistance in seawater is questionable, the copper steel coupons were chosen to provide reliable corrosion rates that were based on general surface corrosion, rather than being associated with zonal corrosion of cast iron or pitting corrosion of wrought iron.

The coupons were characterised by being a semi-lustrous grey metal (Figure 13). The metal composition from wet chemical analysis is outlined in Table 5. The SEM image showed up some small inclusions and the grain boundaries are clearly visible in the unetched sample (Figure 13). The EDX analysis showed up the manganese and silicon impurities and no localised copper concentration. The presence of copper in a solid solution of ferrite or α iron, helps to depolarise the micro-galvanic cells that otherwise tend to rapidly develop on iron on immediate exposure to the marine environment. The more uniform corrosion of the copper steel will provide comparative data for artefacts that are typical of early 19$^{th}$ and 20$^{th}$ century steel, such as used in kitchen utensils, pots, pans and cutlery. This style and form of artefact may well be a significant proportion of objects that require reburial in the future.

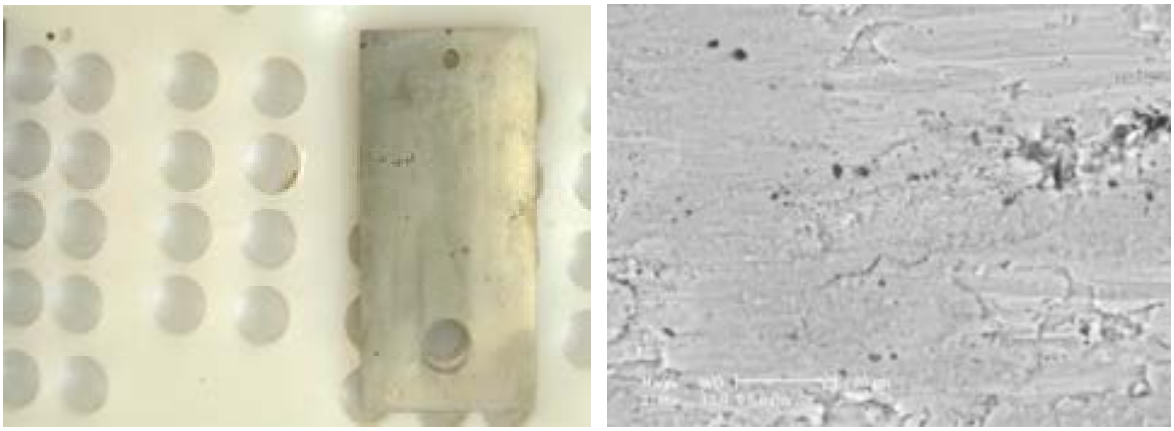

*Figure 13. Copper steel reference coupon (left); SEM image of the copper steel reference coupon (right) indicating some inclusions and the grain boundaries.*

### 3.1.5 Cast Iron Coupons

Cast iron was the most common iron alloy associated with the manufacture of bulky objects such as cannon, bollards, winches, windlasses, etc and simple ordnance in the form of cannon balls. The composition shown in Table 5 of the reference coupons is typical of materials from the 16$^{th}$ to the 21$^{st}$ century and as such, the corrosion data is directly relevant to any historic cast iron object. The cast iron coupons had a rough sand-cast finish and a deep grey semi-lustrous hue (Figure 14). The SEM image revealed the underlying metallurgical structure in that there were well developed zones that showed the presence of ferrite (essentially pure iron), cementite ($Fe_3C$), pearlite (a combination of ferrite and cementite) and graphite, which are the principal components of cast iron (Figure 14). The EDX analysis was adjusted to incorporate the presence of carbon for all cast iron analyses.

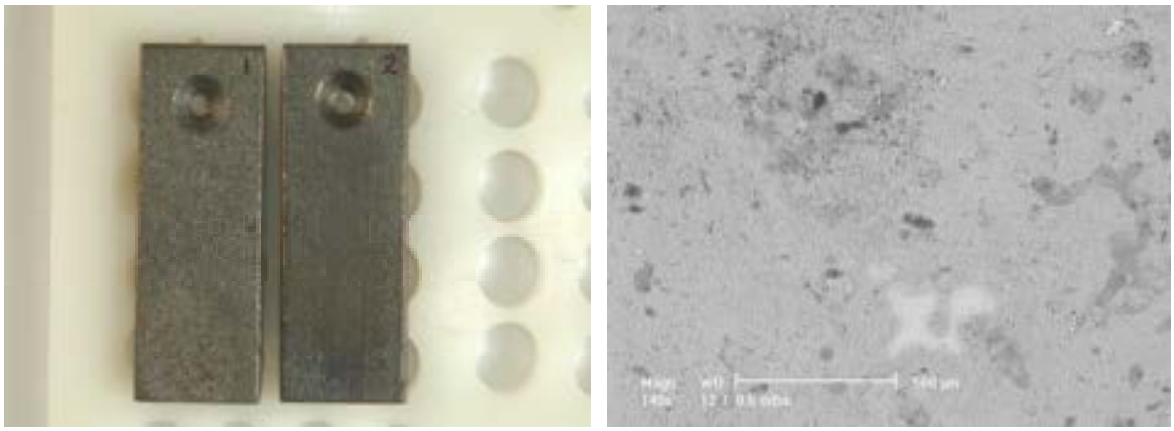

*Figure 14. Cast iron reference coupons (left); SEM image of the cast iron reference coupon (right) indicating the different phases.*

### 3.1.6 Mild Steel Coupons

Mild steel was chosen as a modern substitute for historic wrought iron. Wrought iron and its unique composition and microstructure present very challenging conservation issues to bring about successful stabilisation in the long term. The

overall chemical composition of mild steel is very similar to that of wrought iron and provides the best comparative modern alloy. The coupons had the normal appearance of a dull-grey smooth metal finish and there were no visible inclusions or gross deformations on the surface (Figure 15). The SEM showed up the presence of 45-60µm slag inclusions. Although the amount of silicon in the mild steel does not appear to be great, its localised distribution as slag filaments makes up for the low weight of the element and the zonal corrosion around the inclusions has a most dramatic effect on the penetration of chloride ions. Naturally subtle differences in microstructures associated with being hand and machine wrought, as compared with being rolled in a modern steel mill, may lead to slight differences of interpretation of the impact of the microenvironment on the decay of the objects.

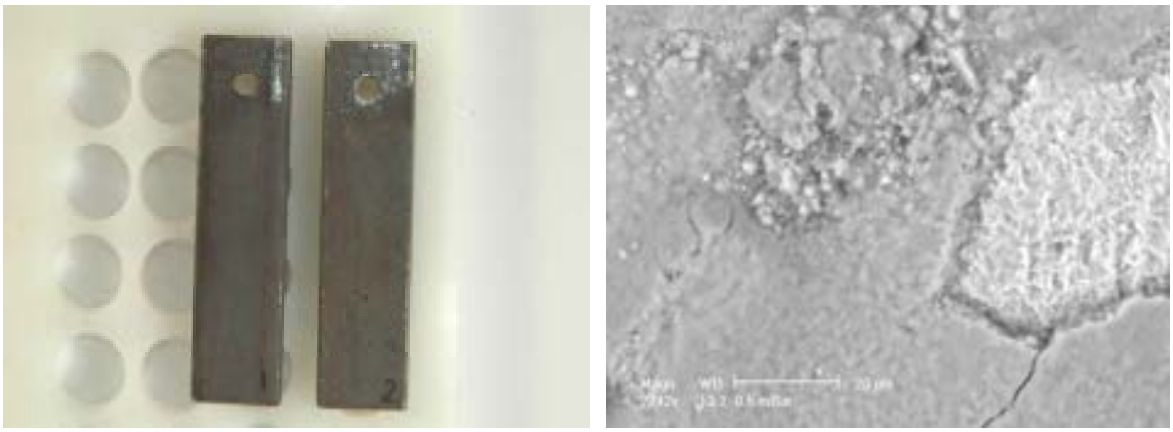

*Figure 15. Mild steel reference coupons (left); SEM image of the mild steel reference coupon (right) indicating the slag inclusions.*

## 3.2 GENERAL OBSERVATIONS

The cable ties used to separate the copper alloy coupons in order to minimise galvanic corrosion caused some differential aeration corrosion in the areas under and directly adjacent to the ties. However the effect was localised and did not seem to affect the primary corrosion mechanisms occurring on the coupons. In addition, the holes drilled in the support plate to allow the flow of seawater and exchange of interstitial water under the sediment also caused differential aeration corrosion on the rear of the coupons. Again these effects were minimal and very localised and did not affect the overall corrosion mechanisms.

Problems were also encountered during the retrieval and packing procedure, which resulted in dehydration and subsequent oxidation of some of the surface corrosion products in transit, storage and during sample preparation. Hence, extreme care must be taken to ensure that minimal post recovery changes occur to the samples prior to analysis. This will ensure that minimal changes occur to the corrosion products and concretion and therefore, any post recovery analysis will be representative of the depositional environment and not a consequence of the storage environment.

It should also be noted that in the SEM images of the stripped iron alloy coupons the bright areas, those of high atomic number contrast, are artefacts of the surface preparation methods using Clarke's solution, which contains concentrated

hydrochloric acid with antimony oxide and tin chloride. Since antimony (III) is only soluble in strongly acidic solutions the consumption of the acid by the concretion and corrosion products matrix clearly decreases the solution pH to the point of precipitation. It is therefore advisable to keep the strength of the hydrochloric acid constant as the calcareous matrices are dissolved during the stripping process to avoid contamination of the stripped metal surfaces with precipitated antimony compounds.

## 3.3 ENVIRONMENTAL CONDITIONS - AEROBIC

### 3.3.1 Copper Coupons: Above Sediment

#### 3.3.1.1 Corrosion

The initial decay patterns on the copper coupons (Cu I & Cu II) recovered after 1, 2 and 6 years (Figure 16) showed the expected corrosion patterns for a kinetically controlled process. The colour of the coupons was generally blue-green typical of the Cu (II) corrosion products for 1 and 2 years of exposure but inspection of the copper coupons after 6 years of exposure showed zonal corrosion due to a mixed exposure environment possibly caused by migration of the sample unit into the sediment which had previously been observed to a lesser extent in 2004 (Figure 16; top left). This reality caused a fundamental change in microenvironment and so the apparent patina from aerobic corrosion was only found on the upper sections of these coupons (Figure 16; bottom).


*Figure 16. Copper alloy coupons – above sediment, immediately after recovery in 2004 after 1 year of exposure (top left), in 2005 after 2 years of exposure (top right) and in 2009 after 6 years of exposure (bottom).*

After recovery from the site in September 2009, the plate was packed in an oxygen free environment for approximately 5 months (See Section 2.1.3). The low oxygenated environment had caused some visual changes to the copper coupons, most markedly a darkening of the corrosion products (Figure 17; right). During storage the bright pink surface changed to a typical mid brown colour associated

with cuprite as the primary copper (I) chlorides were hydrolysed. It was also noted that the patina on the upper exposed sections also changed in storage and this was due to upward migration of the primary copper (I) chlorides through the copper (II) hydroxychloride layer and their subsequent hydrolysis to produce more cuprite.

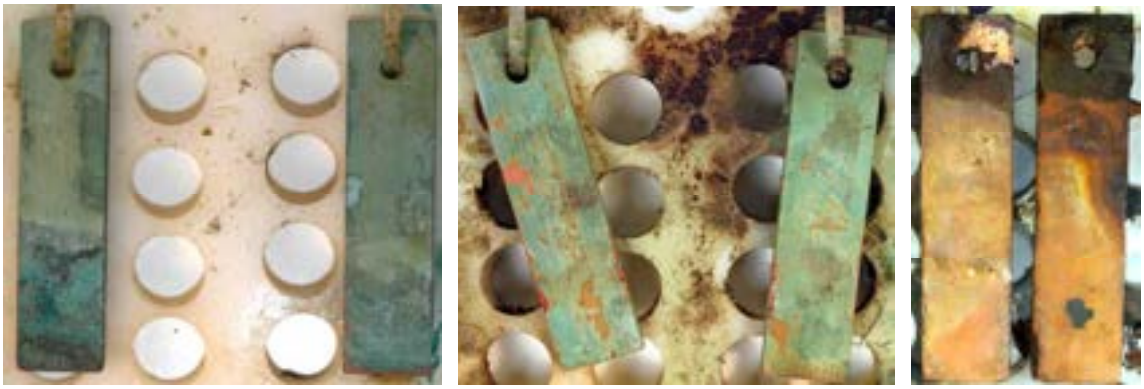

*Figure 17. The copper coupons – above sediment recovered in 2004 after 2 years of storage (left), in 2005 after 1 year of storage (mid) and in 2009 after 5 months of storage (right).*

The SEM image of the unstripped copper coupon in 2004 showed a cracked surface of copper (II) hydroxychloride corrosion products due to dehydration in storage (Figure 18; left). In the same way the 2005 SEM image showed different areas that had developed from the background pavement of cracked copper (II) hydroxychlorides into well defined copper chlorides, likely to be nantokite (CuCl), and cuprite ($Cu_2O$) as seen in Figure 18 (right). These observations are consistent with aerobic corrosion of copper in seawater.

The SEM images of the unstripped copper coupon recovered in 2009 showed dehydrated copper (II) hydroxychloride corrosion product layers similar to those observed in 2004 and 2005 (Figure 19). However, the EDX analysis of the bright areas confirmed that these were regions associated with the formation of $Cu_2S$ (chalcocite) which appear to be due to cracked areas of the copper (II) hydroxychlorides allowing the primary copper (I) chloride complexes to diffuse through and then precipitate as copper sulphides. These corrosion products would have been formed in-situ and not from extended storage in the less oxygenated environment, where the formation of copper sulphides would be kinetically unfavourable under those conditions. The right hand image in Figure 19 showed the intergranular corrosion of the copper coupon where the corrosion products had disbonded from the metal substrate. The corrosion product layers noted in region “b” had essentially the same composition and structural details as the primary layer on the upper section of the coupon.

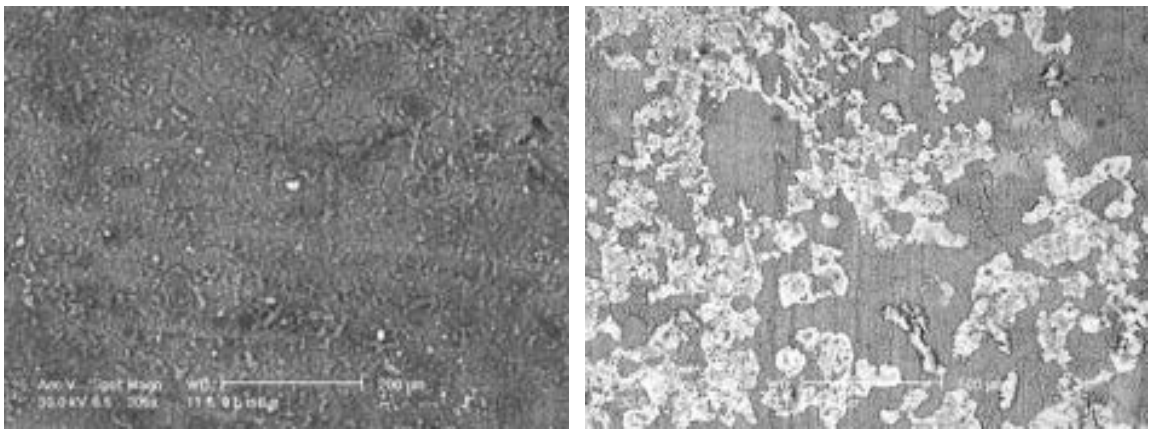

*Figure 18. SEM images of the unstripped copper coupons recovered from above the sediment in 2004 (left): the copper (II) hydroxychlorides (dark grey) and in 2005 (right): the copper (II) hydroxychlorides (dark grey) and the copper chloride and cuprite (light grey).*

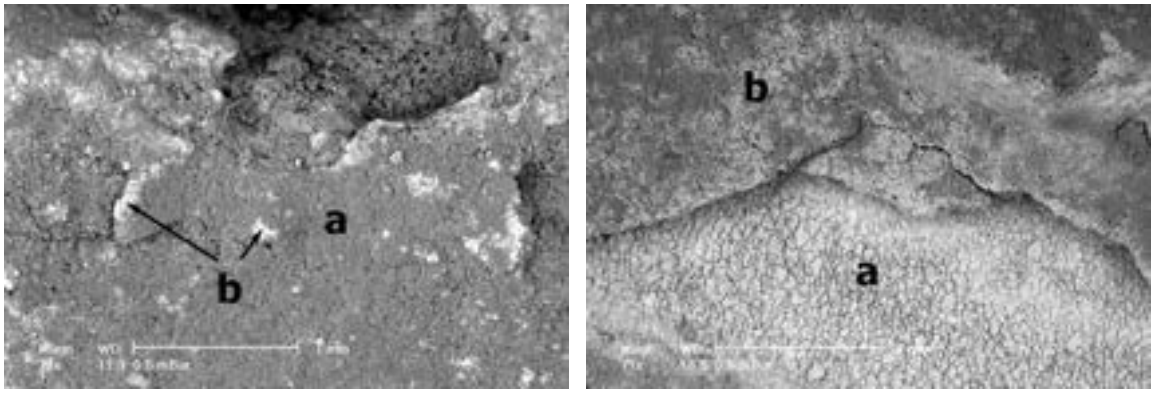


*Figure 19. SEM images of the unstripped copper coupon recovered from above the sediment in 2009 - upper section of the coupon (left): (a) the copper (II) hydroxychlorides (dark grey); (b) copper sulphides (bright areas) - lower section of the coupon (right): (a) the intergranular corrosion pattern of the parent copper metal (b) copper (II) hydroxychlorides (dark grey) and copper sulphides (light grey areas) on the surface of the grains.*

The SEM image of the stripped copper coupon after one year of exposure (Figure 20; top left) highlighted the anticipated intergranular corrosion pattern that is typical of pure copper and where the granular surface was partly occluded the corrosion products were primarily copper (I) chloride. A more detailed inspection of the surface after 2 years of exposure (Figure 20; top right) showed up increased corrosion surrounding the grains. The initial reaction mechanism had been one of surface corrosion of the grains after one year. This had largely changed to intergranular corrosion after 2 years and was fully dominated by this process after a period of six years as shown in Figure 20 (bottom), which is a characteristic of recovered archaeological copper.

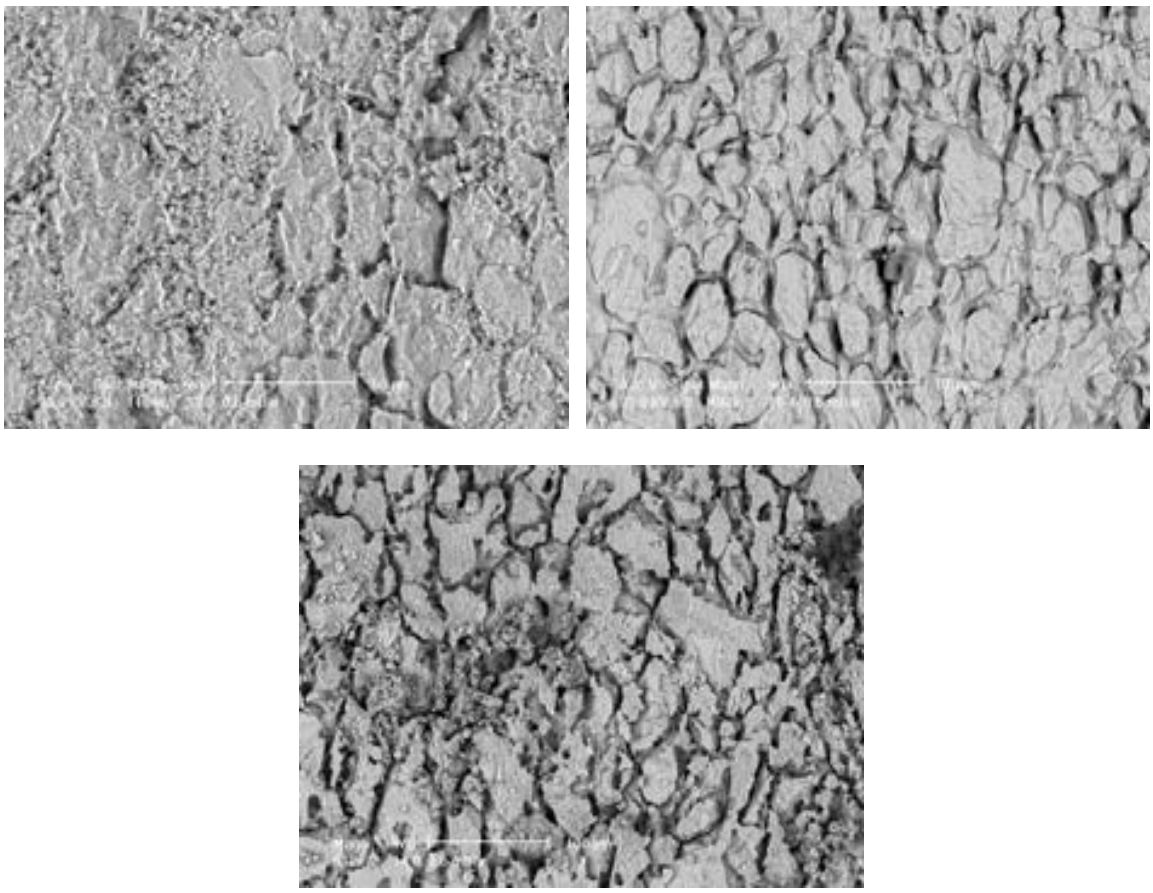

*Figure 20. SEM images of the stripped copper coupons recovered from above the sediment in 2004 (top left), in 2005 (top right) and in 2009 (bottom) showing the increase in intergranular corrosion over this period.*

There is no real difference in the corrosion mechanism causing the degradation of the 2005 coupons as compared to the 2004 coupons but the relative intensity of decay reflects the increased time of exposure. The 2009 coupons show the same basic corrosion profiles in the upper sections (continuous exposure to flowing seawater) but on a more intense basis which leads to exposed grains on the metal surface. The mechanism more applicable to the lower sections of the 2009 copper coupons is best described by reference to corrosion below the sediments (see latter discussions). The presence of the copper chloride mineral in the corrosion product layers supports the increased immersion time in that after 2005 the coupons are slowly equilibrating with the local environment and the typical aerobic corrosion mechanism for historic copper artefacts in an open marine environment is becoming dominant. That is, as the cuprite layer becomes more uniform over the entire copper coupon surface, it acts as a bipolar electrode forming a semi-permeable layer that effectively separates the corrosion reactions, where the anodic reaction (equation 1) occurs on the metal side of the $Cu_2O$ layer while the cathodic reaction, reduction of oxygen (equation 2), occurs on the seaward side.

$$Cu \rightarrow Cu^{+} + e^{-} \quad \text{.....(1)}$$

$$O_2 + 2H_2O + 4e^{-} \rightarrow 4OH^{-} \quad \text{.....(2)}$$

The copper (I) ions diffuse away from the metal surface to the bulk seawater where the pH is about 7.5 to 8.0 and subsequent hydrolysis favours the production of cuprite ($Cu_2O$) rather than CuCl in this pH range (equation 3).

$$2Cu^+ + H_2O \rightarrow Cu_2O + 2H^+ \quad \text{.....(3)}$$

This results in a decrease in the pH at the metal surface and a subsequent increase in chloride ion concentration above that of the surrounding seawater as the chloride ions diffuse in to balance the charge of metal ions. Therefore at the lower pHs (< ~5.60) and higher chloride concentrations under the uniform cuprite layer the formation of the copper chloride, nantokite (CuCl) is favoured (equation 4).

$$Cu_2O + 2H^+ + 2Cl^- \rightarrow 2CuCl + H_2O \quad \text{.....(4)}$$

In addition, at the metal surface the concentration of chloride ions is sufficient for the insoluble CuCl to also form a series of soluble complexes, such as $CuCl_2^-$ under the cuprite layer, which diffuse away from the metal surface towards the seawater, where the increase in pH causes hydrolysis of the copper chloride complexes to produce more cuprite (equation 5).

$$2CuCl_2^- + H_2O \rightarrow 2H^+ + 4Cl^- + Cu_2O \quad \text{.....(5)}$$

In addition, as some of the $CuCl_2^-$ ions approach the seawater interface the redox potential increases and copper (II) hydroxy chlorides precipitate (equation 6).

$$2CuCl_2^- + 3H_2O \rightarrow Cu_2(OH)_3Cl + 3H^+ + 3Cl^- + 2e^- \quad \text{.....(6)}$$

#### 3.3.1.2 Weight Loss and Corrosion Rates

In order to facilitate a comparison of the weight loss data on many coupons it is essential to have a common approach to the management and interpretation of the information. Previous experience in rationalising the rates of release of chloride ions from maritime archaeological items has shown that the apparent weight loss needs to be normalised in terms of the surface area of the different coupons as the forms of the copper, brass and bronze objects all had variable surface area to volume ratios. Since the samples recovered in 2005 had been corroding for two years and those in 2009 for six years it is only natural that the longest immersed samples will have the greatest weight losses. Therefore in order to compare the years of exposure on the net average weight losses, the normalised (for surface areas) weight loss was divided by the number of years of immersion. The results of the copper alloy weight loss data are shown in Figure 21.

The individual weight loss rates for copper expressed as % weight loss.$cm^{-2}y^{-1}$ were 0.034, 0.018 and 0.021 in years 1, 2 and 6 respectively. The initial material loss in the first year is higher than in the subsequent years because of the roughening of the surface and the inherently higher surface reactivity of a bare metal exposed to flowing seawater. The value of the decay rates after 2 and 6 years is similar and this is just a reflection of the fact that it takes a number of

years for the metal to equilibrate with the surrounding environment and attain a quasi steady state.

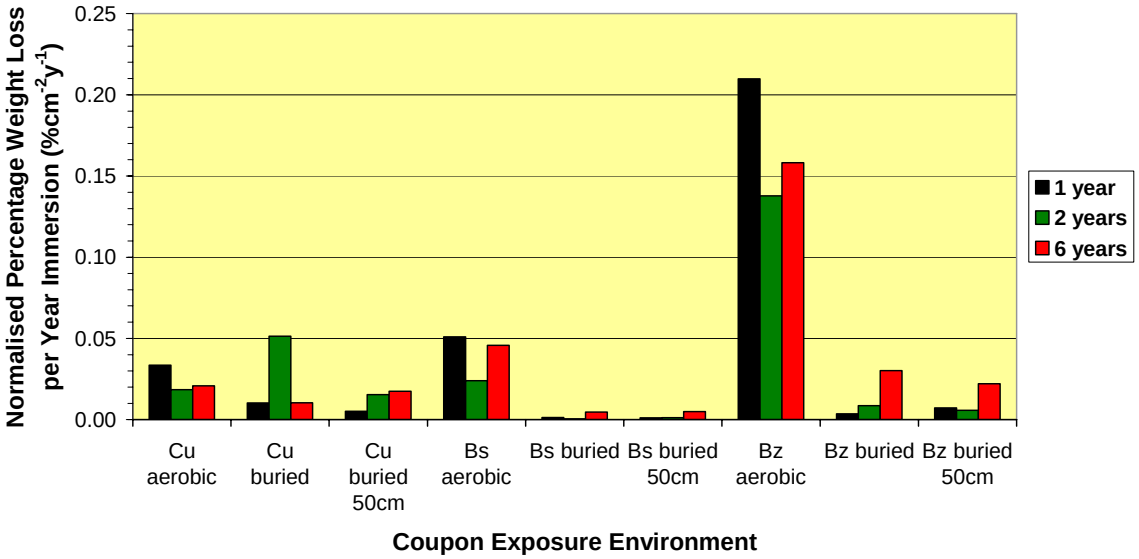


*Figure 21. Normalised percentage weight loss per year of immersion for the copper alloy coupons recovered in 2004, 2005 and 2009.*

In order to better compare the weight loss data between the copper based alloys the normalised weight loss in grams.cm$^{-2}$ was divided through by the time of immersion and the density of the alloy to obtain a more standard decay rate in mmy$^{-1}$ (Table 6). Thus the normalised copper corrosion rate can be expressed as 0.022, 0.012 and 0.030 mmy$^{-1}$ for one, two and six years of exposure, respectively, which showed that the corrosion rate had increased significantly over the past four years and this observation is supported by the SEM images in Figure 20, where after six years a more heavily corroded metal microstructure was evident.

*Table 6. Normalised corrosion rates for the copper alloy coupons.*

| Coupon Type and Environment | Coupon Thickness (mm) | Normalised Corrosion Rate (mmy$^{-1}$) | | |
|---|---|---|---|---|
| | | 2004 | 2005 | 2009 |
| Cu aerobic | 4.76 | 0.022 | 0.012 | 0.030 |
| Cu buried | | 0.007 | 0.034 | 0.022 |
| Cu buried 50cm | | 0.004 | 0.010 | 0.017 |
| Bs aerobic | 4.76 | 0.038 | 0.018 | 0.031 |
| Bs buried | | 0.001 | 0.0004 | 0.003 |
| Bs buried 50cm | | 0.001 | 0.001 | 0.004 |
| Bz aerobic | 5.00 | 0.108 | 0.070 | 0.070 |
| Bz buried | | 0.002 | 0.004 | 0.013 |
| Bz buried 50cm | | 0.004 | 0.002 | 0.011 |

### 3.3.2 Brass Coupons: Above Sediment

#### 3.3.2.1 Corrosion

The physical appearance of the brass coupons (Bs I & Bs II) recovered in 2004 and 2005 (Figure 22; top left and right) predominantly indicate aerobic corrosion mechanisms. However, the mixed patina found in the 2004 samples (Figure 23; left) is consistent with movements in the relative sediment levels by approximately 1-2cm from the original deposition level in 2003. Above the sediment band the patina was not well developed and consisted of light grey corrosion products associated with zinc and some cuprite ($Cu_2O$). Where the band of sediment had encroached on the coupon there were clear signs of differential aeration corrosion (Figure 22; top left and Figure 23; left). The 2005 coupons had a more evenly developed patina than the 2004 samples and had trapped some marine deposits on the surface on top of the straw-green corrosion matrix. There were no tell-tale signs of changed exposure conditions that had been noted on the 2004 coupons (Figure 22; top right and Figure 23; mid).


*Figure 22. Copper alloy coupons – above sediment, immediately after recovery in 2004 after 1 year of exposure (top left), in 2005 after 2 years of exposure (top right) and in 2009 after 6 years of exposure (bottom).*

*Figure 23. The brass coupons – above sediment recovered in 2004 after 2 years of storage (left), in 2005 after 1 year of storage (mid) and in 2009 after 5 months of storage (right).*

On recovery of the copper alloys in 2009 it was obvious that the brass coupons had been almost totally buried in the local sediment (Figure 22; bottom). Only very small sections of the upper parts of the coupons were exposed and this area was characterised by a dark grey surface which on dehydration after 5 months in storage changed to a mottled cream, grey and white patina (Figure 23; right). Clearly the coupons had been largely buried for a significant period of the total exposure time.

The SEM images of the brass coupon surfaces recovered in 2004 were dominated by bright spots of localised brass corrosion products containing varying proportions of copper, zinc and lead, overlying a general amorphous matrix of clay like deposits from the surrounding marine environment due to the partial burial of the coupons (Figure 24; left). The SEM images and the EDX data from 2005 confirmed the visual observation of the mixed corrosion product matrix that had trapped marine based sediments and anions that were precipitated out with mixed copper, zinc and lead cations (Figure 24; right). The surface was also characterised by zinc-rich 40–50µm pustular corrosion products.

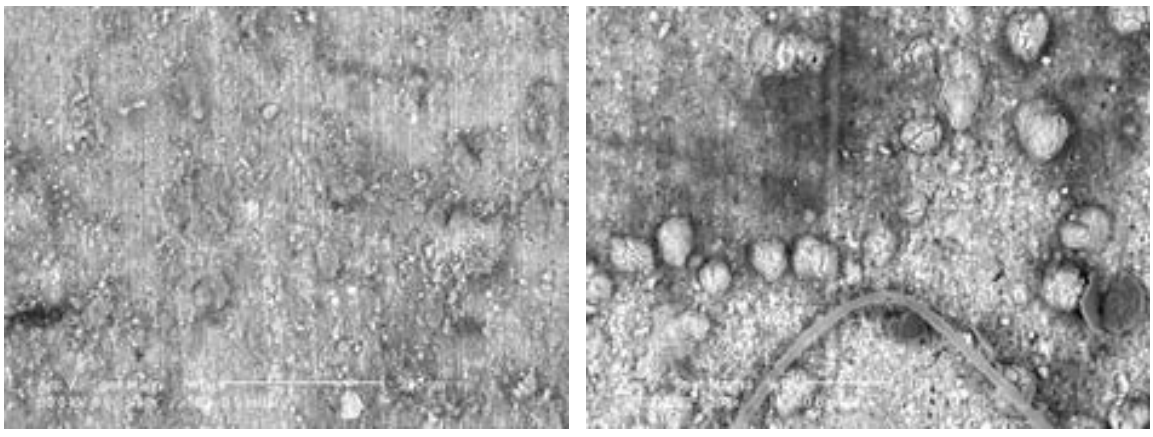

*Figure 24. SEM images of the unstripped brass coupons recovered from above the sediment in 2004 (left): the mixed brass corrosion products (bright areas) and in 2005 (right): the mixed corrosion product matrix (bright areas) and zinc-rich pustules.*

After 6 years of exposure the brass coupons had zones of significant amounts of copper and zinc oxides with relatively high concentrations of lead, confirmed by SEM and EDX analysis. The total absence of chloride on the surface was consistent with the partial burial of the coupons which resulted in the formation of some metal sulfides. Under normal aerobic conditions there would be insufficient concentrations of $Zn^{2+}$ for precipitation of zinc oxide but its presence on the surface showed that within a relatively short period of time the coupon became partly buried and so there was insufficient water movement across the coupon and this allowed the build up of zinc ions to levels where precipitation was possible. The lower sections of the coupons were dominated by the presence of copper (I) oxides and some copper (I) sulphides indicative of a mixed exposure history where initially, the coupons were subjected to an aerobic environment which then changed to an essentially anaerobic microenvironment as the sediment encroached up the support plate.

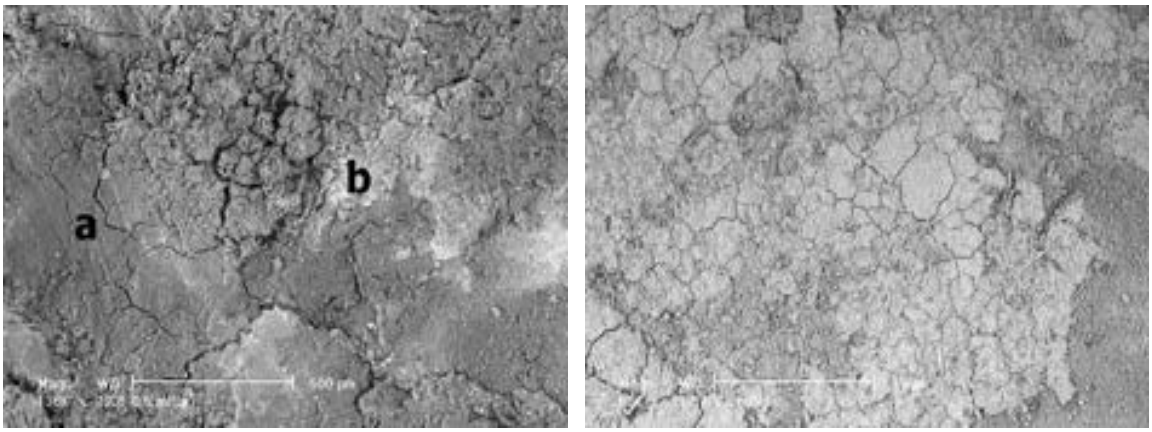


*Figure 25. SEM images of the unstripped brass coupons recovered from above the sediment in 2009 – upper section of the coupon (left): (a) zinc oxide (dark grey); (b) mixture of copper and zinc oxides with some lead sulphide (bright areas) – lower section of the coupon (right): mainly copper oxides with some copper and zinc sulphides (light grey).*

The stripped sample from 2004 showed that there was localised corrosion along the deformation and working lines of the brass and that the dominant mechanism was intergranular corrosion (Figure 26; left). The extent of corrosion of the 2005 stripped coupon was very similar to that of the 2004 sample and again, the major corrosion mechanism was increased corrosion at the grain boundaries. The stripped surfaces of the brass coupon from 2009 showed up the localised corrosion of the lead inclusions which appear to be more concentrated in the zinc-rich β phase at the grain boundaries. Figure 26 (right) showed the α copper-rich phase remaining as isolated islands in a zone that has been extensively corroded through intergranular corrosion. The complex corrosion behaviour this coupon exhibited is due to the mixed burial history it had since the time of deposition in 2003.

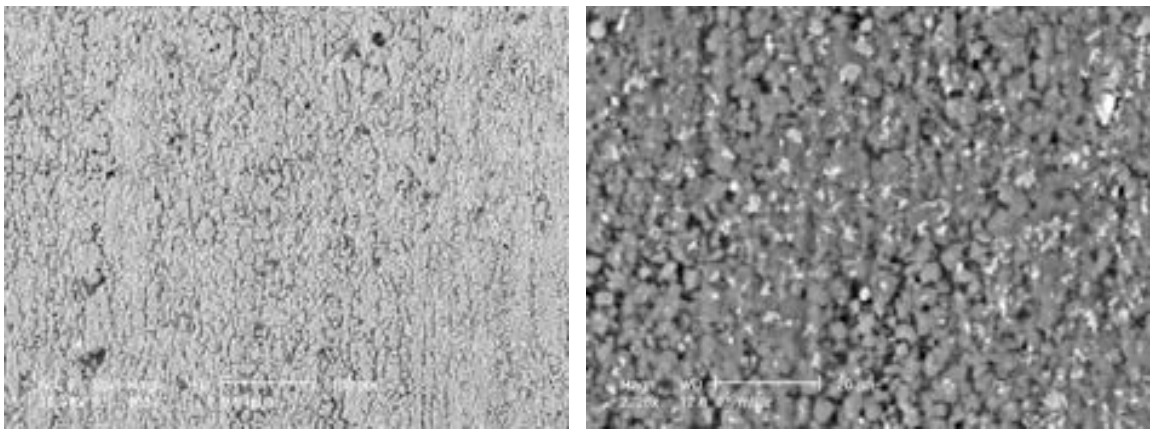

*Figure 26. SEM images of the stripped copper coupons recovered from above the sediment in 2004 (left) and in 2009 (right) showing the increase in intergranular corrosion over this period.*

The corrosion process occurring on brass exposed to aerobic seawater is usually dominated by the corrosion behaviour of the copper which is the major alloying constituent in the alloy. Therefore the typical range of aerobic copper corrosion products, such as copper oxides, chlorides and hydroxy chlorides are usually found in the corrosion product matrix in aerobically corroded brasses. The only chloride containing zinc corrosion product found on brass artefacts recovered from an aerobic marine environment has been anarakite, $[(Cu,Zn)_2(OH)_3Cl]$ where copper has been substituted with zinc in the hydroxy chloride. The absence of simple zinc chlorides is due to their relatively high solubility in seawater and these compounds are not typically found in the corrosion product layers.

The most characteristic form of brass corrosion is dezincification. In this form of corrosion the zinc component of the brass is selectively corroded and the alloy is transformed to a porous mass of copper which has very little mechanical strength but generally retains the original shape of the artefact. Two mechanisms have been proposed for dezincification, namely selective dissolution of the zinc phases which leaves behind the copper or complete dissolution of both the copper and zinc followed by selective deposition of the copper. Possibly both processes may be occurring on these coupons dependent on the local conditions, however dezincification is usually more pronounced in anaerobic environments which is confirmed by the behaviour of the 2004 and 2009 brass coupons, which were partially buried.

The presence of lead corrosion products on these brass coupons is not unusual. The addition of lead to duplex brasses results in the lead concentrating along the interdendritic lines between the α and ß phases. Hence, if the major corrosion mechanism occurring on these coupons is intergranular corrosion then the corrosion of the lead component under aerobic conditions would lead to the formation of a passivating lead sulphate ($PbSO_4$) film along the grain boundaries, which may assist in protecting the underlying brass from general corrosion, however due to the partial burial of the 2004 and 2009 coupons it was difficult to observe any notable differences in corrosion rate due to the presence of the lead.

### 3.3.2.2 Weight Loss and Corrosion Rates

The 2004 normalised percentage weight loss was 0.051%$cm^{-2}y^{-1}$, in 2005 the weight loss amounted to 0.024%$cm^{-2}y^{-1}$ while after six years in 2009 it was 0.046%$cm^{-2}y^{-1}$ (Figure 21). The lower percentage weight loss in 2005 is due to the coupons having been exposed to the full brunt of the oxygenated marine environment, whereas the first and sixth year coupons had been subjected to differential aeration due to partial burial of the samples. This demonstrates that if burial of artefacts is being considered then it is essential to guard against accidental partial exposure or burial scenarios, which is supported by the normalised corrosion rates of 0.038 $mm.y^{-1}$ for 2004, 0.018 $mm.y^{-1}$ in 2005 and 0.031 $mm.y^{-1}$ in 2009 (Table 6).

Brasses with zinc contents above 32%, such as these yellow brass coupons, are generally more reactive than copper and this would explain the increased normalised weight loss of the exposed brass coupons compared to the aerobically corroded copper coupons (Figure 21). These types of brasses have both an α copper-rich phase and a ß zinc-rich phase, which is preferentially attacked at the grain boundaries causing increased interdendritic corrosion (Figure 26; right) as compared to single phase α brasses, such as admiralty or red brass where the loss of zinc is distributed fairly uniformly across the grains.

### 3.3.3 Bronze Coupons: Above Sediment

#### 3.3.3.1 Corrosion

The patina on the bronze coupons (Bz I & Bz II) recovered in 2004 consisted of a green secondary corrosion product layer of copper (II) hydroxychlorides, overlying a pink-brown primary layer of cuprite with some tin oxides. The patina was patchy and not well adhered. There was no visual evidence of the sediment encroaching on these coupons as was readily apparent on the copper and brass coupons (Figure 27; top left and Figure 28; left). The appearance of the coupons recovered in 2005 was very similar to the 2004 samples, however the green-brown patina was more uniform (Figure 27; top right and Figure 28; mid). The main difference with the 2009 samples was the bronze coupons had been half buried (Figure 27; bottom) so the upper sections bore the same characteristics as the previously described coupons recovered in 2004 and 2005 subjected to an aerobic environment while the lower sections were dominated by a mixture of copper and tin oxides and a small amount of copper sulfides (Figure 27; bottom and Figure 28; right) formed in the deoxygenated microenvironment under the sediment.


*Figure 27. Copper alloy coupons – above sediment, immediately after recovery in 2004 after 1 year of exposure (top left), in 2005 after 2 years of exposure (top right) and in 2009 after 6 years of exposure (bottom).*

*Figure 28. The bronze coupons – above sediment recovered in 2004 after 2 years of storage (left), in 2005 after 1 year of storage (mid) and in 2009 after 5 months of storage (right).*

The SEM images of the unstripped bronze coupons recovered in 2004 after one year of exposure was dominated by tin-rich areas as the light grey zones and the middle grey areas were relatively richer in copper and also reflected the greater amount of zinc in the corroded matrix (Figure 29; left). This is a reflection of the underlying metallurgical structure where the zinc in the parent alloy is in solid solution in the copper-rich α phase. The EDX analysis confirmed that the copper corrosion products were rich in chloride while the tin-rich corrosion matrix was dominated by oxides and hydroxides. The SEM images of the 2005 bronze coupons showed that the overall surface was dominated by the presence of copper (II) hydroxychlorides, which was consistent with the mixed bronze patina that appeared to contain at least three distinct phases of oxidation products. In a similar vein to the 2004 sample, the 2005 coupon had well defined plate-like crystals that were consistent with a copper chloride corrosion product. There were large pavements of an apparently amorphous mass of copper (II) hydroxychlorides that was also rich in tin (Figure 29; right).

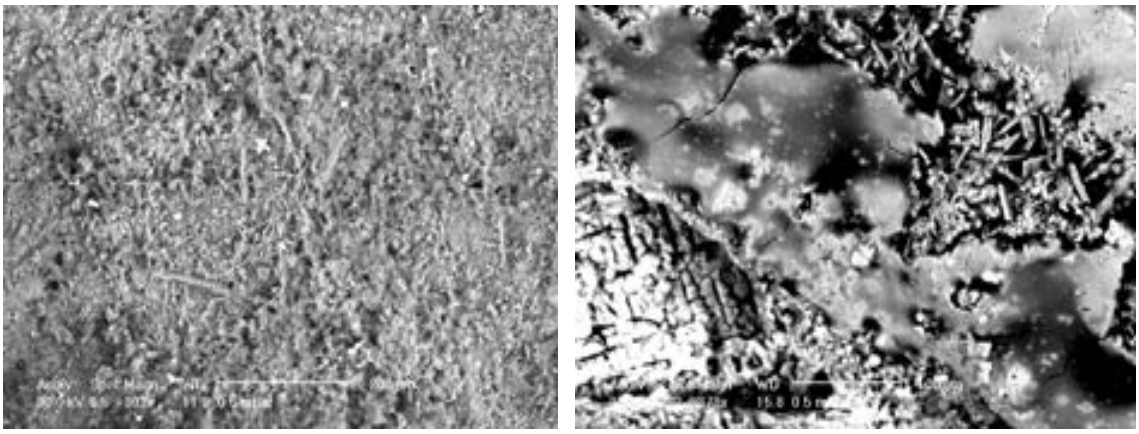

*Figure 29. SEM images of the unstripped bronze coupons recovered from above the sediment in 2004 (left): the copper zinc corrosion products (darker grey areas) and the tin oxides and hydroxides (lighter grey areas) and in 2005 (right): the copper chlorides (angular crystals) and copper (II) hydroxychlorides rich in tin (amorphous mass).*

The partially buried bronze coupons recovered in 2009 after six years of exposure, had corrosion products dominated by cuprite on the upper sections that were exposed to higher concentrations of dissolved oxygen in the open seawater, where the kinetic control of the degradation processes results in the selective corrosion of the copper-rich α phase (Figure 30; left). Progressing down the coupon the microenvironment became deoxygenated due to the coverage of the support plate by the surrounding sediment and the corrosion mechanism changed to one of preferential corrosion of the tin-rich eutectoid phase. However the lowered oxygen activity did not result in the formation of tin sulphides, which are relatively soluble but rather in the formation of a primary layer of the mixed Sn(IV)/Sn(II) oxide ($Sn_3O_4$) which appeared as pseudo morphs of the underlying "Chinese script" phase bronze and an overlying secondary layer consisting of a wide range of other hydrated and mixed tin oxyhydroxides (Figure 30; right).

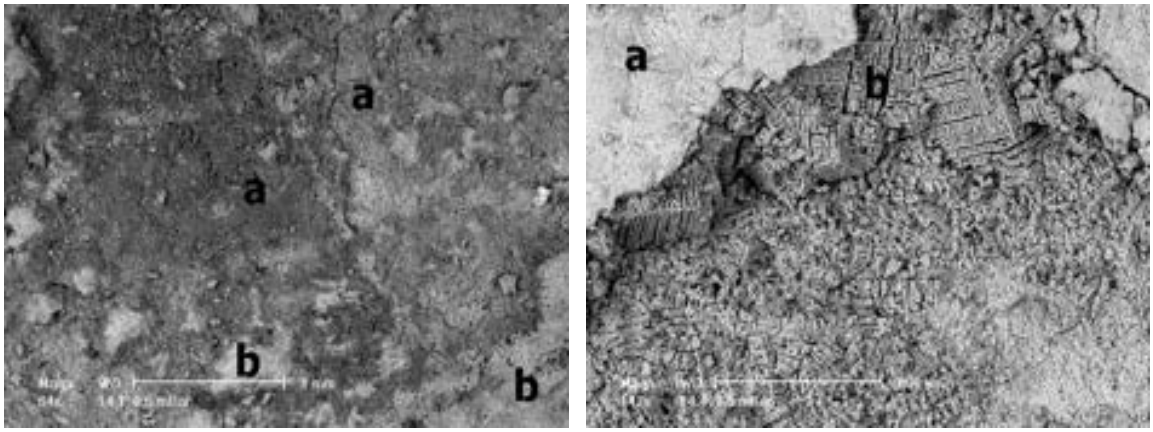


*Figure 30. SEM images of the unstripped bronze coupons recovered from above the sediment in 2009 - upper section of the coupon (left): (a) mainly cuprite corrosion products (darker grey areas); (b) with the lighter grey areas containing higher concentrations of tin - lower section of the coupon (right): (a) hydrated and mixed tin oxyhydroxides; (b) the mixed Sn(IV)/Sn(II) oxide ($Sn_3O_4$) which appeared as pseudo morphs of the underlying "Chinese script" phase bronze.*

The stripped bronze coupon recovered in 2004 showed the strong interdendritic corrosion processes, with the tin-rich eutectoid phase having been vigorously attacked which had left the copper-rich α phase largely unchanged, apart from localised corrosion across the face of the dendrite (Figure 31; left). The stripped surface images of the coupon recovered in 2005 showed very extensive attack on the α phase, which was richest in copper (Figure 31; right).

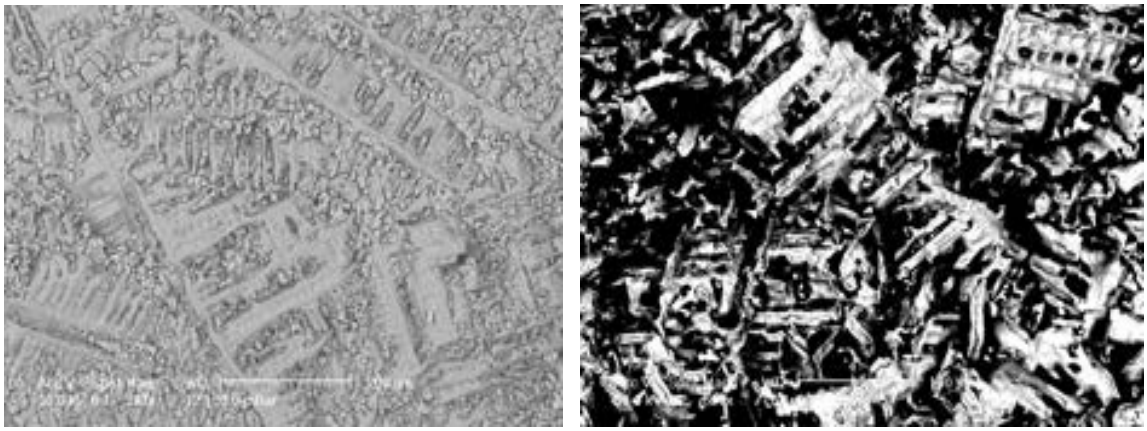

*Figure 31. SEM images of the stripped bronze coupons recovered from above the sediment in 2004 (left): the corrosion of the tin-rich eutectoid phase and in 2005 (right): corrosion of the copper-rich α phase.*

The stripped section towards the top of the bronze coupon recovered in 2009 showed up the presence of copper (I) chlorides with a small amount of lead chloride, $PbCl_2$, which indicates that although originally exposed to the aerobic environment in flowing sea water, this changed to being partially deoxygenated at some point where some preferential corrosion on the tin-rich (α+δ) eutectoid phase occurred. The higher concentration of lead in the matrix is due to the much greater solubility of lead in the eutectic phase as compared to the copper-rich α phase. On the stripped middle section of the coupon the bright SEM phase was shown to be approximately 88% copper and 4% tin, which is consistent with it being residual α phase of the bronze cast coupon (Figure 32; left).

Inspection of the lower section of the stripped coupon showed the preferential corrosion that had taken place at the sharp edges of the metal where the voltage gradient is greatest. The valleys in the structure are indicative of preferential corrosion of the tin-rich eutectoid phase where the overall decay is under thermodynamic control, as distinct from the initial kinetic control of the exposed upper section of the coupon. The tin oxide and hydroxide corrosion products' morphology reflected the underlying dendritic microstructure and some of the residual original dendritic structure is seen in Figure 32 (right).

Despite some of these bronze coupons being subjected to differential oxygenated microenvironments, the main corrosion mechanism of tin bronzes in aerobic seawater is the corrosion of the copper-rich α phase and therefore the typical aerobic copper corrosion products will dominate. The amount of tin in the bronze is the dominant force in determining corrosion rates in bronzes under aerobic conditions. The most commonly found tin mineral on aerobically corroded bronzes is the tin oxide, cassiterite ($SnO_2$). Oxidation of tin proceeds by way of two consecutive electron oxidation steps.

$$Sn \rightarrow Sn^{2+} + 2e^- \quad (7)$$
$$Sn^{2+} \rightarrow Sn^{4+} + 2e^- \quad (8)$$

Tin (II) species are more mobile than tin (IV) ions and although chloride ions form complexes with both tin (II) and tin (IV) the fully oxygenated and alkaline pH of the bulk seawater causes the oxidation, hydrolysis and concomitant precipitation of tin

(IV) oxides. This rapid hydrolysis of $Sn^{4+}$ ionic species in the aerobic marine environment is largely responsible for the retention of the original dimensions of a bronze artefact, however the corrosion product matrix is often crumbly and does not form an effective passivating film.

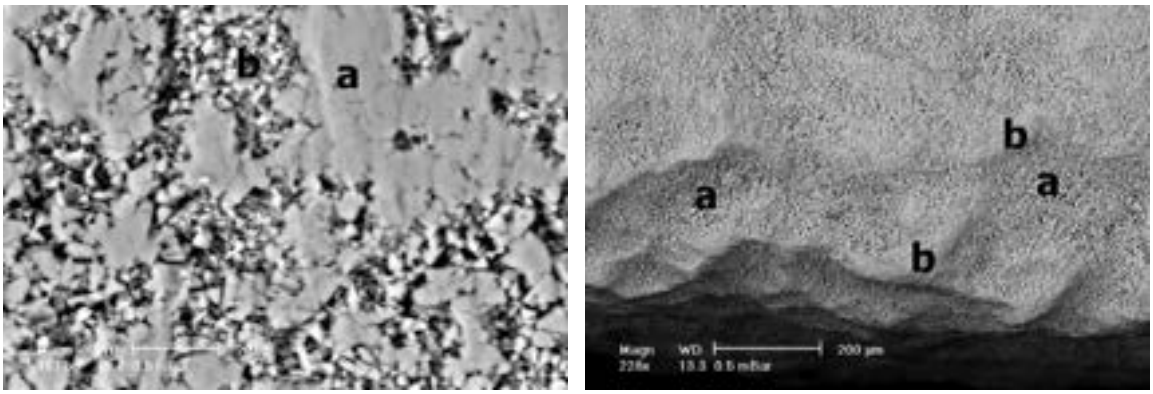


*Figure 32. SEM images of the stripped bronze coupons recovered from above the sediment in 2009 – mid section of the coupon (left): (a) mainly copper (I) chlorides with some lead chloride, $PbCl_2$; (b) residual copper-rich α phase – lower section of the coupon (right): (a) residual original dendritic structure; (b) tin corrosion products morphology reflecting the underlying dendritic structure.*

### 3.3.3.2 Weight Loss and Corrosion Rates

The 2004 normalised percentage weight loss per year of immersion was 0.210%$cm^{-2}y^{-1}$, in 2005 the weight loss decreased to 0.138%$cm^{-2}y^{-1}$ and then after six years in 2009 it had increased again to 0.158%$cm^{-2}y^{-1}$ (Figure 21). The higher percentage weight loss in 2004 and to a lesser extent in 2009 is due to these coupons being partially buried and subjected to differential aeration corrosion where both corrosion of the copper-rich α phase and the tin-rich eutectic phase can occur leading to a significant increase in the overall extent of corrosion. In comparison the bronze coupons exposed to a totally aerobic environment showed a decrease in weight loss as corrosion of the copper-rich α phase is the dominant corrosion mechanism. Unfortunately this trend in percentage weight loss is not supported by the normalised corrosion rates where the rate has not increased over the last four years (Table 6). The normalised corrosion rate for the bronze coupons was 0.108 $mm.y^{-1}$ in 2004 and 0.070 $mm.y^{-1}$ in both 2005 and 2009 (Table 6). However, comparisons between the normalised corrosion rates (Table 6) and the weight loss data (Figure 21) for the aerobic copper, brass and bronze coupons showed that the extent of corrosion of these tin bronzes was much more extensive than for the copper and brass and that the bronzes had corroded, on average, about 3 and 4 times more rapidly than the brass and copper coupons, respectively.

This demonstrates that if copper alloy artefacts, especially multi-phased copper alloys, such as bronzes are being considered for reburial then it is essential to guard against partial exposure or burial cycles, which will cause differential aeration corrosion and increased intergranular galvanic corrosion. On the other hand, the corrosion products present on the bronzes subjected to these different oxygenated environments showed that tin bronzes are very sensitive indicators of the microenvironment and that it is possible to obtain detailed information about

the changing burial environment by carefully examining the nature and the morphology of the corrosion matrices.

### 3.3.4 Copper Steel Coupons: Above Sediment

#### 3.3.4.1 Corrosion

Inspection of the ferrous alloy plate upon recovery in 2004 showed up the presence of zonal corrosion due to a mixed exposure environment due to migration of the sample units into the sediment and/or a localised increase in the sediment level. The copper steel (Cu/Fe) coupon showed significant signs of corrosion attack but with the normal patchy distribution associated with differential aeration cells (Figure 33; top left). The aerial oxidation continued regardless of storage under oxygen scavenging conditions (Figure 34; left). On recovery the 2005 copper steel coupon had voluminous aerobic corrosion products on the surface (Figure 33; top right) and the response of the coupon to aerial oxidation on storage was the same but more intense than the 2004 sample (Figure 34; mid). The corrosion matrix on the copper steel coupon immediately after recovery in 2009 was even more voluminous than on the 2004 and 2005 coupons (Figure 33; bottom) and aerial oxidation occurred during storage (Figure 34; right).


*Figure 33. Ferrous alloy coupons – above sediment, immediately after recovery in 2004 after 1 year of exposure (top left), in 2005 after 2 years of exposure (top right) and in 2009 after 6 years of exposure (bottom).*

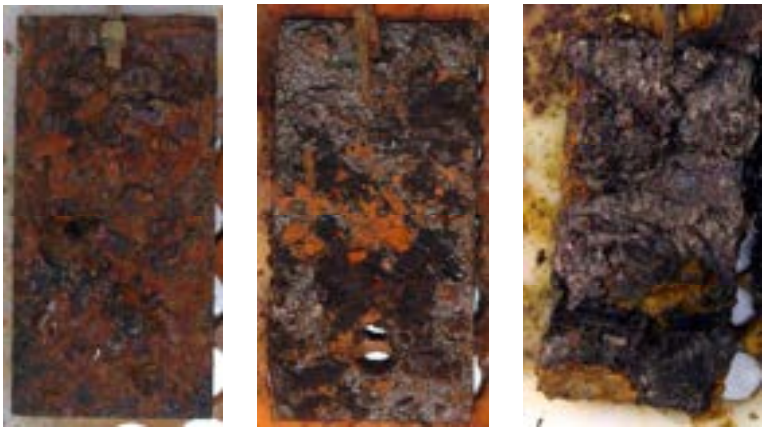

*Figure 34. The copper steel coupons – above sediment recovered in 2004 after 2 years of storage (left), in 2005 after 1 year of storage (mid) and in 2009 after 5 months of storage (right).*

The SEM images of the unstripped copper steel coupon showed up two distinct phases, one of which was amorphous and the other consisted of coherent small crystals (Figure 35; left). There was essentially no significant difference in composition of the phases which consisted of hydrated iron oxides and oxyhydroxides. The crystalline phase appears to replicate the underlying microstructure of the alloy which had undergone very even intergranular corrosion. The SEM images of the 2005 copper steel coupon showed up a more developed zonal corrosion pattern in that there were distinct areas that were rich in calcium and iron corrosion products and those that contained essentially only iron oxides and oxyhydroxides. There was also some evidence of marine colonisation. The presence of increased amounts of marine debris on the 2005 coupon showed that it takes a couple of years before iron begins to stabilise in a marine environment. By 2009 the SEM images and EDX analysis of the unstripped copper steel coupon showed amorphous iron oxides and oxyhydroxides with minor quantities of chloride, calcium and manganese. The amount of incorporated marine debris had increased significantly since 2005.

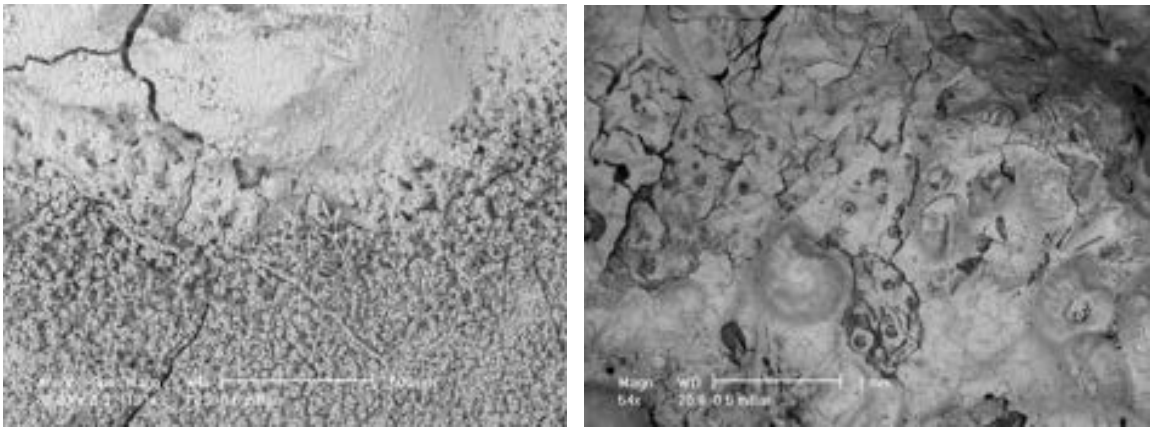

*Figure 35. SEM images of the unstripped copper steel coupon recovered from above the sediment in 2004 (left): the amorphous and crystalline iron oxides and oxyhydroxides and in 2009 (right): the amorphous iron oxides and oxyhydroxides with increased amounts of incorporated marine debris.*

Although the stripping of the 2004 sample was not complete it was observed that there had been general uniform corrosion and where residual crystalline corrosion products remained on the surface their basic morphology matched the underlying microstructure (Figure 36; left). The stripped copper steel coupon from 2005 showed the original structure of equiaxed primary ferrite iron alloy, with typical grain sizes around 20µm. The corrosion pattern of the stripped copper steel sample from 2009 was identical to the 2005 coupon, which showed a more zonal corrosion pattern (Figure 36; right). The EDX analysis of the ferrite grains showed that the 99% Fe and 1% Mn was consistent with the original metal composition (Table 5).

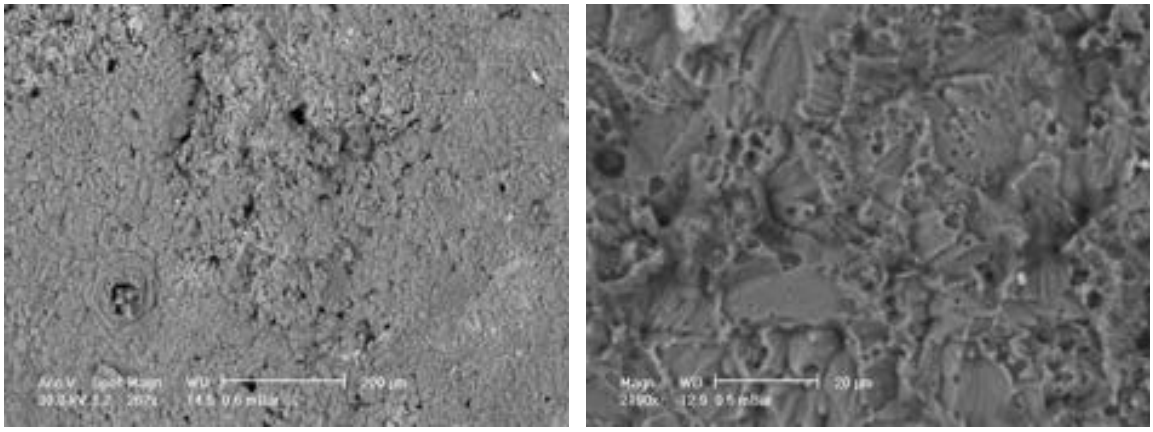

*Figure 36. SEM images of the stripped copper steel coupon recovered from above the sediment in 2004 (left): uniform general corrosion of the grains and in 2009 (right): zonal corrosion of the ferrite microstructure.*

Although there was considerably more marine debris present on the 2009 copper steel coupon compared to the 2004 and 2005 samples, which indicated that the anodic and cathodic sites on the 2009 coupon were beginning to be separated by the formation of a concretion layer, the major corrosion mechanism occurring on all copper steel coupons above the sediment was predominantly that of bare iron exposed to aerobic seawater without complete coverage with concretion.

When iron is immersed in aerobic seawater, corrosion will occur at the anodic areas, where the iron metal is oxidised to $Fe^{2+}$ ions and the electrons enter the residual metal (equation 11).

$$Fe \rightarrow Fe^{2+} + 2e^{-} \quad (11)$$

The corresponding cathodic reaction is the reduction of oxygen and occurs at the cathodic sites on the iron metal surface (equation 12).

$$O_2 + 2H_2O + 4e^{-} \rightarrow 4OH^{-} \quad (12)$$

As the ferrous ions formed in the anodic reaction move away from the metal surface and encounter the more positive electrochemical potential of the bulk seawater they are oxidised to ferric ($Fe^{3+}$) ions. The ferrous and ferric ions can then react with the hydroxyl ($OH^{-}$) ions to form a number of different oxides and hydroxides. The most common aerobic iron corrosion products are the α, ß and γ

iron oxyhydroxides [FeO(OH)], which possess the familiar reddish, brown rust colour and $Fe_2O_3$.

### 3.3.4.2 Weight Loss and Corrosion Rates

Similar to the copper alloy coupons the weight loss rates of the ferrous alloy coupons were normalised for surface areas and divided by the number of years of immersion, expressed as % weight loss.$cm^{-2}y^{-1}$. The results of the ferrous alloy weight loss data are shown in Figure 37.

The individual weight loss rates for the copper steel coupons were 0.094, 0.091 and 0.073%$cm^{-2}y^{-1}$ in years 1, 2 and 6 respectively. The initial material loss in the first and second years of exposure were similar but slightly higher than after six years because of the roughening of the surface and the inherently higher surface reactivity of a bare metal exposed to flowing seawater. After six years of exposure the concretion layer was better formed and subsequently the decay rate decreased slightly.

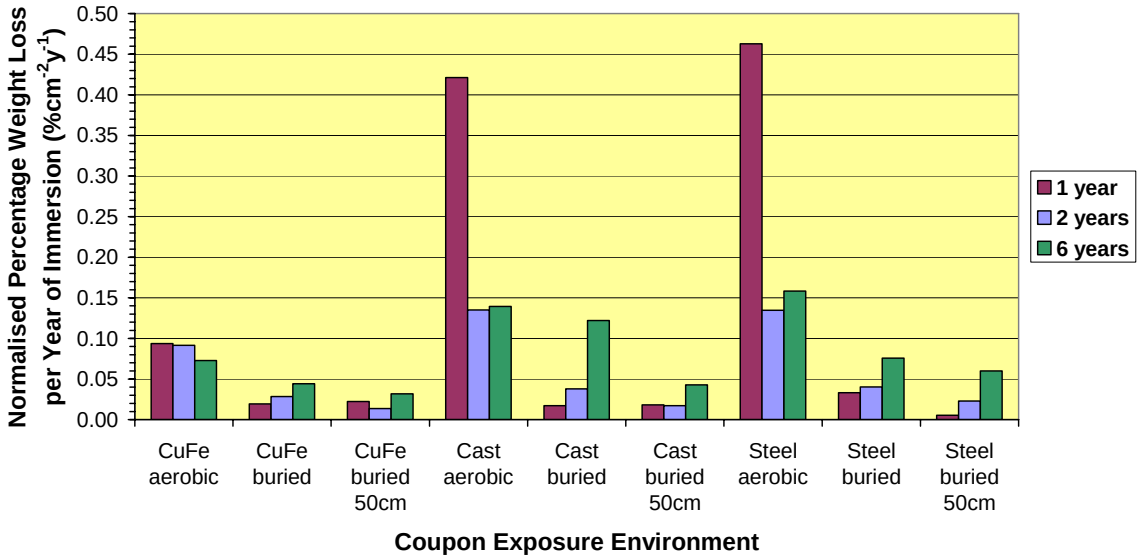


*Figure 37. Normalised percentage weight loss per year of immersion for the ferrous alloy coupons recovered in 2004, 2005 and 2009.*

In order to better compare the weight loss data between the ferrous based alloys the normalised weight loss in g.$cm^{-2}$ was divided through by the time of immersion and the density of the alloy to obtain a more standard decay rate in $mmy^{-1}$ (Table 7). Thus the normalised copper steel corrosion rate can be expressed as 0.169, 0.163 and 0.167 $mmy^{-1}$ for one, two and six years of exposure, respectively indicating that the corrosion rate had not changed over the six year period and the copper steel has reached a steady state of decay.

*Table 7. Normalised corrosion rates for the ferrous alloy coupons.*

| Coupon Type and Environment | Coupon Thickness (mm) | Normalised Corrosion Rate ($mmy^{-1}$) | | |
|---|---|---|---|---|
| | | 2004 | 2005 | 2009 |
| CuFe aerobic | 3.00 | 0.169 | 0.163 | 0.167 |
| CuFe buried | | 0.035 | 0.050 | 0.146 |
| CuFe buried 50cm | | 0.040 | 0.024 | 0.048 |
| Cast Fe aerobic | 5.00 | 0.472 | 0.149 | 0.167 |
| Cast Fe buried | | 0.021 | 0.043 | 0.146 |
| Cast Fe buried 50cm | | 0.021 | 0.019 | 0.048 |
| Steel aerobic | 5.00 | 0.333 | 0.090 | 0.113 |
| Steel buried | | 0.024 | 0.029 | 0.054 |
| Steel buried 50cm | | 0.004 | 0.016 | 0.043 |

### 3.3.5 Cast Iron Coupons: Above Sediment

#### 3.3.5.1 Corrosion

The cast iron coupons (cast Fe I & II) as-recovered in 2004 showed the same physical appearance as that described for the copper steel sample recovered from above the sediment. That is, zonal corrosion was evident on the cast iron coupons due to a mixed exposure environment caused by migration of the sample units into the sediment and/or a localised increase in the sediment level (Figure 38; top left). On desiccation during storage these coupons suffered severe spalling and the overall level of decay was significantly more pronounced than for the copper steel sample (Figure 39; left). This is consistent with the normal challenges of conserving marine iron in that it is commonly the cast iron objects that are the most problematic. The cast iron coupons recovered in 2005 were similar in appearance to the 2004 samples (Figure 38; top right) but the overall extent of surface accretion was greater and the amount of post-recovery spalling had significantly increased compared to the previous year (Figure 39; mid).


*Figure 38. Ferrous alloy coupons – above sediment, immediately after recovery in 2004 after 1 year of exposure (top left), in 2005 after 2 years of exposure (top right) and in 2009 after 6 years of exposure (bottom).*

By 2009 the cast iron coupons were covered in concretion, which consisted of a mixture of calcium carbonate, voluminous iron corrosion products and deposits of local sediment (Figure 38; bottom) however, this concretion layer still did not totally encapsulate the coupons. On drying there was considerably less spalling of

the surface accretion compared to the 2004 and 2005 samples due to the more advanced formation of the concretion layer on the surface of the coupons (Figure 39; right).

*Figure 39. The cast iron coupons – above sediment recovered in 2004 after 2 years of storage (left), in 2005 after 1 year of storage (mid) and in 2009 after 5 months of storage (right).*

The SEM image of the unstripped coupon from 2004 was significantly different to that of the other iron samples in that the corrosion products consisted of three distinct zones, one of which was essentially amorphous but another had a well defined structure, as seen in Figure 40 (left). The globular deposits were rich in calcium and reflected partial conversion of calcium carbonate into siderite, $FeCO_3$, as part of the normal concretion formation process. The corrosion products with the crystalline structure was a pure iron oxyhydroxide which had resulted from corrosion of the α ferrite grains distributed along the lines of the graphite in the cast structure. This morphology is a direct consequence of the large differences in the electrochemical properties of α ferrite and graphite, which are two of the well known phases in cast iron. The SEM images and EDX analysis of the cast iron coupons from 2005 and 2009 showed up a mixture of phases that relate to the increased interaction of iron corrosion products with the marine environment. Thus a mixed collection of partially replaced calcium-iron minerals, iron oxyhydroxides, clay particles and minor amounts of iron sulphides were identified (Figure 40; right) associated with the formation of concretion.

The SEM images of the stripped cast iron coupons recovered in 2004 showed the coarse open structure of the cast metal. The coupons showed a very mottled substrate which consisted of macro-cells 140-100 µm in length. There had been preferential corrosion of the iron-containing phases leaving behind an uneven distribution of carbon. The SEM images and EDX analysis of the stripped coupons from 2005 and 2009 showed that the extent of corrosion of the α ferrite phase in the parent alloy had decreased significantly (Figure 41; right).

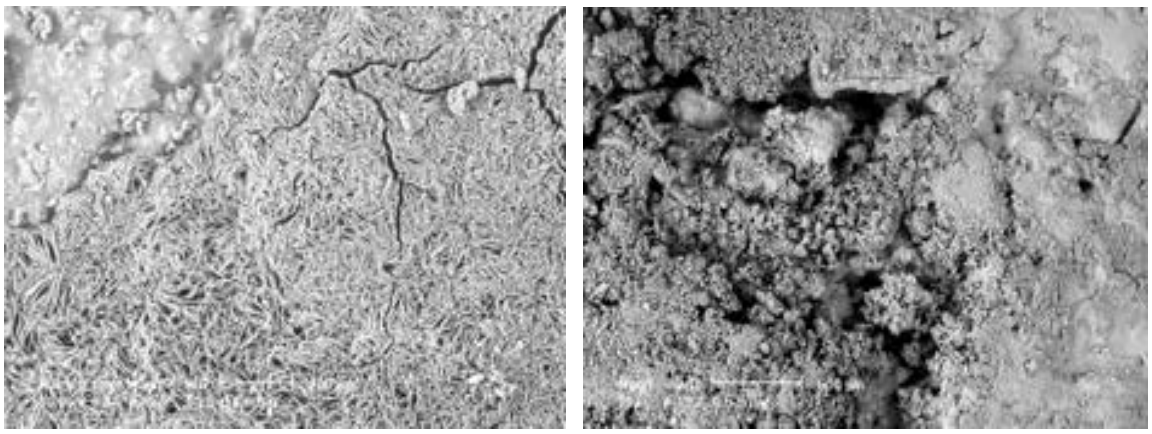

*Figure 40. SEM images of the unstripped cast iron coupons recovered from above the sediment in 2004 (left): the amorphous (top left) and crystalline (bottom right) iron corrosion products and in 2009 (right): the mixture of amorphous, crystalline and globular iron corrosion products with increased amounts of calcium carbonate and incorporated local sediment.*

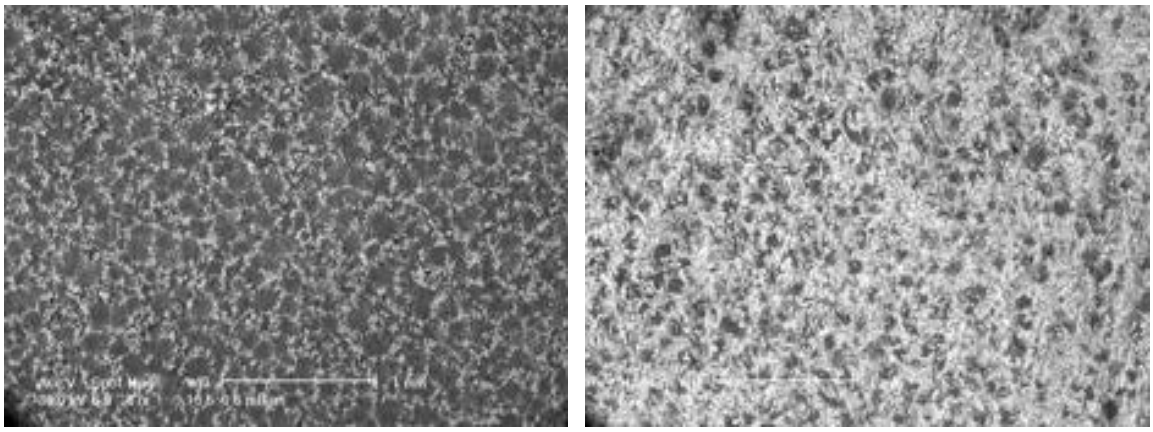

*Figure 41. SEM images of the stripped cast iron coupons recovered from above the sediment in 2004 (left): preferential corrosion of the iron (bright areas) leaving behind a carbon-rich phase (dark grey phase) and in 2009 (right): less corrosion of the α ferrite phase (bright areas).*

During aerobic corrosion of cast iron, the phases containing more iron (e.g. ferrite and pearlite) are preferentially corroded compared to the more inert cementite and graphite phases. The graphite is unaffected by corrosion and remains as a three-dimensional network which retains the shape of the cast iron artefacts and hence, it is not surprising that the areas of the cast iron coupons that have the highest concentrations of carbon are the least corroded.

### 3.3.5.2 Weight Loss and Corrosion Rates

The annualised normalised weight loss of the 2004 cast iron was 0.421%$cm^{-2}y^{-1}$, which decreased significantly in 2005 and 2009 to 0.135% $cm^{-2}y^{-1}$ and 0.140% $cm^{-2}y^{-1}$, respectively (Figure 37). This decrease in overall corrosion in 2005 and 2009 was supported by the normalised corrosion rates which were 0.472 $mm.y^{-1}$ in 2004, 0.149 $mm.y^{-1}$ in 2005 and 0.167 $mm.y^{-1}$ in 2009 (Table 7). This result is typical of the differences in localised corrosion processes associated with cast iron

decay and the overall impact of the different microenvironments experienced in the first few years of exposure before the concretion layer is better developed. The slight increase in the weight loss and corrosion rate for the cast iron recovered in 2009 as compared to the 2005 samples could simply be a reflection of the longer exposure period.

The corrosion reactions for the exposed cast iron coupons would be essentially the same as that explained for the copper steel coupons recovered from above the sediment in that the primary corrosion products are soluble ferrous chloride which undergoes concomitant oxidative hydrolysis to produce the red-brown characteristic rust. In the case of the cast iron there is the major contributing factor of the dissimilarity of the electrochemical potential of the multiple phases present in the alloy. There is a very large difference in the voltages of the half cells involving corrosion of the ferrite (pure iron), pearlite (ferrite and cementite) and graphite (carbon) phases. It is the contiguous relationship of all these phases that exacerbates corrosion of the interior of the cast iron coupons.

Another reason that underlies the cause for the decrease in the extent of corrosion experienced by the 2005 and 2009 coupons could be that the extent of concretion formation was greater on these coupons exposed to the local marine environment as compared to the copper steel coupons recovered from above the sediment. To maintain charge neutrality in the cast iron coupons both the anodic and cathodic reactions must occur at the same rate, there must be a net diffusion of positive ions to the cathodic sites and/or negative ions to the anodic areas and there must be specific movement of reactants and products to and from the reactive areas if corrosion is to continue rapidly. If there is a film of high electrical resistance between the anodic and cathodic sites, such as a concretion layer or a dense corrosion product layer this will retard the movement of electrons and effectively decrease the corrosion rate. The anodic reaction will still occur at the residual metal surface beneath the film but the cathodic reaction will occur at the concretion/seawater interface and the electrons must pass through the high resistance film when moving from the cathodic to the anodic sites, thereby slowing the corrosion rate until the coupons are totally encapsulated by concretion. This concretion separates the iron from the surrounding environment and results in the creation of a significantly different microenvironment on the surface of the residual iron. As a result the iron continues to corrode in an environment which is almost independent of the external conditions and the primary corrosion mechanism is similar to that observed in crevice corrosion.

### 3.3.6 Mild Steel Coupons: Above Sediment

#### 3.3.6.1 Corrosion

Immediately after retrieval in 2004, the appearance of the mild steel coupons recovered from above the sediment was essentially the same as the other iron alloys in that there was evidence of zonal corrosion on the mild steel I coupon and the mild steel II coupon had the typical appearance of the anaerobically corroded iron coupons caused by migration of the sample units into the sediment and/or a localised increase in the sediment level (Figure 42; top left). These coupons had also suffered the same fate in terms of alteration of the surfaces upon exposure to an oxygenated environment in storage (Figure 43; left). Upon recovery of the mild steel coupons in 2005, it was evident that the extent of surface accretion was more pronounced than that observed for the 2004 samples. The mild steel II coupon had also been partially buried and had suffered from some differential aeration corrosion due to settling of the sample unit into the surrounding sediment (Figure 42; top right and Figure 43; mid). Similarly, the mild steel coupons retrieved in 2009 had significantly more concretion formation on the surfaces than those coupons recovered in 2004 and 2005 (Figure 42; bottom and Figure 43; right).

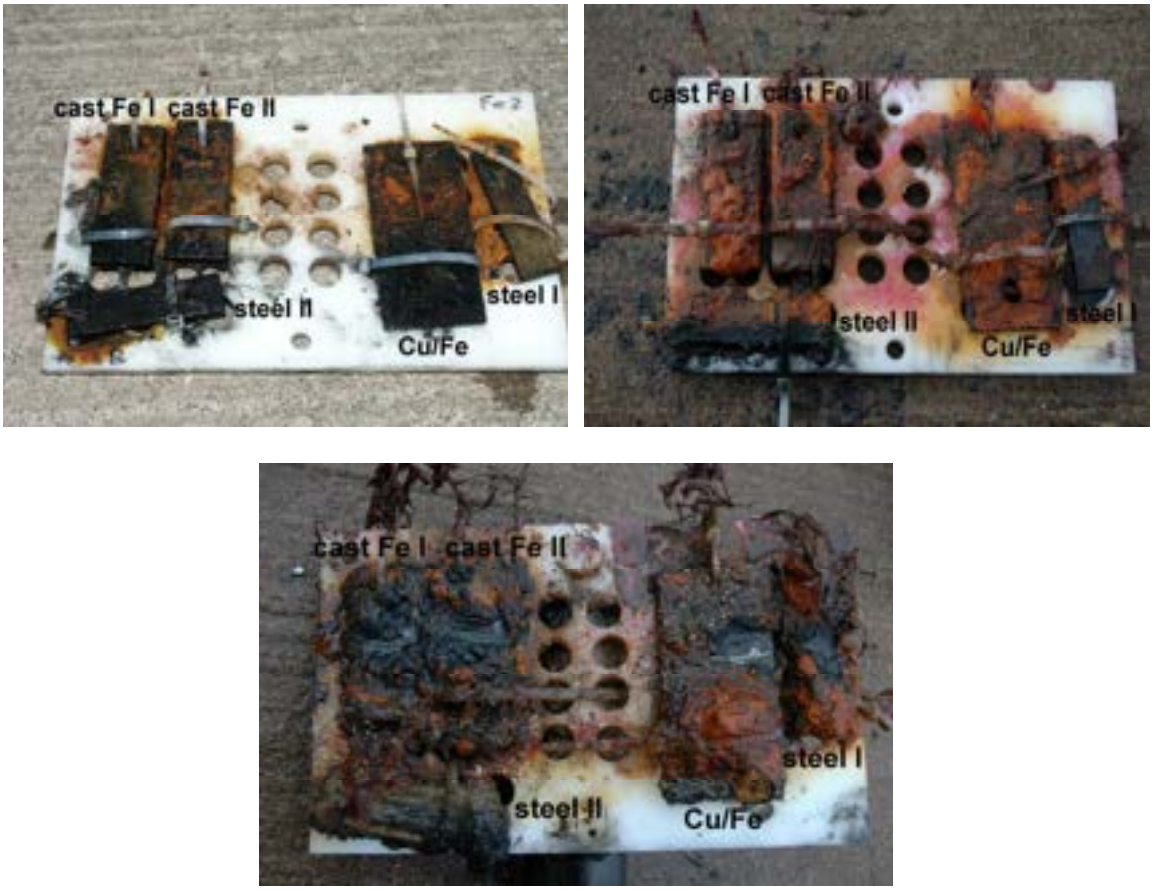


*Figure 42. Ferrous alloy coupons – above sediment, immediately after recovery in 2004 after 1 year of exposure (top left), in 2005 after 2 years of exposure (top right) and in 2009 after 6 years of exposure (bottom).*

*Figure 43. The mild steel coupons – above sediment recovered in 2004 after 2 years of storage (left), in 2005 after 1 year of storage (mid) and in 2009 after 5 months of storage (right).*

The SEM images showed that there was more deposition of calcareous materials on the surface of these coupons and that the mild steel seemed to be responding more rapidly to concretion formation than the other exposed iron alloys. The interaction of marine organisms with the different iron coupons is going to be dependent on the bioavailability of iron and this is greatest for the mild steel coupons, which is almost 99% iron. There is essentially no dilution of the iron in the alloy and so the amount of $Fe^{2+}$ and $Fe^{3+}$ ions is at a maximum for the microenvironment. Since the elemental composition of cast iron is close to 86% iron and 14% carbon it is only to be expected that the amount of growth on the cast iron is significantly less than on the mild steel. The copper steel coupon also had high concentrations of iron (98%), however the presence of copper in the alloy would allow the formation of biologically toxic copper corrosion products to form, which would limit the amount of concretion growth to some extent.

The surfaces of the unstripped 2004 coupons showed up an amorphous aerobic iron oxyhydroxide matrix and some well defined inorganic calcium carbonate crystals which were consistent with localised reduction of oxygen giving a sufficiently elevated pH to cause the soluble $Ca^{2+}$ ions to precipitate (Figure 44; left). The SEM image of the 2005 corrosion products was indistinguishable from the previous years' observations in that the surface was a mixture of amorphous and granular iron oxyhydroxides. The normal milieu of adventitious sediment minerals was also present. By 2009 the amount of concretion on the mild steel coupons had increased significantly. When the EDX data was examined it was clear that the thicker concretion layer had provided an optimal environment for the activation of sulphate reducing bacteria and hence we are now looking at the more classic view of a concreted iron artefact which contains significant amounts of iron sulphides of varying stoichiometry [Figure 44; right (b)]. The amorphous iron oxide phases are shown in area 'a' of the same figure. Additional support for the presence of anaerobic bacteria is also seen in the measurable amounts of the minor alloying element of manganese since these bacteria are known to utilise manganese ions in their metabolic processes and this is precipitated out as insoluble manganese dioxide. However, the relatively low chloride ion concentration in the matrix indicated that total encapsulation of the coupons is not yet complete after six years of exposure.

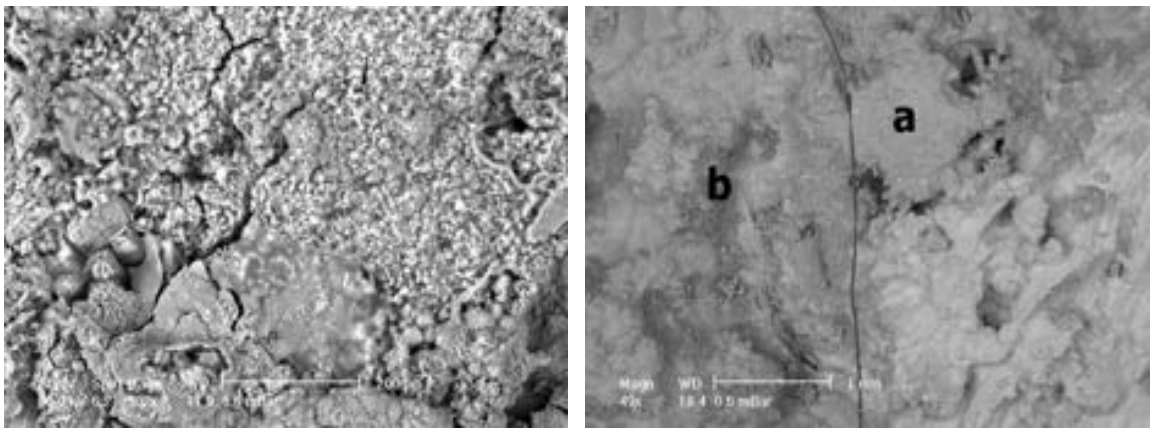


*Figure 44. SEM images of the unstripped mild steel coupons recovered from above the sediment in 2004 (left): amorphous aerobic iron corrosion products with well defined inorganic calcium carbonate crystals (bright crystals) and in 2009 (right): (a) mainly iron oxides and oxyhydroxides; (b) mixture of iron oxides and oxyhydroxides with small amounts of iron sulphides.*

The SEM image of the 2004 stripped mild steel surface showed that there were clearly discerned patterns of localised corrosion, associated with pitting reactions (Figure 45; left), which was not apparent in the copper steel coupon. There was also general surface corrosion of the α ferrite grains. This general surface corrosion of the iron was more pronounced in the 2005 and 2009 samples but there was an apparent change from a dominant pitting corrosion mechanism in the 2004 coupons to a mixture of localised corrosion in and around the slag inclusions as well as generalised attack on the ferritic structure for the 2005 and 2009 coupons (Figure 45; right). This change over in mechanisms is consistent with the formation of the protective concretion layer, which prevents dissolved oxygen direct access to the exposed metal surface. Preferential corrosion along the lines of stress associated with the manufacture of the coupons (rolling) is also clearly seen to be a significant factor in the overall deterioration of the metal from 2005 onwards.

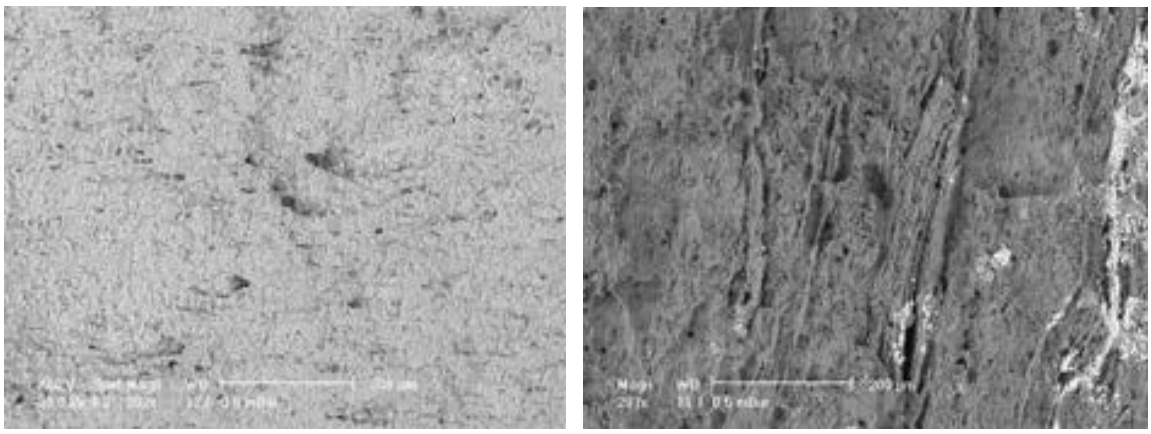

*Figure 45. SEM images of the stripped mild steel coupons recovered from above the sediment in 2004 (left): general corrosion of the α ferrite grains and pitting corrosion and in 2009 (right): general corrosion of ferrite and localised corrosion in and around the slag inclusions.*

### 3.3.6.2 Weight Loss and Corrosion Rates

The 2004 mild steel had an annualised normalised weight loss of 0.463%$cm^{-2}y^{-1}$, in 2005 it had decreased significantly to 0.135%$cm^{-2}y^{-1}$ and in 2009 it had increased slightly to 0.158%$cm^{-2}y^{-1}$. The impact of the increase in concretion formation over the six year period from 2004 to 2009 is seen in the way in which the weight loss decreases over the same period. When the normalised weight loss is expressed as a corrosion rate in $mm.y^{-1}$ there also appears to be a trend towards lower corrosion rates with the passage of time and increasing cover of concretion i.e. the rates were 0.333$mm.y^{-1}$ in 2004, which decreased dramatically to 0.090 $mm.y^{-1}$ and 0.113 $mm.y^{-1}$ in 2005 and 2009, respectively.

It is important in reviewing the data to understand that the initial rates of corrosion for iron are always much higher than in subsequent years, as the formation of concretion begins to separate out the anodic and the cathodic sites and so lowers the corrosion rate. In the initial period of exposure any differences in the extent of exposure and or burial are going to have a dramatic effect on the apparent corrosion rates. Once a significant amount of concretion has formed these differences in the burial microenvironment become less dramatic. Hence, the same explanation for the weight loss anomaly that applied to the 2004 cast iron coupons above the sediment would similarly apply to the 2004 mild steel coupons. The same aerobic corrosion mechanism and deposition of inorganic calcium carbonate described for the copper steel and cast iron coupons recovered from above the sediment would also apply to these mild steel coupons.

## 3.4 ENVIRONMENTAL CONDITIONS – LOW OXYGEN

### 3.4.1 Copper Coupons: Just Below Sediment

#### 3.4.1.1 Corrosion

The copper coupons (Cu I & Cu II) as recovered in 2004 (Figure 46; top left) showed an uneven grey corrosion pattern on their surfaces and there was no evidence of periodic exposure of the support structure. Despite the best attempts to minimise post recovery oxidation, the copper coupons were found to have undergone some changes during storage. The coupons after storage were generally seen as being of a brown to black hue and the presence of the cable ties on the coupons were clearly discerned (Figure 47; left).

There was a marked difference in the appearance of the 2005 copper samples immediately after retrieval. They had a well defined layer of grey/black copper sulphides mixed in with clay and silt grains. This sulphide corrosion product layer had been abraded in areas in direct contact with the cable ties exposing the typical bright pink cuprite layer (Figure 46; top right). After storage and desiccation the ~0.3mm corrosion product layer readily detached from the surface of the coupon, leaving a mixed cuprite and dark grey copper sulphide patina (Figure 47; mid).


*Figure 46. Copper alloy coupons – just below sediment, immediately after recovery in 2004 after 1 year of exposure (top left), in 2005 after 2 years of exposure (top right) and in 2009 after 6 years of exposure (bottom).*

*Figure 47. The copper coupons – just below sediment recovered in 2004 after 2 years of storage (left), in 2005 after 1 year of storage (mid) and in 2009 after 5 months of storage (right).*

The appearance of the 2009 copper coupons immediately after retrieval was considerably different from the samples recovered in 2004 and 2005. In some areas they possessed a secondary blue/green corrosion product layer overlying the typical grey/black patina attributed to copper sulphides (Figure 46; bottom). After desiccation on storage the coupons had a mottled appearance consisting of grey copper sulphides and the typical brown hue of cuprite. Similar to the 2005 samples, this thin corrosion product layer easily peeled away from the residual metal exposing a very black, powdery surface typical of copper sulphides (Figure 47; right).

The SEM image of the unstripped coupon from 2004 (Figure 48; left) showed that there were two distinct copper sulphide phases present, which was supported by the slightly differing ratios of copper and sulphur in the EDX analysis. One corrosion product was isomorphous with the underlying metallographic structure and the other phase had a less clearly defined structure concentrated over the grain boundaries. For the 2005 copper samples, the dominant sulphide phase in the corrosion product matrix was richer in copper than the 2004 surface, which is consistent with the development of chalcocite ($Cu_2S$) as being the primary sulphide corrosion product. In 2009, after six years of exposure, the SEM image of the copper coupons and the EDX analysis showed a less clearly defined corrosion product layer on the surface consisting of an amorphous $Cu_2S$ phase [Figure 48; right (a)] and a more crystalline copper sulphide phase which included some elemental copper and cuprite [Figure 48; right (b)] overlying a very ordered crystalline phase of chalcocite ($Cu_2S$) [Figure 48; right (c)]. Finally there was a thin layer of isomorphous chalcocite overlying the intergranular microstructure of the parent copper metal [Figure 48; right (d)].

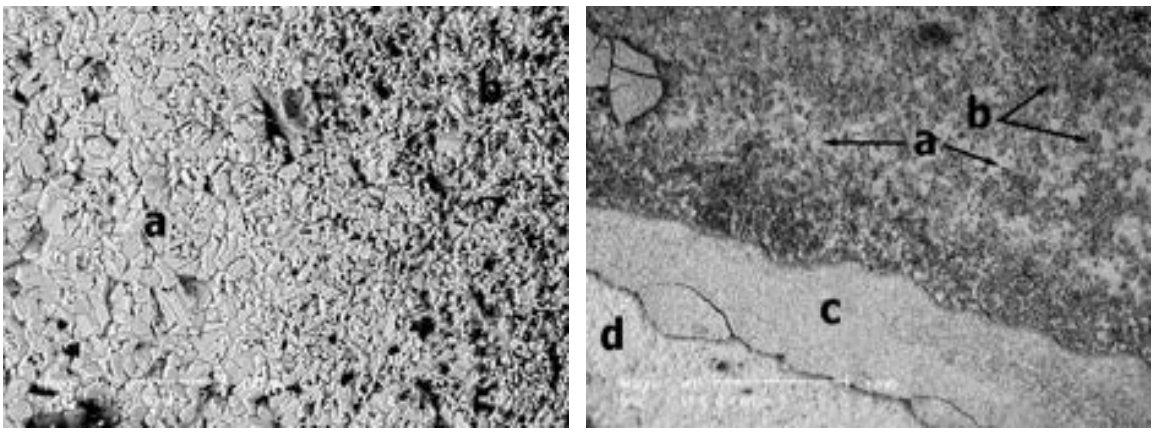


*Figure 48. SEM images of the unstripped copper coupons recovered from just below the sediment in 2004 (left): (a) isomorphous copper sulphide phase (light grey); (b) copper sulphide phase with a less clearly defined structure (dark grey) and in 2009 (right): (a) amorphous copper sulphide phase (light grey); (b) more crystalline copper sulphide phase (dark grey); (c) very ordered crystalline copper sulphide phase; (d) isomorphous copper sulphides overlying the intergranular microstructure of the copper metal.*

All stripped copper coupons showed uniform anaerobic corrosion across the grain surfaces as well as continued intergranular corrosion (Figure 49; left and right) that had been observed in the aerobic samples (Figure 26). Clearly localised corrosion along the grain boundaries is due to the different free energy of the copper atoms which are associated with micro-alloying impurities that naturally accumulate along the boundaries. Owing to the different electrochemical activity of the edges of the grains, as compared with the bulk material, it is not unexpected to find different corrosion products, as reflected in their EDX values. It should be noted that these are subtle effects of the burial process on the fate of the metal.

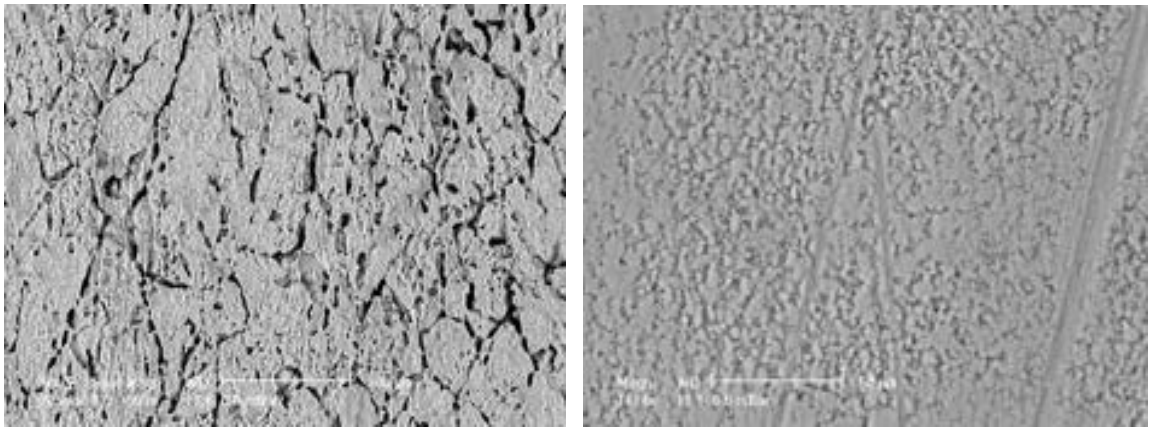

*Figure 49. SEM images of the stripped copper coupons recovered from just below the sediment in 2005 (left): corrosion along the grain boundaries and across the grains and in 2009 (right): more uniform corrosion across the grain surfaces and intergranular corrosion.*

The primary corrosion mechanisms occurring on the copper coupons recovered from the 0-15cm range below the sediment surface were very similar. In low oxygenated environments, such as near the sediment/seawater interface, the

normal aerobic corrosion mechanism will initially form cuprite on the copper coupon surface, however as the oxygen is consumed by corrosion (oxidation) reactions and/or biological activity the environment tends towards anaerobic conditions and the corrosion mechanism will change markedly. Under such conditions the sediment essentially functions as a closed system and the redox potential ($E_h$) of the interstitial water can fall below the hydrogen evolution potential and the main cathodic reaction in the metal corrosion process will be the reduction of water and not oxygen (equation 9).

$$2H_2O + 2e^- \rightarrow H_2 + 2OH^- \quad \text{.....(9)}$$

This reaction is usually slow but the presence of facultative and anaerobic bacteria in the sediment can catalyse this reaction. Sulphate reducing bacteria are especially important and utilise sulphate ions in the interstitial water of the sediment to produce sulphide ions which in turn, provide an alternative corrosion cycle for copper. The sulphide ions produced by these bacteria react with the copper ions released by the anodic reaction and form insoluble copper sulphide precipitates overlying the cuprite layer. An example of one such reaction is shown in equation 10.

$$2Cu + HS^- \rightarrow Cu_2S + H^+ + 2e^- \quad \text{.....(10)}$$

The most common corrosion product found under these conditions is chalcocite ($Cu_2S$), however due to slight variations in the $E_h$ and pH of the sediment during burial, a wide range of copper sulphides [$Cu_xS$ ($1 \leq x \leq 2$)] can be found in the adherent corrosion product film on the copper coupons. Once the initial copper sulphide layer has formed on the surface further corrosion of the metal produces $Cu^+$ ions which diffuse through this corrosion product layer to the sulphide rich region surrounding the coupon where they are precipitated and can trap silica, clay particles and calcareous material as is evident on the 2005 coupons.

#### 3.4.1.2 Weight Loss and Corrosion Rates

The normalised percentage weight losses for the copper coupons were 0.010%$cm^{-2}y^{-1}$ in 2004, which increased to 0.051% $cm^{-2}y^{-1}$ in 2005 and then decreased to 0.010% $cm^{-2}y^{-1}$ again after six years of exposure in 2009 (Figure 21). Similarly the calculated corrosion rates were 0.007 $mm.y^{-1}$ in 2004, 0.034 $mm.y^{-1}$ in 2005 and 0.022% $mm.y^{-1}$ in 2009 (Table 6). It appears that the corrosion behaviour of the 2005 copper coupons is anomalous and possibly there was a change in the microenvironment over the two year period (e.g. reburial/exposure cycles) that caused variations in the dissolved oxygen content and hence increased the extent of deterioration through differential aeration corrosion mechanisms.

### 3.4.2 Brass Coupons: Just Below Sediment

#### 3.4.2.1 Corrosion

All brass coupons (Bs I & Bs II) immediately after retrieval were very similar in appearance to the control samples, just less lustrous indicating very little corrosion (Figure 50 and Figure 11; left). After storage the coupons had become darker with very small amounts of grey/black corrosion products on the surfaces overlying a thin cuprite layer (Figure 51).


*Figure 50. Copper alloy coupons – just below sediment, immediately after recovery in 2004 after 1 year of exposure (top left), in 2005 after 2 years of exposure (top right) and in 2009 after 6 years of exposure (bottom).*

*Figure 51. The brass coupons – just below sediment recovered in 2004 after 2 years of storage (left), in 2005 after 1 year of storage (mid) and in 2009 after 5 months of storage (right).*

The SEM images of all unstripped brass coupons were markedly different from the aerobic brass coupons in that lead sulphide corrosion products were clearly identified, particularly along the grain boundaries while the original striation lines of the parent alloy had suffered from zonal corrosion (Figure 52; left and right). The EDX data indicated that there was general corrosion of the alloy producing a copper and zinc sulphide layer and localised corrosion of the lead-rich phases present in the β phase at the grain boundaries resulting in topical concentrations of the lead sulphide galena (PbS) in these areas (Figure 52; left). There were also distinct zinc-rich mineral phases overlying the background of the mixed copper-zinc sulphide layer. From the EDX data it is clear that the copper is dominated by the presence of $Cu_2S$ but in the mid to upper sections the amount of oxygen is too high to be accounted for by the clay type minerals and the colour and morphology of the corrosion products is consistent with some cuprite being present formed during the initial corrosion phase.

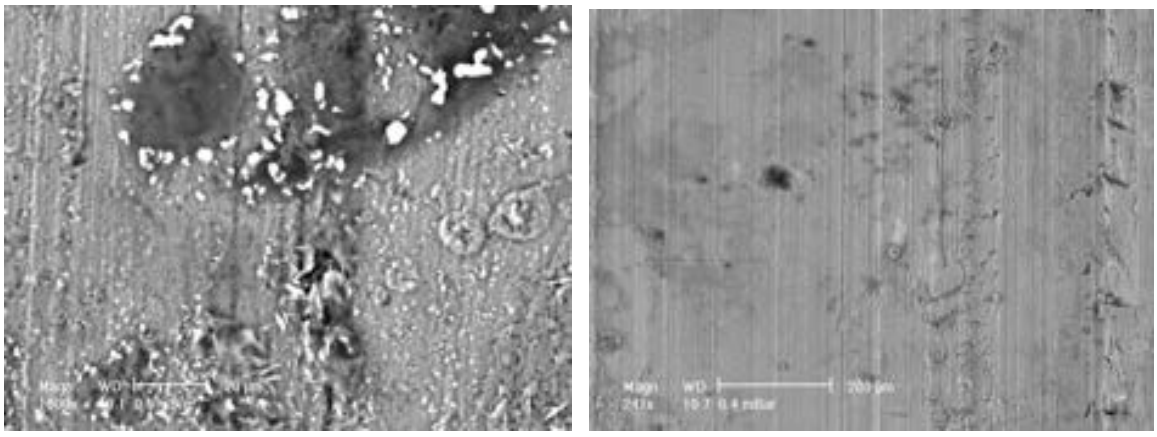

*Figure 52. SEM images of the unstripped brass coupons recovered from just below the sediment in 2004 (left): lead sulphides (bright crystals) and other copper and zinc sulphides (plate-like light grey crystals) and in 2009 (right): copper, zinc and lead sulphides along the original striation lines of the rolled parent brass.*

The 2004 stripped brass coupon showed very clear signs that the dominant corrosion mechanism was selective attack on the β zinc-rich phase (Figure 53; left). The selective corrosion of the zinc-rich phase in the mildly anaerobic microenvironment was not unexpected as dezincification is usually more pronounced under anaerobic conditions. The stripping of the coupon from 2005 showed up the previously observed intergranular corrosion as well as general surface corrosion of the α copper-rich phase. The 2009 stripped coupon showed slightly increased intergranular and surface corrosion across the grains (Figure 53; right).

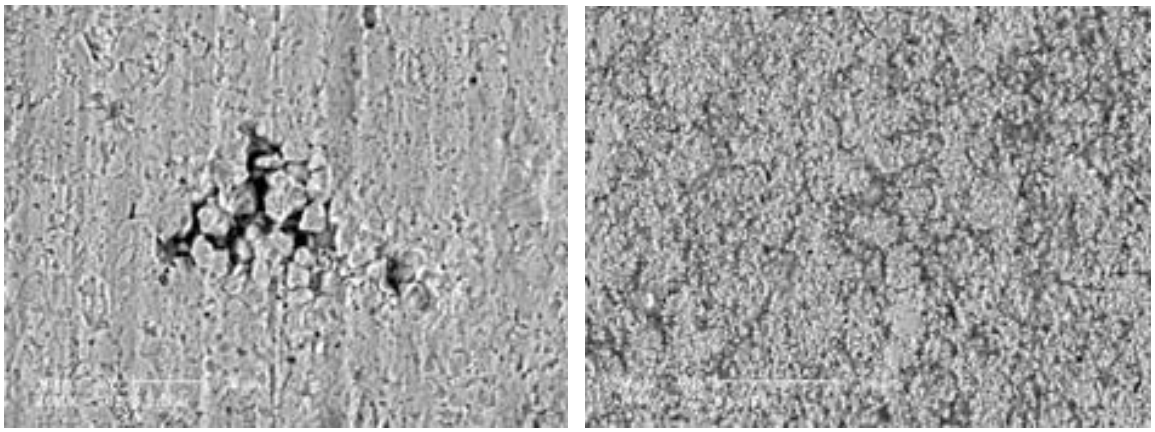

*Figure 53. SEM images of the stripped brass coupons recovered from just below the sediment in 2004 (left): selective attack of the β zinc-rich phase and in 2009 (right): increase in intergranular corrosion and corrosion across the grain surfaces.*

The dominant corrosion mechanisms for the brass coupons recovered from just below the sediment was a combination of general corrosion of the α copper-rich phase with some selective attack of the β zinc-rich phase and the lead concentrated along the grain boundaries of the β phase, which is not unexpected as the dissolved oxygen concentration in the first 15cm of sediment is usually quite variable causing different corrosion processes to occur on the brass coupons.

### 3.4.2.2 Weight Loss and Corrosion Rates

There was very little corrosion of the brass coupons recovered from just below the sediment surface and this was confirmed by the annualised normalised weight loss data and the normalised corrosion rates. The weight loss and corrosion rate of the 2004 sample was 0.001%$cm^{-2}y^{-1}$ and 0.001 $mm.y^{-1}$, the 2005 sample was 0.0005%$cm^{-2}y^{-1}$ and 0.0004 $mm.y^{-1}$ and the 2009 sample was 0.005%$cm^{-2}y^{-1}$ and 0.003 $mm.y^{-1}$, respectively (Figure 21 and Table 6), which was consistent with the visual and SEM observations.

### 3.4.3 Bronze Coupons: Just Below Sediment

#### 3.4.3.1 Corrosion

The bronze coupons (Bz I & Bz II) immediately on retrieval in 2004 had a very thin layer of black corrosion products on the surface (Figure 54; top left). After storage the coupons had a very thin lustrous grey-black layer of sulphide corrosion products adhering to the surface in some areas and the typical brownish hue of cuprite evident in other areas (Figure 55; left). The general appearance of the coupons recovered in 2005 (Figure 54; top right) and after storage (Figure 55; mid) were similar to that of the 2004 samples except that the patina had time to develop a more complex hue that overlaid the original mixed copper and tin oxide patina. The corrosion matrix of small copper sulphide crystals was highly reflective. The appearance of the 2009 copper coupons immediately after retrieval was considerably different from the samples recovered in 2004 and 2005. In some areas they possessed a secondary blue/green corrosion product layer overlying the typical grey/black patina attributed to copper sulphides (Figure 54; bottom). After desiccation on storage the coupons had a light grey mottled appearance consisting of copper sulphides and some incorporated sediment particles (Figure 55; right).


*Figure 54. Copper alloy coupons – just below sediment, immediately after recovery in 2004 after 1 year of exposure (top left), in 2005 after 2 years of exposure (top right) and in 2009 after 6 years of exposure (bottom).*

*Figure 55. The bronze coupons – just below sediment recovered in 2004 after 2 years of storage (left), in 2005 after 1 year of storage (mid) and in 2009 after 5 months of storage (right).*

The SEM images of the unstripped 2004 bronze coupons showed that the patina consisted of a mixture of copper-zinc sulphides as well as tin oxides and possible tin sulphides (Figure 56; left). The very bright areas were richest in lead sulphides and reflected corrosion of the tin-rich eutectoid phase where the lead concentrates. The general surface was characterised by the underlying metallographic structure of the heavily cored high tin bronze. The SEM images of the unstripped 2005 bronze coupons showed the strongly developed cubic crystals of chalcocite (Figure 56; right) and some other mixed phases that appeared to be a copper-lead sulphide and pustular globules of a copper-rich matrix that also contained zinc, lead and tin cations. The low amount of sulphide indicated that these mixed corrosion matrices may be principally composed of oxides and hydroxides which would relate more to changes in the surface after recovery rather than be a direct consequence of corrosion in the low oxygenated burial environment.

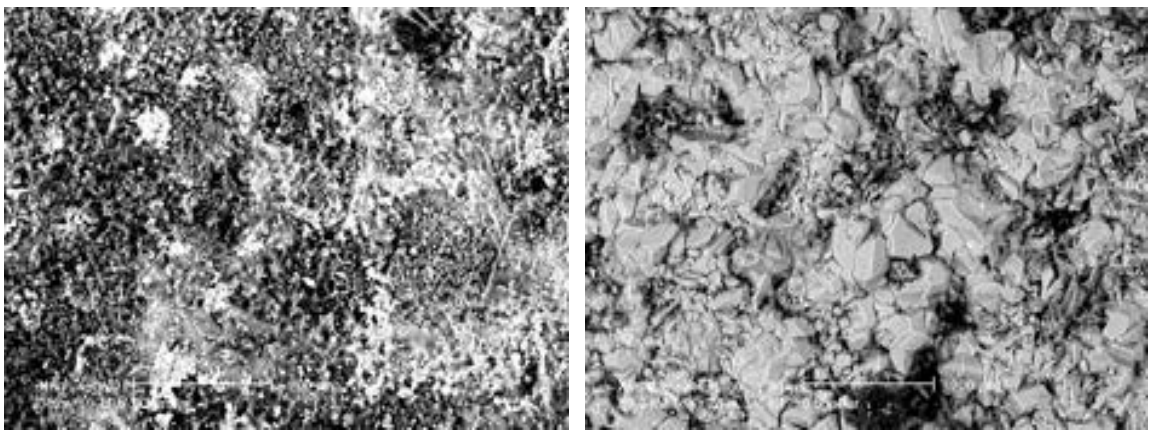

*Figure 56. SEM images of the unstripped bronze coupons recovered from just below the sediment in 2004 (left): the mixed copper and tin corrosion products and lead sulphides (bright areas) and in 2005 (right): the cubic crystals of chalcocite and some mixed phases of copper, lead and tin corrosion products.*

The SEM images and EDX analysis of the unstripped bronze coupons recovered in 2009 showed a much thicker and better developed corrosion product layer of

chalcocite ($Cu_2S$) with only very small traces of zinc and tin towards the top of the coupon (Figure 57).

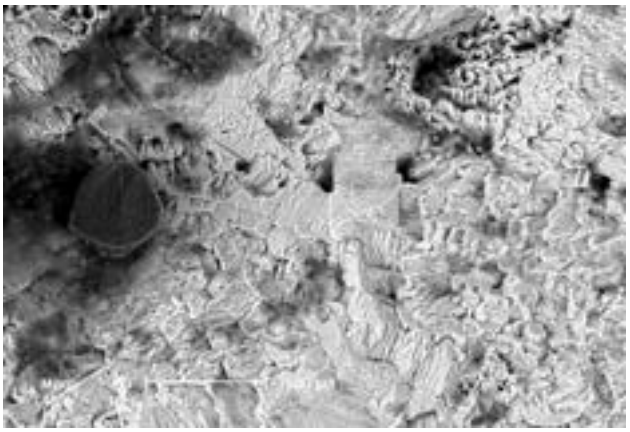

*Figure 57. SEM image of the unstripped bronze coupon recovered from just below the sediment in 2009 showing better developed cubic crystals of chalcocite on the surface with some incorporated interstitial sediment particles (dark grey areas).*

The SEM images of the 2004 stripped bronze coupon showed up well defined localised corrosion zones that had left isolated dendritic islands (Figure 58; left). There were difficulties in obtaining an effective strip of the 2005 bronze coupon owing to the inherent lack of reactivity of the well adhered sulphide patina but localised corrosion zones were evident (Figure 58; right).

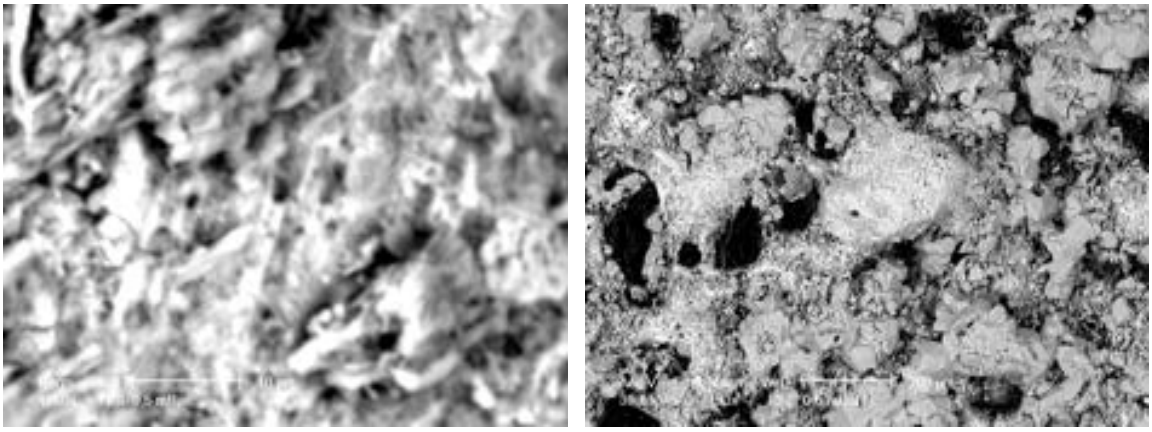

*Figure 58. SEM images of the stripped bronze coupons recovered from just below the sediment in 2004 (left) and in 2005 (right) indicating the localised corrosion zones.*

With the buried bronzes recovered after six years of exposure in 2009 the bright SEM phase was shown to be approximately 88% Cu and 4% Sn, which is consistent with it being residual copper-rich α phase of the bronze cast coupon. In Figure 59 (right) the tin corrosion products morphology reflected the underlying dendritic microstructure of the cast bronze.

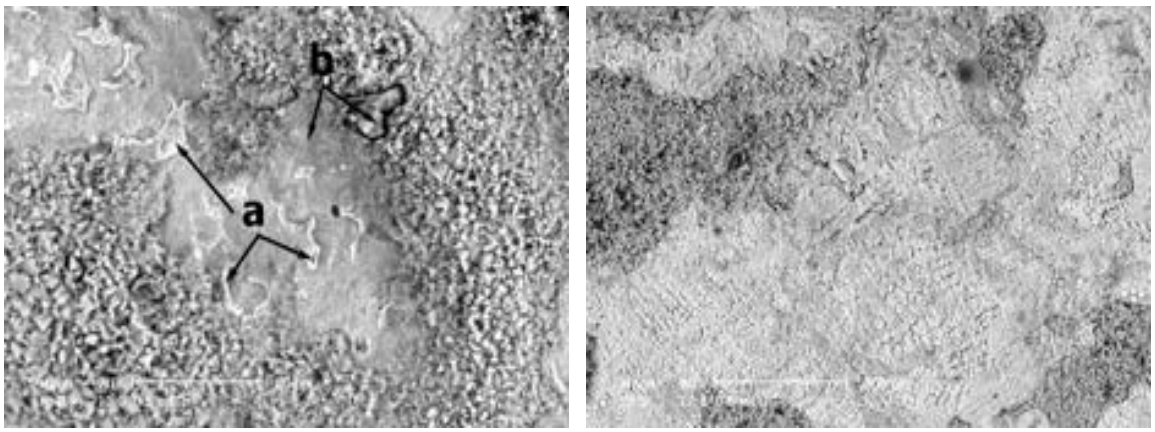


*Figure 59. SEM images of the stripped bronze coupons recovered from just below the sediment in 2009 (left): (a) residual copper-rich α phase; (b) localised differential corrosion of the tin-rich eutectic phase (right): selective corrosion of the cored dendritic structure with the residual tin corrosion products pseudo morphs of the underlying metallographic structure.*

The major corrosion mechanism for the 2004 and 2005 bronze coupons, was one of zonal corrosion where there was corrosion of both the copper-rich α phase and the tin-rich eutectic phase due to differences in the dissolved oxygen gradients in the sediment over the two year time period. However, after six years the major corrosion mechanism occurring on the bronze coupons buried just below the sediment had become selective corrosion of the tin-rich eutectic phase, which is the dominant corrosion mechanism under deoxygenated conditions.

### 3.4.3.2 Weight Loss and Corrosion Rates

The 2004 coupon had an annualised normalised percentage weight loss of 0.004%$cm^{-2}y^{-1}$ , the weight loss of the 2005 coupon was 0.009%$cm^{-2}y^{-1}$ and for the 2009 coupon it was 0.030%$cm^{-2}y^{-1}$ (Figure 21). Similarly the normalised corrosion rate was 0.002 $mm.y^{-1}$ in 2004, 0.004 $mm.y^{-1}$ in 2005 which then increased significantly to 0.013 $mm.y^{-1}$ by 2009 (Table 6). The increase in the weight loss and corrosion rate of the bronze coupons is simply a reflection of the longer immersion period.

### 3.4.4 Copper Steel Coupons: Just Below Sediment

#### 3.4.4.1 Corrosion

The copper steel coupon (Cu/Fe) recovered in 2004 showed a remarkably uniform corrosion pattern on the surface which was a deep charcoal grey to black and there was no evidence of periodic exposure of the support structure (Figure 60; top left). Despite the best attempts to minimise post recovery oxidation, the coupon underwent significant oxidation during storage (Figure 61; left). The as-recovered appearance of the 2005 coupon was similar to the 2004 sample except more interstitial marine sediment was present on the surface (Figure 60; top right). It also had a similar response to the problems of aerial oxidation (Figure 61; mid). However, after post recovery oxidation it became apparent that the amount of corrosion on the 2005 coupon had increased (Figure 61; mid). The coupon recovered in 2009 had significantly more concretion, corrosion products and interstitial sediment with entrained marine debris, such as fragments of waterlogged wood on the surface (Figure 60; bottom). On drying it was noted that there was significant spalling of these surface layers (Figure 61; right).

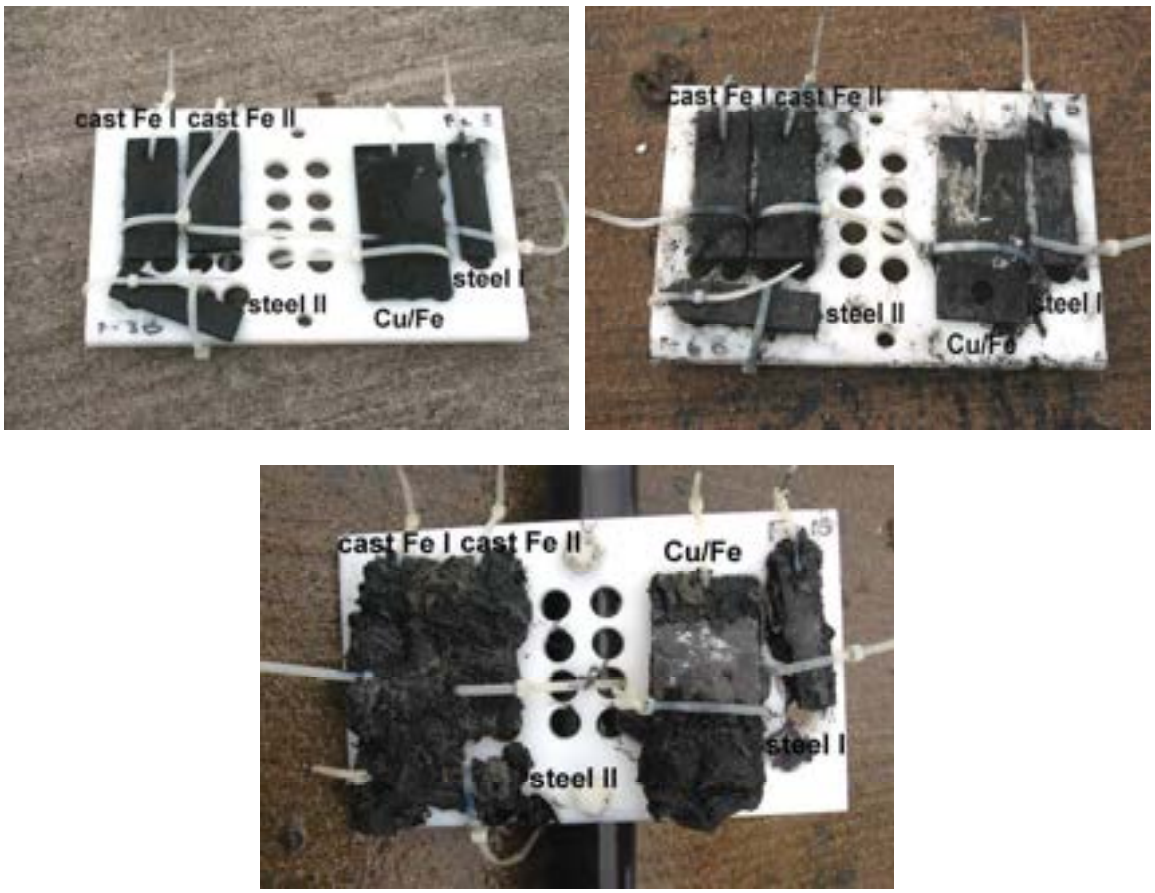


*Figure 60. Ferrous alloy coupons – just below sediment, immediately after recovery in 2004 after 1 year of exposure (top left), in 2005 after 2 years of exposure (top right) and in 2009 after 6 years of exposure (bottom).*

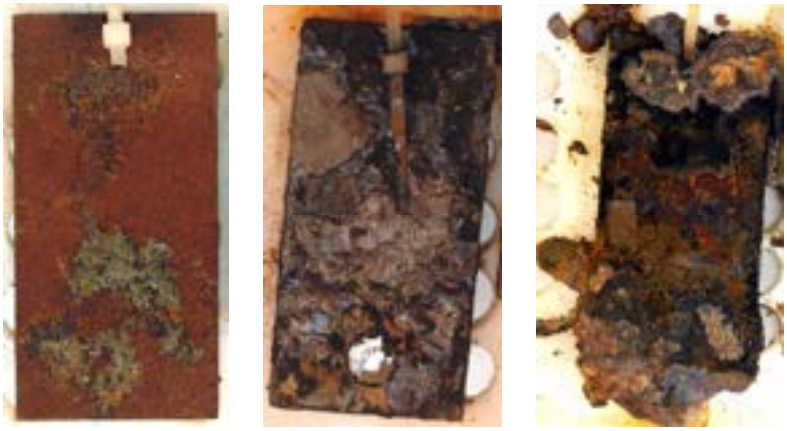

*Figure 61. The copper steel coupons – just below sediment recovered in 2004 after 2 years of storage (left), in 2005 after 1 year of storage (mid) and in 2009 after 5 months of storage (right).*

Where the SEM images focused on original material that had not been subjected to gross change, the underlying corrosion products showed a very uniform crystalline structure (Figure 62; left). There was essentially no calcareous material but the amount of sulphur present was much more marked, with up to 9% as $SO_2$ from the EDX analysis. The SEM images and EDX analysis of the 2005 and 2009 coupons showed up increased amounts of entrained sand grains, along with some calcareous deposits and clay minerals from the sediment as compared to the 2004 sample. Massive deposits of very crystalline iron sulphides (FeS) and large areas of amorphous iron oxyhydroxides associated with high chloride contents typical of lepidocrocite had become the dominant morphological feature of these coupons (Figure 62; right).

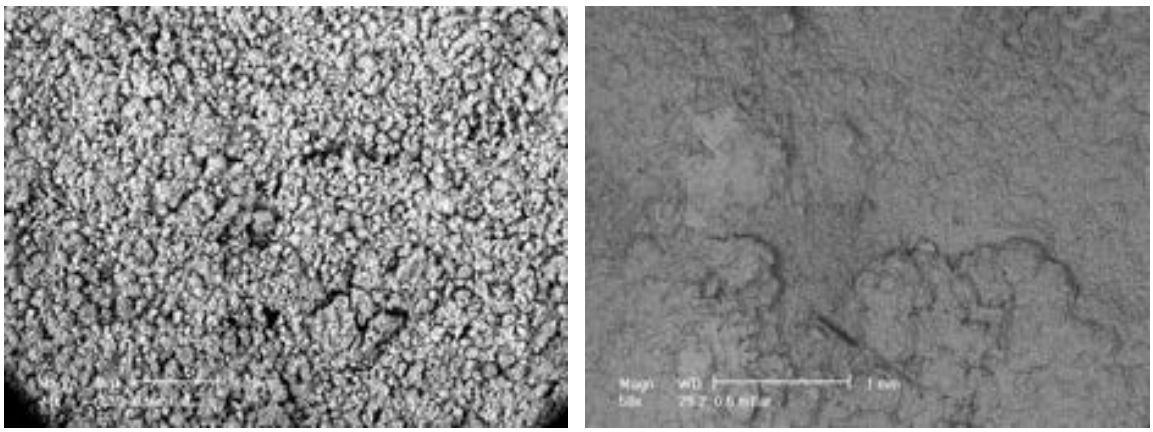

*Figure 62. SEM images of the unstripped copper steel coupon recovered from just below the sediment in 2004 (left): the uniform crystalline structure of the corrosion products and in 2009 (right): the crystalline iron sulphide corrosion products.*

The SEM image of the partially stripped surface from 2004 showed a marked difference in the surface under these burial conditions in that copper sulphides were now seen to be preferentially forming at the edges of macro-grains of the micro-galvanic cells (Figure 63; left). The aerobic samples showed no signs of the presence of copper having exerted a measurable effect. The wisdom of not using very aggressive stripping agents is seen in the retention of the copper sulphides at

the grain boundaries, which provides evidence of the detailed corrosion mechanism.

The stripped coupon recovered in 2005 simply reflected the original microstructure of the alloy with very uniform corrosion across the grains. In comparison to the 2004 sample there was no evidence of copper sulphide accumulation at the macro-grain boundaries in the 2005 coupon. This may indicate that the corrosion mechanism had stabilised somewhat after two years of burial and micro-galvanic corrosion cells present on the coupon in 2004 were not dominant in 2005 due to the overall decrease in dissolved oxygen content in the sediment after two years and the more extensive corrosion of the original surfaces.

In the SEM images of the stripped copper steel coupon from 2009 there was very clear evidence of selective corrosion across the face of the α ferrite grains with high relief of the former intergranular zone (Figure 63; right). The original concentration of manganese in these copper steel coupons was 0.61% but in the 2009 coupon the amount was 2% while the aerobic coupon it was 1% Mn. This data is consistent with reporting of manganese to the grain boundaries which effectively increased their concentration. Thus it would appear that as the burial conditions were altered from fully to partially oxygenated there was a change in corrosion mechanism.

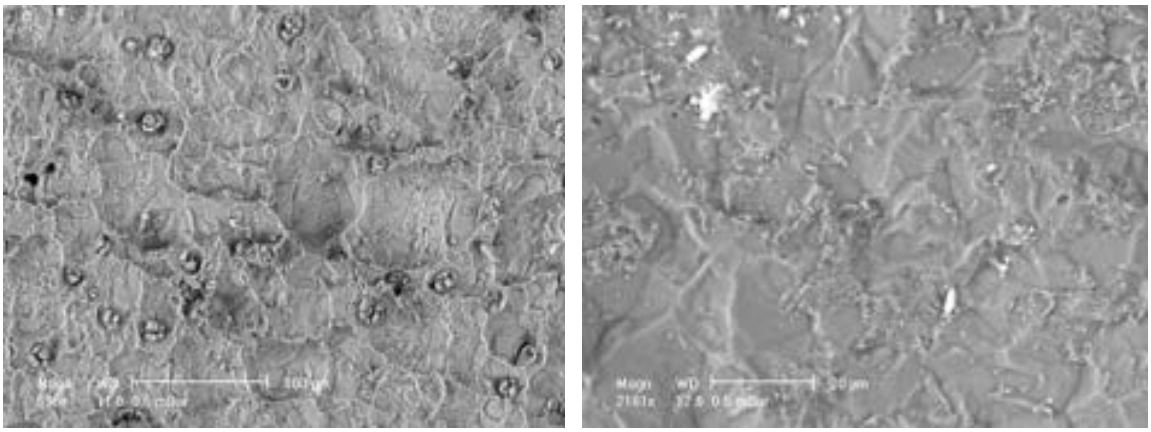

*Figure 63. SEM images of the stripped copper steel coupon recovered from just below the sediment in 2004 (left): intergranular corrosion with copper sulphides at the edges of the macro-grains and in 2009 (right): very uniform corrosion across the ferrite grains.*

### 3.4.4.2 Weight Loss and Corrosion Rates

The normalised weight loss for the 2004 coupon was 0.019%$cm^{-2}y^{-1}$, which increased to 0.028%$cm^{-2}y^{-1}$ in 2005 and again to 0.044%$cm^{-2}y^{-1}$ in 2009 (Figure 37). The corresponding corrosion rates were 0.035 $mm.y^{-1}$ in 2004 increasing slightly to 0.050 $mm.y^{-1}$ in 2005 and then quite dramatically to 0.146 $mm.y^{-1}$ in 2009 (Table 7). The systematic increase in the weight loss data and corrosion rates does not fit in with the general observations on long term marine corrosion experiments, which decrease with length of exposure. It is the opinion of the authors that this increase is a reflection of the change over in corrosion mechanism with time, the amount of concretion cover and the increasing depth of burial.

Near the sediment/seawater interface corrosion processes are dominated by dissolved oxygen and aerobic bacterial degradation. As the concretion builds up the microenvironment becomes less oxygenated the aerobic and facultative bacteria populations will decrease and the anaerobic bacteria will become more dominant. It would appear that several years of exposure to the conditions are required before the corrosion rates settle down towards a long-term value that is characteristic of archaeological metals. Therefore, it is important that the project continues to establish where the turning point is in terms of the rate of deterioration so we can then extrapolate to the effect on archaeological metals.

The primary corrosion mechanism occurring on the 2004, 2005 and 2009 copper steel coupons buried just under the sediment (0-15cm depth range) was essentially the same as that described above for the totally exposed coupons, however as the dissolved oxygen content in the surface sediment decreases by being utilised in the corrosion reactions and biological activity, the main cathodic reaction will be the reduction of interstitial water in the sediment and not oxygen (equation 9). Due to the lower redox potential of the sediment as compared to the oxygenated seawater, reduced iron species, such as magnetite ($Fe_3O_4$) and haematite ($\alpha$-$Fe_2O_3$) will be more prevalent in the corrosion matrix on the coupons buried just under the sediment than on the more exposed samples. As discussed above there is also a fundamental change in corrosion mechanism as the samples are aged and become less aerobic.

Moreover as the micro-environment under the sediment becomes increasingly depleted in oxygen over time, tending towards anaerobic conditions and if there is sufficient organic matter, sulphate reducing and other anaerobic bacteria will become the dominant microbes present under deoxygenated conditions. The action of sulphate reducing bacteria catalyses the cathodic reaction since their metabolism converts sulphate to sulphide ions, which then react with the iron ions produced in the anodic reaction to produce iron sulphides (FeS) and elemental sulphur on which the hydrogen evolution reaction occurs more rapidly than on the metal surface. Hence, the presence of high sulphur levels in the corrosion product matrix on these coupons buried just under the sediment is not unexpected. Further anaerobic corrosion of the metal and subsequent precipitation of the corrosion products surrounding the coupon will trap silica, calcareous material and clay particles as was evident on the 2005 and the 2009 coupons.

### 3.4.5 Cast Iron Coupons: Just Below Sediment

#### 3.4.5.1 Corrosion

Upon recovery the 2004 cast iron coupons (cast Fe I & II) were uniformly black in appearance (Figure 64; top left) but gradually their appearance changed due to the combined effects of dehydration and oxidation on storage (Figure 65; left). The cast iron coupons recovered in 2005 were also uniformly black in appearance, however there was significantly more sediment incorporated in the surface layer (Figure 64; top right). As with all the other iron coupons, there were marked post recovery changes that saw massive amounts of spalling of the corroded surface, which indicated that these coupons were significantly more degraded than the 2004 samples (Figure 65; mid). The coupons recovered in 2009 had significantly more concretion, corrosion products and interstitial sediment with entrained marine debris, such as fragments of waterlogged wood incorporated into the surface layer (Figure 64; bottom). On drying there was significant spalling of these layers (Figure 65; right).

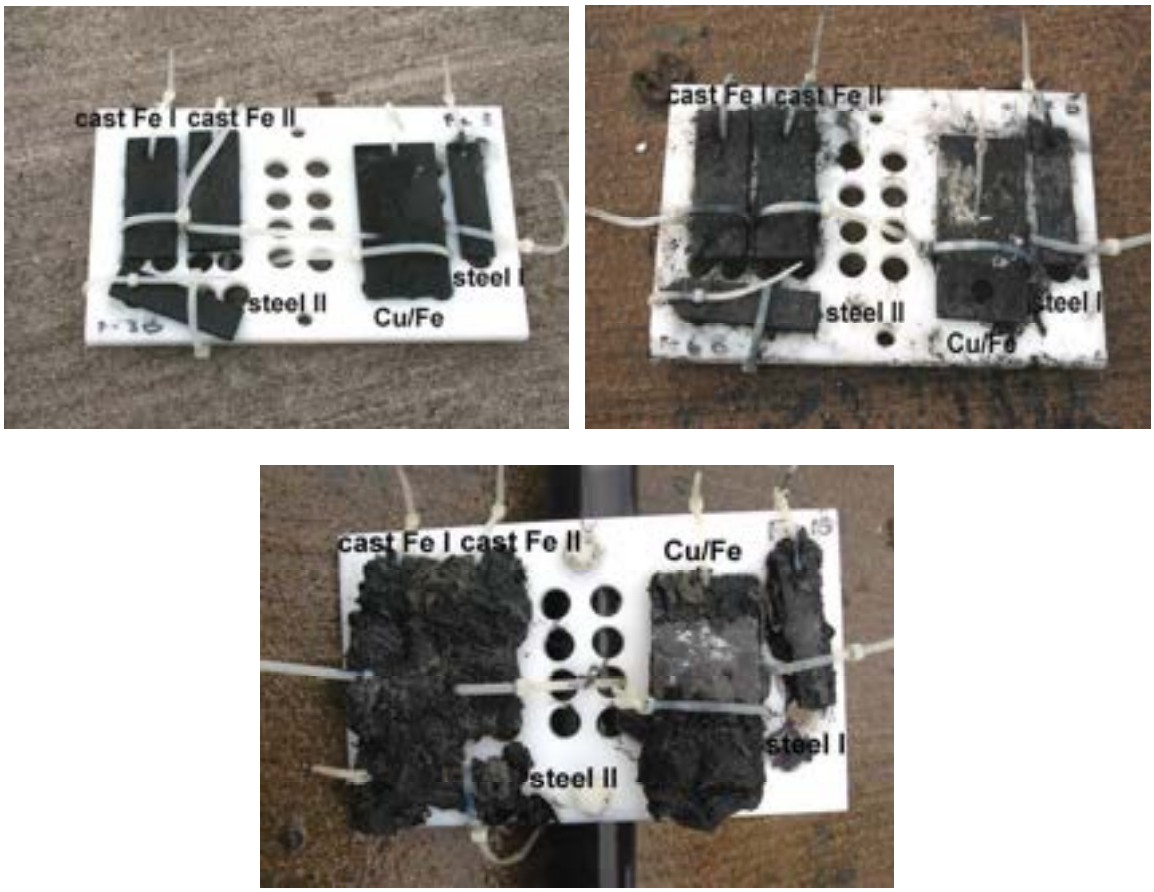


*Figure 64. Ferrous alloy coupons – just below sediment, immediately after recovery in 2004 after 1 year of exposure (top left), in 2005 after 2 years of exposure (top right) and in 2009 after 6 years of exposure (bottom).*

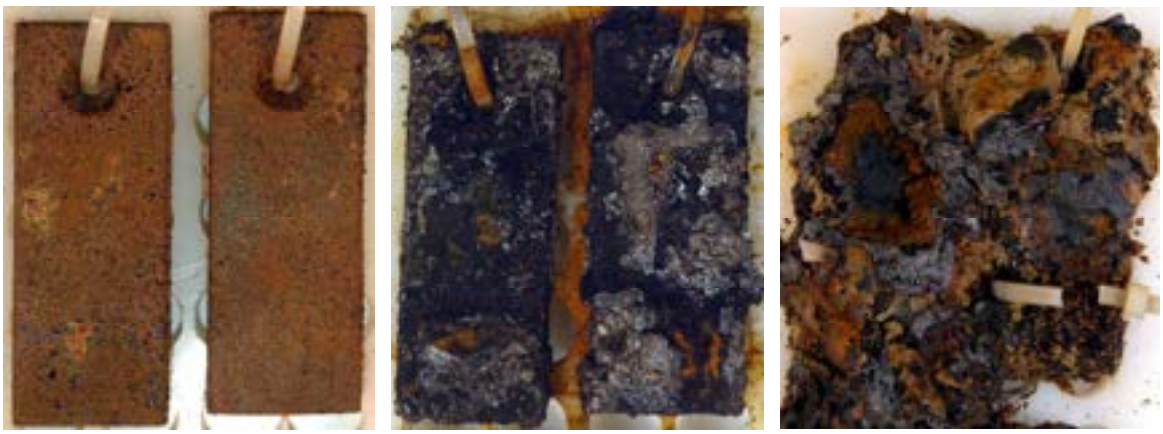

*Figure 65. The cast iron coupons – just below sediment recovered in 2004 after 2 years of storage (left), in 2005 after 1 year of storage (mid) and in 2009 after 5 months of storage (right).*

The SEM images of the 2004 unstripped cast iron coupons showed up a background area of an amorphous deposit of a mixture of iron carbonates, iron sulphides and iron oxyhydroxides (Figure 66; left). The latter are believed to be an artefact of the recovery and storage environments. The SEM images of the 2005 unstripped coupons showed a typical flat pavement area which was a mixed corrosion product with some areas of secondary mineralisation associated with much higher sulphur levels. In the crystalline zone there were clearly defined clusters of calcium carbonate 10µm needles amongst the clay particles and the nearby iron sulphides. The presence of inorganic calcium carbonate shows that in this environment, just below the sediment, there is still sufficient oxygen to allow for it to be used as an oxidising agent. As oxygen is reduced by the cast iron, the increased local pH from the production of hydroxides will result in the precipitation of inorganic $CaCO_3$. The SEM images and EDX analysis of the corrosion products on the 2009 unstripped coupons showed the expected complex mixture of iron oxyhydroxides, iron sulphides, concretion and clay particles and the amount of iron sulphides in the corrosion matrix increased with a concomitant drop in the amount of chloride ions and calcium as the coupon was traversed towards the foot of the coupon indicative of the decrease in the dissolved oxygen gradient as the depth of the sediment increased.

After stripping the cast iron coupon recovered in 2004 showed up the graphite flakes and structure of the grains of the parent alloy and the overall amount of attack on the cast iron was significant. The 2005 stripped sample showed up the normal corrosion pattern expected for marine cast iron and the image in Figure 67 (left) showed up the lamellar nature of the pearlite phase (ferrite and cementite), with preferential corrosion of the iron, which had not been clearly discernable in the stripped aerobic cast iron samples recovered from above the sediment. Thus subtle differences are being discerned between these two microenvironments by the microstructural differences in the metallography of the coupons. The SEM images and EDX analysis of the stripped coupon from 2009 showed very extensive corrosion where the iron was preferentially attacked leaving behind the residual carbon-rich phases (Figure 67; right). The corrosion around some of the ferrite grains was so extensive as to leave them as broken elements on the original surface.

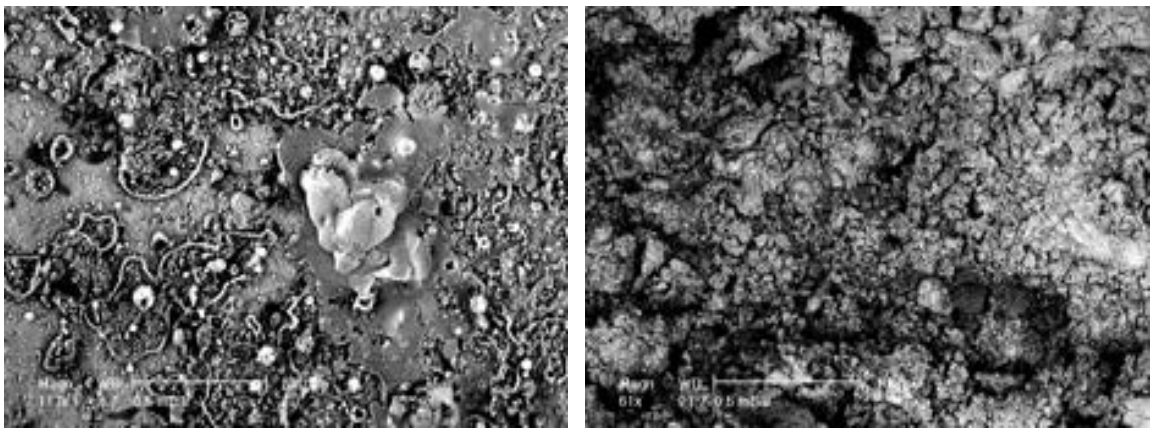

*Figure 66. SEM images of the unstripped cast iron coupons recovered from just below the sediment in 2004 (left): the mixture of different iron corrosion products and in 2009 (right): the mixture of iron oxyhydroxides, iron sulphides, concretion and some clay particles.*

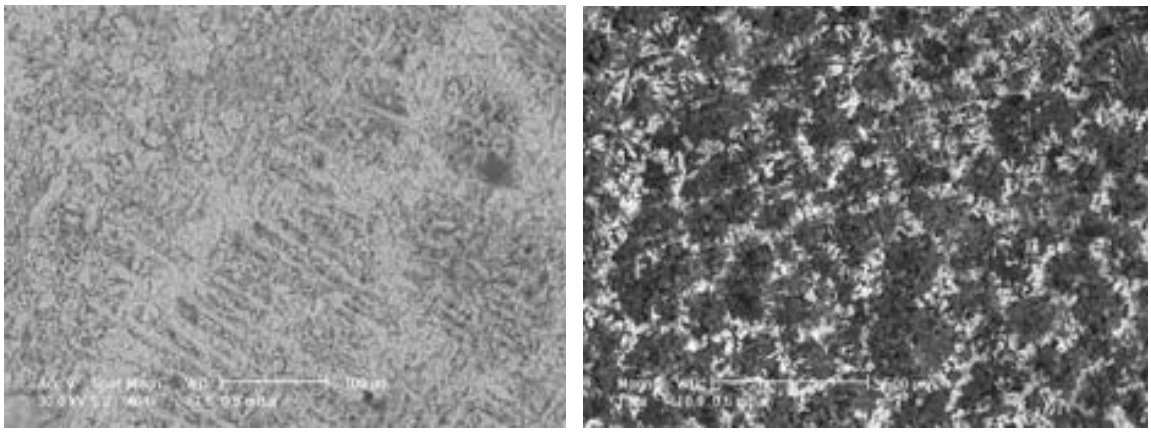

*Figure 67. SEM images of the stripped cast iron coupons recovered from just below the sediment in 2005 (left): lamellar structure of the pearlite phase and in 2009 (right): preferential attack of the iron resulting in carbon enrichment (dark grey areas).*

### 3.4.5.2 Weight Loss and Corrosion Rates

The normalised weight losses for the cast iron coupons increased over the six year burial period. The weight loss after one year of burial was 0.017%$cm^{-2}y^{-1}$ in 2004, which doubled by 2005 to 0.038%$cm^{-2}y^{-1}$ and then increased again to 0.122%$cm^{-2}y^{-1}$ by 2009 (Figure 37). The normalised corrosion rates also increased over this time period i.e. 0.021 $mm.y^{-1}$ in 2004, 0.043 $mm.y^{-1}$ in 2005 and 0.146 $mm.y^{-1}$ in 2009 (Table 7). Again, this systematic increase in the weight loss data and apparent corrosion rates is not typical of long term corrosion where the rates should decrease with increasing time of exposure and is simply a reflection of the longer immersion period. This indicates that even after six years of shallow burial the coupons have yet to fully equilibrate with the microenvironment where extrapolation to long-term corrosion of archaeological materials is possible. However, the actual corrosion mechanisms applicable to the processes occurring on these cast iron coupons were similar to those described for the copper steel coupons recovered from just below the sediment.

### 3.4.6 Mild Steel Coupons: Just Below Sediment

#### 3.4.6.1 Corrosion

In 2004 the mild steel coupons (steel I & II) were recovered with a very thin uniform black corrosion product layer (Figure 68; top left), which only altered slightly during storage (Figure 69; left). There also appeared to be significantly less corrosion of the mild steel coupons compared to the cast iron and the copper steel coupons on the same support plate (Figure 69; top left). The 2005 coupons were recovered with the expected black corrosion product matrix with engrained sediments (Figure 68; top right) that gradually changed to a mottled spalling matrix upon inadvertent exposure to air during storage (Figure 69; mid). There was also far more corrosion on the surface of these coupons than for the coupons recovered in 2004 (Figure 69; left and mid). The coupons recovered in 2009 were very similar in appearance to the cast iron coupons and had significantly more concretion, corrosion products and interstitial sediment with entrained marine debris than the coupons recovered in 2004 and 2005 (Figure 68; bottom). On drying there was significant spalling of this corrosion matrix (Figure 69; right).

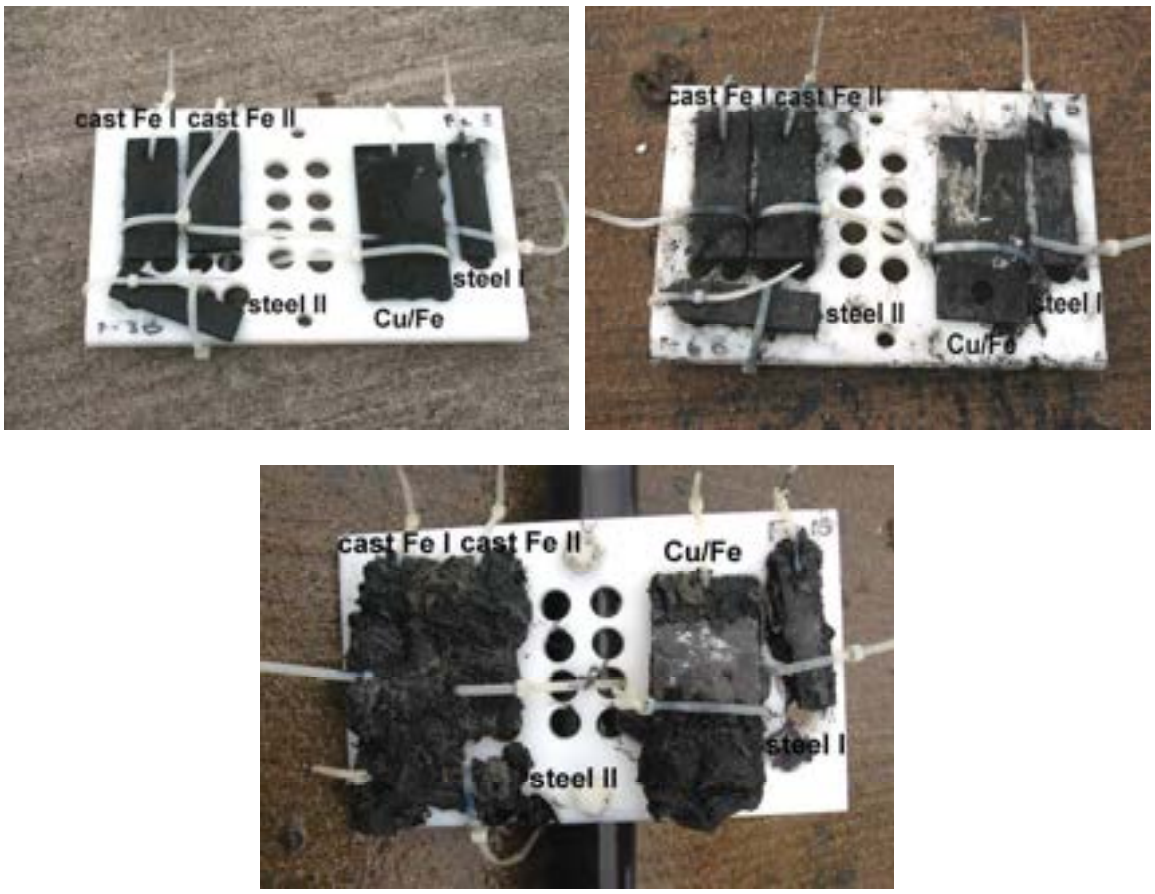


*Figure 68. Ferrous alloy coupons – just below sediment, immediately after recovery in 2004 after 1 year of exposure (top left), in 2005 after 2 years of exposure (top right) and in 2009 after 6 years of exposure (bottom).*

*Figure 69. The mild steel coupons – just below sediment recovered in 2004 after 2 years of storage (left), in 2005 after 1 year of storage (mid) and in 2009 after 5 months of storage (right).*

The SEM images of the 2004 unstripped mild steel coupons showed that the plate was covered with a uniform corrosion layer that was mainly an iron sulphide with a few localised outgrowths of a secondary sulphide (Figure 70; left). This coherent layer of sulphides had much lower sulphur content than the secondary outgrowths. The SEM images of the unstripped 2005 samples were characterised by a mixed matrix of iron sulphides and entrained sediment minerals and there was ample evidence of inorganically deposited calcium carbonate crystals, which confirmed the corrosion processes and mechanisms observed under the same burial conditions for the cast iron samples. The SEM images and EDX analysis of the corrosion product layers on the mild steel coupons recovered in 2009 were similar to the 2005 coupons with iron sulphides, calcium carbonate and clay particles identified (Figure 70; right).

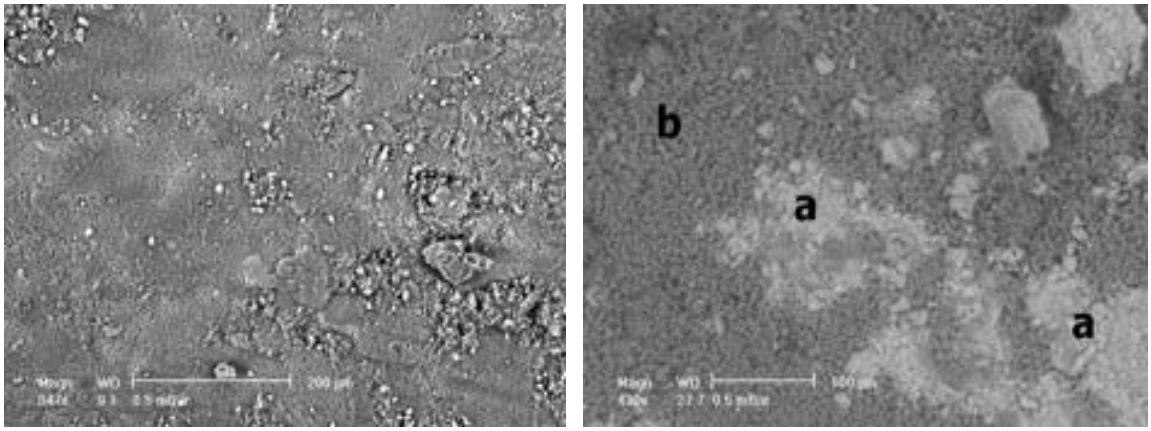


*Figure 70. SEM images of the unstripped mild steel coupons recovered from just below the sediment in 2004 (left): uniform iron sulphide corrosion product layer and in 2009 (right): (a) iron sulphides with calcium carbonate; (b) clay particles.*

The stripped mild steel coupon from 2004 showed deep incisions into the corrosion layer plate due to localised pitting corrosion reactions that would have lead to the secondary mineralisation that was very rich in sulphur, compared with the background levels. The background corrosion pattern was similar to that observed in the aerobically corroded 2005 mild steel coupon recovered from

above the sediment. The 2005 and 2009 stripped samples showed up localised intense corrosion along the lines of the slag inclusions that related to the original deformation associated with the production of the mild steel plates from which the coupons were cut. The SEM images in Figure 71 (left and right) showed up well defined rounded corrosion pits associated with the anaerobic corrosion processes, however these were more extensive in the 2009 sample.

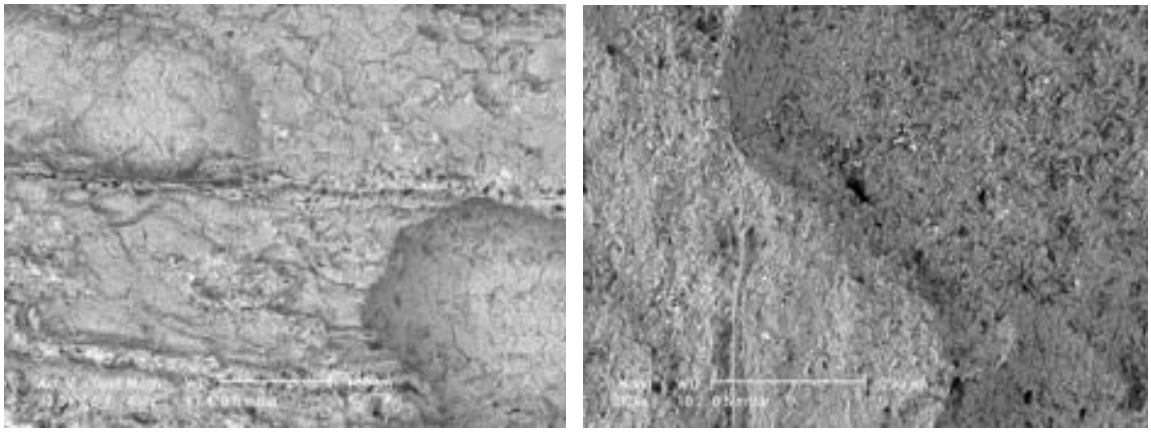

*Figure 71. SEM images of the stripped mild steel coupons recovered from just below the sediment in 2005 (left): corrosion pits and corrosion along the lines of slag inclusions and in 2009 (right): more extensive pitting and corrosion across the ferrite grains.*

### 3.4.6.2 Weight Loss and Corrosion Rates

In 2004 the normalised weight loss for the mild steel coupon was 0.033%$cm^{-2}y^{-1}$, in 2005 it was similar at 0.040%$cm^{-2}y^{-1}$ and in 2009 it had increased to 0.076%$cm^{-2}y^{-1}$ (Figure 37). The corrosion rates also increased over the six year burial period with the rates calculated at 0.024$mm.y^{-1}$ in 2004, 0.029$mm.y^{-1}$ in 2005 and 0.054$mm.y^{-1}$ in 2009 (Table 7). These increasing trends for the weight losses and corrosion rates over the six year burial period supported the SEM observations and were again a direct consequence of the increased immersion period and did not accurately reflect long-term corrosion rates of archaeological metals. The same corrosion mechanisms described for the copper steel and cast iron coupons just under the sediment would also apply to these mild steel coupons.

## 3.5 ENVIRONMENT CONDITIONS - ANAEROBIC

### 3.5.1 Copper Coupons: 50cm Below Sediment

#### 3.5.1.1 Corrosion

On retrieval in 2004, the copper coupons (Cu I & Cu II) recovered from 50cm below the sediment surface possessed a very thin, adherent corrosion product layer, which had the typical black appearance of copper sulphides (Figure 72; top left) and did not disbond upon dehydration during storage. After storage, the underlying cuprite layer was also easily discerned (Figure 73; left). The copper coupons immediately after retrieval in 2005 were very similar in appearance to the 2004 samples except with a thicker corrosion product layer (Figure 72; top right). After drying the coupons were characterised by a thin layer of sulphides, mixed in with some sediment. The underlying cuprite layer was evident on the coupon surfaces after one year of storage (Figure 73; mid). The copper coupons immediately after recovery in 2009 were very similar to those retrieved in 2005 characterised by a slightly thicker black corrosion layer typical of sulphides with some incorporated interstitial sediment (Figure 72; bottom). After desiccation on storage this grey corrosion product layer easily disbonded from the parent metal surface (Figure 73; right).


*Figure 72. Copper alloy coupons – 50cm below sediment, immediately after recovery in 2004 after 1 year of exposure (top left), in 2005 after 2 years of exposure (top right) and in 2009 after 6 years of exposure (bottom).*

*Figure 73. The copper coupons – 50cm below sediment recovered in 2004 after 2 years of storage (left), in 2005 after 1 year of storage (mid) and in 2009 after 5 months of storage (right).*

The overall appearance of the unstripped copper coupons from 2004 (Figure 74; left) was essentially that described for the low oxygen (just below sediment) samples (Figure 48; left). The surface was characterised by well defined copper sulphide deposits that had grown more intensely along the lines of stress associated with the original manufacturing processes of the coupon. There was also a significant amount of mixed calcium and silica containing deposits on the surface which were clearly identifiable through the SEM as well as through their morphology, which was generally flat and plate-like in appearance. There were still two phases of copper sulphide present, one of which still showed the underlying primary grain structure of the parent metal. The SEM images and EDX analysis of the 2005 copper coupons showed that the copper sulphides were becoming the dominant landscape feature of the surface. The unstripped 2009 samples showed a more uniform corrosion product matrix overlying the primary grain structure of the copper metal. The main minerals identified through EDX analysis were chalcocite ($Cu_2S$) and cuprite ($Cu_2O$) with a small amount of copper chloride (Figure 74; right).

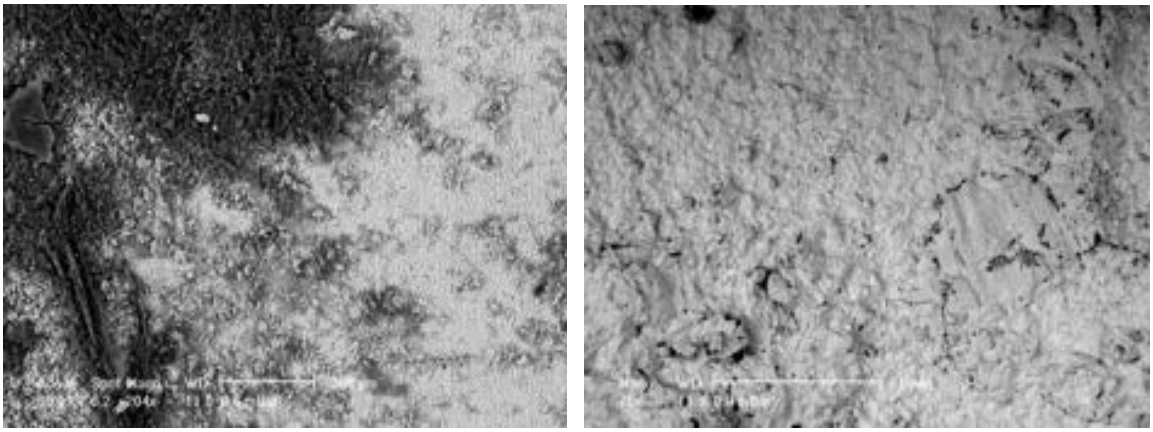

*Figure 74. SEM images of the unstripped copper coupons recovered from 50cm below the sediment in 2004 (left): the two different copper sulphide phases (light grey) and calcium and silica deposits (black areas) and in 2009 (right): chalcocite and cuprite overlying the primary grain structure of the parent copper metal.*

The stripped copper samples from all years showed up the same form of corrosion, which was uniform anaerobic corrosion across the grain surfaces in combination with intergranular corrosion along the grain boundaries (Figure 75).

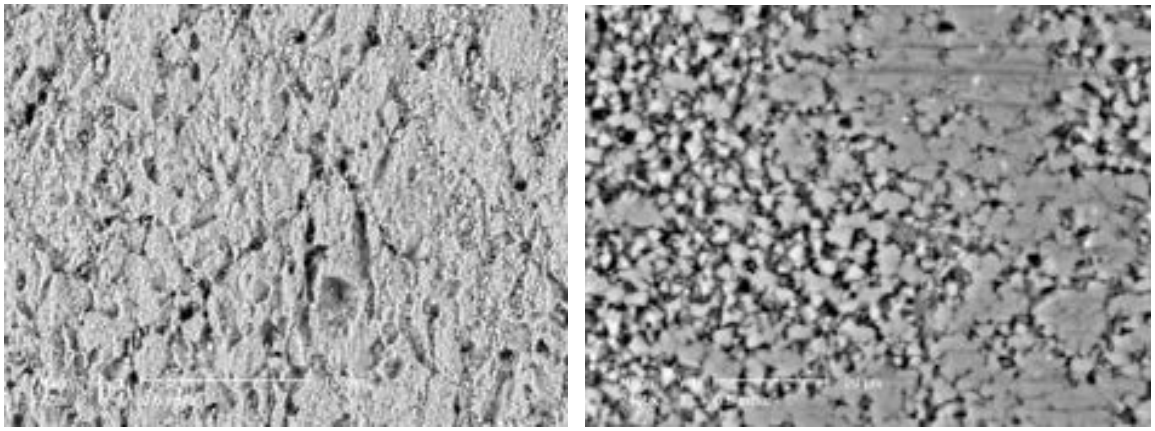

*Figure 75. SEM images of the stripped copper coupons recovered from 50cm below the sediment in 2005 (left) and in 2009 (right): showing the uniform anaerobic corrosion across the grain surfaces as well as intergranular corrosion.*

### 3.5.1.2 Weight Loss and Corrosion Rates

The annualised normalised weight losses for the 2004, 2005 and 2009 copper coupons was 0.005%$cm^{-2}y^{-1}$, 0.015% $cm^{-2}y^{-1}$ and 0.017% $cm^{-2}y^{-1}$, respectively (Figure 21) and this slight increase over the past six years is simply a result of the longer burial period. In support, the corrosion rate for the 2004 coupons was 0.004 $mm.y^{-1}$, which increased to 0.010 $mm.y^{-1}$ in 2005 and again to 0.017 $mm.y^{-1}$ for the 2009 samples (Table 6). The relatively smaller difference in the weight loss data and corrosion rates for the 50cm buried samples, compared with the just below the surface, is consistent with the fact that the most dramatic changes in microenvironment occur in the first 15cm of the sediment and this, in turn leads to increased corrosion in the more shallower burial depths.

The same corrosion mechanisms apply to the copper coupons buried to a depth of 50cm as per the coupons buried just below the sediment. However, small differences were noted as the corrosion product layers were thinner, more uniform and adherent on the 50cm samples and more silica and clay particles were incorporated in these corrosion product matrices, indicating a more rapid establishment of the anaerobic corrosion mechanism and hence, less overall corrosion. In laboratory studies it is generally agreed that the presence of sulphide ions increases the corrosion rate of copper and its alloys above that normally encountered in the same $E_h$ and pH range, however examination of wreck material submerged for several decades indicates that the copper sulphide layer can be protective. Therefore, this may assist in partially explaining the increase in the corrosion rates of the 2005 coupons recovered from just below the sediment which possessed less adherent and less uniform corrosion product layers as compared to the samples buried to a depth of 50cm.

### 3.5.2 Brass Coupons: 50cm Below Sediment

#### 3.5.2.1 Corrosion

All brass coupons (Bs I & Bs II) immediately after retrieval were very similar in appearance to the control samples, just less lustrous indicating very little corrosion (Figure 76 and Figure 11; left). After storage the 2004 coupons had uneven patches of grey black corrosion products on the surfaces overlying the typical brown cuprite layer (Figure 77; left). The appearance of the 2005 coupons after storage was similar to the 2004 sample except there were dark lines of corrosion products running parallel to the striation lines (Figure 77; mid). The 2009 brass samples possessed a patchy patina of grey/black sulphides as well as some typical aerobic blue/green corrosion products on the surface which were also evident on the 2005 coupons. These were likely to have formed during oxidation of the surface during storage (Figure 77; mid and right).


*Figure 76. Copper alloy coupons – 50cm below sediment, immediately after recovery in 2004 after 1 year of exposure (top left), in 2005 after 2 years of exposure (top right) and in 2009 after 6 years of exposure (bottom).*

*Figure 77. The brass coupons - 50cm below sediment recovered in 2004 after 2 years of storage (left), in 2005 after 1 year of storage (mid) and in 2009 after 5 months of storage (right).*

The SEM and EDX analysis of the unstripped brass coupons recovered in 2004 showed the presence of lead sulphide minerals, most likely galena (PbS) overlying a matrix of mixed copper and zinc sulphide-rich corrosion products (Figure 78; left). It should be noted that the surface had a very complex corrosion matrix with at least four distinct phases that could be resolved at moderate magnification. There were small cubic crystals of cuprite, plate-like crystals that appeared to be a mixed copper zinc sulphide and massive block-like deposits of a zinc sulphide. The SEM images of the 2005 coupons showed up the plate-like zinc-rich copper sulphides as well defined crystals, surrounded by a general matrix of marine debris and other corrosion products that included cuprite, zinc oxides/hydroxides and localised precipitates of lead sulphide. The SEM images and EDX analysis of the unstripped brass coupons from 2009 were similar to the 2005 coupons, however with significantly less sulphide and large quantities of cuprite and trapped zinc oxides with localised lead sulphide crystals (Figure 78; right).

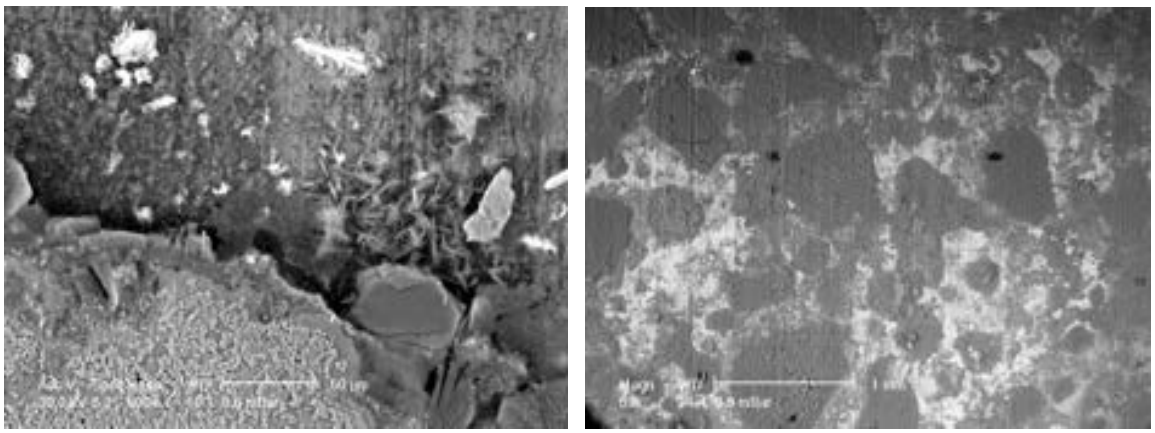

*Figure 78. SEM images of the unstripped brass coupons recovered from 50cm below the sediment in 2004 (left): the lead sulphide (bright crystals) and the other sulphide-rich corrosion products and in 2009 (right): cuprite and zinc oxides (dark grey areas) with some localised lead sulphides (bright crystals).*

Previously noted zonal corrosion around grain boundaries and fabrication stress lines were more clearly developed in the stripped 2004 samples than in the samples recovered from just below the sediment surface. This indicated that the selective corrosion of the zinc-rich β phase was becoming more dominant and is the primary corrosion mechanism of anaerobically corroded brasses. The EDX analysis of the stripped brass coupons recovered in 2005 and 2009 showed up a slight surface enrichment of copper compared to the uncorroded reference sample, which again supports the fact that the primary corrosion mechanism of duplex brass under anaerobic conditions is the selective corrosion of the zinc-rich β phase (Figure 79) and the lead which concentrates long the interdendritic lines between the β phase and the copper-rich α phase.

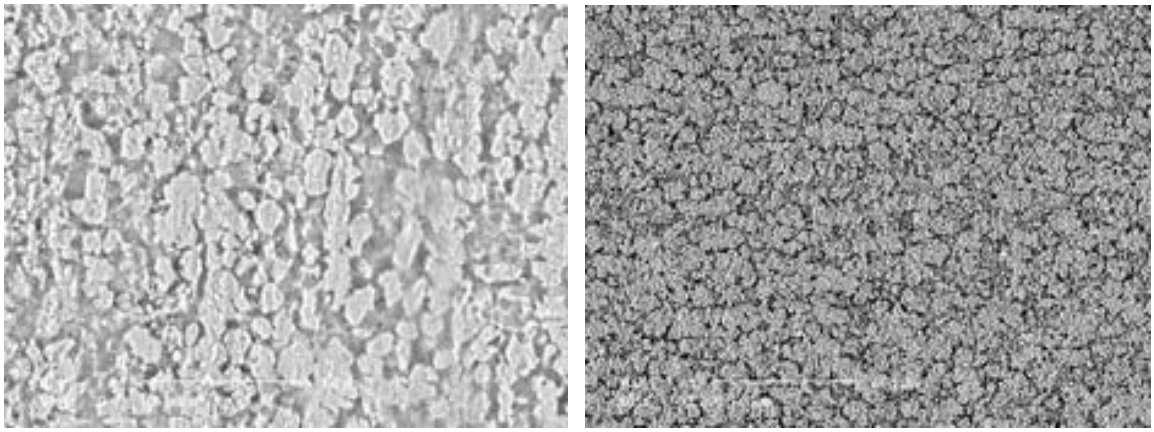

*Figure 79. SEM images of the stripped brass coupons recovered from 50cm below the sediment in 2005 (left) and in 2009 (right) showing the corrosion of the zinc-rich β phase*.

### 3.5.2.2 Weight Loss and Corrosion Rates

The annualised normalised weight loss for the 2004, 2005 and 2009 coupons was 0.001%$cm^{-2}y^{-1}$, 0.001%%$cm^{-2}y^{-1}$ and 0.005%%$cm^{-2}y^{-1}$, respectively (Figure 21). The normalised corrosion rates were 0.001$mm.y^{-1}$ in both 2004 and 2005, which then increased slightly to 0.004$mm.y^{-1}$ by 2009 (Table 6). The percentage weight loss and corrosion rate data is within experimental error of the results observed for the brass coupons recovered from just below the sediment.

These results clearly indicate that the burial environment in Marstrand harbour is very benign with regard to overall corrosion of leaded duplex brass. Usually brasses with zinc contents greater than 32%, such as these yellow brass coupons (36 - 43%; Table 4) are more reactive than pure copper but the addition of relatively high concentrations of lead provides excellent corrosion resistance for these types of copper alloys. Therefore, in comparison to the tough pitch copper coupons recovered from the sediment in this reburial experiment, the buried leaded yellow brass coupons were significantly less corroded. One of the reasons for this decrease in corrosion would be that in low oxygen and anaerobic environments, the lead concentrated at the grain boundaries and the zinc-rich phase of the duplex brass selectively corrodes, forming coherent layers of lead sulphides and voluminous zinc deposits on the surface that block further corrosion. However, at this stage in the project it is difficult to determine the benefits that would accrue from burial at the deeper 50cm depth but it is obvious

that exposure to the aerobic marine environment significantly increases the extent of corrosion of leaded duplex brass.

### 3.5.3 Bronze Coupons: 50cm Below Sediment

#### 3.5.3.1 Corrosion

Immediately after recovery the bronze coupons (Bz I & Bz II) from 2004 had a very thin layer of black corrosion products present on the surface (Figure 80; top left). On drying the 2004 bronze coupons were characterised by an essentially uniform dark grey to black sulphide patina (Figure 81; left). When recovered the 2005 coupons consisted of a uniform patina of a rich lustrous grey-black layer of corrosion products (Figure 80; top right). It was noted that the surfaces were not remarkably stable in that after several months in storage there was underlying corrosion that resulted in the partial loss of the patina and its oxidation to typical aerobic corrosion products (Figure 81; mid). Immediately after retrieval the 2009 bronze coupons possessed a thicker layer of the usual uniform grey black sulphide corrosion products (Figure 80; bottom). On storage the grey black sulphide layer remained relatively unchanged, however there was evidence of oxidation to the typical blue/green aerobic corrosion products in some areas (Figure 81; right).


*Figure 80. Copper alloy coupons – 50cm below sediment, immediately after recovery in 2004 after 1 year of exposure (top left), in 2005 after 2 years of exposure (top right) and in 2009 after 6 years of exposure (bottom).*

*Figure 81. The bronze coupons - 50cm below sediment recovered in 2004 after 2 years of storage (left), in 2005 after 1 year of storage (mid) and in 2009 after 5 months of storage (right).*

The SEM images of the unstripped 2004 bronze coupons showed the characteristic tin-rich and copper-rich corrosion matrices that were indicative of the elemental distribution in the underlying parent alloy. The heavily cored dendritic structure of the coupon was replicated in the micromorphology of the corrosion products (Figure 82; left). The SEM images of the 2005 samples showed greater agglomeration of pustular and warty corrosion products which had zones of very high localised lead concentrations, probably PbS corrosion products. Other zones of high atomic number contrast were characterised by high tin and sulphur values from the EDX analysis. The SEM images and EDX analysis of the unstripped bronze coupons recovered in 2009 showed a more uniform corrosion product layer mainly consisting of cuprite and a copper sulphide, probably chalcocite ($Cu_2S$) and only minor amounts of tin and zinc. Lead sulphide crystals (PbS) were concentrated along the boundaries of the tin-rich (α + δ) eutectoid (20% Sn, 3% Pb) (Figure 82; right) indicating some selective corrosion of this phase.

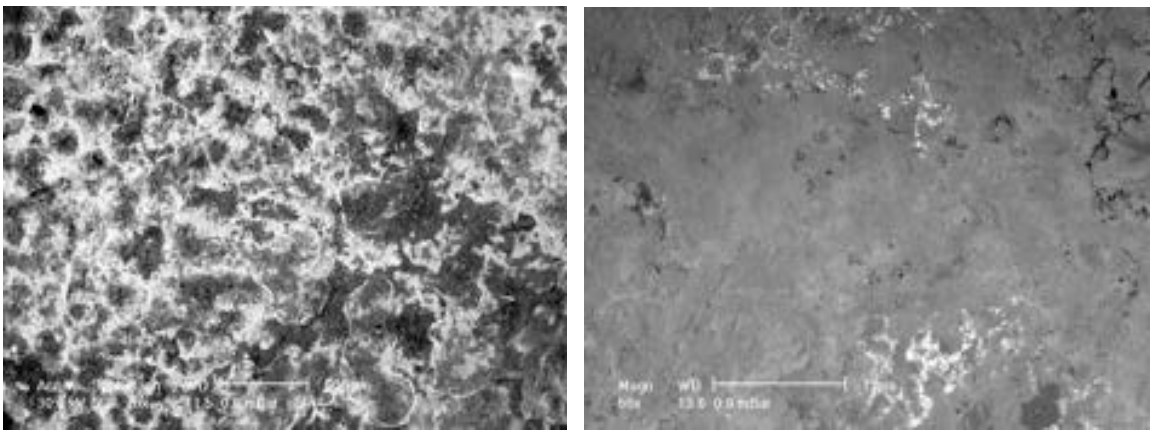

*Figure 82. SEM images of the unstripped bronze coupons recovered from 50cm below the sediment in 2004 (left): the mixed copper-rich and tin-rich corrosion products and in 2009 (right): mixture of zinc-rich copper sulphide and cuprite (grey corrosion products) with lead sulphides (bright areas) concentrated along the tin-rich eutectic phase boundaries.*

The SEM image of the stripped 2005 coupon showed up the underlying corrosion process of selective attack of the tin-rich eutectoid (Figure 83; left) in a similar fashion to that observed in the earlier sample recovered in 2004. The EDX analyses confirmed this general anaerobic corrosion mechanism, which was consistent with a thermodynamically controlled process, as distinct from the kinetically controlled mechanisms in the aerobic coupons located above the sediment. The EDX analysis of the stripped 2009 bronze coupon showed that the bright SEM phase was approximately 88% Cu and 4% Sn, which is consistent with it being residual copper-rich α phase of the bronze cast coupon (Figure 83; right). There were difficulties in completely stripping the coupon so the corrosion products partly occluded the metallographic microstructure of the cast bronze, however there was evidence of selective corrosion of the cored dendritic structure.

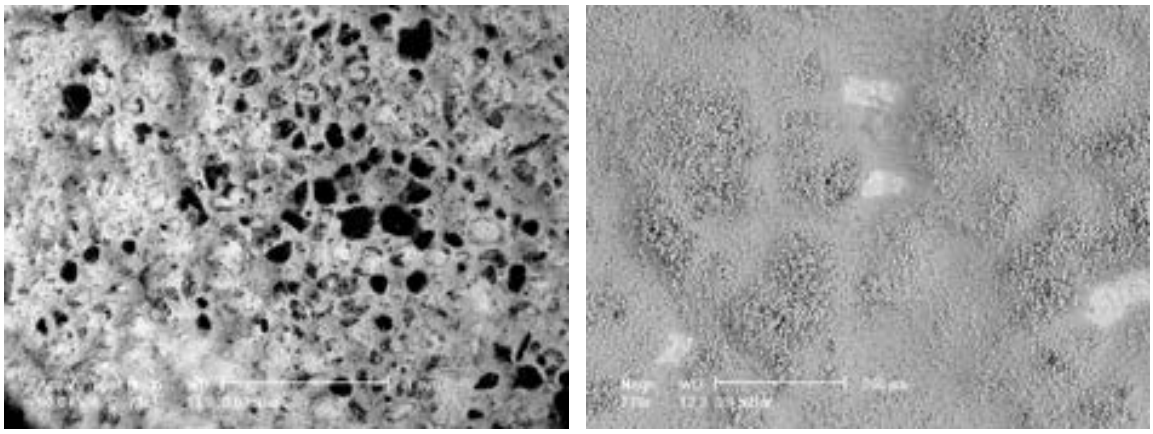

*Figure 83. SEM images of the stripped bronze coupons recovered from 50cm below the sediment in 2005 (left): selective attack of the tin-rich eutectoid phase and in 2009 (right): residual copper-rich α phase (brighter areas) with the corrosion product matrix on the surface partly occluding the underlying dendritic structure of the parent bronze.*

Again, like the brass coupons, the corrosion patterns on the bronze coupons recovered from just below the sediment surface and 50cm below the sediment were similar. However, for the bronze coupons recovered from just below the sediment the presence of less sulphide-rich corrosion products as compared to the coupons recovered from deeper in the sediment may indicate a changeover in corrosion mechanism from corrosion of the copper-rich α phase dominant in partially oxygenated environments to corrosion of the tin-rich (α+δ) eutectoid phase which is predominant under anaerobic conditions. The major corrosion products on the 50cm buried coupons were copper-rich and tin-rich sulphides with some lead sulphide deposits concentrated at the edges of the tin-rich (α+ δ) eutectoid phase, which resulted from the preferential corrosion of this phase. This is consistent with the primary corrosion mechanism of bronzes under anaerobic conditions.

### 3.5.3.2 Weight Loss and Corrosion Rates

The annualised normalised weight loss for the 2004, 2005 and 2009 bronze coupons was 0.007%$cm^{-2}y^{-1}$, 0.006%$cm^{-2}y^{-1}$ and 0.022%$cm^{-2}y^{-1}$, respectively (Figure 21). The normalised corrosion rate for the bronze coupons buried at 50cm in the sediment was 0.004 $mm.y^{-1}$ in 2004, 0.002 $mm.y^{-1}$ in 2005 and then

increased to 0.010 mm.y$^{-1}$ in 2009 (Table 6). Based on these results it appears that there are possible benefits of reburying medium leaded zinc bronzes at depths of 50cm in sediments similar to those in Marstrand harbour. However, it would be prudent to analyse the next set of samples scheduled to be recovered in 2012 in order to confirm this observation. However, it is obvious that exposure to fully aerobic conditions significantly increases the extent of corrosion of medium leaded zinc bronzes. It is also evident that these bronze coupons do not have the same corrosion resistance as the duplex brass samples and this would be due to differences in the composition, microstructure and mechanical stress of the different alloys.

### 3.5.4 Copper Steel Coupons: 50cm Below Sediment

#### 3.5.4.1 Corrosion

The ferrous alloy plate as-recovered in 2004 from 50cm below the sediment was indistinguishable from the shallower sample buried just below the sediment (Figure 84; top left) and had similar post storage problems (Figure 85; left). The overall appearance of the as-recovered 2005 coupon was much the same as for the 2004 sample but the depth of the corrosion matrix was naturally greater (Figure 84; top right). After some aerial oxidation the mottled or marbled pattern, that typifies population distribution of anaerobic bacteria on the metal surface, was readily apparent (Figure 85; mid). The appearance of the 2009 copper steel coupon immediately after recovery was similar to the 2005 sample but the thickness of the corrosion matrix had increased. It was typified by a grey/black corrosion product layer with extraneous sediment on the surface and no visual evidence of concretion formation (Figure 84; bottom). There appeared to be considerably less oxidation of the corrosion layer after storage (Figure 85; right).

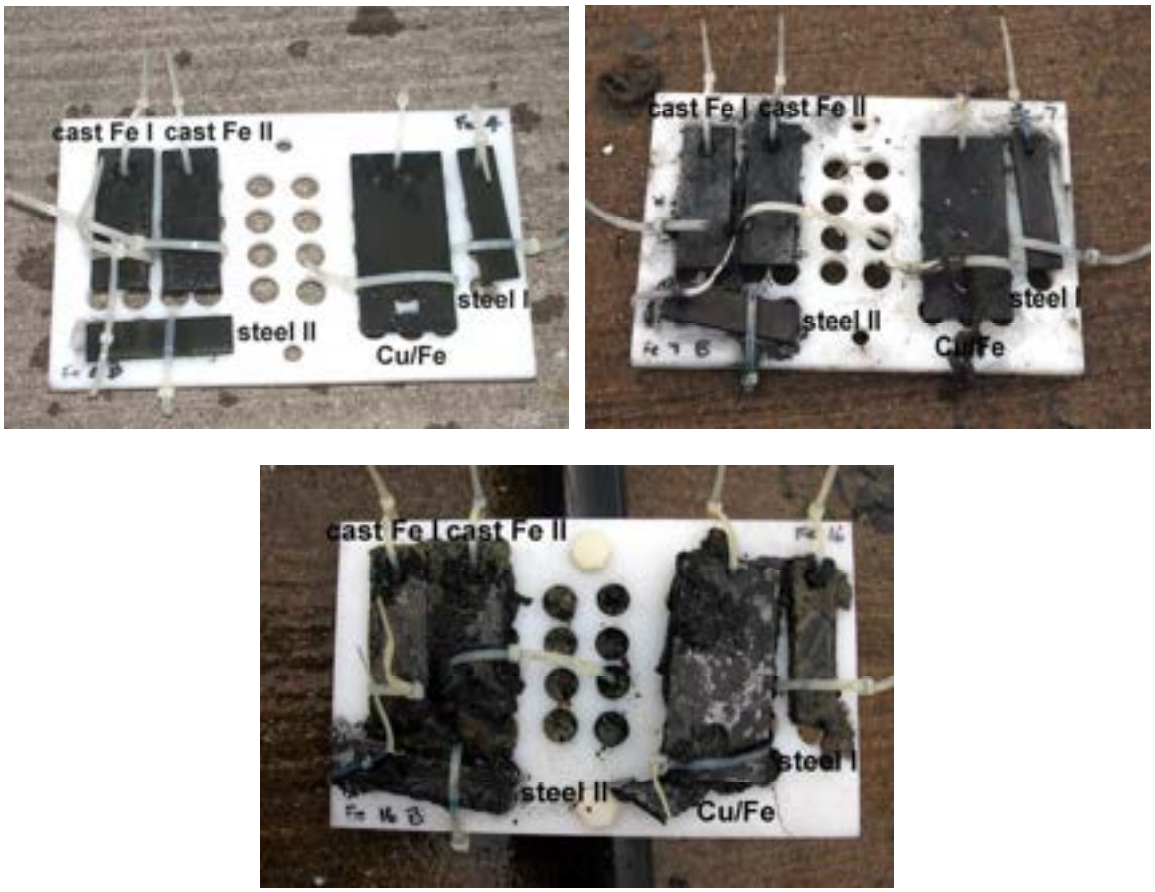


*Figure 84. Ferrous alloy coupons – 50cm below sediment, immediately after recovery in 2004 after 1 year of exposure (top left), in 2005 after 2 years of exposure (top right) and in 2009 after 6 years of exposure (bottom).*

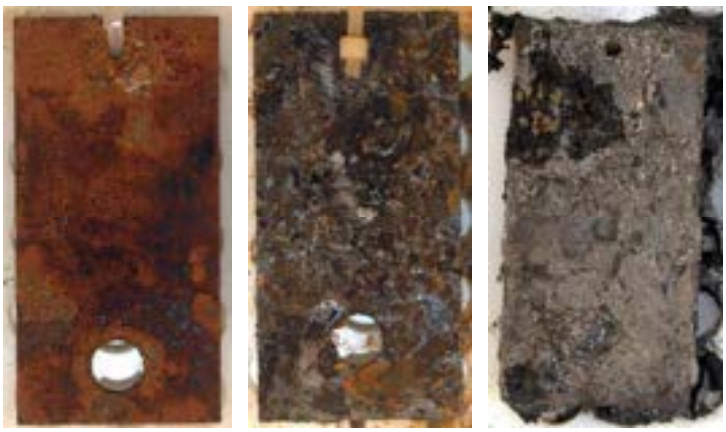

*Figure 85. The copper steel coupon - 50cm below sediment recovered in 2004 after 2 years of storage (left), in 2005 after 1 year of storage (mid) and in 2009 after 5 months of storage (right).*

The SEM images of the unstripped 2004 coupon showed well developed roseate crystalline corrosion products of iron sulphides which had grown up from a remarkably uniform background of corroded metal (Figure 86; left). The SEM images of the 2005 coupon showed the presence of more than one iron sulphide phase. The EDX analysis of the surface indicated massive mineral deposits, containing 14% $SO_2$ that appeared to have grown up from a general pavement of an iron sulphide that had 7-8% $SO_2$. It cannot be determined if the localised corrosion processes underneath the more sulphur-rich deposits are due to direct differences in microbiological activity. The SEM images of the unstripped copper steel coupon recovered in 2009 showed a more developed iron sulphide corrosion product layer with incorporated sand and clay particles. The EDX analysis showed up minor quantities of chloride, calcium, manganese and copper.

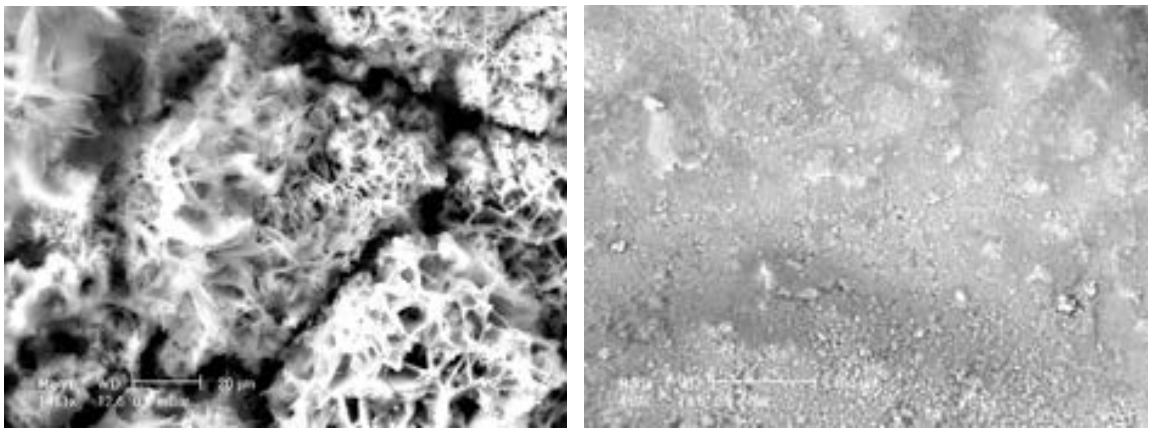

*Figure 86. SEM images of the unstripped copper steel coupon recovered from 50cm below the sediment in 2004 (left): the roseate crystalline iron sulphides and in 2009 (right): more developed iron sulphide corrosion product layer.*

The partially stripped 2004 sample showed up increased amounts of copper sulphides which in some areas had grown over the original iron corrosion products that had come from uniform attack of the primary ferrite grains of the metal (Figure 87; left). The stripped coupons from 2005 and 2009 had a generally similar

appearance to the 2004 coupon but as seen in Figure 87 (right) there were some areas that had marked attack on the primary α iron grains.

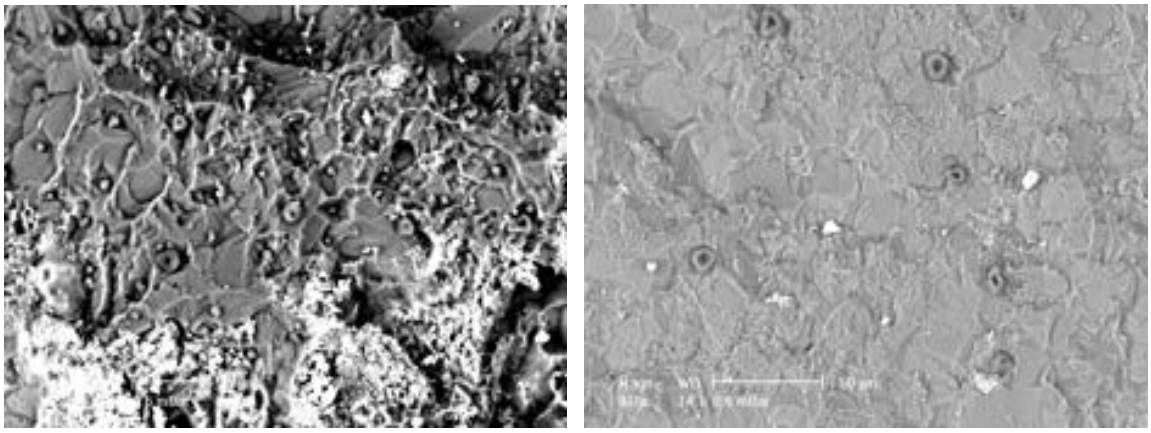

Figure 87. SEM images of the stripped copper steel coupon recovered from 50cm below the sediment in 2004 (left): intergranular corrosion and uniform attack of the primary ferrite grains and in 2009 (right): general corrosion of the α ferrite phase.

### 3.5.4.2 Weight Loss and Corrosion Rates

The visual and SEM observations for the extent of corrosion of this coupon was supported by the normalised weight loss data; in 2004 the loss was 0.022%$cm^{-2}y^{-1}$, in 2005 it was 0.014%$cm^{-2}y^{-1}$ and in 2009 it was 0.032%$cm^{-2}y^{-1}$ (Figure 37). Similarly the corrosion rates were 0.040$mm.y^{-1}$ in 2004, 0.024$mm.y^{-1}$ in 2005 and 0.048$mm.y^{-1}$ in 2009. There was a slight decrease in the rate of corrosion of the copper steel coupon in 2005 but by 2009 it had increased again to values slightly higher than the initial 2004 corrosion rate, indicating that small changes in the microenvironment can significantly affect the extent of corrosion.

The corrosion of the copper steel coupons buried at 50-65cm below the sediment would primarily be caused by sulphate reducing bacteria, such as *Desulphovibrio* species. The presence of organic material stimulates these organisms' reducing power whereby sulphate is reduced to sulphide, but some species appear to grow as chemolithotrophs and reduce sulphate according to equation 13.

$$SO_4^{2-} + 4H_2 \rightarrow S^{2-} + 4H_2O \quad \text{.....(13)}$$

The sulphide can then react with hydrogen ions to produce hydrogen sulphide (equation 14).

$$2H^+ + S^{2-} \rightarrow H_2S \quad \text{.....(14)}$$

Reactions between iron ions produced by the anodic reaction and the sulphide ions produced by the sulphate reducing bacteria results in the formation of FeS and elemental sulphur (equations 15, 16 and 17).

$$2Fe^{3+} + S^{2-} \rightarrow 2Fe^{2+} + S \quad \text{.....(15)}$$

$$Fe^{2+} + S^{2-} \rightarrow FeS \quad \text{.....(16)}$$

$Fe + H_2S \rightarrow FeS + H_2$ .....(17)

Under anaerobic conditions the cathodic reaction in the iron corrosion process becomes the reduction of hydrogen ions or water to hydrogen gas and the sulphate reducing bacteria increases this reaction as it occurs more rapidly on iron sulphides and sulphur than on the bare metal surface itself. The enzyme hydrogenase produced by the bacteria also catalyses this reaction. The sulphate reducing bacteria may also increase the corrosion rate by direct chemical action of metabolic products such as sulphuric acid and organic acids. The resulting corrosion rates are much higher than in similar environments with lower bacterial counts.

### 3.5.5 Cast Iron Coupons: 50cm Below Sediment

#### 3.5.5.1 Corrosion

There was no readily discernable difference between the appearance of the cast iron coupons recovered from 50cm below the sediment in 2004 and from just below the sediment surface the same year (Figure 88; top left). These coupons also suffered from the same post recovery oxidation problems as the other iron coupons (Figure 89; left). The overall appearance of the 2005 cast iron coupons as-recovered was dark grey to black (Figure 88; top right) but on oxidation during storage the surfaces gradually took on a patchy mottled grey/red-brown hue of microbially corroded iron (Figure 89; mid). By 2009 the as-recovered cast iron coupons had the same grey/black corrosion product layer, however there was considerably more interstitial sediment on the surface (Figure 88; bottom). There was much less post storage oxidation on these coupons (Figure 89; right).

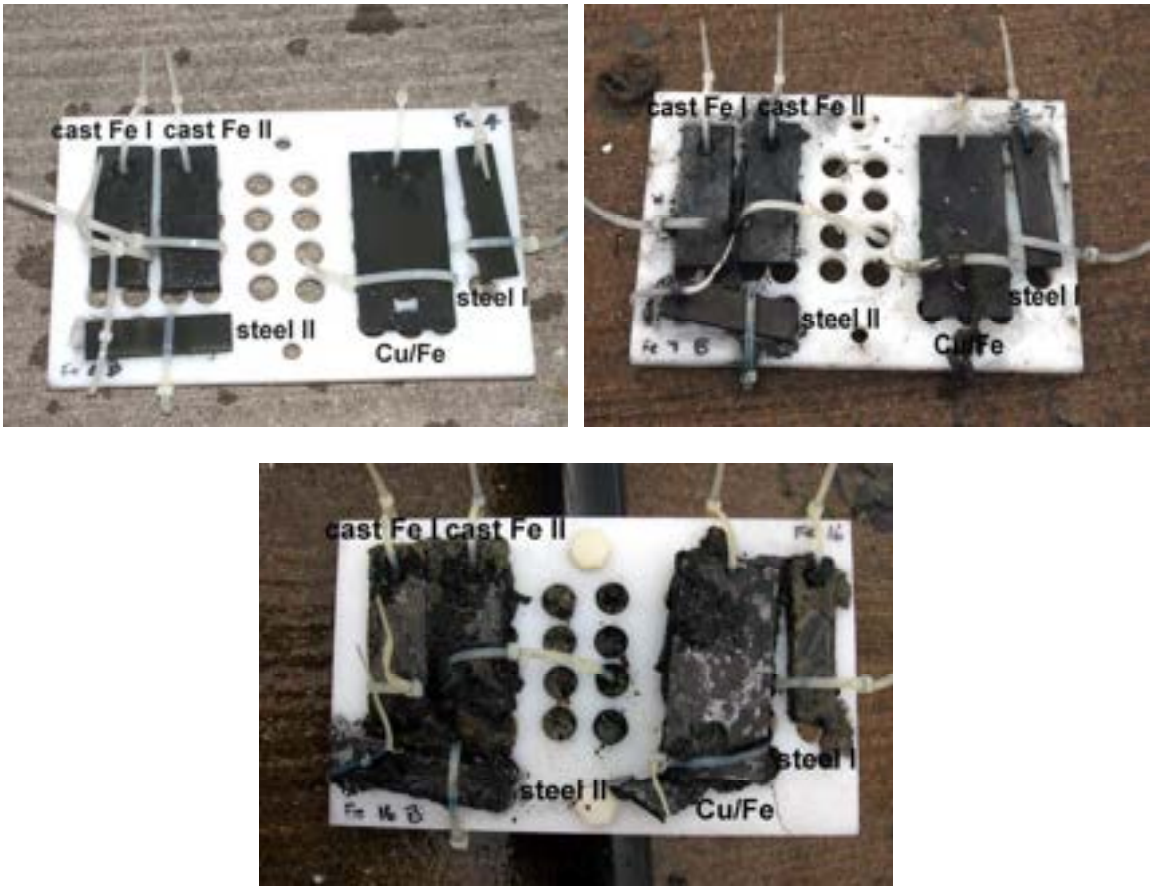


*Figure 88. Ferrous alloy coupons – 50cm below sediment, immediately after recovery in 2004 after 1 year of exposure (top left), in 2005 after 2 years of exposure (top right) and in 2009 after 6 years of exposure (bottom).*

*Figure 89. The cast iron coupons - 50cm below sediment recovered in 2004 after 2 years of storage (left), in 2005 after 1 year of storage (mid) and in 2009 after 5 months of storage (right).*

The SEM images of the 2004 cast iron coupons showed up a much more uniformly corroded surface, with the boundaries around the graphite flakes clearly defining some of the localised corrosion phenomena. It was noted that in all the 2004 SEM/EDX analyses there was no specific distribution form, mineral or chemical corrosion product associated with the manganese and silicon contents of the original parent alloy. However, on closer inspection and in conjunction with the EDX analysis the mobilisation of iron has resulted in the residual phases containing 40% $SiO_2$ and 30% MnO becoming a dominant feature inside the residual grain structure, as seen in Figure 90 (left). The SEM images and EDX analysis of the 2005 and 2009 samples showed up a mixture of iron corrosion products that contained at least two different forms of iron sulphides, along with adventitious materials from the sediment. The general appearance of the coupons was more like the uniform corrosion of the copper steel at 50cm buried (Figure 90; right).

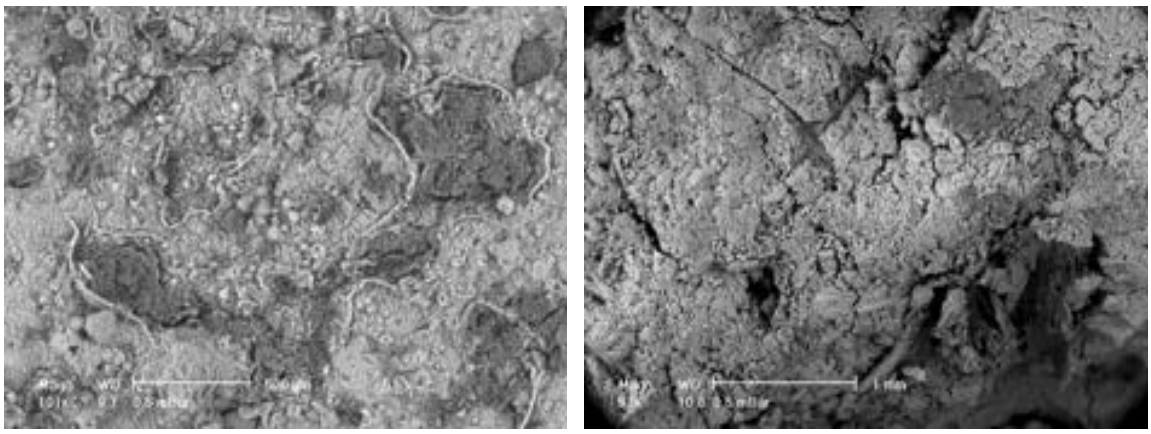

*Figure 90. SEM images of the unstripped cast iron coupons recovered from 50cm below the sediment in 2004 (left): residual grain structure (dark grey areas) and in 2009 (right): iron sulphides (light grey areas) with some interstitial sediment incorporation (darker grey areas).*

The stripped cast iron sample from 2004 showed evidence of more intense localised corrosion, which was seen in the development of “holes” in the metal

structure (Figure 91; left). The SEM also showed more details of the underlying microstructure, with the EDX analysis of the residual phases containing up to 40% silicon as $SiO_2$. The stripped surface on the 2005 coupon showed that the corrosion processes were pitting the surface of the coupon, which resulted in the secondary outgrowths of sulphur rich deposits. By 2009, the pitting corrosion was more severe and more of the underlying microstructure of the cast iron was becoming apparent compared with the 2004 coupon (Figure 91; right). There was also increased corrosion along the lines of working caused during the manufacturing process of the coupons.

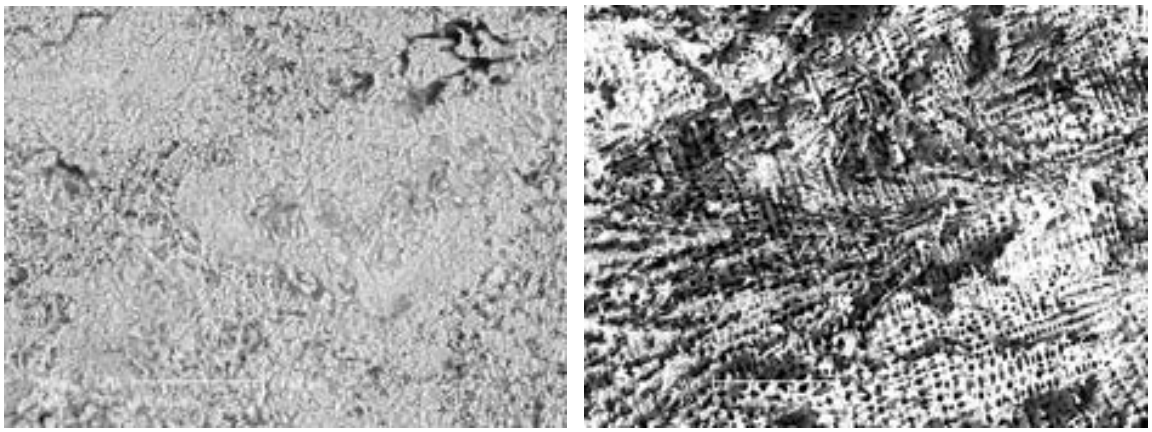

*Figure 91. SEM images of the stripped cast iron coupons recovered from 50cm below the sediment in 2004 (left): residual grain structure and development of 'holes' (upper right) in the metal structure and in 2009 (right): extensive pitting of the iron-rich phases (bright areas) and increased corrosion along the lines of working.*

### 3.5.5.2 Weight Loss and Corrosion Rates

In 2004 the cast iron coupon had lost 0.018%$cm^{-2}y^{-1}$ of its normalised weight, in 2005 the loss was similar at 0.017%$cm^{-2}y^{-1}$ and then doubled to 0.043%$cm^{-2}y^{-1}$ by 2009 (Figure 37). Similarly the corrosion rates were 0.021$mm.y^{-1}$ in 2004, 0.019$mm.y^{-1}$ in 2005 and 0.048$mm.y^{-1}$ in 2009 (Table 7). These increasing trends for the weight losses and corrosion rates over the six year burial period supported the SEM observations and were again a direct consequence of the increased immersion period and did not accurately reflect long-term corrosion rates of archaeological metals. However, the weight loss and corrosion rate data is in stark contrast to the much greater and relatively unpredictable nature of the weight loss associated with the exposed coupons. The primary corrosion mechanism occurring on these cast iron coupons buried 50-65cm in the sediment is basically microbial corrosion due to sulphate reducing bacteria and the mechanism is described in detail for the copper steel coupons recovered from 50cm below the sediment surface. In addition, the normalised weight loss and rates for the cast iron coupons recovered from 50cm below the sediment surface in 2009 was considerably less than the loss experienced by the 2009 coupons recovered from just below the sediment. This indicates that differential aeration corrosion due to residual dissolved oxygen in the surface sediments is generally more extensive than anaerobic microbial corrosion induced by sulphate reducing bacteria after the coupons have equilibrated with the local microenvironment.

### 3.5.6 Mild Steel Coupons: 50cm Below Sediment

#### 3.5.6.1 Corrosion

In 2004 the mild steel coupons were recovered with a uniform black corrosion products layer (Figure 92; top left) that resisted aerial oxidation much more noticeably than the exposed and partly buried coupons (Figure 93; left). This is entirely consistent with the difference in the nature of both the corrosion products and the corrosion mechanism of aerobic and anaerobic decay. Immediately after retrieval, the coupons recovered in 2005 were indistinguishable from the appearance of the 2004 samples (Figure 92; top right), however they were subjected to a greater degree of post recovery alteration than the coupons from the previous year (Figure 93; mid). The as-recovered 2009 coupons had the usual grey/black corrosion product layer with more incorporated extraneous sediment (Figure 93; bottom). After storage there was some oxidation but the sulphide layer was relatively stable (Figure 93; right).

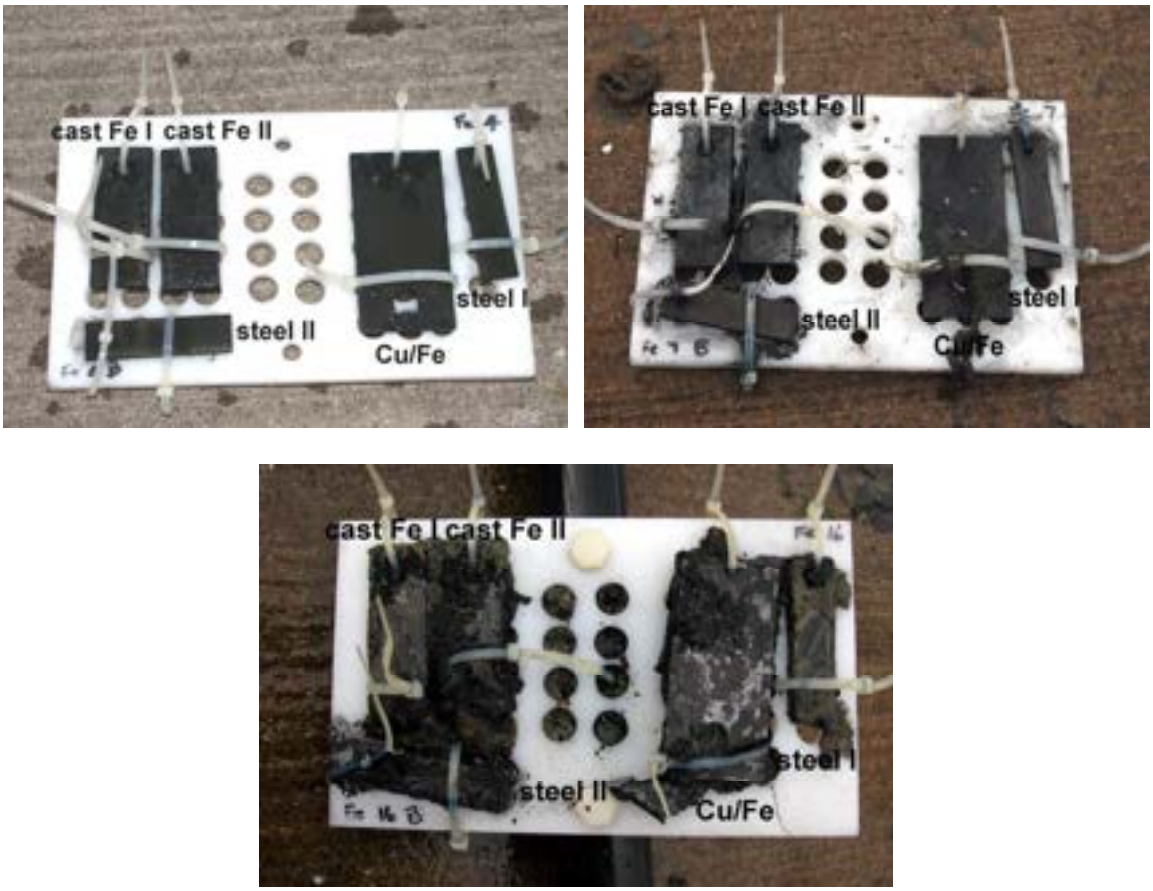


*Figure 92. Ferrous alloy coupons – 50cm below sediment, immediately after recovery in 2004 after 1 year of exposure (top left), in 2005 after 2 years of exposure (top right) and in 2009 after 6 years of exposure (bottom).*

*Figure 93. The mild steel coupons - 50cm below sediment recovered in 2004 after 2 years of storage (left), in 2005 after 1 year of storage (mid) and in 2009 after 5 months of storage (right).*

The SEM images of the 2004 mild steel coupons showed a remarkably uniform corrosion layer of iron sulphides with little sign of localised corrosion processes (Figure 94; left). However, the amount of iron sulphides containing higher concentrations of sulphide and/or lower quantities of iron had increased compared with the coupon recovered from just below the surface. The SEM images of the 2005 samples showed a thick layer of iron sulphide corrosion products, which was compact with little space between the mounds of iron sulphides and this was even more pronounced for the 2009 coupons (Figure 94; right).

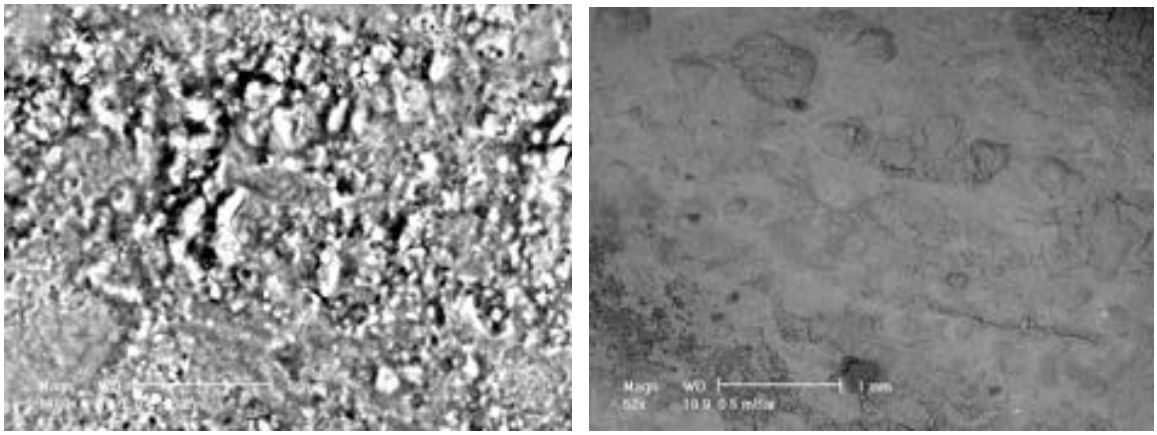

*Figure 94. SEM images of the unstripped mild steel coupons recovered from 50cm below the sediment in 2004 (left): uniform corrosion layer of iron sulphides and in 2009 (right): more developed iron sulphide corrosion product layer.*

The SEM images of the stripped mild steel coupon recovered in 2004 showed up a mixture of localised pitting and general surface corrosion of the α ferrite grains (Figure 95; left). The stripped sample from 2005 showed the deeply pitted nature of the steel along the inclusion lines and also strong corrosion across the faces of the α-iron grains leading to the very rough surface topography and this was more pronounced in the images of the stripped 2009 mild steel coupon.

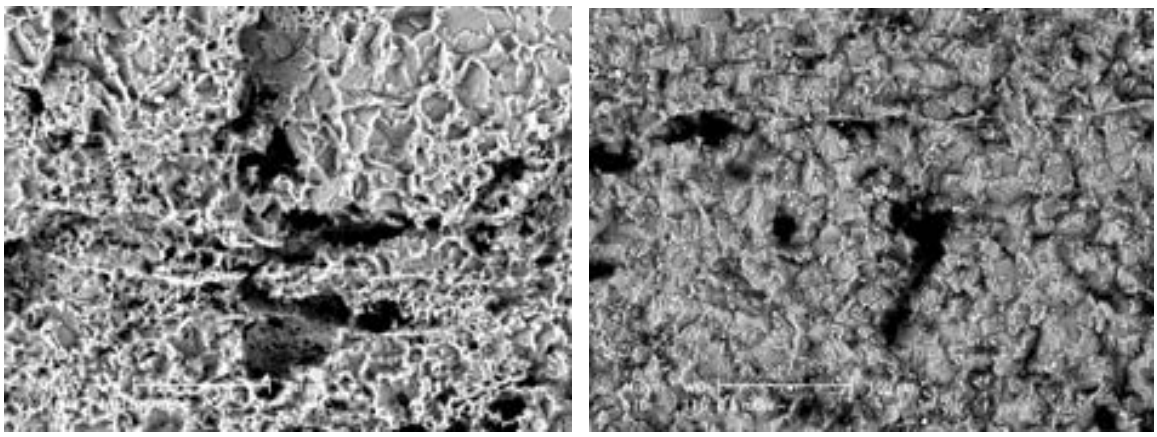

*Figure 95. SEM images of the stripped mild steel coupons recovered from 50cm below the sediment in 2004 (left): localised pitting and general surface corrosion of ferrite grains and in 2009 (right): increased pitting corrosion, corrosion along the slag inclusions and lines of working and across the ferrite grain surfaces.*

### 3.5.6.2 Weight Loss and Corrosion Rates

The 2004 sample had suffered minimal corrosion with a normalised weight loss of 0.005%$cm^{-2}y^{-1}$ while the 2005 and 2009 coupons had much higher levels of loss at 0.023% $cm^{-2}y^{-1}$ and 0.060%$cm^{-2}y^{-1}$, respectively. Similarly the normalised corrosion rates increased over the six year burial period and the results were 0.004$mm.y^{-1}$ in 2004, 0.016$mm.y^{-1}$ in 2005 and 0.043$mm.y^{-1}$ in 2009. This is consistent with the greater amount of the secondary iron sulphide minerals on the surface of the 2009 coupons indicating more extensive corrosion after six years of burial in the sediment.

The corrosion mechanisms of aerobic and anaerobic corrosion of wrought iron are the same as that for cast iron, however as wrought iron consists almost entirely of ferrite with silicate (slag) inclusions with no graphite present the corrosion products of wrought iron are soft and non-adherent with no retention of the original shape and surface of the artefact. The slag inclusions in wrought iron allow deeper penetration of chlorides into the bulk of the iron and subsequent corrosion along the walls of the slag inclusions widens the gaps between the inclusions and the ferrite and pushes out the slag. As a result of this corrosion, deep crevices or pits are formed in the residual metal, which is evident from the SEM images of the 2009 stripped mild steel coupons. Thus although it could be argued that there is little relevance of using mild steel for such studies, the actual microstructure of the degraded coupons reflects the same corrosion mechanisms and processes that typify historical wrought iron.

Comparisons of the normalised weight losses of the different ferrous coupons from the three different depths indicated that the extent of corrosion increased in order from copper steel, to cast iron to mild steel coupons, which suffered the most corrosion. This is simply a reflection of the differences in metal composition and metallurgical structure. The addition of copper to mild steel obviously has an enobling effect and decreases the extent of corrosion of mild steel, especially when exposed to the aerobic marine environment. The extent of corrosion of the cast iron coupons was only slightly less than that of the mild steel coupons and this would simply be due to the slight enobling effect of carbon present in some of

the cast iron phases. However, there were only small differences in the weight losses noted for all coupons recovered from 50cm below the sediment surface and this indicates that deeper burial in sediment does in fact, lower the corrosion rates and the eventual extent of overall corrosion after six years of immersion.

## 3.6 COMPARISON OF WEIGHT LOSS AND CORROSION RATES

Comparisons between the normalised percentage weight loss per year of immersion (Figure 96) and the normalised corrosion rates (Table 8) for all metals coupons over the six year experimental period should provide additional information regarding the stability and hence, suitability of the different metal types for reburial.

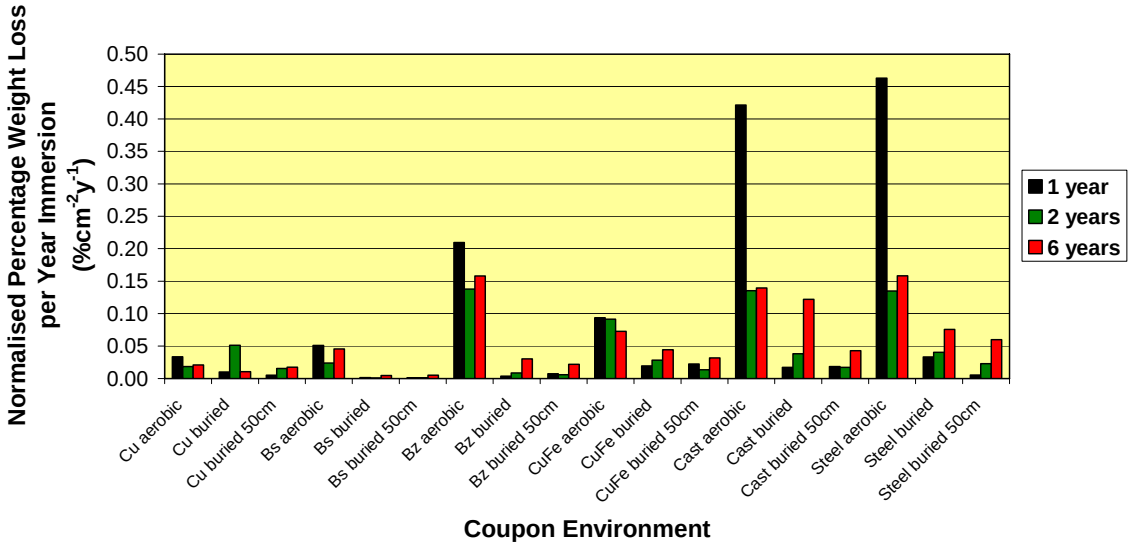


*Figure 96. Normalised percentage weight loss per year of immersion for all metal coupons.*

*Table 8. Normalised corrosion rates for all metal coupons and the estimated years to total loss.*

| Coupon Type and Environment | Normalised Corrosion Rate ($mmy^{-1}$) | | | Estimated Years to Total Loss |
|---|---|---|---|---|
| | 2004 | 2005 | 2009 | |
| Cu aerobic | 0.022 | 0.012 | 0.030 | 124 |
| Cu buried | 0.007 | 0.034 | 0.022 | 169 |
| Cu buried 50cm | 0.004 | 0.010 | 0.017 | 215 |
| Bs aerobic | 0.038 | 0.018 | 0.031 | 118 |
| Bs buried | 0.001 | 0.0004 | 0.003 | 1077 |
| Bs buried 50cm | 0.001 | 0.001 | 0.004 | 990 |
| Bz aerobic | 0.108 | 0.070 | 0.070 | 55 |
| Bz buried | 0.002 | 0.004 | 0.013 | 294 |
| Bz buried 50cm | 0.004 | 0.002 | 0.011 | 366 |
| CuFe aerobic | 0.169 | 0.163 | 0.167 | 14 |
| CuFe buried | 0.035 | 0.050 | 0.146 | 16 |
| CuFe buried 50cm | 0.040 | 0.024 | 0.048 | 48 |
| Cast Fe aerobic | 0.472 | 0.149 | 0.167 | 23 |
| Cast Fe buried | 0.021 | 0.043 | 0.146 | 26 |
| Cast Fe buried 50cm | 0.021 | 0.019 | 0.048 | 80 |
| Steel aerobic | 0.333 | 0.090 | 0.113 | 34 |
| Steel buried | 0.024 | 0.029 | 0.054 | 71 |
| Steel buried 50cm | 0.004 | 0.016 | 0.043 | 89 |

The estimated years to total loss was calculated from the 2009 normalised corrosion rates and the initial thicknesses of the coupons (Table 8). The 2009 corrosion rates were used for this calculation as plots of the corrosion rates versus time using a number of mathematical functions (i.e. linear, logarithmic, exponential, 2$^{nd}$ and 3$^{rd}$ order polynomials) gave a range of equations where the correlation coefficient of the lines of best fit were inconsistent. In addition, since corrosion is not unidirectional and occurs on both sides of the coupon the initial calculations were divided by a factor of 1.3, which takes into account the slower corrosion on the reverse sides of the coupons lying against the support plate where the dissolved oxygen concentration and total water movement is more limited as compared to the exposed front surfaces. This calculation is obviously not ideal and is only an estimation based on only three sets of experimental data but it does provide some idea of the overall stability of the different metal alloys in that particular environment in an easily understandable format.

Analysis of the annualised weight loss data, normalised corrosion rates and estimated years to total loss shows that for pure copper there is only a relatively modest positive effect with increasing burial depth and this would be due to the fact that the tough pitch copper is a single phase alloy with a very uniform composition and thus less intergranular corrosion can occur under different environmental conditions. There was an anomalous increase in the extent of corrosion of the 2005 copper coupon buried just under the sediment but this was explained by increasing differential aeration corrosion caused by the changing depth of sediment coverage during the term of the experiment. There also appears to be a systematic trend towards higher annualised corrosion rates in the coupons buried to a depth of 50cm, which is consistent with the fact that copper sulphides do not form a passivating layer on the residual metal surface so the copper continues to corrode and the sulphide layer grows as the copper (I) ions diffuse to the sediment interface where they are precipitated as copper sulphides.

The aerobic brass coupons shows a relatively consistent corrosion loss and although there was some scatter of the data this was probably due to the variable nature of the sediment coverage in the area of burial. However, in this aerobic environment the brass coupons are corroding at a slightly higher rate than the pure copper coupons. This can easily be explained by the fact that under normal aerobic conditions the presence of the zinc-rich β phase, present in these coupons owing to the relatively high concentration of zinc in the parent alloy, dominates the corrosion microenvironment and so the brass objects suffer from extensive dezincification in part due to the opening up of the microstructure of the metal to penetration by chloride ions which accelerate the corrosion of the copper-rich α phase. At the intermediate (just below sediment) and lower burial depths (50cm below sediment) the long term corrosion rate of brass is very satisfactory in terms of providing long-term protection since even after 50 years the average total weight loss is about 0.15%cm$^{-2}$ and the average estimated time for total loss is about 550 years for the buried brasses. At this very low corrosion rate even thin, flat surfaced objects, such as brass metal sheathing, should be suited to this form of reburial.

The corrosion rates of the exposed bronze coupons shows that the aerobic microenvironment is very aggressive compared with the effect on the parent copper and brass alloys. This is due primarily to the high tin and zinc

concentrations which give a combined tin equivalent of nearly 13% in terms of the microstructure. This results in quite marked interdendritic corrosion since the electrochemical potential difference between the copper-rich α phase and the mixed tin-rich α + δ phases of the eutectic mixture is large. Since corrosion of bronzes in oxygenated seawater is dominated by corrosion of the copper-rich α phase, the coupons demonstrate this effect to a high degree. Correspondingly when the coupons are buried and the corrosion mechanism changes over to attack on the thermodynamically more reactive eutectoid phases and any other tin-rich phases the overall corrosion rate drops dramatically from a mean annualised level of 0.169%$cm^{-2}y^{-1}$ under aerobic conditions to 0.014%$cm^{-2}y^{-1}$ under partially oxygenated conditions and 0.012%$cm^{-2}y^{-1}$ under essentially anaerobic conditions. Essentially the dramatic 13 times reduction in average corrosion rate on burial just under the sediment surface and at depths of 50cm means that even after 50 years there is still only roughly 0.65%$cm^{-2}$ weight loss on buried medium leaded zinc bronzes. Hence, the estimated average time to total loss based on the 2009 corrosion rates for the two depth of burial would be about 330 years. This loss is certainly manageable in terms of care of shipwreck artefacts owing to the retention of the corrosion products on the surface of the artefacts. Whilst this corrosion loss is relatively low, care should be exercised when considering the surface area to volume ratio of the objects since thin sheets of metal will be effectively mineralised over this extended time period.

The aerobic copper steel samples showed an apparent systematic trend towards slightly lower corrosion rates as the immersion time increased over the period of the experiment. This is due to the activation of the surface by the presence of the copper to promote uniform corrosion and this data indicates that increased time should result in a further lowering of the average corrosion rate. When the actual corrosion rates for the aerobically corroded copper steel are examined it is not characterised by the massive drop between 2004 and 2005 that dominates the aerobic cast iron and the mild steel and this is due to the uniformity of the microstructure of the copper steel compared with the wrought iron, with its slag inclusions, and the cast iron with its multiply dissimilar phases. Part of the reason for the very rapid aerobic corrosion of the cast and wrought iron in the first year is that the reactivity differences in the various phases were exacerbated by the direct exposure to dissolved oxygen where the overpotentials associated with the reduction of oxygen on the different phases have a major effect on how the microstructure degrades.

When comparing the aerobic cast iron and the mild steel coupons, which show relatively similar behaviour in terms of the overall corrosion rates, they are roughly four times greater than the copper steel coupons. The reason for this significant increase lies in the underlying metallurgical structures. In the case of the cast iron coupons, the as-cast microstructure and the carbon content of between 3.0–3.6% is typical of cast iron objects from shipwrecks, ranging from cannon and windlass fitting, capstans etc. This high carbon content results in phases of very different electrochemical activity and so the pure ferrite is preferentially corroded in the cast iron and this is a form of internal galvanic corrosion since there is a large amount of electrically conducting graphite present which facilitates the oxidation process by providing a low resistance pathway to the chemical reactions. In the case of the mild steel the behaviour is very similar to the corrosion of wrought iron as there is a large amount of slag inclusions present and there are also marked lines of

working where there has been preferential corrosion along the lines of rolling and general fabrication with no annealing of the metal. Thus there is severe localised corrosion attack across the metal surface which is also very prone to pitting corrosion.

In contrast the copper steel samples buried just under the sediment and at a depth of 50cm show the reverse trend, which is also observed for the cast iron and the mild steel coupons, which is consistent with the impact of sulphate reducing bacteria changing the corrosion mechanism that is taking place underneath the corrosion product matrix and the slow formation of a protective encapsulating concretion layer under these deoxygenated conditions.

If the approximate average normalised weight losses are calculated for the copper steel, cast iron and mild steel the results indicate that even after 50 years the amount of loss from iron alloy objects would be greater than 3% which may result in the loss of surface detail and important archaeological information as the iron corrosion tend to be voluminous and non-adherent, especially for the copper steel and mild steel. In addition, if the very large statistical variations in the estimated time to total loss values calculated for the buried iron alloys are taken into account then it could be easily suggested that the extent of corrosion would be excessive after 50 years and therefore they could not be recommended for reburial. On the other hand, reburial of the copper alloys might be feasible.

It should be noted, however, when there is an apparent systematic trend to either higher or lower annualised corrosion rates with time, it is not accurate to use the arithmetic averages for comparative purposes as the standard deviation in the data shows the results are too variable for any form of reliable statistical evaluation. This mathematical calculation was only used as the amount of data obtained over the three point recovery period (2004, 2005 and 2009) was not adequate in order to obtain any statistical relevant mathematical trends. This is one of the fundamental reasons why there is a compelling need for more data measurements. Hence, additional data is required to ensure that the observed trends in the apparent corrosion behaviour and response to the burial microenvironments of all the coupons, especially the iron alloys are correct and that the recommendations for reburial are indeed appropriate for each metal alloy tested and extrapolation to archaeological metals is appropriate.

# 4 CONCLUSIONS

The results obtained from this metals reburial experiment have proven to be quite interesting and informative, despite the relatively short time period (6 years) for the two initial phases of the project. The different analytical techniques appear to compliment each other and positively support the conclusions drawn based on the results. The basics of the experimental design were very sound as was shown by the fact that there was almost no cross contamination of the copper alloy coupons with corrosion products from adjacent coupons of different metal composition. There was also no evidence of galvanic or proximity corrosion occurring between the copper alloy and ferrous alloys sample units or between individual coupons in close proximity on the support plates. Hence, these observations give greater confidence to the conclusions drawn about the validity of the general methodologies and the effectiveness of reburial as a means of protecting metallic underwater cultural heritage.

Unfortunately there were some minor problems encountered with the experimental design and they will be briefly discussed. The cable ties used to separate the copper alloy coupons in order to minimise galvanic corrosion caused some differential aeration corrosion in the areas under and directly adjacent to the ties. However the effect was localised and did not seem to affect the primary corrosion mechanisms occurring on the coupons. In addition, the holes drilled in the support plate to allow the flow of seawater and exchange of interstitial water under the sediment also caused differential aeration corrosion on the rear of the coupons. Again these effects were minimal and very localised and did not affect the overall corrosion mechanisms. However, it does illustrate that the manner in which metals are packed for reburial is extremely important and care should be taken not to cause further deterioration of the artefacts by inadvertently changing the local micro-environment. For example, it is common knowledge that metals of significantly different composition must be separated, however even artefacts of similar composition should be physically separated in some way (e.g. geotextile barrier) to minimise direct contact with other artefacts in order to decrease the chances of differential corrosion cells being established which could increase the corrosion rates over time. Also the physical barrier should minimise the possibility of abrasion and possible disbondment of surface corrosion product layers, which also causes increases in corrosion rate by promoting pitting corrosion in the exposed areas.

Problems were also encountered during the retrieval and packing procedure, which resulted in dehydration and subsequent oxidation of some of the surface corrosion products in transit, storage and during sample preparation. Hence, extreme care must be taken to ensure that minimal post recovery changes occur to the samples prior to analysis. It has been a long established fact that copper alloy artefacts recovered from the marine environment could be temporarily stored and transported in a dry environment (relative humidity (RH) < 45%), which minimises the cyclic bronze disease process. However, from the results obtained from this sub-project it is advisable that copper alloy artefacts, as is always the case with ferrous alloys, are always stored wet. In addition, all metal artefacts should be stored in a similar environment to that from which they had been recovered (e.g. deoxygenated environments if the artefact is recovered from under the sediment) if further analysis of the corrosion product layer and underlying

residual metal will be undertaken in the context of the deposition and site formation processes. Significant change in the nature of the corrosion products could lead to misinterpretation of the local microenvironment and the corrosion mechanisms and hence, the associated archaeological record.

Generally, the results obtained from the analysis of the metal coupons have shown that the resistance of a metal to initial corrosion is very much dependent on the initial elemental composition, the metallurgical microstructure and the method of manufacture of the parent metal. The reburial environments surrounding the metal coupons have finally stabilised and as a result the long term corrosion processes and associated mechanisms are becoming better indicators of the final corrosion outcomes. The concretions and corrosion product layers on the metal coupons are more extensively developed than after the first two years of exposure/reburial and therefore, the coupons are beginning to more accurately reflect the corrosion behaviour of marine archaeological metal artefacts.

On the other hand, it was obvious that compared to the extent of deterioration suffered by the metal coupons exposed to the aerobic seawater column, the extent of corrosion of all metal coupons decreased significantly once the coupons were buried, even at very shallow depths and this protective effect generally increased with increasing burial depth. This decrease was most marked for the brass and bronze coupons, but much less dramatic for the ferrous alloy coupons. Burial seemed to have the least effect on the pure copper coupons, however the extent of corrosion of the exposed copper coupons was also very low. It should be noted, however, that the metal coupons, especially the copper alloys were very susceptible to differential aeration corrosion and therefore, it is vitally important that metals are reburied to depths where there is no chance of partial exposure to the aerobic marine environment through sediment movement due to strong wave action or currents.

Despite a general decrease in the extent of corrosion with burial, all metal coupons exposed to the three different environments (exposed, buried just below the sediment and buried 50cm below the sediment), showed some increase in corrosion rate over the past four years. The greatest increases were found for the bronze and ferrous metal coupons buried at both depth intervals but the rate increases for the buried brass and copper coupons were considerably less. These results indicate that the greatest microenvironmental changes are occurring in the sediment and these changes are mainly affecting the corrosion behaviour of the buried bronze and ferrous alloy coupons.

It appears that reburial has the most positive effect on brasses and to a lesser extent, bronzes. This significant decrease in corrosion would be primarily due to the biological toxicity of copper, zinc and tin corrosion products, which inhibit concretion formation and corrosion by effectively limiting bacterial counts in the surrounding sediment. The bronze coupons show more corrosion than the brass coupons as the three different phases in the bronze microstructure have significantly different electrochemical voltages as compared to the brass microstructure, which causes increased intergranular (micro-galvanic) corrosion. Reburial has less affect on the preservation of pure copper as it is a single phase alloy, with uniform composition and therefore, exhibit less intergranular galvanic corrosion.

This positive effect of burial is significantly reduced on ferrous alloys due to the fact that iron corrosion products can be utilised by microbes and therefore, microbially induce corrosion (MIC) can become more significant in controlling the corrosion rates than direct access to dissolved oxygen. Since the major process ongoing in the Marstrand sediments is sulphate reduction and the metals trench contains sulphate, albeit at low concentrations at deeper depths and significant quantities of organic matter, it is probable that sulphate reducing bacteria are causing microbially influenced corrosion of the buried ferrous alloy coupons.

Based on the 2009 results, copper alloys could be recommended for reburial in these types of sediments for a period of six years. It is probable that pure copper and brass alloy types may be buried for longer periods of time and at shallower depths, however more information from the next phase of the experiment is required to support this inference. On the other hand, due to the significant increase in corrosion rate of the leaded zinc bronze coupons over the past four years, it is not possible to recommend longer term reburial times for these alloy types at this point in time.

Conversely, ferrous alloys could not be recommended for reburial even in the medium term, based on their extensive degradation after six years and the significant increases in their corrosion rates since 2005, which may indicate that corrosion will increase parabolically over time. Evidently, even after six years, it is still difficult to make any definitive statements regarding the longer term stability of these alloy types and therefore, it is of paramount importance that this project continues to the next phase, so as much information as possible regarding the corrosion processes of these metal coupons can be obtained, to establish whether or not the present conclusions are real indicators of the effects of the different microenvironments on long-term metal corrosion and whether reburial is indeed, an appropriate preservation strategy for maritime archaeological metals.

# 5. REFERENCES

Nyström Godfrey, I. and Bergstrand, T. (eds), 2007, *Reburial and Analyses of Archaeological Remains – Studies on the Effect of Reburial on Archaeological Materials Performed in Marstrand, Sweden 2003-2005*. *The RAAR Project*, Bohusläns Museum and Studio VästSvensk Konservering, Sweden, pp. 91-179.

Richards, V.L. and MacLeod, I.D., 2007, Reburial and analyses of archaeological remains: Investigations into the effects of reburial on metals in *Reburial and Analyses of Archaeological Remains – Studies on the Effect of Reburial on Archaeological Materials Performed in Marstrand, Sweden 2003-2005*. *The RAAR Project,* eds I. Nystrom-Godfrey & T. Bergstrand, Bohusläns Museum and Studio VästSvensk Konservering, Sweden, pp. 91-179.

# REBURIAL AND ANALYSES OF ARCHAEOLOGICAL REMAINS

# THE RAAR PROJECT

## Investigation into the Effects of Reburial on Artefacts made of Ceramics and Glass

## Phase II – results from the 4th retrieval 2009

Carola Bohm, Eva Christensson, Anders G. Nord and Kate Tronner

## Background

After the completion of Phase I of the RAAR project in 2006, with analyses and interpretation of the samples from three consecutive retrieval periods, the results were extremely varied for the different material categories included in the silicate sub-project. The status of the glass samples in particular indicated that the potential for acceptable preservation in the reburial sediments at Marstrand was poor. By contrast, some of the ceramic wares, notably porcelain and modern stoneware samples, appeared consistently unaltered over the three years. These observations allowed us to suggest some tentative recommendations for artefact categories that might be considered for reburial – and some that ought not.

For several of the ceramic samples of a more porous quality, such as e.g. earthenware and flint ware, the results were considered inconclusive. A longer period of exposure to the burial environment and further investigations were necessary to make an informed statement.

Naturally, the first phase of the project also gave rise to a series of new questions to focus upon for the retrieval 2009.

- What is the nature and the implications of the biological growth in the zip lock bags?
- Does the material, if undisturbed, reach a state of equilibrium with its environment?
- Does the rate of deterioration, seen particularly on the model glass, abate?
- Is the discolouration, seen on some samples, exacerbating future conservation needs?

## Sample handling

All samples retrieved in 2009, excepting the model potash glass and the clay pipe packed in zip lock bags were handled in the same manner as for the previous retrievals. They were removed from their reburial crate, repacked with sediment and sent to The National Heritage Board in Visby. There, they unpacked, lightly rinsed from excess sediment, dried, weighted and documented. The elemental analyses were carried on using the same SEM/EDAX instrument that was used for all samples in Phase I. For a more detailed description of the analytical procedured, see the extensive report published in 2007 (Bergstand & Nyström Godfrey, eds).

### *For microbiological analysis*

On all the samples from the three previous retrievals, micoorganisms had been observed on model potash glass packed in zip lock bags. The sample from 2009 was kept wet and undisturbed in cold storage and passed on to Margareta Ekroth Edebo at the Department of Conservation, Göteborg University for study of the biological growth. The clay pipe sample in zip lock bag was also included, as there were vague indications that microorganisms might also be present on these.

## Results

The analyses of the silicate samples retrieved in 2009, after seven years of burial, have in many instances confirmed the results from the first phase of the project. Tendencies of degradation, of alterations in the elemental composition – or indeed the absence of any alterations – that had been observed after the first three years, were generally also seen on the samples from this fourth retrieval. Deposition and, by inference, absorption of salts that had been registered on the more porous ceramic wares, seems to continue increasing. At this stage, the infiltration of salts MAY still depend on the type of packaging and further investigations should include desalination and monitoring of the concentration of soluble salts in these samples.

### *Glass*

The glass samples, particularly the model glass, have displayed the clearest alterations and interesting features throughout the project. In this phase, we therefore concentrated the investigation of these samples.

*Model potash glass*

Early on, the model potash glass samples had black stains when still in the wet state. Upon drying, the discoloration mellowed to a pale yellow. This phenomenon has increased over the years of retrievals (figures 1 b & c), but has not been attributable to any corresponding increase in either carbon, sulphur or iron. It is more likely due to the reduced state of one or more of these elements, which then re-oxidize upon drying under atmospheric conditions.


*Figure 1a. Reference sample*



*Figure 1b & c. Sample deposited in geotextile and retrieved after 7 years, in wet condition (b) and after drying (c)*

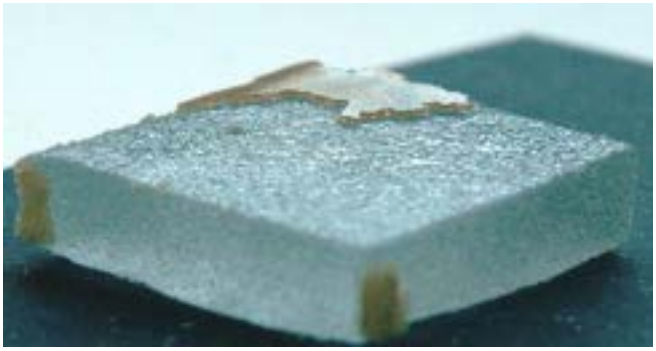

*Figure 2. Same sample as figures 1b&c (above) after removal of the weathered layer*

| Retrieval year | Zip lock | Netting | Geotextile |
|---|---|---|---|
| 2003 | 0,85 | 3,74 | 2,51 |
| 2004 | 2,75 | 7,42 | 8,45 |
| 2005 | 1,99 | 7,83 | 7,55 |
| **2009** | **5,59** | **20** | **16,61** |

*Table 1. Percent weight loss on model potash glass samples over the seven years reburial period*

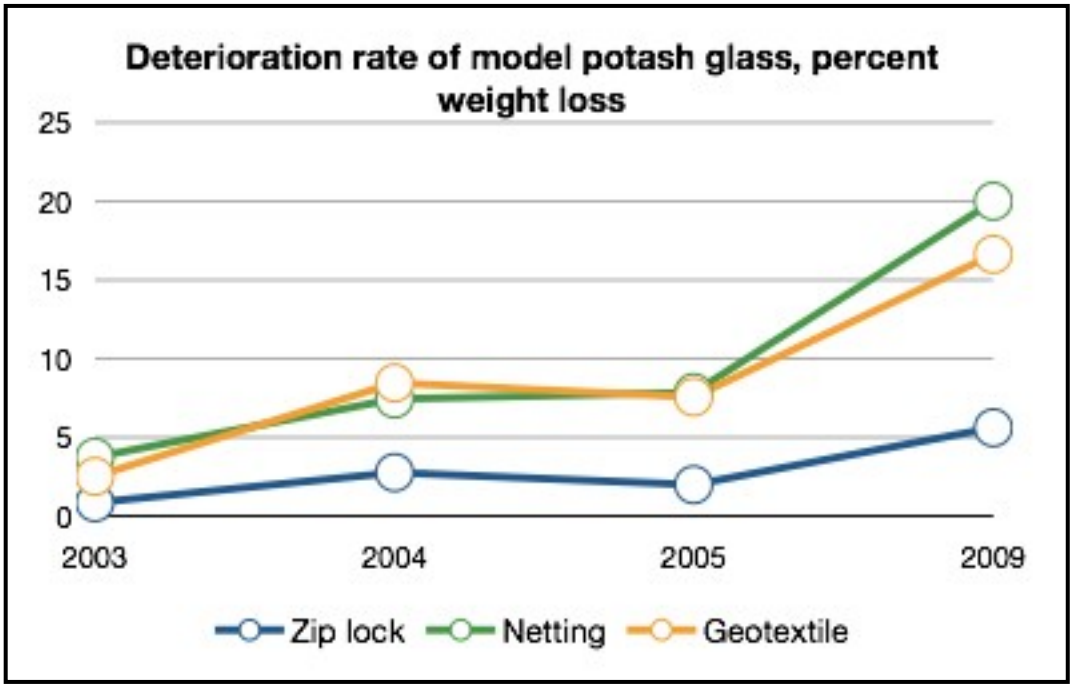


*Figure 3. Continuous deterioration of model potash glass, calculated as the weight percentage of weathered matter related to the samples' initial weight, prior to reburial*

We continued to monitor the rate of degradation of these samples by removing the weathered layers with pressurized air. On the samples packed in netting and geotextile, the layer had a distinctly stronger adherence to the glass substrate than was experienced for the samples from previous retrievals. It was thought that this might be attributed to a different microenvironment in the burial trench, but this hypothesis has not been corroborated by the environmental data – and remains unexplained.
There is very clearly an unabated deterioration rate on these samples, most obvious on the samples packed in netting with a mass decrease of 20%. Deterioration also continues in the zip lock bags, but at a much slower rate. The results can been seen in table 1 and the diagram above (figure 3). "Percentage weight loss" is calculated as the difference between the original weight of each sample before burial and its weight after retrieval every given year.

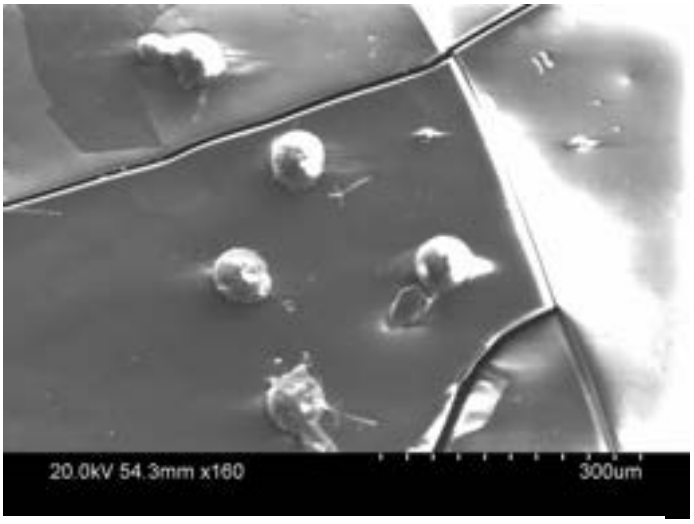


*Figure 4. After seven years burial. Microorganisms ever present on the model potash glass deposited in zip lock bags*

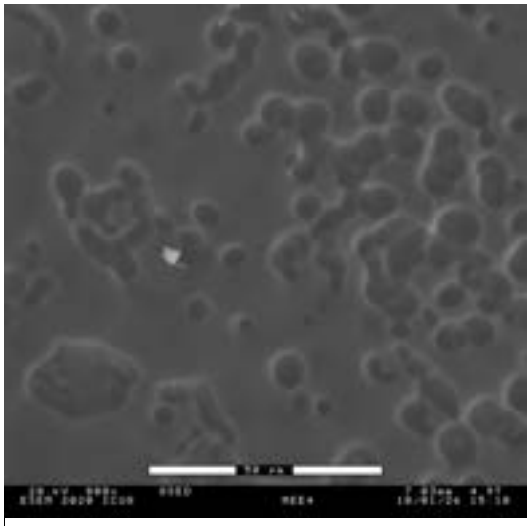

*Figure 5. "Pit corrosion" or etching beneath the weathered layer on the same sample as in figure 3*

As mentioned above, the biological growth on samples in zip lock bags were studied more closely this year. The small rounded particles (figure 4), approx. 50 micrometers in size, that sometimes are seen in groups or small clusters, have not been seen to increase or spread out over the years. Elemental analysis show that they have a higher content of both phosphorous and calcium than does the surrounding glass substrate. Few known organisms are known to exist in anoxic environments. Sulphur-reducing bacteria spring to mind, but these particles are apparently too large in size. Spores of yeast or algae have been contemplated and it has actually been suggested that they might be attributed to contamination prior to burial. The definitive identity of these organisms remains unresolved, but investigations will continue.
The pit corrosion or etching seen in figure 5 has a conspicuous correspondence in size as compared to the microorganisms and we have speculated if there might be any connection. It is worth noting that small, shallow and more or less densely distributed pits are a quite common feature on deteriorated glass surfaces – appearing beneath the fragile (and fugitive) weathering layers. It may be observed on archaeological glass from both land and marine sites as well as on medieval window glass exposed to atmospheric weathering. And, studies conducted on medieval

window glass exposed in polluted environments have indeed shown that microorganisms have a role in the deterioration process.

### *Ceramics*

Results for the ceramic wares continue along the same lines registered during the first phase of the project. In general, the non-porous wares display little or no alteration, whereas the porous earthenware, flintware and clay pipes continue to absorb soluble salts from the environment. The porous samples are also consistently black-stained when still wet, a feature that was only sporadically observed in the previous retrieval series. Archaeological flintware samples are offered as examples in the images below.

*Flint ware*



*Figures 6 a & b. Archaeological flintware packed in netting, after seven years of reburial. In wet condition (a) and dried (b)*

*Tables 2 & 3. Summary of the results for the glass and ceramic samples*

**Glass**

| **Archaeological samples** | | **Model samples** | |
|---|---|---|---|
| Clear table glass | Bottle glass, green | Soda glass | Potash glass |
| Thin iridescent surface layers with reduced alkali levels.<br><br>Surface exfoliation<br><br>One sample in Zip-lock® bag broken | Thick silica-rich surface layers with areas of elevated NaCl, S, Fe<br><br>Heavy surface exfoliation<br><br>No clear difference between reburied sample and reference | Accelerating depletion of Na | Depletion of alkali components in surface layers<br><br>Severe disintegration and loss of surface<br><br>Zip-lock® bag represses leaching, but promotes biological growth<br><br>Discolouration of weathered layers, black-stained in wet condition |

**Ceramics**

| **Archaeological samples** | | | | **Modern samples** | | | |
|---|---|---|---|---|---|---|---|
| Porous | | | Non-porous | Porous | | Non-porous | |
| Earthenware, lead glazed | Flintware, lead glazed | Clay pipes | Stoneware, salt glazed | Earthenware, low-fired | Flintware, lead glazed | Stoneware, feldspatic glaze | Porcelain, feldspatic glaze |
| No visible alteration<br><br>Black-stained in wet condition<br><br>Absorption of NaCl, S | No visible alteration<br><br>Black-stained in wet condition<br><br>Absorption of NaCl, S | Black stained in wet condition<br><br>Absorption of NaCl, S, Fe | No visible alteration<br><br>Traces of NaCl, S | Severe disintegration<br><br>Black-stained in wet condition<br><br>Absorbed NaCl, S | No visible alteration<br><br>Increased absorption of NaCl | No alteration | No alteration |

# Reburial and Analyses of Archaeological Remains. (RAAR)

## Investigation of the effects of burial on materials used at archaeological excavations to separate and mark objects.

**Final report, phase 2**
**4th retrieval 2009**

Co-ordinator: Inger Nyström Godfrey
Studio Västsvensk Konservering, Västarvet
Gamlestadsvägen 2-4, 415 02 Göteborg, Sweden.

With contribution from
Stefan Almström
SP Swedish National Testing and Research Institute

STUDIO
VÄSTSVENSK KONSERVERING

## Table of contents

# Reburial and Analyses of Archaeological Remains. (RAAR)

## Investigation of the effects of burial on materials used at archaeological excavations to separate and mark objects.

### Final report, phase 2
### 4th retrieval 2009


## Summary

In archaeology a range of modern products are used to separate, label and support archaeological objects during an excavation. These products are often polymeric in nature. As reburial of archaeological material is anticipated to last for an extended period, the packing and labelling materials need to be able to survive for just as long. Consequently the durability of these products is of great importance. Although reburial environments are likely to be benign for the preservation of polymer material, present knowledge of their long-term stability is limited. Better knowledge of the most suitable products and materials to use will not only improve the quality of cultural heritage management but will also improve the efficiency of the work that is to be conducted. The correct material can be used and unknown or problematic material can be avoided from the start of an excavation.

The objectives of this sub-project are to investigate how a reburial environment will effect the mechanical properties of some relevant packing products/materials and also to determine the legibility of a number of labelling materials subjected to a marine sediment environment. The materials chosen in the investigation are products that are often used during underwater archaeological excavations. The study compares and assesses the usefulness of these materials in relation to reburials.

The study includes a variety of products and materials (table X), mainly of polymeric origin, including polyethylene (PE), polypropylene (PP), polyester, polyamide or nylon (PA) and polyether/polyurethane. Stainless steel labels have also been included and compared with polyvinyl chloride (PVC) labels. Samples of pinewood, to imitate a pine container, were also tested and compared to a PE container.

Four different types of pens have been used on two different supports. Two different brands of permanent marking pens, one is especially designed for writing on overhead plastic sheets, a ball-point pen with archival proof ink and a pencil have been tested. All text has been written both on polyethylene bags and on polyethylene tags.

The products can be placed in the following groups according to their uses.

- Materials to separate objects (crates/containers, bags, nets and sacks).
- Materials for tying or attaching labels to object (different kind of cords).
- Materials for support and protection, e.g. geotextile and synthetic rubber tarpaulin.
- Materials to identify objects, e.g. tags with embossed or prefabricated numbers, but also text written with pencil, permanent markers and an archival proof ballpoint pen.

The lack of funding for the 4th retrieval 2009 meant that the tensile strength of some of these materials could not be tested (table 1). The materials that had to be excluded were chosen on the basis of bad preservation result from phase 1 or their importance in the archaeological process

The test materials were exposed i*n-situ* in the actual sediments in the harbour under the same conditions as during a normal reburial at a depth of approximately 50 cm. The previous phase of the project (2002-2005) also included accelerated ageing in the laboratory of some materials. Those results were reported in the final report for the RAAR project phase 1 (Reburial and analyses of archaeological remains, 2007 & Nyström Godfrey, 2009).

After retrieval from the burial environment samples were inspected and documented. They were photographed and examined under the microscope. The labelling materials were investigated using ocular inspection and colorimetric analyses and the mechanical strength of the packing materials was evaluated by tensile testing. Results were compared with references and previously retrieved samples.

This study on packing and labelling material investigates products are (or have been) used in archaeological and reburial contexts. It is important that these products are easy available and not too expensive, which is the case with most of the studied products.

When commercial products are studied a few problems arise. One is that the complete content of a specific product can be difficult to obtain because of trade secrets. Therefore only the main ingredient(s), the base material, of each product can be given in a study like this. The fact that additives, such as plastisicers and colours, are mixed with base materials complicates the interpretation of degradation analyses. Processes such as the extraction of additives in different environments may affect the mechanical properties in various ways. Different products made of the same base material are likely to have different additives, which may cause them to degrade differently. Hence conclusions from the analyses in this study are valid primarily for the tested products and to a lesser extent for the base materials.

We know from previous results (Nyström Godfrey, 2009) that the wooden crate (B) and the polyethylene net (D) already after 3 years had lost considerable strength. However, after seven years in the marine sediments the mechanical strength of the HDPE crate (A), the polyethylene bag (C), the polyethylene/polypropylene geotextile (F), the polyethylene rope and the PETR/PUR prefabricated tag (N) is unchanged. The polyester rope (J) is still strong, but the Max Load has decreased from 800 to 625 N and it could be considered a trend (Figure 15), which would make a polyester rope less suitable for long term reburials; however this will have to be confirmed through future analyses.

The interpretation of the tensile tests on the polyamide products cord (L) and yarn (M) was after phase I inconclusive. Although polyamide is known to be a very strong and durable material, often used in marine environments (e.g. Kevlar sails) little was known about the degradation processes in an anaerobic environment. (Brydson, 1995 ). Polyamide is a material sensitive to humidity. Moisture does not affect the ageing, but it strongly affects the strength of the material. (Almström, pers.comm.) The inconclusive and odd results for the mechanical strength in phase I was thought to be a result of differences in moisture content and re-cristallisation, despite all samples being conditioned in the same manner. The tests performed on the 2009 *in situ* samples showed no degradation of the mechanical properties (figure 21), smaller variations are within standard deviation. This suggests that it is suitable for reburials. However, it would be wise to wait for future analyses before making statements of the long term preservation of polyamide in anaerobic reburial environments.

In short one can state that most of the polymer materials tested are very stable and can be used in situations where archaeological artefacts are to be reburied. Crates should be made of HDPE and not from wood. Nets of PE should be avoided and certainly not used for heavier objects. A possibility would of course be to use a PE net with coarser and stronger strings or using nets made from other material, such as polyamide or maybe polyester. For short-term reburials (7 years) ropes and yarns made of PE, polyester or polyamide could be used, for longer-term reburial it would, until further investigations are made, be wise to use the PE cord.

After seven years of burial all labels were easily readable with the naked eye. Ocular inspection and chromaticity readings show, however, that text written with (R) the black marker (R) [1] and the blue archival proof pen (S) [2] had continued to deteriorate and change quite considerable. As expected the pencil (T) writing had not change at all, likewise with the permanent marker (Q). [3]

It is therefore recommended to use pencils or markers of good permanent quality and not for example, over-head markers, as the one tested. As the archival ink pen (S) showed signs of degradation in this particular environment it is not suitable for anaerobic clay sediments. Another reason to avoid this pen is the fineness of the tip of the pen, which makes the lines very thin and difficult to read when the ink fades and changes in colour.

Although the prefabricated and Dymo labels all looked good after seven years of burial, the steel label is difficult to read. It is also known that stainless steel corrodes in anaerobic environments due the action of the sulphate reducing bacteria, which would make it a less good choice. (Evans 1963 & Richards, Appendix 2 this publication) A better choice for labelling artefacts reburied in sediments would be to use PVC Dymo labels or prefabricated embossed tags, so called “ear-tags”. Table 7 summarise the results and evaluations of the stability of the tested materials

## Introduction

In archaeology a range of modern products are used to separate, label and support archaeological objects during an excavation. These products are often polymeric in nature. As reburial of archaeological material is anticipated to last for an extended period, the packing and labelling materials need to be able to survive for just as long. Consequently the durability of these products is of great importance. Although reburial environments are likely to be benign for the preservation of polymer material, present knowledge of their long-term stability is limited. Better knowledge of the most suitable products and materials to use will not only improve the quality of cultural heritage management but will also improve the efficiency of the work that is to be conducted. The correct material can be used and unknown or problematic material can be avoided from the start of an excavation.

### *Objectives*

The objectives of this sub-project are to investigate how a specific reburial environment will effect the mechanical properties of some relevant packing products/materials and also to determine the legibility of a number of labelling materials subjected to a marine sediment environment. The materials chosen in the investigation are products that are used during underwater archaeological excavations. The study compares and assesses the usefulness of these materials in relation to reburials.

The previous phase of the project (2002-2005) has been reported in the project report Reburial and analyses of archaeological remains (2007) and in Nyström Godfrey (2009).

### *Material*

The study includes a variety of products and materials (*Table 1*), mainly of polymeric origin, including polyethylene (PE), polypropylene (PP), polyester, polyamide or nylon (PA) and polyether/polyurethane. Stainless steel labels have also been included and compared with polyvinyl chloride (PVC) labels. Samples of pinewood, to imitate a pine container, were also tested and compared to a HDPE container.

Four different types of pens have been used on two different supports. A ball-point pen with archival proof ink and a pencil have been tested as well as two different brands of permanent marking pens, of which one is especially designed for writing on overhead plastic sheets. All text has been written both on polyethylene bags and on polyethylene tags.

The products can be placed in the following groups according to their uses.[1]

- Materials to separate objects (crates/containers, bags, nets and sacks).
- Materials for tying or attaching labels to object (different kind of cords).
- Materials for support and protection, e.g. geotextile and synthetic rubber tarpaulin.
- Materials to identify objects, e.g. tags with embossed or prefabricated numbers, but also text written with pencil, permanent markers and an archival proof ballpoint pen.

[1] For a complete list of materials, data and suppliers see List on page 33 ff.

The lack of funding for the 4th retrieval 2009 meant that the tensile strength of some of these materials could not be tested (*Table 1*). The materials that had to be excluded were chosen on the basis of bad preservation result from phase 1 or their importance in the archaeological process.

*Table 1 . Materials tested in the study.*

| Sample ID | Product | Material | Abbreviation | Tested in phase 1 | Tested in phase 2 - 2009 |
|---|---|---|---|---|---|
| | | | | | |
| A | Crate | Polyethylene | HDPE | X | X |
| B | Crate | Pine | | X | |
| C | Bag | Polyethylene | LDPE | X | X |
| D | Net | Polyethylene | PE | X | |
| E | Sack, woven | Polypropylene | PP | X | |
| F | Geotextile | Polyethylene/ Polypropylene | PP/PE | X | X |
| G | Geotextile | Polyester | | X | |
| H | Tapaulin | Synthetic rubber | EPDM | X | |
| J | Cord | Polyester | | X | X |
| K | Cord | Polyethylene | PE | X | X |
| L | Cord, spun | Polyamide | PA | X | X |
| M | Yarn | Polyamide | PA | X | X |
| N | Tag, prefabricated | Polyether/ Polyurethane | PETR/PUR | X | X |
| O | Tag, Dymo ® | Polyvinyl chloride | PVC | X | X |
| P | Tag, Dymo ® | Steel | | X | X |
| Q | Marker | Permanent ink on PE bag | | X | X |
| R | Marker for OH | Permanent ink on PE bag | | X | X |
| S | Pen, ball point | Archival proof ink on PE bag | | X | X |
| T | Pencil | Graphite on PE - bag | | X | X |

## Experimental

The test materials were exposed i*n-situ* in the actual sediments in the harbour under the same conditions as during a normal reburial. The previous phase of the project (2002-2005) also included chemical and microbiological accelerated ageing in the laboratory of some materials (70˚C, 26 weeks and 23˚C, 135 weeks respectively). Those results were reported in the final report for the RAAR project phase 1 (Reburial and analyses of archaeological remains, 2007) and in Nyström Godfrey, I. (2009). The results can also be seen in the diagrams for the different materials below.

Eight units with samples were buried in the reburial trench in Marstrand harbour in September 2002. The burial depth is approximately 50 centimetres from the bottom of the container, which means that all samples were covered by 30-50 centimetres of sediment.


*Figure 1. Display of unpacked material*

Each unit contains three samples of each material category, all three buried at the same depth. A ninth unit was kept as a reference in cool storage conditions at Studio Västsvensk Konservering (SVK).[2] After the retrieval 2009 the unit was immediately packed in plastic and taken to SVK, where it was stored in cool storage before excavation.[3]

*Figure 2 & 3. The unit from 2009 during and after excavation*

[2] Fridge temperature approx. 2-4 °C
[3] Ibid.

The sediment covering the samples consisted of clay and mud mixed with shells, pieces of wood and other organic material. It had a very unpleasant smell of hydrogen sulphide or rotten egg, which indicated an anaerobic condition. After excavation all samples were rinsed under tap water and air-dried.

## *Analyses*

After excavation the samples were inspected and documented. They were photographed and examined under microscope. The labelling materials were also investigated using colorimetric analyses and changes in weight were recorded. The mechanical strength of the samples from the 4th retrieval after 7 years of exposure was tested and compared with reference and previously analysed *in situ* samples.

### Tensile strength test

The mechanical strength of all material was evaluated by tensile testing according to table 2. The tensile test results are reported as the arithmetic mean of five or more test samples. Reference material and all samples were conditioned at 23±2 ºC and 50±5% RH until their weight became constant before tensile tests[4].

*Table 2. Tensile strength test set up.*

| **Material** | **Test specimens** | **Clamping type** | **Initial clamping distance mm** | **Elongation measurement** | **Test speed mm/minute** |
|---|---|---|---|---|---|
| A | Dumbbell ISO 37 type 2 | Manual mechanical | 55 | Video extensometer | 100 |
| C | 25 mm strips (backside of bag) | Rubber friction rolls | 50 | Distance between rolls c/c | 100 |
| F | 50 mm strips | Rubber, friction rolls | 100 | Distance between rolls c/c | 100 |
| J | about 300 mm | Steel friction rolls | 100 | Distance between rolls c/c | 50 |
| K | about 300 mm | Steel friction rolls | 100 | Distance between rolls c/c | 50 |
| L | about 300 mm | Steel friction rolls | 100 | Distance between rolls c/c | 50 |
| M | about 300 mm | Steel friction rolls | 100 | Distance between rolls c/c | 50 |
| N | Dumbbell ISO 37 type 4 | Manual mechanical | 25 | Video extensometer | 100 |

[4] According to ISO 527-1

**Chromaticity analyses**
The written or prefabricated text samples were assessed as to its legibility. Three categories were used; easy readable, partially readable and not readable. Comments have been made to specify type of change such as discolouring, blurring etc. Visible deterioration of the material onto which the text has been written or embossed has also been recorded. The ocular inspection was performed with the naked eye and under binocular (X10 – X60).

However, human assessment of colour change is subjective. Therefore colour changes were measured with a colorimeter.[5]

Colour as perceived has three dimensions: hue, chroma and brightness. Hue stands for what we call colour in everyday life, e.g. red, green etc, chroma gives us the saturation level, e.g. vivid or dull colours and brightness is how light or dark the colour is. For colours to appear similar, these three quantities must be identical. The L*a*b* measuring mode is designed to approximate human vision. The three coordinates represent lightness of the colour (L*), its position between red and green (a*) and between yellow and blue (b*).The dE colour deviation measuring mode represents the total colour difference between the sample and the standard.[6] (Minolta, 1984 & Wikipedia)

Chromaticity of the samples was measured in the L*a*b* measuring mode and colour deviation with deltaE (dE). The illuminant source used was D65. The previous chromaticity analyses performed during phase 1 used another colorimeter[7], with a different light source. This colorimeter was no longer available which meant that all the samples including the old ones (references and samples from 2005) had to be analysed again.

The measuring area of the new colorimeter was bigger (8mm in diam.) than the previously used meter, which meant that measurements taken directly on the PVC dymo tags (material O) and on the written text on the bags (material Q, R, S & T) would record not only the colour of the sample material but also of the surrounding background. To overcome this, measurements were taken on enlarged prints of the sample material itself.[8]

Three chromaticity measurements at three different positions were taken on every sample to overcome uneven degradation. Since each unit contained three samples of each material category; nine measurements were taken in total for each material category and retrieval. The mean value and standard deviation were calculated from these nine measurements. It is important to note though, that the values recorded from the prints do not reflect the actual colour of the material, but was merely a way of getting comparable data.

---

[5] Minolta colorimeter CR 400

[6] dE is the square root of the sums of the squares of the three components representing the difference between coordinates of the samples and the standard. $dE = [(dL^*)^2+(da^*)^2+(db^*)^2]^{1/2}$

[7] Minolta colorimeter CR 100

[8] To get comparable prints when the tag/text was enlarged, the following procedure was adopted. Bags and tags were scanned using a Canon scanner (CanoscanN12OU). It was set to use workspace RGB1998 standard, colour photo mode and 1200 dpi resolution. The images were saved as tiff-images. From each bag and tag a digit[8] was cropped and enlarged to the same size before printed on archival matte paper an Epson Stylus Photo 2100 printer.

## Results
### *Packing material*

**A. Crate, High Density Polyethylene (red).**


*Figure 4 & 5. Close up of HDPE crate. Reference sample and sample after seven years of in-situ exposure in the sediments*

After seven years in the sediments a very slight shift in the colour was noticed. The red colour had turned a fraction darker. Apart from that, no visible degradation on the HDPE crate was detected.The mechanical strength of all exposed samples has not changed significantly.[9](*Figure 6).*

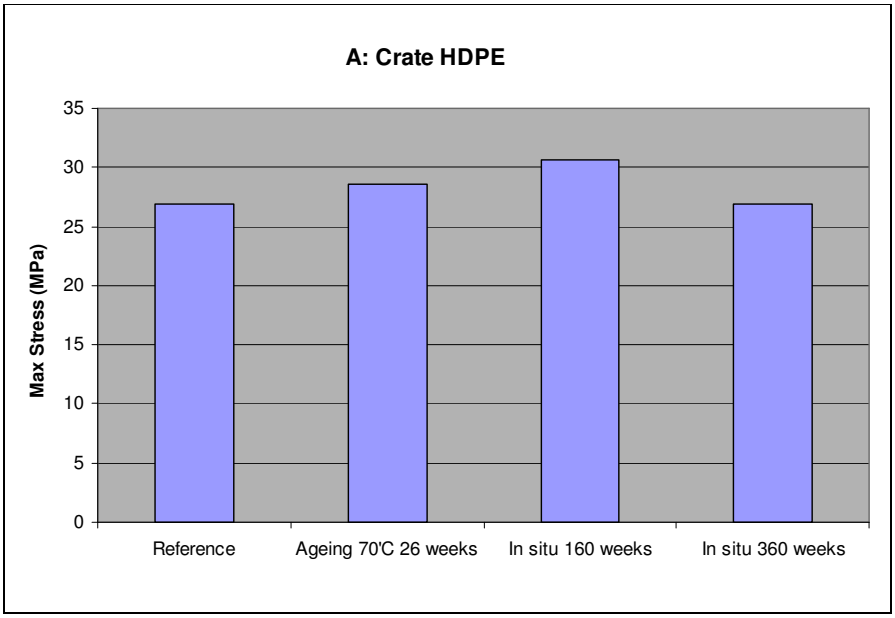


*Figure 6. Diagram of stress at break point (Mpa) for the HDPE crate (A) exposed in different environments.*

[9] It was decided to show the results of the tensile strength test as Max stress values in stead of the previously used Stress at break, since it was considered a more just way to portray the physical properties of the material

## C. Bag, Polyethylene (transparent + white text panels)


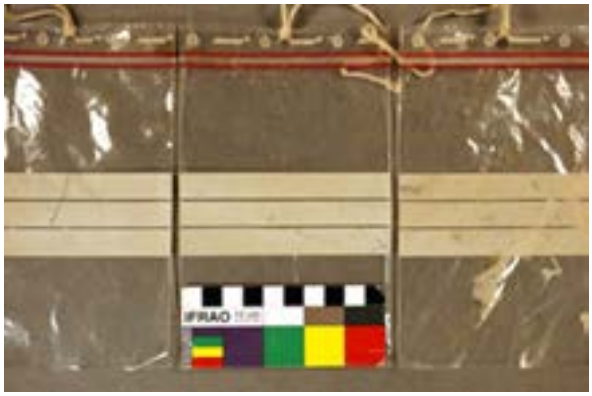

*Figures 7 & 8. PE-bags. Reference and samples retrieved after seven years of in-situ exposures in the sediments.*

The PE –bags, particularly the white text panels, have become discoloured (yellow), indicating that some changes are taking place in the material. The chromaticity readings taken confirmed that the discolouration has increased since 2005. *(Table 13*). No change in weight has occurred. *(Table 12).*

The mechanical strength of the samples from all of the three exposure conditions is insignificantly changed. The small differences noted in the diagram for mechanical strength (*figure 9*) are within standard variations.

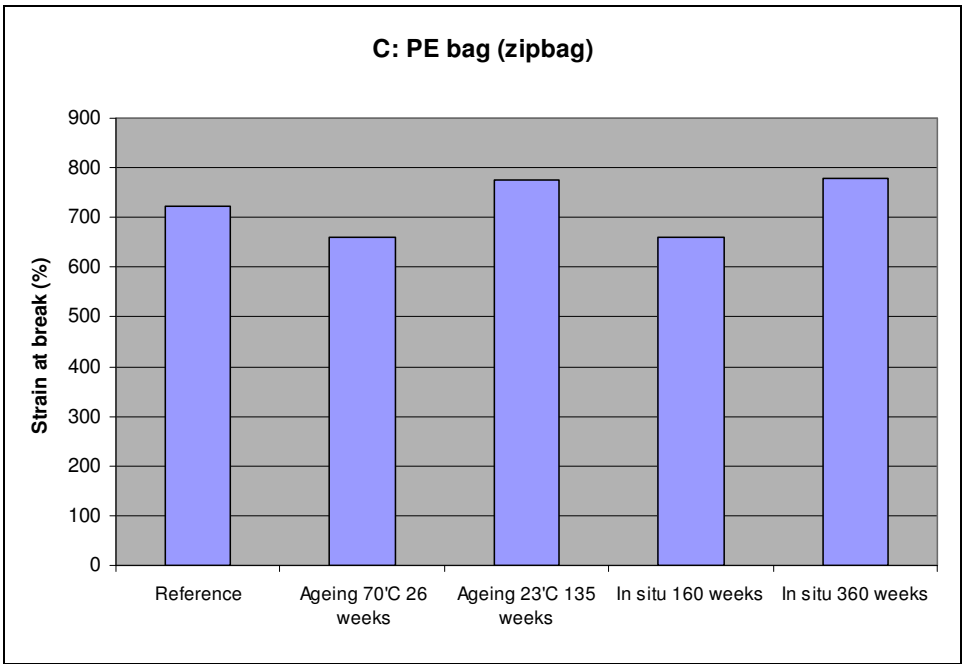


*Figure 9. Diagram of the strain at break point for the polyethylene bag samples (C), exposed in different environment.*

**F. Geotextile, Polypropylene/Polyethylene (white).**


*Figure 10 & 11. Geotextile of PP/PE. Reference and sample retrieved after seven years of in-situ exposures in the sediments.*

No visible degradation could be seen using the microscope or the naked eye on any of the samples. The result of the tensile test show a decrease in strength (7.9→7.5→6.2 N/mm),[10] however the non-woven geotextile material is not homogenous. *(Figure 12)* The distribution of different sized fibres is irregular and therefore different parts of the material can behave differently. The result is therefore not conclusive.

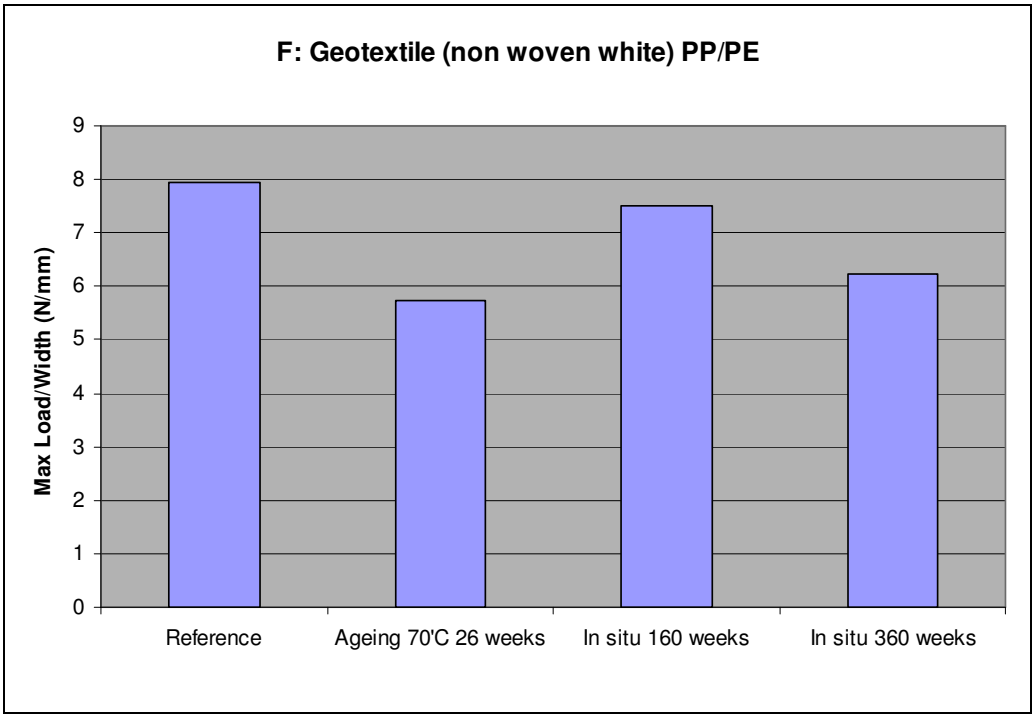


.[10] The tensile strength result for the *in situ* samples from 2005 was incorrectly reported after phase 1as 12 Mpa should have been 7.5 N/mm (Stefan Almström, pers. comm.]

*Figure 12. Diagram of Max Load/Width for the PP/PE geotextile samples (F), exposed in different environment.*

**J. Cord, Polyester (white).**


*Figure13 & 14. Polyester cord. Reference and samples retrieved after seven years of in-situ exposures in the sediments.*

No visible degradation could be seen using the microscope or the naked eye on any of the samples. A slightly yellow tinge is probably due to dirt. However, there has been no visible change between the samples retrieved 2005 and the samples retrieved 2009.

The exposure in the different environments has changed the mechanical properties of the samples very little. However, looking at the *in situ* samples, the strength slowly decreases from 800 → 770 → 630 N which could possibly be called a trend. (*Figure 15).*

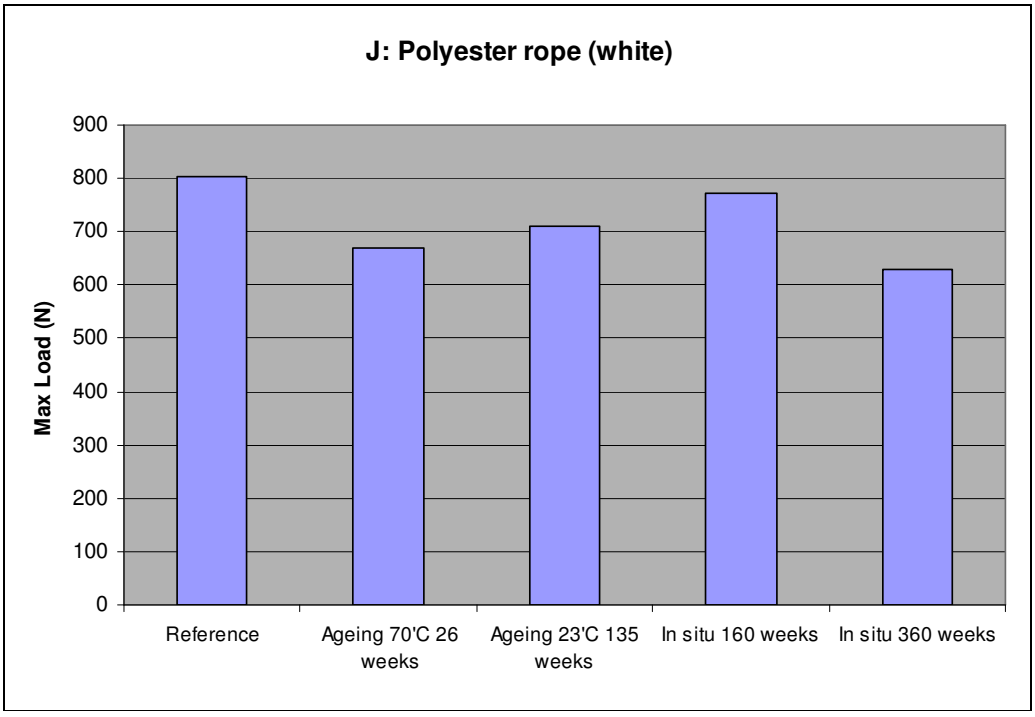


*Figure 15. Diagram of the max load (N) of the polyester cord samples (J) exposed to different environments.*

**K. Cord, Polyethylene (green).**

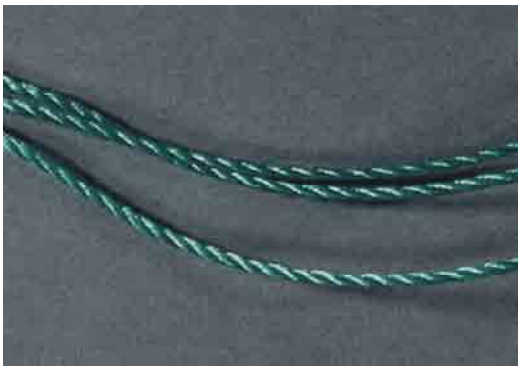


*Figures 16 & 17. PE cord. Reference and samples retrieved after seven years of in-situ exposures in the sediments.*

No visible degradation could be seen using the microscope or the naked eye on any of the samples. The mechanical strength of the samples is intact after seven years in-situ in the sediments. The small differences noted in the diagrams for mechanical strength *(figure 18)* are within standard variations.

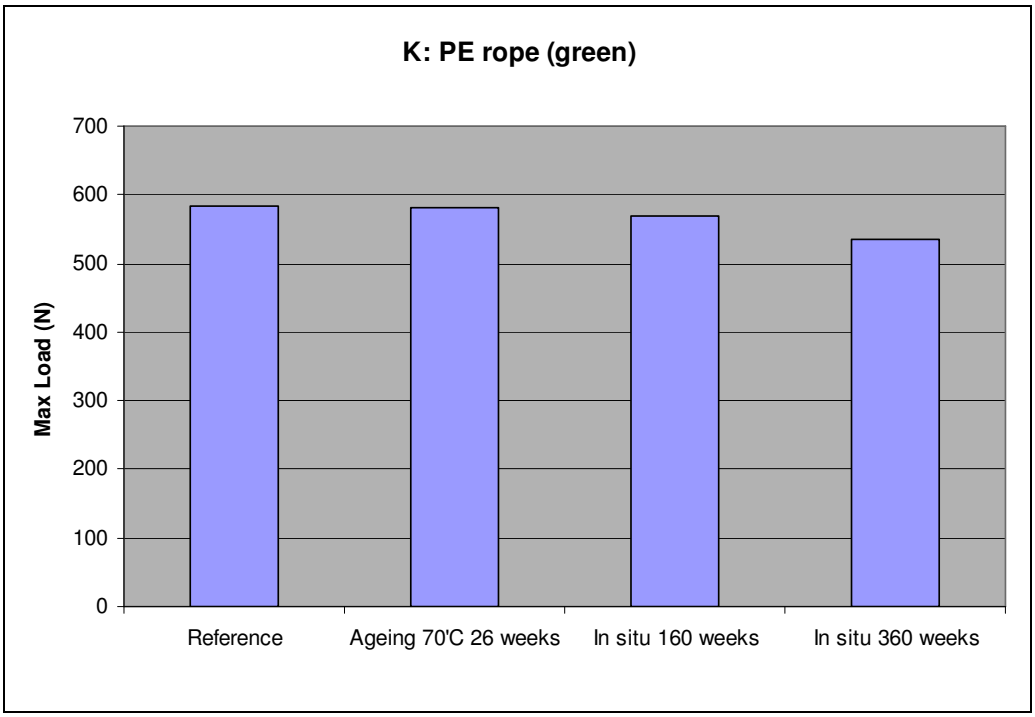


*Figure 18. Diagram of max load (N) for the polyethylene cord samples (K) exposed in different environments.*

**L. Cord, Polyamide (white).**


*Figures 19 & 20. Polyamide cord. Reference and samples retrieved after seven years of in-situ exposures in the sediments.*

No visible degradation could be seen using the microscope or the naked eye on any of the samples. A slightly yellow tinge is probably due to dirt

Polyamide is a material highly sensitive to humidity, moisture does not effect the ageing, but it strongly effects the strength of the material. (Stefan Almström, pers. comm.). The inconclusive and odd results for the mechanical strength in phase 1 was thought to be a result of differences in moisture content and recristallisation, despite all samples being conditioned in the same manner.The results from 2009 show no real loss of strength compared to the reference, the small difference noted in the diagram for mechanical strength is within standard variations. *(Figure 21*)

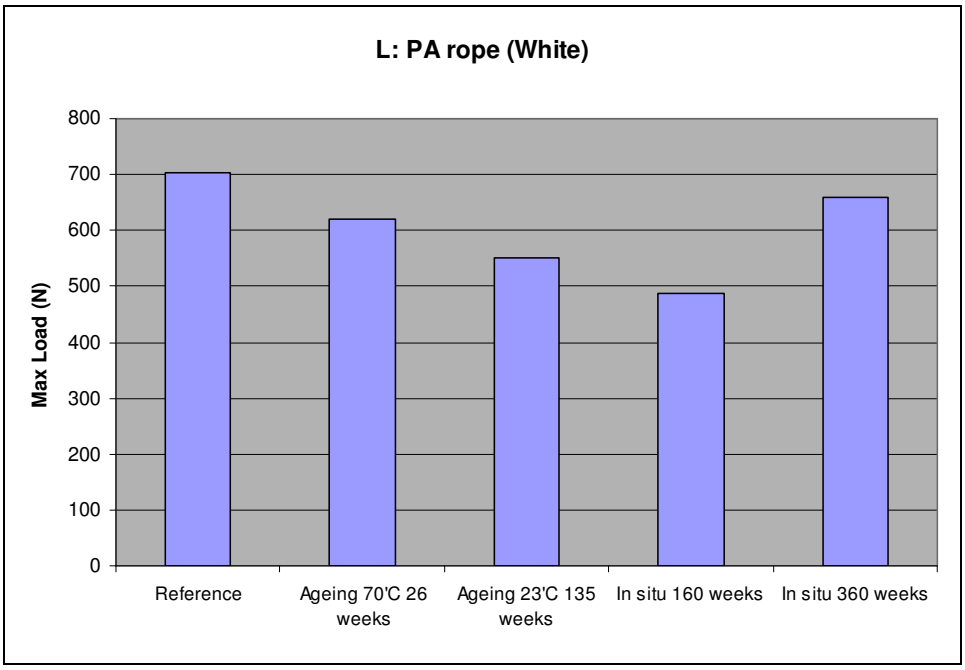


*Figure 21. Diagram of max load (N) for the polyamide yarn samples (L)) exposed*

*in different environments.*

**M. Yarn, Polyamide (green).**

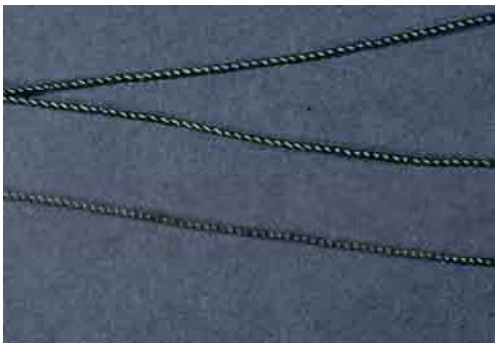

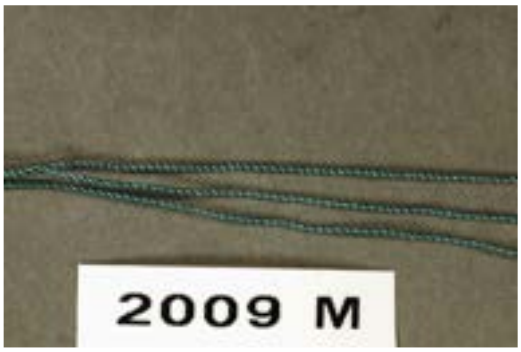


*Figures 22 &23. Polyamide yarn. Reference and samples retrieved after seven years of in-situ exposures in the sediments.*

Only a very small change could be seen using the microscope or the naked eye. The green colour of the 2009 samples has a slightly more bluish tinge than the reference and the previously retrieved samples.

As with the polyamide cord mentioned above (material L) the inconclusive and odd results for the mechanical strength in phase 1 was thought to be a result of differences in moisture content and recristallisation, despite all samples being conditioned in the same manner. The result from 2009 shows no loss of strength compared to the reference, the small difference noted in the diagram for mechanical strength is within standard variations. (*Figure 24*).

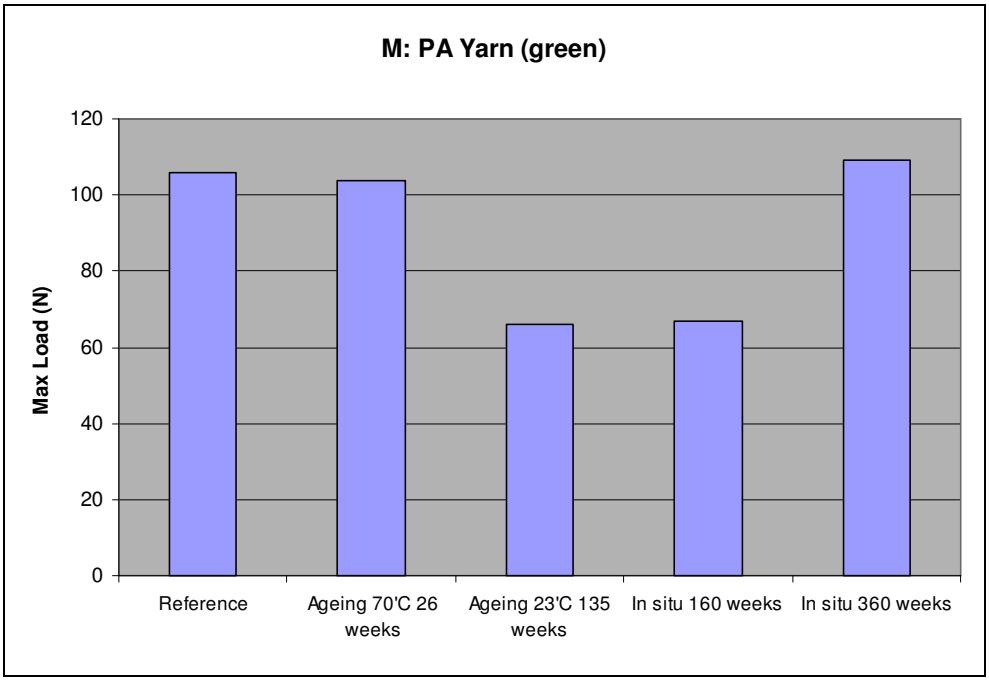

*Figure 24. Diagram of max load (N) for the polyamide yarn samples (M) exposed in different environments.*

**N. Prefabricated tags of polyether/polyurethane (yellow with black text)**


*Figure 25. Tags PETR/PUR. Reference and sample retrieved after seven years of in-situ exposures in the sediments.*

The yellow colour of the tag has become slightly darker, but apart from that no visible degradation or changes in weight could be noted on any of the samples. *(Table 3)*
The mechanical properties do not seem to be affected by any of the burial environments. *(Figure 26 & 27)*. Small differences are within standard variation.

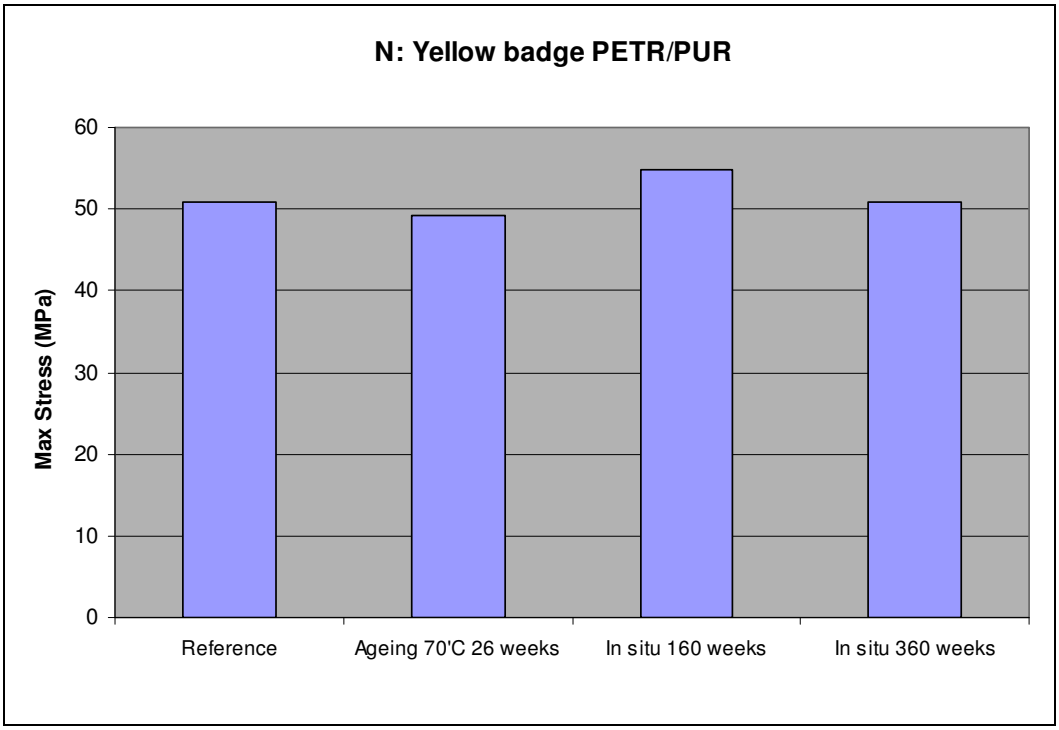


*Figure 26. Diagram of the stress at break point (MPa) for the PETR/PUR tag samples (N) exposed in different environments.*

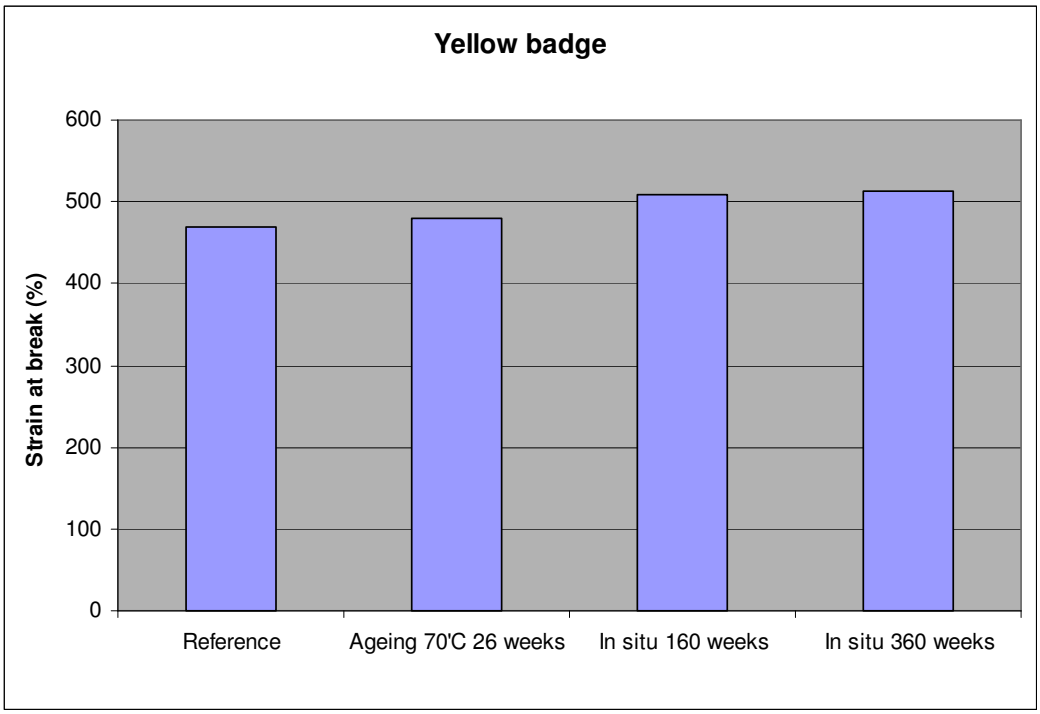


*Figure 27. Diagram of strain at break point (%) for the PETR/PUR tag samples (N) exposed in different environments.*

*Table 3. PETR-PUR tag. Weights before and after burial.*

| **Sample** | **Before burial, 2002.** | | **After burial, 2009** | |
|---|---|---|---|---|
| | g | % | g | % |
| N:1 | 9.2 | 100 | 9.2 | 100 |
| N:2 | 9.0 | 100 | 9.0 | 100 |
| N:3 | 9.0 | 100 | 9.0 | 100 |

## *Labelling material*

All of the labels were easily legible after 7 years of exposure in-situ in the sediments. However, some changes were noted by the ocular inspection and confirmed by the chromaticity readings. These alterations had begun early and were detected in 2003, after one year of exposure in the sediments.

Comments and results are noted below for each material. The ocular and weight inspections of the labels retrieved from the in-situ sediments are summarised in table 4. The chromaticity readings from 2009 are compared with the reference samples and samples from 2005.

*Table 4. A summary of the degradation on labels retrieved from the burial sediments in 2009 assessed using ocular inspection and weighing.*

| Sample | Text | Comments | Material | Comments | Weight loss |
|---|---|---|---|---|---|
| N | Easy readable | | No visible deterioration | | No |
| O | Easy readable | | No visible deterioration | | No |
| P | Easy readable | | | Spots of tarnish | No |
| Q | Easy readable | Reduced blackness. Spots with material loss.. | | Discoloured, yellow | |
| R | Easy readable | Changed colour, blue instead of black. Reduced intensity. Slightly chafed. | | Discoloured, yellow | |
| S | Easy readable | Slightly changed colour, greenish blue instead of blue. Slightly reduced intensity. | | Discoloured, yellow | |
| T | Easy readable | | | Discoloured, yellow | |

**N. Prefabricated labels of polyether/polyurethane PETR/PUR (yellow with black text).**

No visible degradation apart from a slightly darker yellow tone or change in weight (*table 7*) was recorded on the samples exposed in-situ.

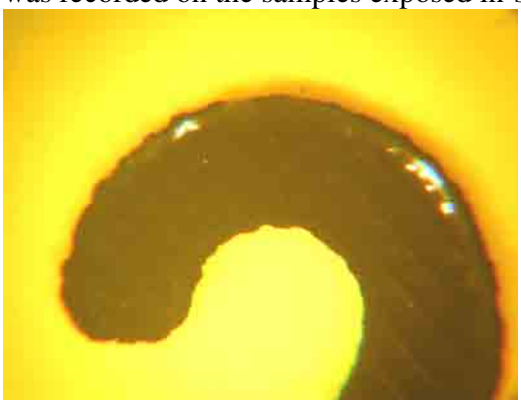
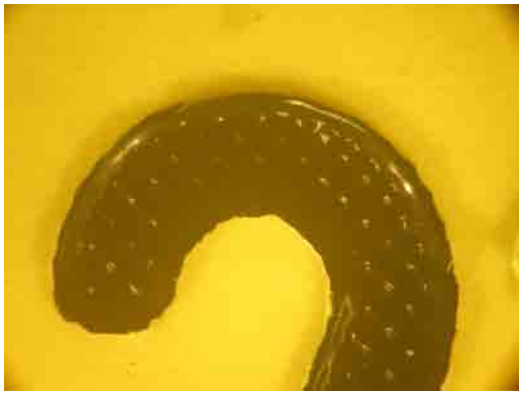

*Figure 28 & 29. Label of PETR/PUR. Details of reference sample and sample retrieved after seven years of in-situ exposures in the sediments*

Chromaticity readings were taken on the yellow background and on the black digits. These readings confirmed the ocular inspection, showing a total colour change (dE) less than 1 for the black digits and a low but slightly increasing dE for the yellow material.*(Table 5).*

*Table 5. Chromaticity readings for the prefabricated labels of PETR/PUR*

| **N - prefabricated tag** | | **L*** | **a*** | **b*** | **dL*** | **da*** | **db*** | **dE*ab** |
|---|---|---|---|---|---|---|---|---|
| Yellow PETR/PUR material | Reference | 91,64 | -11,41 | 74,17 | | | | |
| | St. dev. Ref. | 0,233 | 0,0565 | 3,429 | | | | |
| | 2005 | 89,36 | -9,3 | 74,51 | -2,28 | 2,11 | 0,34 | **3,13** |
| | St.dev 2005[11] | - | - | - | | | | |
| | 2009 | 87,53 | -9,61 | 70,58 | -4,11 | 1,8 | -3,6 | **5,75** |
| | St. dev. 2009 | 0,232 | 0,2426 | 2,574 | | | | |
| | | | | | | | | |
| Black digit | Reference | 22,64 | 0,89 | 2,1 | | | | |
| | St. dev. Ref. | 0,113 | 0,106 | 0,063 | | | | |
| | 2005 | 22,13 | 0,76 | 2,03 | -0,51 | 0,13 | 0,07 | **0,53** |
| | St.dev 2005[12] | - | - | - | | | | |
| | 2009 | 22,02 | 0,69 | 1,96 | -0,62 | -0,2 | 0,14 | **0,67** |
| | St. dev. 2009 | 0,068 | 0,036 | 0,0378 | | | | |

[11] Only one sample, therefore no standard deviation.
[12] Ibid

**O. Labels of PVC with embossed text so called "Dymo labels".**

No visible degradation or change in weight was recorded (*table 6*) on the samples exposed in-situ. This was also confirmed by the chromaticity analyses *(table 7*). The total colour change (dE) is negligible for the black background. The slightly higher dE value for the pressed whitish digits on the 2009 samples is likely to be explained by the fact that they are pressed into the material and therefore the original character is uneven.


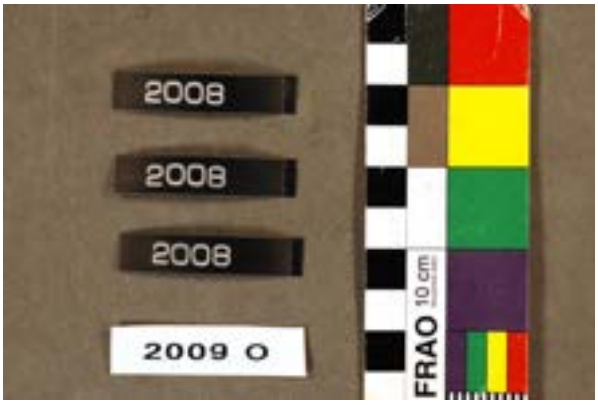


*Figures 30 & 31. PVC Dymo labels. References and samples retrieved after seven years of in-situ exposures in the sediments.*

*Table 6. PVC tags. Weights before and after burial*

| **Sample** | **Before burial, 2002.** | | **After burial, 2005** | |
|---|---|---|---|---|
| | g | % | g | % |
| O:1 | 0.15 | 100 | 0.15 | 100 |
| O:2 | 0.15 | 100 | 0.15 | 100 |
| O:3 | 0.15 | 100 | 0.15 | 100 |

*Table 7. Chromaticity readings for the DYMO label (PVC)*

| **O - DYMO label** | | **L*** | **a*** | **b*** | **dL*** | **da*** | **db*** | **dE*ab** |
|---|---|---|---|---|---|---|---|---|
| Black PVC material | Reference | 22,86 | 2,42 | 1,79 | | | | |
| | St. dev. Ref. | 0,05 | 0,007 | 0,007 | | | | |
| | 2005 | 22 | 1,97 | 1,67 | -0,87 | -0,45 | -0,12 | **0,98** |
| | St. dev. 2005 | 0,13 | 0,2 | 0,01 | | | | |
| | 2009 | 22,05 | 1 | 1,78 | -0,81 | -1,42 | -0,02 | **1,63** |
| | St. dev. 2009 | 0,36 | 0,02 | 0,21 | | | | |
| | | | | | | | | |
| Pressed whitish digits | Reference | 73,86 | 0,44 | -7,43 | | | | |
| | St. dev. Ref. | 2,99 | 0,565 | 0,64 | | | | |
| | 2005 | 74,89 | 0,56 | -7,77 | 1,03 | 0,12 | -0,34 | **1,1** |
| | St. dev. 2005 | 1,89 | 0,86 | 1,06 | | | | |
| | 2009 | 80,83 | 2,4 | -7,62 | 6,97 | 1,95 | -0,19 | **7,24** |
| | St. dev. 2009 | 1,94 | 0,47 | 0,675 | | | | |

**P. Labels of stainless steel with embossed text so called "Dymo labels".**

Tarnished spots have been visible on the samples from all the retrievals, including the last one. However none of the samples were considered heavily tarnished, which was confirmed by the fact that no change in weight was recorded. (*Table 8).* Despite that the chromaticity measurements were taken on tarnished spots if available, the total colour change of the in-situ samples is negligible and have not change much since 2005. (*Table 9*)


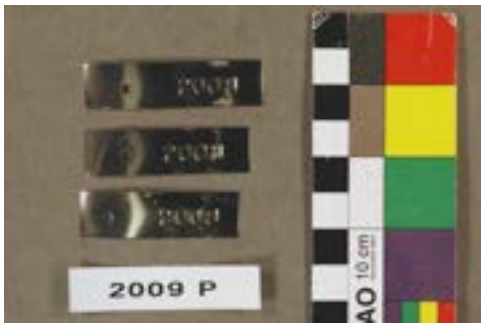


*Figures 32 & 33. Steel Dymo labels. References and samples retrieved after seven years of in-situ exposures in the sediments.*

*Table 8. Stainless steel tags. Weights before and after burial*

| **Sample** | **Before burial, 2002.** | | **After burial, 2005** | |
|---|---|---|---|---|
| | g | % | g | % |
| P:1 | 0.619 | 100 | 0.619 | 100 |
| P:2 | 0.554 | 100 | 0.554 | 100 |
| P:3 | 0.579 | 100 | 0.579 | 100 |

*Table 9. Chromaticity readings for the DYMO label (steel)*

| **P - DYMO steel label** | | **L*** | **a*** | **b*** | **dL*** | **da*** | **db*** | **dE*ab** |
|---|---|---|---|---|---|---|---|---|
| | Reference | 70,21 | 0,21 | 3,84 | | | | |
| | St. dev. Ref. | 0,445 | 0,08 | 0,34 | | | | |
| | 2005 | 73,83 | 0,41 | 4,19 | 3,62 | 0,21 | 0,34 | **3,64** |
| | St. dev. 2005 | 0,61 | 0,04 | 0,2 | | | | |
| | 2009 | 75,14 | 0,22 | 3,14 | 4,93 | 0,01 | -0,71 | **4,98** |
| | St. dev. 2009 | 1,37 | 0,16 | 0,085 | | | | |
| | | | | | | | | |

**Q, R, S & T. Written text on PE-bags.**

As stated before, text had been written with three different pens and one pencil on PE-bags, so called zip-lock bags. No change in weight of the PE bag after burial was recorded, but the white text panels have turned more yellow. (*Table 10 &11*)

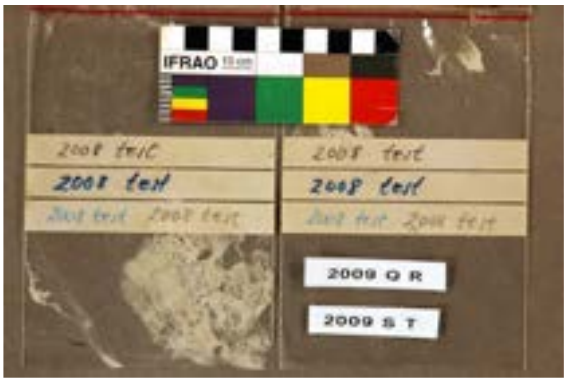


*Figures 34 & 35. Written text on PE bags. References and samples retrieved after seven years exposure in-the sediments.*

*Table 10. PE bags. Weights before and after burial.*

| **Sample** | **Before burial, 2002.** | | **After burial, 2005** | |
|---|---|---|---|---|
| | g | % | g | % |
| PE bag:1 | 2.00 | 100 | 1.99 | 99.5 |
| PE bag:2 | 1.98 | 100 | 1.92 | 97 |
| PE bag:3 | 1.99 | 100 | 1.99 | 100 |

*Table 11. Chromaticity readings for the PE bag (white areas for writing)*

| **PE bag** | | **L*** | **a*** | **b*** | **dL*** | **da*** | **db*** | **dE*ab** |
|---|---|---|---|---|---|---|---|---|
| | Reference | 95,45 | -0,69 | 4,27 | | | | |
| | St. dev. Ref. | | | | | | | |
| | 2005 | 92,57 | -0,38 | 11,33 | -2,87 | 0,32 | 7,06 | **7,63** |
| | St. dev. 2005 | 2,04 | 0,22 | 4,99 | | | | |
| | 2009 | 88,97 | 0,65 | 17,94 | -6,48 | 1,34 | 13,68 | **15,19** |
| | St. dev. 2009 | 51,3 | 0,52 | 6,47 | | | | |

**Q. Permanent marker. Written text on PE-bags.**

The ocular inspection recorded no major visible degradation on the samples exposed in-situ. The written text was clearly visible, but the black ink had turned paler than its reference. The chromaticity readings could confirm that there was a small colour change, but it seemed to have stabilized since 2005. (Table 12).

*Figure 36 & 37. Permanent marker (Q) on PE bag. Reference and samplee after seven years of exposure in situ.*

*Table 12. Chromaticity readings for the Black marker Q.*

| **Q – Black marker on PE bag** | | **L*** | **a*** | **b*** | **dL*** | **da*** | **db*** | **dE*ab** |
|---|---|---|---|---|---|---|---|---|
| | Reference | 23,72 | 3,21 | 1,76 | ------ | ------ | ------ | ------ |
| | St. dev. Ref. | 0,35 | 0,17 | 0,22 | | | | |
| | 2005 | 28,51 | 5,02 | 2,66 | 4,78 | 1,81 | 0,91 | **5,19** |
| | St. dev. 2005 | 2,09 | 0,65 | 0,28 | | | | |
| | 2009 | 26,26 | 0 | 4,44 | 2,54 | -3,21 | 2,68 | **4,9** |
| | St. dev. 2009 | 2,39 | 0,7 | 1,025 | | | | |

**R. Permanent marker OH. Written text on PE-bags.**

The written text is clearly visible, both on the PE bags, but the ink has not only lost some intensity, but also changed its colour from originally black to blue. This change in colour did occur all ready after one year exposure in the sediments.

The chromaticity readings confirm the result of the ocular inspection. All three dimensions: lightness (L*) and the two colour opponent dimensions (a* green/red and b* blue/yellow) have undergone changes. The 2009 samples are lighter and bluer than both the reference samples and the 2005 samples. *(Table 13).*

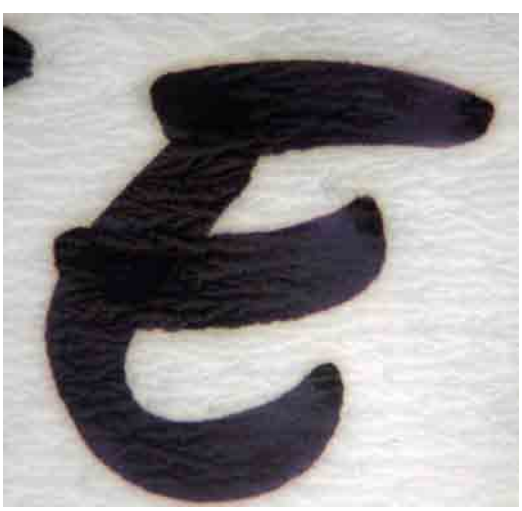

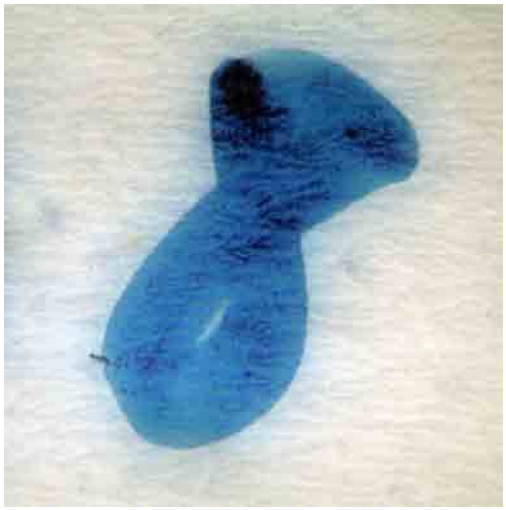

*Figure 38 & 39. Permanent marker OH (R) on PE bag. Reference sample and sample after seven years of exposure in-situ in the sediments.*

*Table 13. Chromaticity readings for the Black OH marker R*

| R - Black marker on PE bag | | L* | a* | b* | dL* | da* | db* | dE*ab |
|---|---|---|---|---|---|---|---|---|
| | Reference | 22,5 | 1,71 | 1,72 | | | | |
| | St. dev. Ref. | 0,12 | 0,06 | 0,1 | | | | |
| | 2005 | 26,93 | 3,88 | -11,16 | 4,44 | 2,17 | -12,89 | **13,8** |
| | St. dev. 2005 | 1,65 | 2,12 | 1,09 | | | | |
| | 2009 | 34,88 | -5,39 | -9,83 | 12,38 | -7,1 | -11,55 | **18,36** |
| | St. dev. 2009 | 2,83 | 0,56 | 0,76 | | | | |

**S. Archival proof ink. Written text on PE-bags.**

The ocular inspection recorded no major visible degradation on the samples exposed in-situ. The written text was clearly visible, but to the eye it seemed that the blue ink had turned paler and had changed to a more greenish blue colour than its reference

The chromaticity analyses again confirmed the result of the ocular inspection. The 2009 samples are lighter, more green (a*) and less blue (b*).The total colour change dE has continued to increase since the previous retrieval. *(Table 14).*

Though archival proof the ink has undergone some degradation in the sediments.

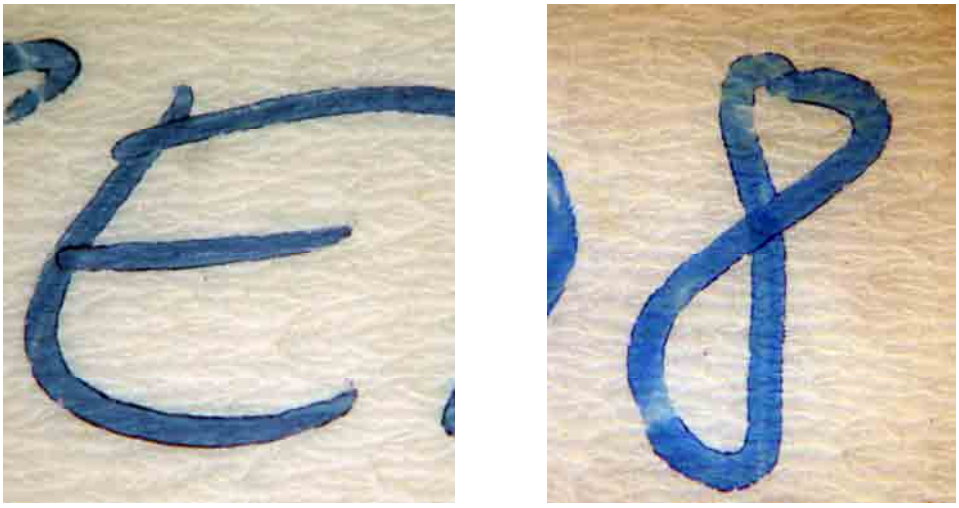

*Figure 40 & 41. Archival proof ink (S) on PE bag. Reference and sample after seven years of exposure in situ.*

*Table 14. Chromaticity readings for the archival ink – ball point pen S.*

| **S - Blue archival ink on PE bag** | | **L*** | **a*** | **b*** | **dL*** | **da*** | **db*** | **dE*ab** |
|---|---|---|---|---|---|---|---|---|
| | Reference | 45,53 | -0,97 | -18,43 | | | | |
| | St. dev. Ref. | 2,1 | 1,33 | 0,13 | | | | |
| | 2005 | 50,7 | -6,23 | -21,51 | 5,17 | -5,26 | -3,08 | **7,99** |
| | St. dev. 2005 | 1,63 | 0,53 | 1,77 | | | | |
| | 2009 | 53,02 | -8,84 | -14,56 | 7,48 | -7,87 | 3,87 | **11,53** |
| | St. dev. 2009 | 1,9 | 0,11 | 3,11 | | | | |

**T. Pencil. Written text on PE-bags and tags.**

The ocular inspection recorded no visible degradation on the samples exposed in-situ. The written text was clearly visible, both on the PE-bags and on the tags. This was also confirmed by the chromaticity readings. The total colour change (dE) of the 2009 samples is within the standard variation of the samples. *(Table 15).* The slightly increased +value for b* indicates a more yellow colour. This change is probably due to yellowness of the PE –bag it self. *(Table 11)*

*Figure 42 & 43. Pencil (T) on PE bag. Reference sample and sample after seven years of exposure in situ.*

*Table 15. Chromaticity readings for the pencil T.*

| T - pencil on PE bag | | L* | a* | b* | dL* | da* | db* | dE*ab |
|---|---|---|---|---|---|---|---|---|
| | Reference | 52,03 | -2,55 | -0,05 | | | | |
| | St. dev. Ref. | 4,43 | 0,35 | 1,61 | | | | |
| | 2005 | 52,39 | -2,43 | 3,77 | 0,36 | 0,13 | 3,81 | **3,83** |
| | St. dev. 2005 | 2,31 | 0,22 | 0,41 | | | | |
| | 2009 | 51,57 | -3,76 | 3,57 | -0,46 | -1,21 | 3,61 | **3,84** |
| | St. dev. 2009 | 3,76 | 0,51 | 1,26 | | | | |

## Discussion and conclusions

This study on packing and labelling material investigates products are (or have been) used in archaeological and reburial contexts. It is important that these products are easy available and not too expensive, which is the case with most of the studied products.

When commercial products are studied a few problems arise. One is that the complete content of a specific product can be difficult to obtain because of trade secrets. Therefore only the main ingredient(s), the base material, of each product can be given in a study like this. The fact that additives, such as plasticisers and colours, are mixed with base materials complicates the interpretation of degradation analyses. Processes such as the extraction of additives in different environments may affect the mechanical properties in various ways. Different products made of the same base material are likely to have different additives, which may cause them to degrade differently. Dimensions, form and production technique also play a role in the degradation of products. Hence conclusions from the analyses in this study are valid primarily for the tested products and to a lesser extent for the base materials.

Initially the study hoped to find relationships between temperature and ageing time in the current environment in order to predict the acceleration factors and lifetime for the materials. However, most materials did not show any significant change that could be used to calculate a possible lifetime for a material and, as was realised during the project, very few previous studies have been made on plastics in a marine anaerobic environment that could be used to relate to (Yarahmadi, pers comm.) Therefore it was not possible to estimate life span for different materials.

In the result from phase 1 it was noted that the microbiological activity seemed to play a bigger role in the deterioration of the polymers than did the chemical content of the sediments. We also know from previous results that the wooden crate (B) and the polyethylene net (D) already after 3 years had lost considerable strength. (Nyström Godfrey, 2009)

However, apart from these two materials, the most of the other polymers seem stable and could be used when archaeological artefacts are to be reburied. After seven years in the marine sediments the mechanical strength of the HDPE crate (A), the polyethylene bag (C), the polyethylene/polypropylene geotextile (F), the polyethylene rope and the PETR/PUR prefabricated tag (N) is unchanged.

The reason why the degradation of the different PE products (net, bag and cord) vary is likely to found in the facts mentioned above, which is differences in dimensions, form, production technique and additives.

The polyester rope (J) is still strong, but the Max Load has decreased from 800 to 625 N and it could be considered a trend (*Figure 15*), which would make a polyester rope less suitable for long term reburials; however this will have to be confirmed through future analyses.

The interpretation of the tensile tests on the polyamide products cord (L) and yarn (M) was after phase I inconclusive. Although polyamide is known to be a very strong and durable material, often used in marine environments (e.g. Kevlar sails) little was known about the degradation processes in an anaerobic environment. (Brydson, 1995 ). Polyamide is a material sensitive to humidity. Moisture does not affect the ageing, but it strongly affects the strength of the material. (Almström, pers.comm.) The inconclusive and odd results for the mechanical strength in phase I was thought to be a result of differences in moisture content and re-cristallisation, despite all samples being conditioned in the same manner. The tests performed on the 2009 *in situ* samples showed no degradation of the mechanical properties (*figures 18 &21*), smaller variations are within standard deviation. This suggests that it is suitable for reburials. However, it would be wise to wait for future analyses before making statements of the long term preservation of polyamide in anaerobic reburial environments.

In short one can state that most of the polymer materials tested are very stable and can be used in situations where archaeological artefacts are to be reburied. Crates should be made of HDPE and not from wood. Nets of PE should be avoided and certainly not used for heavier objects. A possibility would of course be to use a PE net with coarser and stronger strings or using nets made from other material, such as polyamide or maybe polyester. For short-term reburials (7 years) ropes and yarns made of PE, polyester or polyamide could be used, for longer-term reburial it would, until further investigations are made, be wise to use the PE cord.

After seven years of burial all labels were easily readable with the naked eye. Ocular inspection and chromaticity readings show, however, that text written with (R) the black marker (R) [1] and the blue archival proof pen (S) [2] had continued to deteriorate and change quite considerable. As expected the pencil (T) writing had not change at all, likewise with the permanent marker (Q). [3]

It is therefore recommended to use pencils or markers of good permanent quality and not for example, over-head markers, as the one tested. As the archival ink pen (S) showed signs of degradation in this particular environment it is not suitable for anaerobic clay sediments. Another reason to avoid this pen is the fineness of the tip of the pen, which makes the lines very thin and difficult to read when the ink fades and changes in colour.

Although the prefabricated and Dymo labels all looked good after seven years of burial, the steel label is difficult to read. It is also known that stainless steel corrodes in anaerobic environments due the action of the sulphate reducing bacteria, which would make it a less good choice. (Evans 1963 & Richards, Appendix 2, this publication) A better choice for labelling artefacts reburied in sediments would be to use PVC Dymo labels or prefabricated embossed tags, so called “ear-tags”. Table 16 summarise the results and evaluations of the stability of the tested materials

*Table 16. Recommendations on packing and labelling materials suited for reburial in anaerobic sediments with low microbiological activity*

| ***Sample ID*** | ***Product*** | **Material** | **Long term reburial possible*** | **Medium term reburial possible – at least 7 years** | **Reburial not recommended** |
|---|---|---|---|---|---|
| A | Crate | Polyethylene, HDPE | x | x | |
| B | Crate | Pine | | | x |
| C | Bag | Polyethylene, LDPE | x | x | |
| D | Net | Polyethylene | | | x |
| E | Sack, woven | Polypropylene | | x** | |
| F | Geotextile | Polyethylene/ Polypropylene | x | x | |
| G | Geotextile | Polyester | | x** | |
| H | Tarpaulin | Synthetic rubber | x | x** | |
| J | Cord | Polyester | | x | |
| K | Cord | Polyethylene | x | x | |
| L | Cord, spun | Polyamide | | x | |
| M | Yarn | Polyamide | | x | |
| N | Tag, prefabricated | Polyether/ Polyurethane | x | x | |
| O | Tag, dymo ® | Polyvinyl chloride | x | x | |
| P | Tag, dymo ® | Stainless steel | | x | x |
| Q | Marker | Permanent ink | x | x | |
| R | Marker for OH | Permanent ink | | x | x |
| S | Pen, ball point | Archival proof ink | | x | x |
| T | Pencil | Graphite | x | x | |

* That long term reburial is possible have been predicted for these materials, but are to be confirmed through future retrievals.

** These materials were only tested after 3 years of exposure, hence short term reburial can only be safely recommended for at least 3 years; however it is highly likely that at least the EPDM tarpaulin is suitable for long term reburial.

## References

Brydson, J. A. (1995) *Plastics Materials*, 6th edn. Butterworths – Heinemann

Evans, U. R. (1963) *An introduction to metallic corrosion*. London, Edward Arnold Publishers.

Nyström Godfrey, I. (2009) Reburial and Analyses of Archaeological Remains (RAAR). Investigation of the effects of burial on materials used at archaeological excavations to separate and mark objects. In K. Streatkvern, D.J. Huisman (eds). *Proceedings of the 10th ICOM-CC Working group on wet organic archaeological materials conference.* ICOM Amersfort 2009, 215-251.

Minolta. *Chroma meter CR-100/CR-110. Operation manual* (1984) 1ff.

Reburial and analyses of archaeological remains. Studies on the effect of reburial on archaeological materials performed in Marstrand, Sweden 2002-2005, (2007), Eds. T. Bergstrand & I. Nyström Godfrey. Uddevalla, Bohusläns Museum and Studio Västsvensk Konservering, Kulturhistoriska dokumentationer nr 20.

WIKIPEDIA: Lab color space.
http://en.wikipedia.org/wiki/Lab_color_space (2010-12-10)

Personal communication
Stefan Almström, The Swedish National Testing and Research Institute, Borås. Personal communication.

Nazdaneh Yarahmadi, The Swedish National Testing and Research Institute, Borås. Personal communication.

## List of Materials

*A. Crate*
Material: HDPE
Supplier: WITRE, Göteborg
Measurements: 60x40x27 cm, thickness: 3 mm
Weight: approx. 1690 g each (after being labelled)

*B. Crate*
Material: pine, with one side sawed and the other planed
Supplier: SVK.
Measurements: 14.7x10.5x0.9 cm
Weight: individually weighed

*C. Bag, "Ziplockbag"*
Material: Polyethylene + plasticizer
Supplier: Joka Plastemballage, Kungsbacka
Measurements: 15x10 cm
Weight: 1.95g/bag

*D. Net, "Layflat", AXI-85-LF43*
Material: Polyethylene
Supplier: Lars-Göran Danielsson, 018-108720
Measurements: tube diam: c 21 cm, loops/cm: c 1.5, sample length: approx. 30 cm.

*E. Sack*
Material: polypropene, woven
Supplier: SK Stok, Århus
Measurements: th. 0.5-1 mm, samples approx. 20x20 cm
Weight: 110g/m

*F. Geo-textile, Terram 900 Pr*
Material: 70% polypropene, 30% polyethylene
Supplier: Allt i mark, Göteborg
Measurements: th. Approx. 1 mm. Samples approx. 20x20 cm
Weight: 115g/$m^2$

*G. Geo-textile, Weedkiller*
Material: 100% polyester
Supplier: Allt i mark, Göteborg
Measurements: th. Approx. 1 mm
Weight: 180g/$m^2$

*H. Tarpaulin*
Material: EPDM, etenpropendienmonomer, a synthetic rubber.

Återförsäljare: Scandinavian Terra Tec
Supplier: Trelleborg Building System
Measurements: th. 1 mm. Samples approx. 20x20 cm
Weight: 1,11 kg /$m^2$.

*I. Wadding. Fiberfill, carded, non-vowen*
Material: Polyester
Supplier: Nevotex
Measurements: th. 2 cm. Samples approx. 20x20 cm.
Weight: approx. 200g/m2

*J. Cord, s-spun*
Material: polyester
Supplier: Asperö Handels AB. V. Frölunda
Measurements: th. Approx. 3 mm. Sample length approx. 30 cm

*K. Cord, z-spun.*
Material: polyethylene
Supplier: Asperö Handels AB. V. Frölunda
Measurements: th. approx. 2.5 mm. Sample length approx. 30 cm

*L. Cord, plaited.*
Material: Polyamide, nylon
Supplier: Asperö Handels AB. V. Frölunda
Measurements: th. Approx. 2 mm. Sample length approx. 30 cm

*M. Yarn, z-spun.*
Material: Polyamide, nylon
Supplier: Asperö Handels AB. V. Frölunda
Measurements: th. Approx. 0.5 mm. Sample length approx. 30 cm

*N. Label, embossed – prefabricated. Normally used for marking animals, so called "ear tags".*
Name: Combi
Material: "Elastollan", from BASF. Polyether and polyurethane
Supplier: Stallmästaren, Lidköping
Measurements: 92x57x1.5 cm
Weight: approx. 9.1 g, individually weighed as well.
The numbers are pressed into the plastic with heat and dyed black

*O. Label with embossed text, DYMO, black.*
Material: Polyvinyl chloride
Supplier: Akademibokhandeln or any stationary
Measurements: w. 10 mm
Weight: individually weighed

*P. Label with empossed text, DYMO.*
Material: Steel
Supplier: via Bohus County Museum
Measurements: w. 13 mm
Weight: individually weighed

*Q. Pen, permanent marker. Black.*
Brand: Edding 404, permanent marker.
Material: ink
Supplier: Akademibokhandeln

*R. Pen, permanent marker designed for writing on over-heads. Black.*
Brand: Stabilo OHpen Universal. Art no 843/46
Material: ink
Supplier: Akademibokhandeln

*S. Pen, ball-point. Blue.*
Brand: BIC svenskt arkiv SP.SBF 202 (543.91)
Material: ink
Supplier: Akademibokhandeln

*T. Pencil*
Brand: Rexel Cumberland, Derwent Graphic, 4B
Material: Graphite
Supplier: Akademibokhandeln

Text has been written on ziplock bags according to the following.

| | |
|---|---|
| Q. Permanent marker, Edding 404 | |
| R. Permanent marker, Stabilo OH pen | |
| S. Ball-point pen BIC | T. pencil |

Text has been written on polyethylene tags according to the following

Side 1:

| | |
|---|---|
| Q. Permanent marker, Edding 404 | R. Permanent marker, Stabilo OH pen. |

Side 2:

| | |
|---|---|
| S. Ball-point pen BIC | T. Pencil |

# Reburial and analyses of archaeological remains The RAAR project

Eds. Inger Nyström Godfrey, Thomas Bergstrand and Håkan Petersson

Bohusläns museum

Västra Götalandsregionen
Västarvet